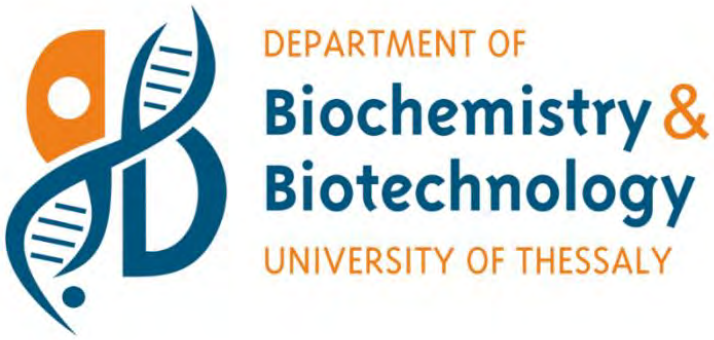

University of Thessaly

School of Health Sciences

Department of Biochemistry & Biotechnology

Doctoral Thesis

"Development of nanocarriers for the encapsulation of cannabinoids and other bioactive compounds"

Demisli Sotiria

Chemist

Larissa, 2023

Development of nanocarriers for the encapsulation of cannabinoids and other bioactive compound

Examination committee

- **Papadimitriou Vassiliki (supervisor)**
  Researcher B' – Group of Biomimetics & Nanobiotechnology
  Institute of Chemical Biology, National Hellenic Research Foundation (NHRF)

- **Leonidas D. Demetres**
  Professor – Biochemistry
  Department of Biochemistry & Biotechnology, University of Thessaly (UTH)

- **Pletsa Vasiliki**
  Researcher B'– Environment and Health Program
  Institute of Chemical Biology, National Hellenic Research Foundation (NHRF)

- **Psarra Anna-Maria**
  Associate Professor – Biochemistry
  Department of Biochemistry & Biotechnology, University of Thessaly (UTH)

- **Skamnaki Vasiliki**
  Assistant Professor – Biochemistry-Metabolism
  Department of Biochemistry & Biotechnology, University of Thessaly (UTH)

- **Giannouli Persefoni**
  Assistant Professor – Technology and Quality Control of Foods of Plant Origin
  Department of Biochemistry & Biotechnology, University of Thessaly (UTH)

- **Savić Snežana**
  Professor – Faculty of Pharmacy
  Department of Pharmaceutical Technology and Cosmetology, University of Belgrade, Belgrade, Serbia

Demisli Sotiria

Development of nanocarriers for the encapsulation of cannabinoids and other bioactive compounds

Abstract

The main goal of the present thesis was the development of novel biocompatible nanodispersions to be used as carriers for diverse lipophilic bioactive compounds. The purpose of these systems was the effective delivery of the encapsulated substances while providing alternative routes of administration, other than the oral which is the most commonly used. Two different nanodispersions were developed namely, oil-in-water nanoemulsions and nanoemulsion-filled hydrogels. These systems were used as carriers for the encapsulation and delivery of various lipophilic substances with pharmacological interest.

Initially, the structure of the developed systems was elucidated in order to reveal possible differences and determine the localization of the encapsulated compounds. It was also essential to investigate whether the nanoemulsions' structure was affected after its incorporation into the hydrogel matrix. In order to obtain the structural characterization of the formulated nanocarriers Dynamic Light Scattering (DLS), Electron Paramagnetic Resonance Spectroscopy (EPR), Confocal Fluorescence Microscopy (CFM), Cryo-Electron Microscopy (Cryo-EM) and Small-angle X-ray Scattering (SAXS) were performed. The investigation was carried out for both systems in the absence and presence of bioactive compounds. Regarding the nanoemulsions, the structural study revealed that the localization of the encapsulated compounds was dependent on their structure and had an effect on the size of the nanodroplets and the surfactant monolayer. Nevertheless, no significant changes in the structure of the nanoemulsion were observed after its incorporation into the hydrogel.

In order to evaluate the suitability of the formulated nanodispersions to act as delivery vehicles of bioactive compounds different *in vitro* methods were implemented for their biological evaluation. The cytotoxic effect of both nanocarriers in the absence and presence of the encapsulated molecules was assessed through a cell viability assay using the cell lines RPMI 2650 and WS1 as models of the human nasal epithelium and skin, respectively. Subsequently, *in vitro* permeation study through Franz difussions cells and tape stripping experiments were conducted indicating that the nanoemulsion-filled hydrogels could be more effective for the delivery of bioactives through the skin since it demonstrated increased penetration and improved release profiles compared to the bioactive released from the nanoemulsions.

Consequently, the proposed nanodispersions could be promising candidates as carriers for the effective delivery of various substances of pharmacological interest through the skin providing increased efficacy as well as the possibility of alternative delivery routes.

Περίληψη

Βασικός στόχος της παρούσας διατριβής ήταν η ανάπτυξη βιοσυμβατών νανοδιασπορών ως φορέων χορήγησης λιπόφιλων βιοδραστικών ενώσεων. Συγκεκριμένα αναπτύχθηκαν νανογαλακτώματα ελαίου-σε-νερό και υδρογέλες με ενσωματωμένο νανογαλάκτωμα με στόχο την αποτελεσματική χορήγηση των ενθυλακωμένων ουσιών με φαρμακολογικό ενδιαφέρον.

Αρχικά, διευκρινίστηκε η δομή των συστημάτων που αναπτύχθηκαν ώστε να εντοπιστούν πιθανές διαφορές μεταξύ τους και να προσδιοριστεί η θέση των βιοδραστικών ουσιών. Βασική ήταν επίσης η μελέτη της δομής των νανογαλακτωμάτων μετά την ενσωμάτωσή τους στην υδρογέλη. Για τον δομικό χαρακτηρισμό χρησιμοποιήθηκαν Δυναμική Σκέδαση Φωτός (DLS), Φασματοσκοπία Ηλεκτρονικού Παραμαγνητικού Συντονισμού (EPR), Συνεστιακή Μικροσκοπία Φθορισμού (CFM), Κρυογονική Ηλεκτρονική Μικροσκοπία (Cryo-EM) και Σκέδαση Ακτίνων Χ σε μικρές γωνίες (SAXS). Η έρευνα διεξήχθη και για τα δύο συστήματα απουσία και παρουσία βιοδραστικών ενώσεων. Η δομική μελέτη των νανογαλακτωμάτων αποκάλυψε ότι η δομή των ενθυλακωμένων ουσιών επηρέαζε τον προσανατολισμό τους μέσα στα νανοσταγονίδια, είχε επίδραση στο μέγεθος των νανοσταγονιδίων και στη μονοστιβάδα των επιφανειοενεργών. Ωστόσο, δεν παρατηρήθηκαν σημαντικές αλλαγές στη δομή του νανογαλακτώματος μετά την ενσωμάτωσή του στην υδρογέλη.

Για την αξιολόγηση της καταλληλότητας των προτεινόμενων νανοδιασπορών να δρουν ως φορείς για τη χορήγηση βιοδραστικών ουσιών, εφαρμόστηκαν διαφορετικές μέθοδοι *in vitro* για τη βιολογική τους αποτίμηση. Η κυτταροτοξικότητα και των δύο νανοφορέων απουσία και παρουσία των ενθυλακωμένων μορίων αξιολογήθηκε μέσω μελέτης αναστολής της κυτταρικής βιωσιμότητας με χρήση των κυτταρικών σειρών RPMI 2650 και WS1 ως μοντέλα του ανθρώπινου ρινικού και δερματικού επιθηλίου αντίστοιχα. Μέσω πειραμάτων *in vitro* μελετήθηκε η διαπερατότητα της βιοδραστικής στο δέρμα με χρήση της κυψελίδων διάχυσης Franz και με την τεχνική tape stripping. Βρέθηκε ότι οι υδρογέλες γεμάτες με νανογαλάκτωμα θα μπορούσαν να είναι πιο αποτελεσματικές για την χορήγηση βιοδραστικών μέσω του δέρματος, καθώς τους παρείχε αυξημένη διαπερατότητα και βελτιωμένα προφίλ απελευθέρωσης σε σύγκριση με τα νανογαλακτώματα. Συνεπώς, οι προτεινόμενες νανοδιασπορές είναι κατάλληλες για την αποτελεσματική χορήγηση διάφορων ουσιών μέσω του δέρματος παρέχοντας αυξημένη αποτελεσματικότητα καθώς και δυνατότητα εναλλακτικών οδών χορήγησης.

Demisli Sotiria
Larissa, 2023

“Development of nanocarriers for the encapsulation of cannabinoids and other bioactive compounds”

Doctoral Thesis

University of Thessaly
School of Health Sciences
Department of Biochemistry & Biotechnology

Number of primary pages: 17

Total number of pages: 190

Total number of figures: 58

Total number of tables: 13

Total number of references: 548

Prologue

The principal purpose of the present thesis was the development of novel biocompatible nanodispersions to act as carriers for various lipophilic compounds of pharmacological interest. In addition, their biological evaluation as suitable delivery systems was of paramount importance. Two types of nanocarriers were formulated namely oil-in-water nanoemulsions and nanoemulsion-filled hydrogels and were used as carriers for the encapsulation of diverse lipophilic compounds of interest. The proposed systems were structurally characterized by implementing various techniques and then their efficacy as potent vehicles for the delivery of bioactives through the skin was assessed through *in vitro* studies.

This thesis was carried out during the years 2018-2023 at the Biomimetics & Nanobiotechnology group of Institute of Chemical Biology (ICB) at National Hellenic Research Foundation (NHRF) in collaboration with the Department of Biochemistry and Biotechnology of the University of Thessaly. Supervisor of this dissertation was Dr. Vassiliki Papapdimitriou. Part of this project was financially supported by the project “CO2-BioProducts” (MIS 5031682), which is funded by the Operational Programme “Competitiveness, Entrepreneurship and Innovation” (NSRF 2014-2020) and co-financed by Greece and the EU (European Regional Development Fund). Additional funding was received by the European Union and Greek national funds through the Operational Program Competitiveness, Entrepreneurship and Innovation, under the call RESEARCH – CREATE – INNOVATE (QFytoTera, T1EDK-00996).

Acknowledgements

Accomplishing the following work was a dream and a milestone for my academic career. A lot of effort, mental strength and perseverance were required so that the result presented in this doctoral thesis exists today. Particularly important were the people who supported me and accompanied me all these years on this sometimes difficult and sometimes beautiful journey. Therefore, I would like to thank these people from the bottom of my heart.

Firstly, I would like to deeply thank my supervisor Dr. Vassiliki Papadimitriou for her invaluable guidance and support throughout my PhD research. Her expertise and assistance were invaluable to me and have played a crucial role in order to achieve the present work. I would also like to thank Dr. Vasiliki Pletsa who introduced me to the world of cells by passing me her knowledge and who was by my side every step of the way. Her insights and guidance were crucial in helping me to shape my research and write this thesis. I would like to extend my sincere thanks to Prof. Demetrios Leonidas for serving on my thesis committee, who has provided important feedback and his professional expertise. I truly appreciated that he gave me the opportunity to conduct my PhD in the Department of Biochemistry & Biotechnology in the University of Thessaly.

I would like to express my profound appreciation and gratitude to Dr. Aristotelis Xenakis for his trust, support, and encouragement. His vast wisdom and wealth of experience have inspired me throughout my research. In addition to the above I would like to thank my thesis examination committee: Prof. Anna-Maria Psarra, Prof. Vasiliki Skamnaki, Prof. Persefoni Giannouli, and Prof. Snežana Savić for accepting the invitation to be a valuable part of my public defense and for their important contribution. A special thanks to Prof. Snežana Savić, for giving me the opportunity to work in her lab, broadening my scientific horizons. Thank you for the amazing collaboration which has been the real basis for understanding exactly what scientific life is all about. A special thanks to Tanja Ilić and Ines Nikolić who helped me during this time in Belgrade and made me feel at home.

I could not have undertaken this journey without my beloved fellow travelers, the Biomimetics and Nanobiotechnology group of National Hellenic Research Foundation. I would like to express my deep appreciation to Dr. Maria Zoumpanioti, Dr. Spyridon Avramioti and George Sotiroudi for teaching, advising and supporting me at every step of this way. In addition, I owe a huge thanks to Dr. Evgenia Mitsou and Dr. Maria Chatzidaki for their support and the fruitful conversations who gave me the push to keep going. My heartfelt thanks to Eleni Galani for all her emotional and moral support and for being my companion through this

journey. I would like to thank Eva Vassiliadi, Konstantina Matskou, Dr. Ioanna Theochari and Dr. Ilias Matis for creating a pleasant and warm environment.

Finally, I would like to express my gratitude to my family for their constant support through difficult times and good times that helped me bloom and become the person I am. Their belief in me has kept my spirits and motivation high during this process.

Contents of Figures & Tables

Table of Contents

Chapter 1

Introduction

Chapter 1 – Introduction

1.1. Nanotechnology and Types of Nanodispersions

Nowadays, nanotechnology is one of the most intriguing scientific fields attracting the attention of both the research community and industry since it offers an extensive range of applications. The term nanotechnology is referred to the development and manufacturing as well as the investigation, measurement, and manipulation of formulations or structures which possess size at the nanometer scale [1,2]. Particularly, according to the National Nanotechnology Initiative (NNI) in the United States nanotechnology is defined as a science, engineering, and technology conducted at the nanoscale that contributes to the development of novel applications in several fields including chemistry, biology, engineering, materials science and physics due to its unique properties [3]. However, the acceptable particle size in order to characterize a formulation as "nano" is still under debate with literature references reporting nanodispersions up to 100 nm or even 500 nm in size [4–10]. One of the most valuable branches of nanotechnology is nanomedicine where nanosized materials are applied for the prevention or treatment of pathological conditions. These materials can be employed as delivery vehicles for active therapeutic agents, diagnostic tools [11], biosensors, and biomaterials. They are also useful for tissue engineering, and bioimaging [12].

Amongst the aforementioned applications, the use of nanocarriers for the delivery of bioactive compounds is one of the most studied. This arises from the fact that both the conventional drug formulations that are utilized until now and the natural substances that are recently gaining ground as pharmaceutical actives demonstrating great pharmacological action and simultaneously less toxicity than the synthetic ones [13,14] present certain drawbacks. Even though the potential efficacy of a bioactive compound depends on some features of the molecule itself including solubility, molecular weight, pK_a, and receptor affinity, the influence of some external factors such as pH, presence of interacting substances in the surrounding environment, and, the enzymatic function is also crucial. As a result, the bioactive compound of interest presents limited permeation through the natural barriers or undergoes high systemic clearance which reduces its bioavailability and efficacy creating the need for additional and repeating application or higher doses leading to adverse effects [11,15,16]. However, implementing nanotechnology for the development of pharmaceutical formulations is a cutting-edge solution for the aforementioned limitations since nanocarriers provide the ability to effectively protect, transport, and release diverse drugs [17–19] and also natural compounds of pharmaceutical interest [20–23].

Hence, nanocarriers have been extensively investigated as vehicles for the delivery of multiple molecules with therapeutic potential since they present a plethora of benefits. There are indications that nanocarriers improve the delivery and efficacy of the encapsulated bioactive substances in multiple ways including the increase of solubilization of highly lipophilic drugs, their enhanced penetration, and targeted delivery leading to increased bioavailability. In addition, nanocarriers provide the ability of surface flexibility or functionalization and can be used as delivery vehicles for miscellaneous pharmaceutical agents. Thus, they enable the administration of large macromolecules or the simultaneous delivery of two or more therapeutic agents with synergistic action. Simultaneously nanocarriers protect the encapsulated molecules against metabolic degradation increasing their stability upon storage or administration. Overall, nanocarriers have been proven beneficial for drug delivery by changing the absorption pathways and affecting the pharmacokinetics and biodistribution of pharmaceutical substances reducing the frequency or the dose of administration and preventing cytotoxic or adverse effects [11,24–29].

There are various types of nanocarriers each of them owing different properties and being suitable for different applications. Some of the most studied and used nanocarriers for the encapsulation of active compounds are liposomes, solid lipid nanoparticles, Pickering emulsions, micelles, dendrimers, biopolymer-based and inorganic nanoparticles [26,27,30–33]. Nanocarriers can be classified into two broad groups according to their physicochemical properties and the method of encapsulation of the bioactives and are characterized either as “hard” or “soft” through adsorption or covalent bonding including inorganic nanoparticles, metal oxides, carbon nanotubes, and quantum dots. On contrary, the latter term refers to the nanocarriers encapsulating the bioactive molecule in their core. Some of the most commonly used soft nanocarriers are dendrimers, micro- and nano-emulsions, liposomes, and Pickering emulsions and they are illustrated in figure 1 below [26,34,35].

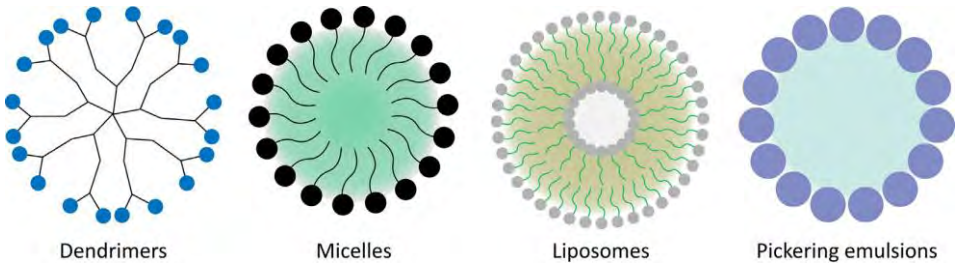

Figure 1. Some of the most widely used “soft” nanocarriers [26].

In order for a nanocarrier to be considered ideal for biomedical applications there are some crucial technical and also economical parameters that need to be fulfilled. Some of the essential requirements are the use of biocompatible and inexpensive materials and the development of formulations demonstrating high chemical stability over time and producing non-toxic degradation by-products. Furthermore, rapid, robust, scalable, and cost-effective formulation procedures are required to provide consistent results in every batch regarding the size, homogeneity, encapsulation efficiency, and stability of the formulated nanocarrier [1,15,36]. Particularly, size and shape are two characteristics of paramount importance affecting the efficacy of the nanocarriers as delivery vehicles since their uptake and permeation through the epithelia as well as their absorption profile are directly dependent on them. Thus, smaller nanoparticles with sizes between 50 nm and 300 nm are usually preferred as delivery vehicles for active molecules [1,37].

In the present thesis, the nanodispersions of interest that were developed and investigated were nanoemulsions (NEs) and nanoemulsion-filled hydrogels (NE/HGs). These particular systems were formulated to be used as carriers for various natural lipophilic bioactive compounds of pharmacological interest. The developed nanocarriers were studied to determine their potential efficacy for the transdermal delivery of bioactive compounds and were compared in terms of the release of the encapsulated substance and skin penetration and permeation ability by implementing *in vitro* techniques.

1.2. Nanoemulsions – terminology and advantages in drug development

Since the development of nanotechnology, there has been increasing interest in diverse industries including food, cosmetic, agrochemical, pharmaceutical, and others in the application of colloidal dispersions to encapsulate lipophilic molecules in order to protect them and provide enhanced delivery. Specifically, NEs have attracted particular interest for many decades and remain appealing due to their wide versatility. Especially in the field of drug development a significant number of therapeutic agents of interest present extremely poor water solubility making challenging their effective delivery and reducing their bioavailability. Hence, NEs present great potential due to their unique characteristics making them ideal candidates for drug delivery. Hence, they have been studied extensively for use as carriers for multiple hydrophobic therapeutic compounds through diverse routes of administration providing the possibility of improved delivery via alternative routes [4,38,39].

NEs are colloidal nanodispersions and they are usually comprised of oil, water, surfactants, and occasionally co-surfactants. They are defined as two immiscible liquids stabilized by an amphiphilic surfactant with one liquid being dispersed as spherical nanosized droplets within the other. One phase is referred to as dispersed and the other as the continuous phase. Depending on the nature of the dispersed phase, NEs are classified as oil-in-water (O/W) when the oil phase is dispersed in the aqueous while in the opposite case they are referred to as water-in-oil (W/O) as illustrated in figure 2 [4,8,40,41].

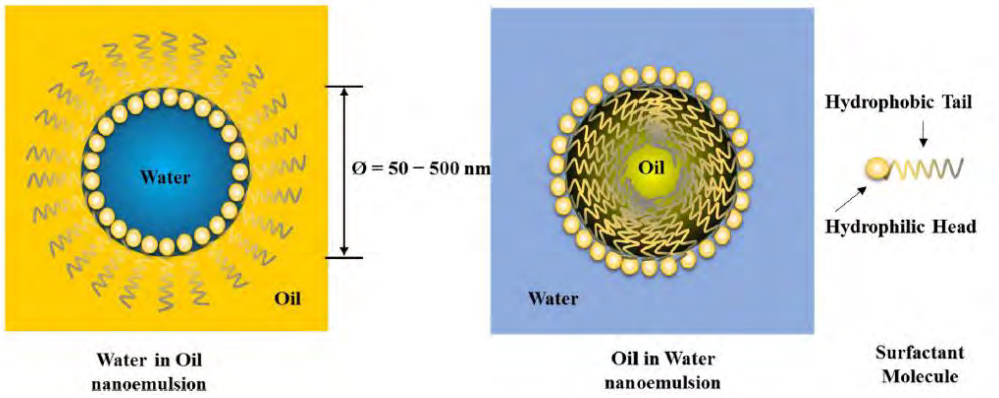

Figure 2. Water-in-oil (W/O) and oil-in-water (O/W) NEs with the schematic representation of the composition and the structure of the amphiphilic surfactants used for their stabilization [42]

Since they are thermodynamically unstable systems, energy input is required for their formulation and they tend to destabilize over time. However, the nanodroplet size and the selection of suitable components of the formulation can affect the stability with nanodroplets of smaller diameter leading to increased stability [43,44]. The acceptable upper limit of the mean droplet diameter values in order for a formulation to be considered as NE range from 200 nm to 500 nm depending on the literature [26,45]. Their appearance could be clear, turbid, or even milky according to their composition and also the size and concentration of the dispersed nanodroplets. Nevertheless, the features of NEs are adjustable providing the possibility to develop systems with distinct characteristics and properties depending on the use and route of administration for which they are intended. This optimization is of paramount importance since the properties of the formulation influence the overall bioavailability and hence the efficacy of the encapsulated lipophilic compound and lead to enhanced protection against environmental factors such as pH and temperature during both storage and administration [41,46,47]. More specifically, physicochemical attributes such as size, optical properties, and rheology as well as the type of the formulated NE (O/W or W/O) are

considerably affected by the nature of the selected components. For instance, the composition of the surfactant mixture favors the formulation of different types of NE with the water-soluble ones leading to O/W type and the oil soluble to W/O ones and *vice versa*. In addition, the nature and viscosity of the oil have a great influence on the size and stability of the formulated NEs since more viscous oils produce larger nanodroplets [38,41]. Functionalization of NEs can also be obtained by surface modification of the formulated nanodroplets providing prolonged circulation times or even targeted delivery [48].

In general, NEs have emerged as promising delivery vehicles for use in nanomedicine due to their aforementioned ability of functionalization. In addition, they are easy to produce and can be optimized to demonstrate long-term stability. Since NEs typically require lower concentrations of surfactants for their formulation compared to other nanocarriers they demonstrate reduced toxicity and can be formulated entirely from generally recognized as safe (GRAS) components [43,46]. In addition, NEs present favorable properties for medical applications such as enhanced solubilization of highly lipophilic drugs increased loading capacities, and efficient masking of unpleasant after taste which could cause nausea resulting in reduced patient compliance [38,49,50]. All these features that NEs provide result in increased protection and bioavailability, controlled release, and enhanced permeability of the encapsulated lipophilic molecules making them promising carriers for use in drug development [51–53].

1.3. Emulsification methods and destabilization phenomena

Since NEs are thermodynamically unstable and usually contain low surfactant concentrations, they cannot be formulated spontaneously and the application of external energy is essential in order to prepare the colloidal nanodispersion from the separate components. *T*he required energy input for their preparation could be either mechanical or physicochemical. More specifically, the necessary overall free energy change (ΔG) for colloidal dispersion formation is expressed by the following equation (1):

$$\Delta G = \Delta A\gamma - T\Delta S \quad (1)$$

Where Δ*A*γ* refers to the required free energy to obtain an increase in the oil-water interface. The term A is the interfacial area and γ is the interfacial tension. On the other

hand, as T*ΔS is mentioned the free energy is related to increasing the number of possible arrangements of dispersed droplets in a NE in comparison to the separated phases with the term T expressing the temperature and S the entropy [43]. For the successful formulation of a NE equation 1 expressing the required external free energy (ΔG) must produce a positive result.

There is a variety of emulsification methods used, each demonstrating different advantages and limitations and providing diverse results leading to systems with distinct characteristics. Thus, the selection of the appropriate formulation method is crucial for the development of a system with the desired properties depending on the intended application. In general, the implemented fabrication methods can be broadly classified into two categories namely high-energy or low-energy methods depending on the physicochemical mechanism that occurs resulting in the droplet disruption [4,46,54]. The selection of a suitable emulsification method is often related to the surfactant–oil-water systems, for example, depending on the oil phase or the concentration of the surfactants that are used high-energy methods could provide better systems in terms of nanodroplet size or/and stability [43].

High-energy emulsification methods

As high-energy methods are described those where the aforementioned free energy derives from mechanical forces resulting in the splitting of the dispersed phase into smaller droplets at the nanoscale range. Special devices known as “homogenizers” are utilized for this purpose generating powerful disruptive forces including shear, turbulence, or cavitation [38,43,54]. Some of the most commonly used devices used to obtain the required disruptive forces including high-pressure homogenizers, microfluidizers, and ultrasonicators are illustrated in figure 3 below [55].

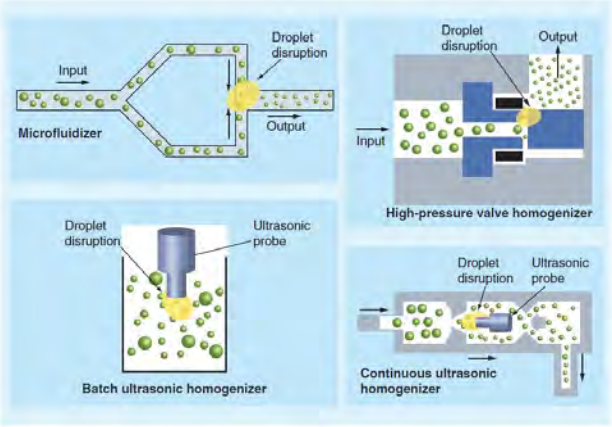

Figure 3. Overview of the most commonly used mechanical devices (homogenizers) applied in high-energy methods for the preparation of NEs [55]

High-energy methods are often used since they are easily scalable enabling industrially application [41]. In addition, they are able to formulate a wide range of formulations since they do not present any limitation on the type of oil that can be used for nanoemulsification and provide the ability to manipulate the size of the final nanodroplets by optimizing the system components as well as the operating conditions of the homogenizer such as the time period and intensity of the applied disruptive energy. However, the use of high-energy approaches is not always feasible due to the instrumental cost and the heat produced due to friction during the procedure making challenging the encapsulation and overall use of thermosensitive compounds [41,43,46]. In the present study, high-pressure homogenization was employed for the development of some systems. During the specific nanoemulsification method, a coarse emulsion produced by the mixture of oil and aqueous phases is pumped through the restrictive valve of a high-pressure homogenizer, and the applied high-shear stress results in the formation of smaller droplets [56,57].

Low-energy emulsification methods

On the other hand, the low-energy emulsification methods are based on the spontaneous formation of nanodroplets within the mixture of the components since the free energy required derives from physicochemical processes as opposed to the high-energy approaches. In order for this procedure to take place, the composition of the system or the environmental conditions have to be changed appropriately. Some of the most widely known low-energy methods include spontaneous emulsification, phase inversion temperature or composition, and emulsion phase inversion [43,58,59]. During the preparation of NEs by these methods the composition of the system, as well as the preparation conditions (temperature, stirring, addition rates), play a crucial role in the formation of nanodroplets of smaller size [46].

These approaches are often preferred over high-energy techniques since no expensive equipment is required, they are simple to implement and are appropriate for the encapsulation of thermosensitive due to the mild preparation conditions. However, their implementation is not always feasible since a higher amount of surfactant-to-oil ratio (SOR ≈ 1) is often recommended and the type of oils and surfactants that can be used are occasionally restrictive including natural emulsifiers such as proteins and polysaccharides [41,43,46]. Specifically, some of the systems developed and will be presented in the following chapters were produced using the method of isothermal spontaneous emulsification. The mechanism of this particular method is depicted in figure 4. For the implementation of this method, the oil and a surfactant of a slightly hydrophilic nature are mixed thoroughly resulting in the oil

phase which is then titrated into the water phase. The addition is performed at controlled rate in order to enable the formulation of oil droplets at the nanoscale. In order to ensure that effective homogenization has been accomplished by the end of the titration additional mixing is required to fully break down any residual bicontinuous system method [43].

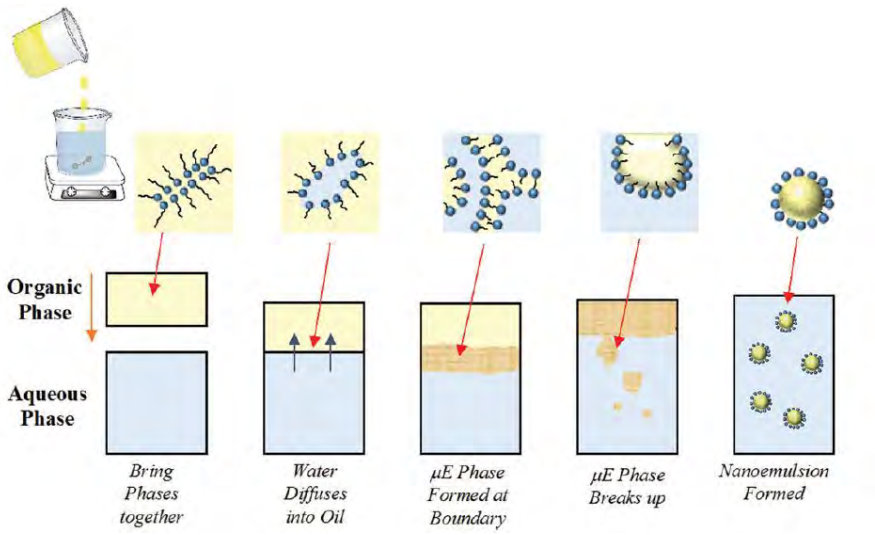

Figure 4. Schematic representation of the potential mechanism of NE formulation by the isothermal spontaneous low-energy emulsification method [43]

Destabilization phenomena

Due to their metastable nature NEs tend to separate over time through various physicochemical mechanisms causing destabilization. This phenomenon occurs due to the gradual increase of droplet size causing a decrease in their interfacial area and reduced free energy. The predominant mechanisms causing a NE to break down including gravitational separation (creaming/sedimentation), flocculation, Ostwald ripening, and coalescence are illustrated in figure 5 below. The time period between the formulation of a NE and its destabilization could be affected by a variety of environmental factors including storage temperature and pH values. However, the appropriate selection of the systems components and the formulation optimization can minimize the occurrence of these phenomena leading to NEs with high stability over time.

The method of gravitational separation arises from the different densities between the dispersed droplets and the continuous phase and could be described either as creaming or sedimentation depending on the movement of the aggregated droplets. The first phenomenon occurs when the dispersed phase has a lower density than the continuous

leading to the floating of the droplets and the formation of a thick layer while when the reverse happens sedimentation takes place [38,46,60].

Flocculation and coalescence are two more destabilization mechanisms and in spite the fact that both have as result the aggregation of nanodroplets are considerably dissimilar. More specifically, during flocculation nanodroplets collide due to attractive forces forming larger aggregates. However, the joint nanodroplets do not fuse and remain stick together as an entity [61,62]. The distinct difference between coalescence, as opposed to flocculation, is that in this case the colliding nanodroplets are merged forming larger ones due to the collapse of their interfacial membrane. The use of surfactants generating strong repulsive forces between the dispersed nanodroplets can be used to minimize this process and prevent both flocculation and coalescence phenomena [4,38].

Finally, Ostwald ripening is one of the primary mechanisms of physicochemical instability in NEs and often acts simultaneously with coalescence accelerating their destabilization [41]. Ostwald ripening manifests due to the diffusion of oil molecules through the aqueous phase resulting in the growth of the larger nanodroplets at the expense of smaller ones leading ultimately to phase separation [63]. Nonetheless, this phenomenon can be avoided with the selection of an appropriate oil phase with very low aqueous solubility hence lipidic mixtures of medium chain triglycerides (MCT) and long chain triglycerides (LCT) are regularly employed to minimize this mechanism [4,41,63,64].

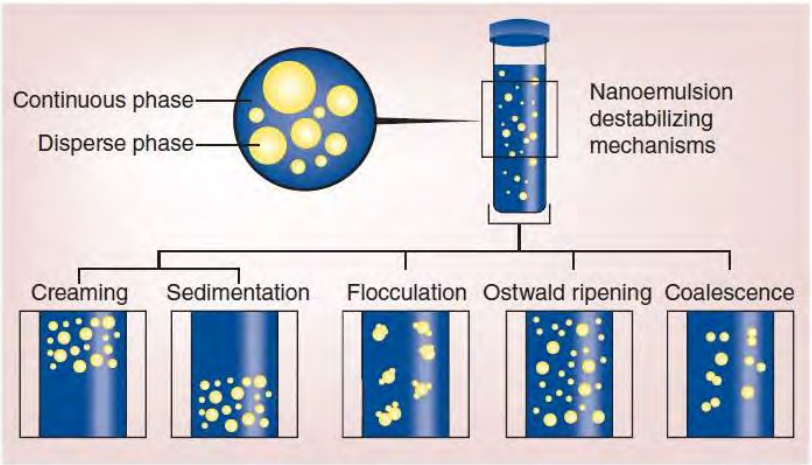

Figure 5. Schematic representation of the five dominant destabilization mechanisms of nanoemulsions. The dispersed and the continuous phases are illustrated in yellow and blue, respectively [38].

1.4. Nanoemulsions components

The main components that comprise NEs are oils, surfactants, co-surfactants, and aqueous phases [4]. The careful selection of components is substantial since they affect the emulsification process and the structure and stability of the developed systems. The most popular excipients used are biocompatible and generally recognized as safe (GRAS) and they play a crucial role in the development of an effective nanocarrier with the desirable properties depending on the intended method of delivery [65]. In these systems are solubilized and encapsulated the bioactives of interest which may also affect the structural characteristics and the stability of the formulated systems.

Since the components of the systems under study are particularly important, below will be presented the materials used for the formulation of the O/W NEs and the NE/HGs which were the object of study of the present thesis as well as the compounds that were selected for encapsulation.

1.4.1. Oils

Nowadays, a plethora of novel bioactive compounds and active pharmaceutical ingredients (APIs) are being developed at a rapid pace. However, the majority of these substances demonstrate poor water solubility [66] which is a significant problem influencing important properties such as the pharmacokinetic and pharmacodynamic profiles and therefore their efficacy and fate in the human organism. For that reason, oils are used for the formulation of O/W NEs to obtain the maximum aqueous solubility of the bioactive compound of interest.

The choice of the appropriate type of oil is crucial since its lipophilicity is directly proportional to the solubility of drugs [67,68]. Other factors apart from the drug solubility that should be considered for the selection of a proper oil phase are the bioavailability, the use for which the final nanocarrier is intended, and the degree of digestion [25]. The digestion rate influences the oral bioavailability of the bioactive compound since faster release is obtained when the oil phase can be easily digested [69]. Moreover, the type and concentration of the oil used for the development of the NEs also affect the size of the nanodroplets [70–72] which is associated with the ability of the nanocarrier to protect the encapsulated compound and the degree of its digestion. Furthermore, specific types of oils could demonstrate emulsification and permeation-enhancing properties as well [73,74]. Thus, the oil phase must be selected prudently in order to have the suitable lipophilicity to solubilize the bioactive

compound but at the same time must be able to be incorporated into the NE in a sufficiently large quantity without affecting its stability.

Considering that the choice of the appropriate oil is influenced by miscellaneous factors, sometimes is selected a mixture of oils in order to obtain an oily phase with the desired requirements [75]. The oils that are frequently used for the formulation of NEs are castor oil, olive oil, corn oil, and omega 3- and 6- containing polyunsaturated fatty acids (PUFA) such as pine seed oil, fish oil, flaxseed oil, sunflower oil, hemp, and wheat germ oil, etc. [68–70,76,77]. Hence, for the present study, various oils and their combinations were tested in order to obtain stable NEs with the appropriate properties.

Extra Virgin Olive Oil (EVOO)

Extra virgin olive oil (EVOO) is one of the most popular and widely used ingredients in the Mediterranean diet and attracts great interest in the research community due to its unique composition and properties. Nowadays there is a vast number of studies providing evidence concerning the multiple health benefits that EVOO presents. The most frequently observed effects are reduced risk of cardiovascular and neurodegenerative disease as well as action against metabolic conditions (such as type 2 diabetes mellitus or metabolic syndrome) and some types of cancer [78–80]. Specifically, there are indications that EVOO could provide protection against age-related cognitive decline and Alzheimer's disease [79]. Furthermore, there are strong pieces of evidence concerning the anti-inflammatory [81–83], antimicrobial [84] and anti-oxidant properties that EVOO demonstrates. All the aforementioned actions are strongly related not only to the fatty acids of the specific oil but also to the variety of its phenolic compounds which are powerful antioxidants that are proven to be effective against the oxidative stress associated with several diseases and cannot be found in other oils [85,86].

The composition of EVOO could vary remarkably since it is affected by multiple factors such as olive fruit ripeness, technological process, variety, and environmental factors, the extraction technology that is applied in order to obtain oil from the fruits [87–90]. However, it mainly consists of triacylglycerols (98–99%) with the major fatty acid being the monounsaturated oleic acid (68–82% of the total fatty acids in olive oil) which is a substance that has been proven to present health benefits [91–94]. Moreover, there are numerous lipophilic and amphiphilic microconstituents in EVOO among them, phytosterols, squalene, tocopherols, phenolic compounds, terpenic acid derivatives, etc. [95–97]. Oleuropein, tyrosol, and hydroxytyrosol, as well as other micro-constituents, are depicted in figure 6. There is an abundance of studies concerning their actions among them protection against coronary artery

disease [98,99] or cancer [100,101]. Last but not least, of great importance are their antimicrobial, antiviral, and antioxidant effects [102–105].

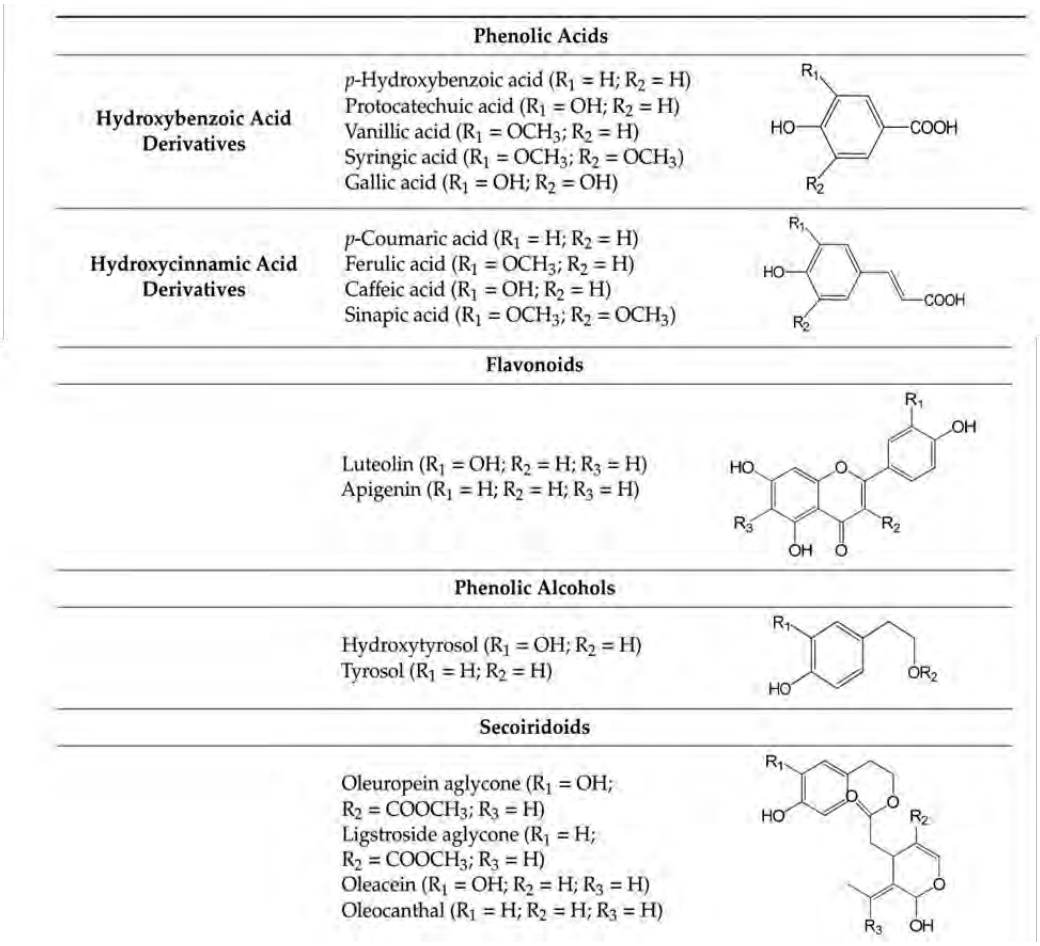

Figure 6. The most abundant compounds found in Extra Virgin Olive Oil [106].

Isopropyl myristate (IPM)

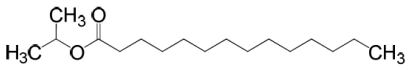

Figure 7. Isopropyl myristate (IPM) structure

Typically, alkyl esters are concerned to be safe and non-irritating [107] thus they are widely used for both cosmetic and pharmaceutical applications. Specifically, isopropyl myristate (IPM) is the ester of isopropanol and myristic acid and is an emollient with medium polarity. It is the most commonly used alkyl ester due to its intriguing properties [108,109]. Since 2012 IPM has been reported in 1149 formulations in concentrations up to 77.3% [107] as it provides moisturizing effects to the developed formulation [110] while acting as a

penetration enhancer. As penetration enhancer can be characterized a compound that has the ability to alter the skin barrier function in order to enable a desired bioactive to obtain a faster rate of permeation [111]. It is obvious that in topical applications the use of an excipient with these properties is especially beneficial since it improves the action of the bioactive of interest by achieving therapeutic plasma levels of many drugs [112].

The interesting thing concerning IPM is that despite its penetration enhancing properties it is largely retained in the stratum corneum [112] preventing systemic side-effects. Various studies have focused on the examination of IPM's mode of action as a penetration promoter. It is suggested that IPM could affect the diffusivity of bioactives by incorporating them into the stratum corneum lipid matrix [113] and facilitating the partition of drugs and from vehicles into the stratum corneum [114]. Hence, it can be concluded that IPM could be a useful excipient for the development of topical applications for the treatment of skin diseases or other conditions that require transdermal delivery by overcoming the skin barrier by increasing the permeation of the necessary bioactives through the skin temporarily [115].

1.4.2. Surfactants & Co-surfactants

Surfactants or as they can be alternatively called emulsifiers and co-surfactants are of paramount importance for the formulation of NEs since they promote emulsification of the two immiscible phases, the oily and the aqueous, forming the nanodroplets. The surface-active compounds comprising of a polar hydrophilic head and a non-polar lipophilic tail are referred to as surfactants [116,117]. Their structure is depicted in figure 8. Surfactants make possible the formulation of NEs regardless of the emulsification method by absorbing to droplet surfaces, enabling droplet disruption, and protecting them against aggregation [118,119].

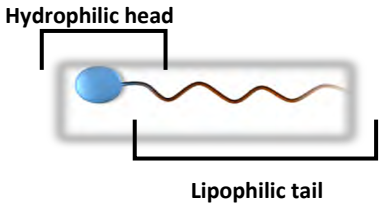

Figure 8. General structure of a surfactant molecule.

The ideal surfactant should have certain properties in order to be suitable for use in formulations intended for industries such as food, cosmetic, or pharmaceutical. Specifically, it is important to be stable, biocompatible, and non-toxic with satisfactory taste and odor.

Equally significant are the effects that an emulsifier could attribute to the developed system such as good emulsification properties which can influence the oil concentration in the system, and effective solubilization of the bioactive compound in order to achieve adequate bioactive loading in the NE [65,75].

Surfactants can be categorized according to their a) surface charge or b) hydrophilic-lipophilic balance (HLB) as depicted in figure 9. Concerning the surface charge of the hydrophilic head group, surfactants can be characterized as ionic, zwitterionic, and non-ionic. Ionic surfactants could be either cationic or anionic which means they could bear positive or negative charge respectively. This type is not used very frequently in the preparation of NEs since there are indications that they could induce toxicity, especially in high concentrations [59,120,121]. Surfactants containing both cationic and anionic groups are referred to as zwitterionic or amphoteric and their behavior depends on the pH of their environment. Hence, in alkaline media where they gain a negative charge, they adopt an anionic behavior and vice versa in an acidic ph. Zwitterionic surfactants are often preferred due to their good water solubility and improved stability. Moreover, they can be combined effectively with diverse surfactants and be functional within different disperse media [122]. Phospholipids belong to this category and they are used frequently due to their GRAS status [55]. Finally, non-ionic surfactants as the name suggest comprise of uncharged hydrophilic groups which can be highly hydrated thus being more soluble in the aqueous phase of the NEs. They are the most preferred category for the development of NEs due to their ability to create nanodroplets of smaller size by both high-energy and low-energy approaches and they present low toxicity [55,122,123].

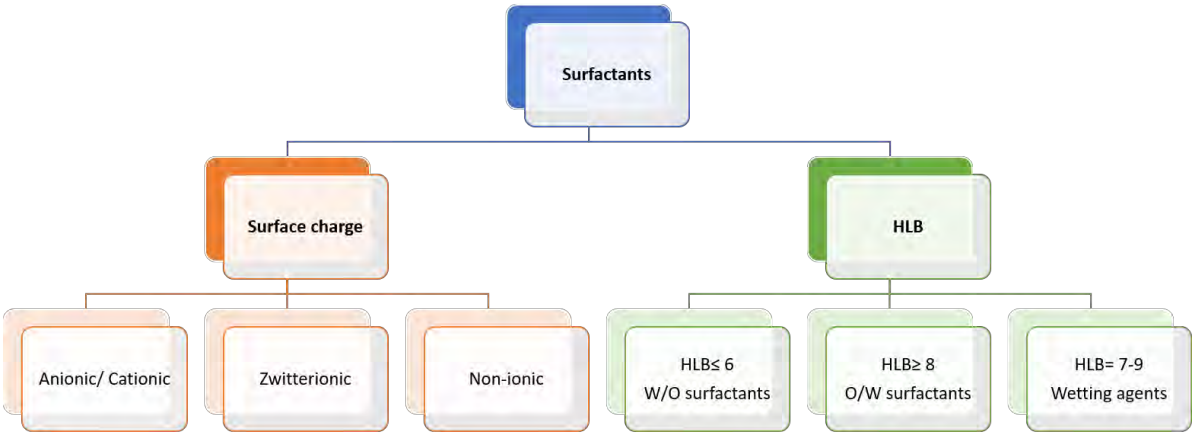

Figure 9. Categorization of surfactants depending on their surface charge and HLB values.

The classification according to HLB values, was mentioned for the first time by Griffin in 1949 and was described as a scale depending on the ratio of the weight percentage of hydrophilic to lipophilic groups in non-ionic surfactant molecules [124]. It is used for the evaluation of the emulsification capability of a surfactant and it could be between 1 to 20. Particularly, non-ionic surfactants with HLB<10 are considered as hydrophobic and tend to formulate W/O NEs (i.e., glycerol esters, propylene glycol fatty acid esters, polyglycerol esters, sorbitan monoesters) while those with HLB>10 such as phospholipids or polysorbate 80 have hydrophilic nature and are useful for the development of O/W NEs [121,122,125]. In figure 10 are depicted some of the surfactants used for the formulation of the O/W NEs that will be presented consequently in this thesis classified according to their HLB values.

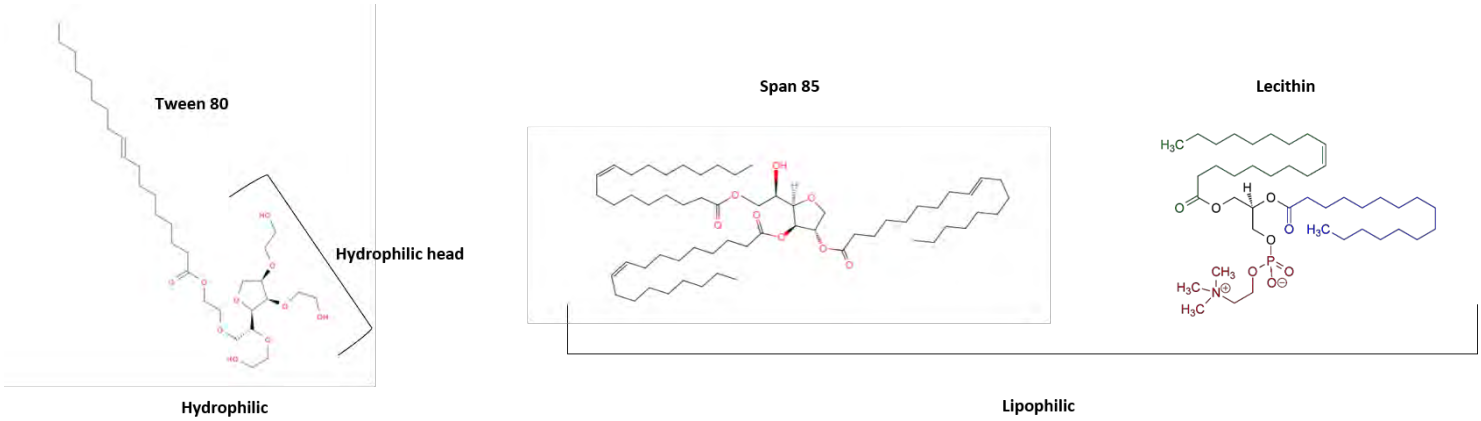

Figure 10. Hydrophilic and lipophilic surfactants used for the formulation of the developed oil-in-water nanoemulsions.

Selecting the appropriate surfactant or mixture of surfactants is critical for the design of stable and effective NEs [55]. Surfactants have the ability to stabilize NEs by preventing the coalescence of nanodroplets and thus the phase separation [65,126]**.** Hence, the selection of a suitable surfactant could provide significant stability against various environmental conditions such as pH, ionic strength, heating, cooling, or long-term storage [55]. Furthermore, throughout the years numerous studies have been performed in order to evaluate the effect of surfactants on various properties of the formulated lipid vesicles. So far, there are indications that the type and concentration of the surfactants used may affect various characteristics of the system such as the size and polydispersity index (PdI) [122,127]. Additionally, it suggested that the entrapment efficiency, permeation, pharmacokinetics and pharmacodynamics of the bioactive compound [122,128] are also dependent on the surfactants. Nonetheless, as a general rule, a combination of hydrophilic and lipophilic surfactants may be necessary in order to achieve the suitable HLB value leading to the optimal

size and stability [55,129–132]. The combination of two or more surfactants provides the possibility to obtain a very wide range of HLB values in order to obtain the optimal value to achieve the formation of nanodroplets with small size with improve stability against aggregation with the desired solubilization effect [55,117,133].

However, sometimes the utilization of surfactants is not effective enough for the formulation of a NE with the desired characteristics. For that reason, co-surfactants are used complementarily for the optimization of the system. As co-surfactants are characterized small, surface-active amphiphilic molecules that usually comprise of a hydrocarbon chain and a hydroxyl group but they are not able to formulate and stabilize NEs on their own due to the small size of their polar head group [55]. Generally, as co-surfactants are preferred molecules of intermediate chain length since they can facilitate the spontaneous formation of NEs by reducing the oil/water interface [134,135]. Some of the most commonly used co-surfactants are diethylene glycol monoethyl ether (commercial name treanscutol), butan-1-ol, chiral alcohols, sorbitol, and polyethylene glycol [136]. It is suggested that co-surfactants facilitate the formulation of NEs through various physicochemical mechanisms such as 1) penetration into the surfactant monolayer increasing the fluidity [129], 2) reduction of the interfacial tension leading to improved stabilization the NE [126]; 3) reduction of the electrical repulsion that could present the head groups of ionic surfactants, and 4) boost the solubilization of oil into the system [65,137–139] .

For the formulation of the NEs that will be presented in this thesis were used Tween 80 and Labrasol as non-ionic hydrophilic surfactants, Span 80 and Maisine CC as non-ionic lipophilic surfactants, phosphatidylcholine as a naturally derived zwitterionic surfactant and last but not least Transcutol HP was used as a co-surfactant to improve the oil solubilization and act as a penetration enhancer. Below are presented some of the main characteristics and properties of the excipients used for the development of the oil-in-water NEs under study.

Polysorbate 80 (Tween 80)

One of the most widely used surfactants for the formulation of diverse products in the pharmaceutical, cosmetic, and food industries is polysorbate 80, mostly known by the commercial name tween 80 (T80). It is a synthetic, non-ionic, viscous yellow liquid that is comprised of the lipophilic group ethylene oxide and a long hydrophilic hydrocarbon chain domain [140]. Due to its hydrophilic nature (HLB 15) it is mostly used for the dispersion of oil into a water phase in order to develop oil-in-water nanodispersions. Over the years, numerous studies have highlighted T80 as a biodegradable, non-toxic, non-mutagenic and, non-

carcinogenic excipient presenting insignificant rates of skin carcinogenesis, with very little potential for skin irritation in humans [141]. In addition, T80 demonstrates various actions since it has been reported to be used not only as an emulsifier but also as a solubilizer and penetration enhancer [133,142] of the encapsulated bioactive compounds. In fact, polysorbates are often reported to interact with biological membranes affecting their structure and function hence the penetration enhancement properties of T80 have been reported in multiple studies increasing the delivery and efficacy of the encapsulated bioactive compound [140,143–145]. For these reasons, T80 has been applied in miscellaneous formulations for the delivery of various lipophilic bioactive compounds without exhibiting any significant adverse effects.

Caprylocaproyl Polyoxyl-8 glycerides (Labrasol® ALF)

An excipient that is gaining constantly ground and is used increasingly for the preparation of nanodispersions for various delivery routes is Caprylocaproyl Polyoxyl-8 glycerides widely known by the trade name Labrasol® ALF (LS). It is a non-ionic, hydrophilic excipient (HLB 12) consisting of a mixture of mono- and diesters of poly(ethylene glycol) (PEG) and fatty acids with the predominant ones being the medium chain fatty acids caprylic- (C8) and capric acid (C10) [146,147]. Due to its safety, low toxicity, and high tolerance labrasol is listed in the inactive ingredients list of the Food and Drug Administration (FDA) [148]. In addition, its excellent bioavailability and the fact that it is easily biodegradable by enzymes present in the human organism [149–151] reinforce its use for topical, transdermal, and oral pharmaceutical preparations [152].

Specifically, LS either alone or in combination with other excipients has been mentioned in various studies to improve the bioavailability of diverse bioactive compounds of interest [150,153–157]. There are multiple studies suggesting that this property is derived from two ways of action. First, LS can serve as a solubilizer providing the possibility of dissolving a larger amount of the bioactive substance and hence, improving its transdermal delivery [146]. Secondly, it has the potential to act as a penetration enhancer for the therapeutic agents of interest in a dose-dependent manner [149,158] since it is mainly comprised of medium-length alkyl chains (C8-C10) which are observed to penetrate more easily the lipid bilayer of the membranes [150]. The penetration-enhancing properties of labrasol have been investigated in various studies for oral delivery as well as for the transdermal route of administration. Its action as a penetration enhancer lies in its ability to change the structure and permeability of the intestinal [150,159] or transdermal [152,160]

epithelia enabling the penetration and thus the bioavailability of the bioactive compounds. However, an important advantage is that these changes are reversible and do not cause any damage to the site of action. Thus, due to the substantial benefits that LS provides, it is widely used for various drug delivery formulations.

Glyceryl monolinoleate (Maisine® CC)

Another liquid excipient with appealing properties that was used for the formulation of the systems that were developed in the present study was Glyceryl monolinoleate or Maisine® CC (MS). It is a lipophilic excipient (HLB 1) derived from corn oil and is actually a mixture of mono-, di- and triglycerides of mainly linoleic (C18:2) and oleic (C18:1) acids with the diglyceride fraction being the most abundant (40-55%). Maisine® is generally recognized as safe (GRAS status) and it has already been utilized for the formulation of approved pharmaceutical preparations acting as a solubilizer and bioavailability enhancer for highly lipophilic bioactive compounds.

In general, there are indications that certain features of glycerides such as type, chain length, and degree of saturation could affect the delivery of lipophilic bioactives [161]. Specifically, the chain length has been identified as a significant factor that could influence the successful formulation of nanodispersions. Long chain monoglycerides have been observed to be more effective due to their co-surfactant and solubility properties [162,163] while they can also enhance the loading capacity and bioavailability of the encapsulated bioactives [162,163]. In addition, the chain length of the glycerides used for the formulation of nanodispersions plays a crucial role in the bioavailability of the encapsulated bioactive compound suggesting that long chain glycerides including MS could provide enhanced oral bioavailability [164] since they are easily digestible and due to the induction of lymphatic absorption instead of being eliminated through first-pass metabolism [165–169]. Furthermore, MS provides effective solubilization of highly lipophilic bioactive substances and has the ability to maintain them in a solubilized state in vivo during digestion and absorption resulting in enhanced bioavailability [170]. Another intriguing property of unsaturated long chain monoglycerides with special reference to Glyceryl monolinoleate, is their ability to open tight junctions [171] indicating their possible use for permeation enhancement through the skin providing effective transdermal administration as well. Hence, unsaturated long chain lipids including Maisine® CC could be beneficial excipients for the development of formulations in order to be used for various routes of administration of lipophilic substances [172,173].

Lecithin (Phosphdylcholine)

Occasionally, in order to avoid the potential toxicity that synthetic surfactants could present, research groups and industry turn towards the utilization of natural substances that have the ability to act as emulsifiers. A well-known compound widely used in various formulations is lecithin which can be easily obtained by chemical or mechanical extraction from a variety of natural sources such as egg yolk, soybeans, cottonseeds, and sunflower oil. In general, lecithin is a mixture of different phospholipids like phosphatidylcholine, phosphatidylinositol, phosphatidylethanolamine, phosphatidylserine, and phosphatidic acid in different concentrations depending on the source. Phospholipids are amphiphilic molecules comprised of two fatty acid chains containing 10-24 carbon atoms which constitute the lipophilic part of the molecule and a polar end which is mainly phosphoric acid bound to a water-soluble molecule. Due to their amphiphilic nature, they demonstrate excellent emulsifying properties so they are often provided with their highly purified form with the most commonly used being phosphatidylcholine (PC) which is utilized for the formulation of various nanodispersions for oral or transdermal delivery.

Over the years, numerous studies have highlighted the advantages of colloidal dispersions containing PC compared to those that do not, with the first and most important being their compatibility with the skin and the internal membranes (i.e., intestine) [174]. Since PC is a fundamental component of all the biological membranes it is biodegradable and non-toxic thus, it is frequently selected as a surfactant. Furthermore, there are various studies indicating that PC has the ability to act as a transmembrane transport enhancer as well, improving the passage of the encapsulated bioactive compounds through the skin and/or the digestive tract depending on the route of administration providing increased bioavailability [159,175–178]. It is also suggested that PC when combined with non-ionic surfactants could demonstrate synergistic action improving transdermal permeation of the therapeutic agent [175]. There are indications that PC exerts this action through various mechanisms. First of all, it has the ability to interact with the encapsulated bioactive compound altering its hydrophilic-lipophilic balance and improving absorption kinetics [179]. In addition, when embedded at the interface of the nanocarriers, PC could act as an adhesion agent to the site of action and modify the epidermal lipid barrier properties and fluidity increasing the permeability and absorption of the active molecule through the skin [180]. Apart from the aforementioned benefits, the nanodispersions formulated containing PC on their interface are frequently utilized for the delivery of various bioactive compounds and even larger therapeutic molecules such as peptides and proteins. The formulated systems are passive, non-invasive, and non-

toxic so they could be immediately commercialized [181]. Hence, PC is a highly attractive molecule among research groups as well as the food, pharmaceutical, and cosmetic industries.

Diethylene glycol monoethyl ether (Transcutol® HP)

As mentioned before, the solubility of an encapsulated bioactive compound into the developed nanocarrier and its effective penetration through the epithelia are crucial factors affecting its action. To that end, an excipient gaining increasing attention due to the appealing properties it presents is the highly purified diethylene glycol monoethyl ether (DEGEE) with the trade name Transcutol® HP (TRSC). It is a penetration enhancer and powerful but safe solvent with the ability to solubilize both hydrophilic and lipophilic bioactive compounds even those that are insoluble in common solvents. Thus, it is extremely useful as a pharmaceutical excipient for the formulation of diverse drug products for various routes of delivery [182,183]. It is a transparent liquid, non-volatile, and practically odorless that has a very low viscosity. Being compatible with a wide variety of other pharmaceutical excipients can be solubilized in common solvents like glycerin, EtOH, PG, and water and can be mixed with polar lipids and polyethylene glycol-based surfactants [182]. One of the most valuable characteristics of TRSC is its functionality even at low concentrations resulting in favorable safety and tolerability profiles [184].

There are numerous studies demonstrating that TRSC has the ability to act as a penetration enhancer in two ways. First, it is capable of altering the structure of the stratum corneum in a reversible manner in order to facilitate the diffusion of the bioactive compound resulting in improved local or even systemic absorption [183,185]. In addition, TRSC provides hydration to the skin thus facilitating the penetration of the bioactive compound. This hydration phenomenon could result either from skin protection and occlusion [185,186] or due to the interaction of TRSC with the lipid filled intercellular spaces of the stratum corneum [182,187]. In order for an excipient to be widely utilized, it is particularly important to evaluate its potential toxicity. Particularly, transcutol ® HP is FDA approved and listed in the Inactive Ingredients Database nevertheless, numerous toxicological studies have been conducted for the evaluation of its toxicity for various routes of administration [184] like dermal [188], and oral [184]. It is suggested that TRSC especially compared to other commonly used solvents exhibits the lowest skin damage ratio [189] while presenting local tissue tolerance in various sites such as skin, eye, and, epithelia [190]. Furthermore, it is non-mutagenic, non-carcinogenic, biocompatible, and rapidly metabolized leading to excretion within 24 hours [184]. Hence, it has already been extensively reported in the literature either alone or in

combination with other surfactants and has been utilized for the development of a broad spectrum of formulations such as creams, gels, and emulsions used for topical [183,186,191], transdermal [192–196], intranasal [197,198], ocular, oral and, intravenous [184,199] administration.

1.5. Bioactive compounds

In recent years, there is a growing interest towards the use of natural bioactive compounds for therapeutic or preventing use against various conditions. Since there is increasing evidence that various natural compounds demonstrate salutary effects on the human organism, in the present thesis were selected for encapsulation three lipophilic bioactive compounds namely vitamin D_3 (VD), curcumin (CU), and cannabidiol (CBD) as well as C-phycocyanin (C-PC) which is hydrophilic. The interesting thing about the aforementioned bioactive compounds is that they demonstrate multiple biological actions and present health benefits when administered either in the systemic circulation or topically. Their biological actions will be summarized below.

1.5.1. Vitamin D (VD)

One of the most essential substances for maintaining a healthy body is vitamin D or the "sunshine vitamin" as it is also referred to, since it is synthesized in the human body through a photoreaction activated by the sun radiation [200]. It is a lipophilic, steroid hormone which is easily solubilized in fats and organic solvents but is insoluble in water [201]. The two predominant dietary forms of Vitamin D are ergocalciferol (vitamin D_2) which is mainly synthesized by plants and, cholecalciferol (vitamin D_3, VD) which can be obtained by animal sources such as salmon, herring, sardines, mackerel, tuna, egg yolks, and cod liver oil [202–205].

The latter, whose main source is the synthesis in the human organism, is the most stable towards degradation and demonstrates biological activity interacting with diverse targets. Hence, this bioactive compound is vital for the proper functioning of the organism but also for the prevention of some severe chronic and neurodegenerative disorders [71,206].

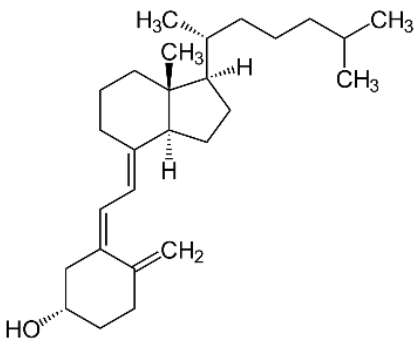

Figure 11. Molecular structure of cholecalciferol (Vitamin D_3).

The significant role of VD for the preservation of a healthy musculoskeletal system is known for many years. However, there are indications of its implication in diverse targets throughout the entire human body such as immune, nervous, and cardiovascular systems [207]. Nowadays, numerous studies support the immunomodulatory, anti-inflammatory and antimicrobial properties of VD making it useful for the treatment of skin diseases such as psoriasis, atopic dermatitis, vitiligo and others [200,208–210]. In addition, driven by the effect of VD on the immune system, some research teams have even been able to link COVID-19 to VD deficiency [211–214]. Furthermore, the presence of vitamin D receptors in diverse sites of the brain indicates its importance for the prevention and treatment of several neurological and psychiatric disorders including multiple sclerosis, stroke, Alzheimer's and Parkinson's diseases, schizophrenia and, autism diseases [206,215,216].

Nevertheless, due to the modern way of life and the prolonged stay indoors during the day, VD insufficiency or even deficiency have become evident all over the world causing significant health problems. Thus, the administration of supplements is often essential in order to obtain the proper daily intake. A substantial limitation to this approach is the unstable nature of VD and its high lipophilic nature, leading to low bioavailability and efficacy. Thus, the formulation of suitable nanocarriers is considered as an efficient therapeutic strategy to obtain a satisfactory administration of VD not only orally but also through transdermal and intranasal routes of delivery [217–220].

1.5.2. Curcumin (CU)

One of the most widely-known natural-source bioactive compounds is curcumin (figure 12) which is the most abundant substance of the Curcuma longa L. rhizome. Curcumin is a lipophilic polyphenol which has the ability to interact with multiple targets in the human body affecting diverse signaling pathways and therefore demonstrating numerous health

benefits. This bioactive compound is universally accepted nowadays since it is naturally derived and demonstrates no adverse effects even in high doses [221].

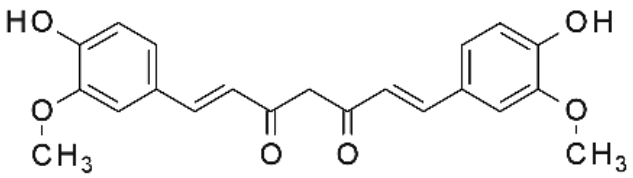

Figure 12. Molecular structure of curcumin.

Curcumin is suggested to be beneficial for the skin due to its anti-inflammatory [222,223], antibacterial [221,224] and wound healing properties [222] and has been used for many years to treat skin conditions [225,226].

In addition, there are indications that curcumin alone or in combination with other therapeutic molecules [25] could be beneficial for the treatment of chronic diseases including heart and liver diseases, arthritis, gastrointestinal problems or even cancer [222,223,227]. Furthermore, due to its neuroprotective effects, curcumin could be beneficial for various neurodegenerative disorders such as Alzheimer's disease [228,229] or psychiatric conditions like depression and anxiety [221].

Nonetheless, the use of curcumin as a therapeutic molecule is limited due to its highly lipophilic nature leading to poor intestinal absorption and bioavailability. Moreover, it is a sensitive compound which is rapidly metabolized losing its activity [230,231]. To address these issues, the encapsulation of curcumin in suitable nanocarriers is often necessary.

1.5.3. Cannabidiol (CBD)

Cannabis is a plant with a long history as there are reports of its medicinal use since antiquity in various parts of the world [232]. Despite the fact that cannabis has been known for more than 5000 years for its health benefits, it is not very easily used as a medicinal product due to the complex legislation surrounding it. Nonetheless, in the recent years the interest towards the use of cannabis for pharmaceutical purposes is revived as new techniques have been developed that make the administration of bioactive phytocannabinoids more effective.

Figure 13. Cannabis plant picture.

There are various species of cannabis each with different major compounds which are used throughout the years for various applications from the production of textiles to recreative drugs and therapeutic purposes. Particularly, *Cannabis sativa Linnaeus (Cannabis sativa L.)* has attracted great interest for the use in treatment or prevention of various diseases due to the pharmacological action of its extract. This species contains numerous bioactive compounds among them terpenoids, flavonoids, alkaloids and, of course phytocannabinoids with some examples of them illustrated in figure 14 [233,234]. Until now, over 100 phytocannabinoids have been identified in these plants with the most potent being either cannabidiol (CBD) which demonstrates a plethora of health benefits or trans-Δ-9-tetrahydrocannabinol (D9-THC) which displays psychoactive action, depending on the species of cannabis [235].

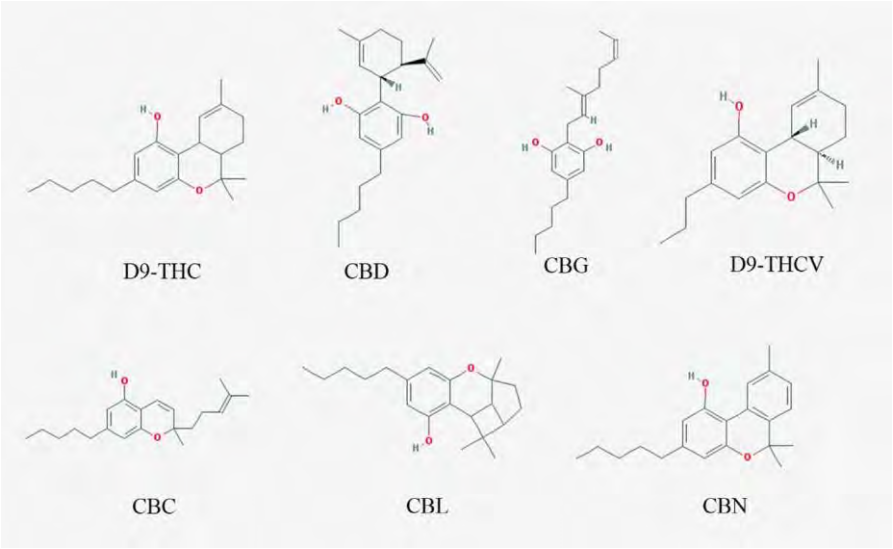

Figure 14. Examples of phytocannabinoids of Cannabis sativa. Δ-9-tetrahydrocannabinol (D9-THC), cannabidiol (CBD), cannabigerol (CBG), Δ-9-tetrahydrocannabivarin (D9-THCV), cannabichromene (CBC), cannabicyclol (CBL), cannabinol (CBN) [232].

The major phytocannabinoid of Cannabis sativa L. is CBD and attracts great attention due to the plethora of health benefits it demonstrates by acting in various receptors such as adenosine receptors, glycine receptors, opioid receptors, serotonin receptors etc. [236]. It also interacts with multiple receptors of the endocannabinoid system which is present within the brain and immune system [237] affecting diverse bodily functions and regulating numerous pathophysiological phenomena [238]. Due to its interaction with diverse pharmacological targets, it is now evident that cannabidiol exerts important pharmacological actions. Specifically, over the years a number of studies have been published supporting the positive effect of CBD against different neurological and psychiatric disorders. There are indications of the neuroprotective, anti-inflammatory, antipsychotic and anxiolytic properties of this specific phytocannabinoids [235,239,240]. Moreover, CBD could be used as an effective treatment against severe neurodegenerative disorders such as epilepsy, Alzheimer's and Parkinson's disease, and schizophrenia [241–245] for the relief of the symptoms.

Despite the aforementioned beneficial properties of CBD in the human organism, nowadays its use for therapeutic purposes remains challenging as its most common form is in oil which presents important limitations. Some crucial drawback concerning the CBD oil are the highly variable composition of the CBD extract, the complicated determination of the suitable dosage, the limited bioavailability, the possibility of toxic solvent residues used for the extraction etc. [246,247]. Hence, the use of synthetic CBD and its encapsulation in appropriate nanocarriers could be proven beneficial for the effective and safe use of this bioactive compound.

1.5.4. C-Phycocyanin (C-PC)

Currently, algae arise great interest as natural dietary supplements. One of the most popular species is *Arthrospira (Spirulina) platensisis* or *A. maxima*, a Gram-negative, non-toxic species of photosynthetic cyanobacteria that is considered to demonstrate significant health benefits being a source of high content of protein, lipid, vitamins, minerals, and antioxidants [248].

One of the active pigments of *A. maxima*, which is present in large concentrations, is C-Phycocyanin (C-PC), a light harvesting bioactive compound [249]. It is a hydrophilic, blue-colored biliprotein which comprises of a protein with the chromophore phycocyanobilin attached to it. The protein consists of two subunits α and β with molecular weights approximately 18 and 20 kDa, respectively. On these subunits are attached the chromophore molecules and specifically as figure 15 demonstrates subunit α is connected with one

phycocyanobilin while β with two [250]. Usually, C-PC is organized in oligomers with the most common being the hexamer complex.

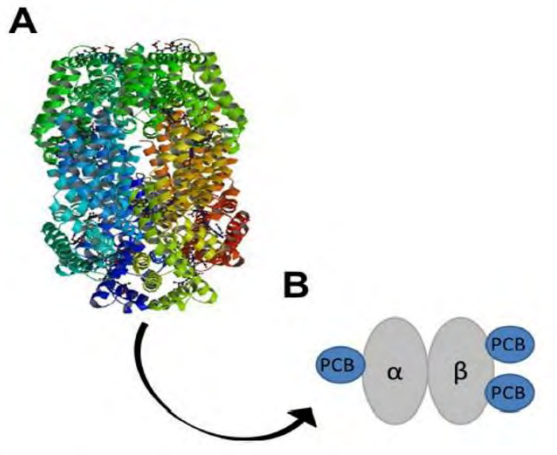

Figure 15. C-Phycocyanin (C-PC) structure. A) Demonstrates the crystal of a C-PC hexamer, B) Schematic representation of C-PC assembly.

Due to its intense color, C-PC is often used as a natural additive for food or cosmetic applications [251,252] however there are currently various studies indicating its significant therapeutic value. Since C-PC is a natural bioactive compound with no toxicity, it could be a promising alternative of conventional, synthetic drugs that often present side effects or insufficient efficacy option [253]. Particularly, in the course of time numerous studies have been performed attributing to C-PC a wide range of biological activities such as stimulation of the immune system, neuroprotection, protection against viruses.

The antioxidant, antimicrobial, anti-inflammatory and therapeutic properties of this substance have been widely studied and can be used through various routes of administration [253–255]. Despite the plethora of health benefits that C-PC demonstrates, there are indications that when administered orally it could be easily degraded in the gastrointestinal tract lowering its pharmacological effect. Hence, encapsulation of C-PC in suitable nanocarriers depending on the intended application could be a promising solution to protect it and increase its efficacy in the human organism.

1.6. Hydrogels

As hydrogels can be described soft materials comprised of two phases, a phase of hydrophilic polymers composing a three-dimensional network and, a liquid phase retained in intermolecular space that could be either water or biological fluids [256–260].

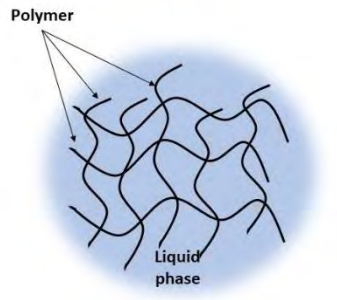

Figure 16. Schematic representation of a polymer network.

Polymers have the ability to absorb different amounts of liquids depending on their hydrophilicity which is determined by the hydrophilic functional groups attached to their polymeric backbone [261].

There are various suggestions for the classification of hydrogels depending on the source of the polymer, the method of cross-linking, the electrical charge, or the responsiveness to environmental changes [262]. However, most frequently hydrogels are classified according to the source of polymers (synthetic or natural) and the cross-linking method (physical or chemical) since these two parameters can have a considerable impact on the biocompatibility of the formulated systems. Concerning the formulation method, in applications requiring biocompatibility, physical crosslinking is preferred predominantly, since it avoids the use of possibly toxic organic solvents [263]. Furthermore, natural polymers are generally selected since they are sustainable, biocompatible, biodegradable, non-toxic, and have low cost [264]. Some of the polysaccharides most frequently utilized for the development of hydrogels are starch, alginate, carrageenan, xanthan gum, and chitosan [262].

Specifically, chitosan is one of the most popular biopolymers since it demonstrates numerous favorable properties. It is a hydrophilic biopolymer derived by alkaline hydrolysis of chitin which is one of the most abundant polymers in nature extracted from the exoskeleton of crustaceans but also fungi [258,265]. As illustrated in figure 17, the arrangement of a chitosan monomer is linear and is composed of glucosamine and N-acetyl-glucosamine linked by (1-4) glycosidic bonds [262,266].

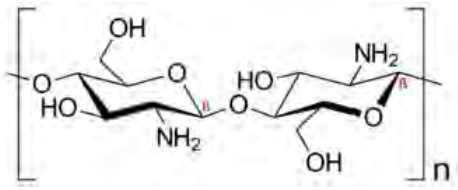

Figure 17. Structural arrangement of a chitosan monomer comprised of glucosamine and N-acetyl-glucosamine linked by (1-4) glycosidic bonds.

The chitosan chain is rich in amino (-NH_2) and hydroxyl (-OH) groups which can act as cross-linkable functional groups. It has also the ability to be solubilized in acetic medium due to the presence of free amino groups from D-glucosamine units which can interact between the polymer chains creating hydrogen bonds formulating hydrogels [267–269].

Nowadays, there is a great interest towards the use of chitosan for the development of functional hydrogels since it possesses intriguing characteristics. Chitosan can adopt diverse forms and is pH-responsive being an ideal candidate for the development of "smart" materials [264,270]. In addition, it is a non-toxic ingredient, biocompatible, and easily biodegradable by enzymes of the human organism resulting in non-toxic by-products. Another important aspect is the biological functions that chitosan demonstrates including antimicrobial, immunological, and wound-healing properties [265,271]. Furthermore, of paramount importance are the mucoadhesive properties of chitosan arising from the strong electrostatic actions of its positively charged amino groups with the negative charged mucosal surfaces and enabling the prolonged contact with the site of action thus making the delivery of the bioactive compound more effective [272].

Recently, the interest in the utilization of hydrogels for diverse biomedical applications has increased immensely since hydrogels can adopt various forms including films, gels, membranes, and fibers [273]. Furthermore, their unique physicochemical, mechanical, and biological features [264] renders them ideal candidates for a number of applications including contact lenses, tissue engineering, cell growth, regenerative medicine, and wound-healing [262,264]. In addition, controlled release of bioactives administered through oral, topical or transdermal, pulmonary, and intranasal delivery routes is widely reported in the literature [71,265,274]. Nonetheless, when the size of the entrapped bioactive compound is smaller than the pores of the hydrogels, can occur burst release and the controlled delivery becomes challenging [261]. Moreover, since the majority of therapeutic agents are lipid soluble, hydrogels lack the ability to entrap them due to their hydrophilic nature [275,276].

Hence, in order to tackle the aforementioned limitations, novel strategies are examined in order to improve the efficacy of hydrogels including their combination with NEs and liposomes [71,277] as will be described in more detail in the next chapter.

1.7. Emulgels

For decades now, natural bioactive compounds have been in the spotlight and research groups all over the world are seeking a suitable carrier in order to protect them against environmental conditions and improve their performance for a vast number of applications. NEs and hydrogels have been at the center of attention for many years however, they still present some limitations. Thus, research groups are constantly on the lookout for new and more effective systems to act as vehicles for the therapeutic agents of interest. To this end, currently, the focus has turned towards the development of novel nanocarriers such as emulsion gels (EGs), in order to combine the benefits of both NEs and hydrogels.

Emulsion gels are characterized as soft, solid-like materials which generally comprise of a polymer network with water as the dispersed medium and emulsified lipid nanodroplets incorporated inside the gel matrix [278] and have the ability to encapsulate lipophilic bioactive compounds. They are multifunctional systems that can be used for diverse applications in the food, cosmetic, and, pharmaceutical industries and display tunable structural and physicochemical characteristics enabling the formulation of miscellaneous structures [71,277,279,280].In particular, EGs are complex colloids and are the result of the combination of an emulsion dispersion and a polymeric gel matrix [281,282]. These systems, as illustrated in figure 18, can be further characterized as a) emulsion-filled gels or b) emulsion-particulate gels. As a) emulsion-filled gels are characterized the systems comprised of a polymeric matrix into which are incorporated emulsion droplets and they are obtained by the partial or total substitution of the dispersion medium of the hydrogel by an emulsion. On the other hand, b) emulsion-particulate gels are formulated by aggregated emulsion droplets comprising a network [283,284]. Even though these two structures are quite distinct in theory, practically in an EG often these arrangements coexist resulting in a hybrid network of both incorporated and partially aggregated droplets of oil [285].

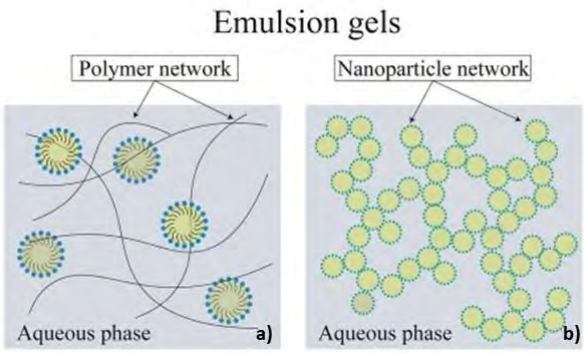

Figure 18. Schematic representation of the two main types of emulgels. a) Emulsion-filled gels and, b) Emulsion-particulate gels [278].

The oil droplets which are incorporated into the polymeric matrix are defined as active or inactive fillers and depending on their effect and possible association with the network they can affect significantly the EGs rheology [286]. As is illustrated in more detail in figure 19, active fillers interact with the polymeric network and their ability to either strengthen or weaken the gel strength is correlated to their interfacial composition and the interactions between the surfactant monolayer of the oil droplets and the polymers of the gel matrix. Contrariwise, inactive fillers are not connected to the polymer matrix and do not demonstrate chemical and physical affinity with the polymers resulting always in decreased network strength [287–291].

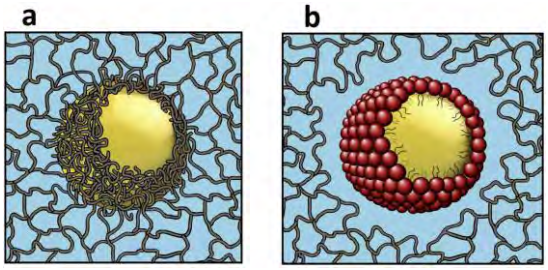

Figure 19. Schematic representation of a) active and b) inactive fillers inside emulgels [286].

Apart from the type of fillers, there are various other factors affecting the EGs rheology resulting in systems with a wide range of mechanical and physicochemical properties. It is well established from a variety of studies that some major determinants involved in the EGs structural features are the morphology and stiffness of the gel matrix [292], the method of formulation of the gel matrix (cold-set, hot-set, acidification, and enzymatic) [293–295] and, the physicochemical properties of the dispersed emulsion (dispersed oil volume fraction, oil-water interfacial composition, size, properties of the surfactants) [283,284,287,288,296–299]. Finally, the distribution of the emulsion droplets and

their interaction with the gel matrix can have a great impact on the structural features of the resulting system [289,290,292,300].

This type of nanocarrier is intriguing and attracts increasing attention since it is reasonably simple and inexpensive to formulate [301]. Furthermore, EGs being complex systems provide a combination of the benefits of both the NEs and the hydrogels. Thus, an improved system arises, enhancing the efficacy of these nanocarriers. This hybrid nanodispersiondemonstrates various important advantages making it suitable for the encapsulation and delivery of both lipophilic and hydrophilic bioactive compounds [281,286,302,303]. In addition, there are various studies indicating that the dispersion of a drug-loaded NE into a hydrogel matrix could improve its stability [304,305] and, provide improved protection of the encapsulated substance [306] while enhancing its release profile [307]. Specifically, as far as the pharmaceutical industry is concerned, EGs are often selected since they exhibit enhanced delivery, reducing adverse effects since they demonstrate regulated [308,309] and targeted release to the desired site of action [71,310]. This feature is a result of the prolonged contact with the administration area due to the mucoadhesive properties that many hydrogels present [311–314]. Last but not least, these carriers are frequently preferred over conventional NEs and hydrogels since they offer favorable sensory features to the consumers. Among their most valuable characteristics are long shelf-life and environmentally friendly, tunable rheology, compatibility with a large variety of excipients, masking undesirable flavors and aromas, and water solubility. Moreover, they have a pleasant transparent appearance and have a moisturizing effect while being greaseless, easily administrated and removed [315–322].

Due to their tunable composition and structure and the plethora of benefits they present, EGs have become an appealing delivery system for miscellaneous applications in the pharmaceutical, food, and cosmetic industries [309]. Specifically, to date, EGs have been investigated for the delivery of bioactive compounds through multiple routes of administration including oral [309]**,** buccal [323], topical [324,325], vaginal [326] and, transdermal [327–329].

1.8. Advantages and drawbacks of the most commonly used delivery routes (oral/ intranasal/ transdermal)

The use of the appropriate nanocarrier is crucial for the encapsulation and protection of the bioactive compound of interest. Their ability to enhance the efficacy of the encapsulated therapeutic agent due to their unique physiochemical properties is widely known and was described in the previous chapters (Chapters 1.1 and 1.2.). However, the route of administration of the nanocarrier and its properties are also decisive factors affecting the fate and efficacy of the therapeutic agent as well as the short- or long-term biological effects. Hence, it is important to select the proper delivery route in order to provide a suitable channel to obtain targeted delivery of the nanocarriers and avoid the rapid metabolism but also increase the efficacy and bioavailability of the therapeutic agent [330,331].

In general, the term bioavailability describes the rate and extent to which an administered bioactive compound is absorbed into the systemic circulation and thereby its availability for therapeutic response. In other words, it refers to the *in vivo* performance of a drug and is directly dependent on the selected route of administration [332]. More specifically, intravenous administration of a drug results in 100% bioavailability by definition [333,334]. On the other hand, when an alternative delivery route is selected the bioavailability of the compound of interest is in general lower due to various parameters including first-pass metabolism, the stability of the drug in the gastrointestinal tract, epithelium permeability and others administration [332].

Thus, the advantages and limitations of the three most prominent delivery routes namely oral, intranasal and transdermal are presented all together in Table 1 and will be discussed in this chapter.

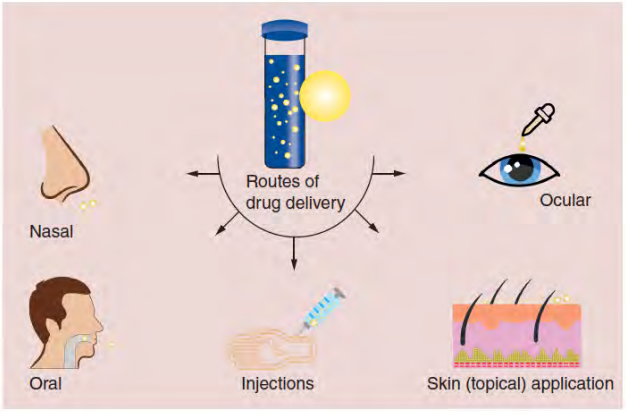

Figure 20. Illustration of the most studied routes of administrations of NEs including nasal, oral, intravenous, topical/transdermal, and ocular [38].

Oral route of administration

Throughout the years, diverse routes of administration have been developed and studied as illustrated in figure 20 since each of them demonstrates both favorable features and shortcomings thus requiring a suitable nanocarrier to tackle the respective barriers and obtain potent action of the therapeutic agent. In particular, non-invasive delivery methods have been the most preferred among research groups and patients since they are convenient for the delivery of bioactives requiring chronic administration [335].

Until recently, one of the most commonly used routes of delivery has been oral administration since it is non-invasive and simple leading to patient compliance. Due to the possibility of self-administration that provides, without the requirement of specialized healthcare professionals or hospitalization, improves the quality of life of the patients while also reducing the treatment cost. In addition, the oral route is promising for the delivery of drugs with poor water-solubility and a variety of formulations including a wide range of nanocarriers such as liquid, hydrogel, as well as solid formulations which demonstrate in general better storage stability over time [25,166,335,336].

However, oral administration also presents some important drawbacks such as the rapid degradation of the drug through first-pass metabolism or by the changes in the pH value and the digestive enzymes present in the gastrointestinal (GI) tract. Another obstacle is the possible interaction of the administered therapeutic agent with the stomach contents and other orally administered compounds [337]. An additional challenge of paramount importance is the controlled release of the therapeutic agent [332]. In these cases, the application of NEs as delivery vehicles could be beneficial in protecting the ingested therapeutic agents from endogenous environmental conditions, minimizing the adverse effects and prolonging their residence in the GI tract with the result of their enhanced absorption and efficacy [38,338]. Moreover, when patient compliance is not feasible for example due to nausea, epilepsy, or age (geriatric/ pediatric patients) or in urgent circumstances, oral administration is not applicable since it demonstrates slow absorption and presents multiple levels of physiological barriers that need to be addressed in order for the bioactive to be efficient [330,335,339].

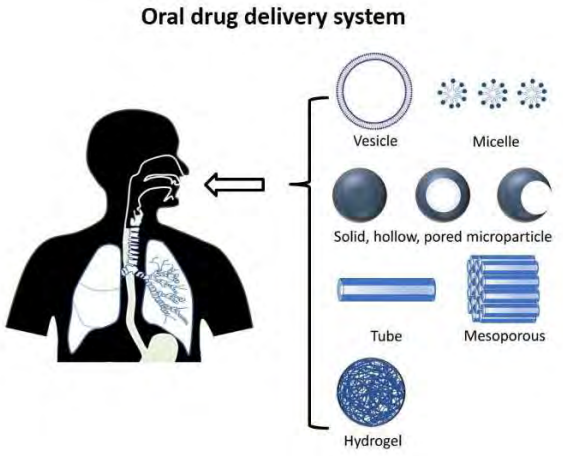

Figure 21. Schematic representation of some of the major nanocarriers used as delivery vehicles for oral route [335].

Intranasal route of administration

Recently, attempts are being made in order to surpass the aforementioned limitations of the oral route of administration. For that reason, various approaches have been employed such as the use of functional excipients. However, the most promising way of improving the absorption and bioavailability of the administered bioactive compound seems to be the use of nanocarriers. So, nowadays research groups as well as the pharmaceutical industry are investigating the use of alternative routes of delivery to improve the efficacy and targeting of the nanocarriers and hence the bioactive compounds. One of the most substantial benefits of nanocarriers is that they offer the possibility of alternative routes of administration avoiding the limitations that oral administration demonstrates. Specifically, NEs have emerged as promising delivery vehicles for nearly all the routes of administration that are known and utilized so far [65].

The nasal cavity has been investigated as an alternative site of drug delivery since it also provides a simple, non-invasive, painless, and well-tolerated route which are favorable characteristics widely acceptable by the patients. Considering that there is a wide range of therapeutic agents that can be administered intranasally intended for diverse sites of action including topical, systemic, and central nervous system (CNS) and that sterilization is not necessary, formulations intended for intranasal administration are attractive for the pharmaceutical industry too [340–342]. The unique physiological and anatomical characteristics of the nasal cavity such as reduced enzymatic activity and reasonably epithelial permeability it has been established as one of the most efficient administration sites providing

the potential of rapid systemic absorption and action hence being an ideal method for emergencies [335,342,343]. Compared to the oral route of administration, intranasal demonstrates enhanced systemic bioavailability and provides the possibility of effective delivery of molecules demonstrating reduced stability in GI tract or easily degraded through first-pass metabolism including polar drugs, proteins, and peptides [330,342,344]. In addition, for the treatment of topical conditions, intranasal administration offers advantages over oral providing the possibility of topical administration of bioactives with the result the efficient delivery even with the application of relatively low concentrations of the formulations. This leads to reduced systemic toxic effects and permits prolonged contact with the site of action resulting in extended drug absorption when it is necessary [345,346]. Last but not least, through intranasal administration the risk of over-dosage could be avoided since the excess formulation can be removed and due to the low volume of the nasal cavity that does not permit the administration of high doses [347].

On the other hand, when the administration of higher concentrations of the bioactives is required, the low volume of the nasal cavity could be a major drawback restricting the administered formulation to approximately 100- 150 μL which occasionally is not an adequate amount [348]. In addition, pathological conditions affecting the nasal mucosa or possible interaction of the administered therapeutic agent with it could compromise the absorption reducing the efficacy of the molecule of interest [340,348,349]. Other physiological barriers considerably reducing the therapeutic action of the drugs are capillary barriers, nasal metabolism, and mucociliary clearance which limits the contact with the site of action [350,351]. Thus, components with mucoadhesive properties such as chitosan and poloxamer are now being exploited in order to prolong the residence time on the nasal mucosa and enhance the bioavailability of the administered compounds [352]. Another formulation that is often selected in order to tackle several of the aforementioned limitations of intranasal delivery is NEs in the form of a spray. However, since it is challenging to achieve a uniform and steady spray deposition the dosage control is troublesome leading to repeated and long-term administration which could cause irritation or even permanent damage due to the presence of surfactants in the NEs [353,354].

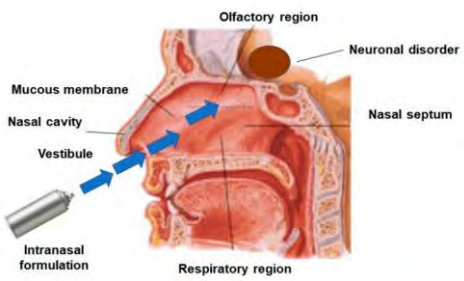

Figure 22. Illustration of the intranasal route of delivery providing the possibility of drug transportation to the brain through the blood-brain barrier [126].

Transdermal route of administration

Although the oral mode of administration is conventionally used for the treatment of dermatological conditions as well, nowadays efforts are being made to replace it with topical formulations since as mentioned above oral administration demonstrates numerous constraints [355]. Skin is the largest organ of the human body reaching about 10% of the overall body mass and performs various physiological functions acting as the first defense mechanism and protecting the body from environmental conditions and pathogens. However, it has also emerged as an ideal site of action for the application of diverse bioactive compounds for both topical and transdermal delivery [38,356].

Skin is a multilayered organ with the outer layer being the stratum corneum (SC) constituting the main barrier of the skin which has to be overcome in order to achieve topical or percutaneous delivery. As illustrated in figure 23 the structure of the SC consists of the epidermis, dermis, and subcutaneous tissues. Specifically, SC is comprised of keratinocytes, ceramides, fatty acids, and cholesterol [357–359]. As figure 23 depicts, skin provides the possibility of both dermal and transdermal delivery of a bioactive compound each with different therapeutic targets and results. In particular, to achieve dermal delivery of a drug, the formulation is administered directly on the site of action. Dermal delivery is preferred over oral administration for the treatment of topical conditions since it provides a higher localized concentration of the bioactive while simultaneously reducing the systemic concentration minimizing the adverse effects [360]. On the other hand, the transdermal route refers to the delivery across the skin layers and requires the transportation through the skin and into the systemic circulation of a drug concentration high enough to achieve a therapeutic effect [361]. This mode of delivery is convenient for the treatment of numerous pathological conditions

and in combination with the use of drug-loaded nanocarriers has been established as a promising delivery method for various therapeutic agents [330,362].

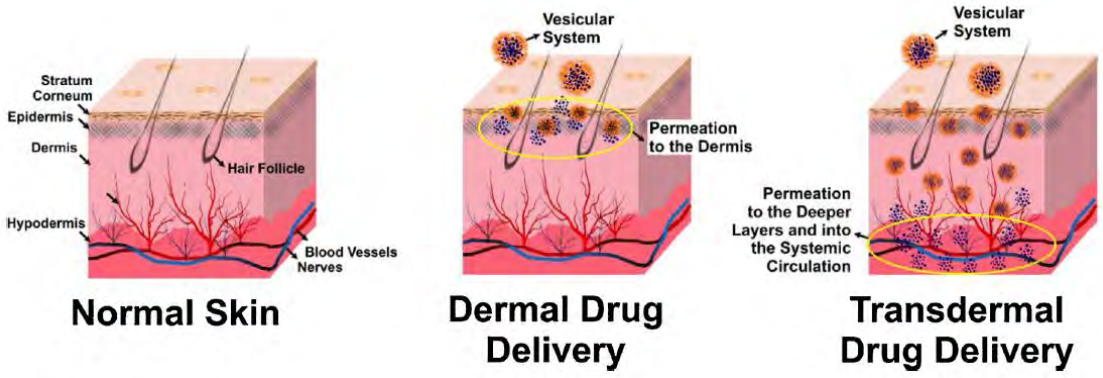

Figure 23. Illustration of the architecture of skin and representation of drug release from delivery vehicles for topical and transdermal applications [360].

It is a fact that (trans)dermal route of administration likewise with the aforementioned methods of delivery is self-administered, non-invasive, and painless [41,363]. However, a benefit of paramount importance that dermal administration presents compared to oral, is its ability to bypass the GI tract similar to intranasal administration. Because of this, the effectiveness of the administered substance increases as metabolism is avoided and the manifestation of adverse effects is decreased. However, transdermal administration is more effective compared also to intranasal administration since it avoids mucociliary clearance and even the slightest metabolism that occurs in the nasal cavity due to the presence of specific enzymes even if they exist in small amounts [350]. Thus, the circumvention of both the first-pass metabolism and mucociliary clearance that occurs during oral and intranasal administration, respectively, reduces the likelihood of drug degradation [65,364–366]. Transdermal formulations provide the possibility of prolonged contact with the site of action resulting in controlled delivery over extended periods of time (hours or even days) and sustained plasma level of the bioactives. Thus, enhanced bioavailability is achieved reducing the need for frequent re-application and minimizing the possibility of skin irritation or systemic side effects [330,335,367,368]. In addition, the systems that are selected for dermal application offer a pleasant sensation on the skin, provide the possibility of targeted action to a specific site and can be easily removed eliminating the formulation and interrupting the delivery of the drug and as a result, minimize the possibility of skin irritation and adverse effects [330,343,366]. With the continuous advancement of the field of nanotechnology, various nanocarriers have proven to be ideal systems for enhancing drug delivery through the

skin highlighting the advantages of this mode of administration over the oral and intranasal. Specifically, NEs due to their ability to solubilize in their oil core and deliver highly lipophilic drugs as well as their components (surfactants and/or oils), can interact with the SC improving the penetration of the bioactives [369]. Hence, over the years transdermal delivery has been preferred for the delivery of lipophilic molecules that were already administered orally in order to overcome the GI adverse effects. Formulations for numerous conditions have been developed including inflammations, various infections, cardiovascular disease, and skin cancer [370]. Specifically, (trans)dermal administration of analgesics demonstrates important benefits compared to oral administration including improved relief of topical pain, while reducing the systemic side effects and minimizing the risk of addiction when analgesia is required for longer periods of time [371].

This particular route of delivery also presents some disadvantages which, however, can be easily encountered with the selection of suitable delivery systems for encapsulation of the therapeutic agents of interest possessing appropriate characteristics and ingredients. The foremost obstacle that needs to be addressed to obtain effective (trans)dermal delivery is the skin itself. Since the skin acts as a barrier demonstrating relative impermeability and high selectivity some specific physicochemical requirements need to be fulfilled in order for a bioactive substance to penetrate it and act either topically or systemically. The most important features of a molecule to be considered for dermal application are low molecular weight and moderate lipophilicity thus providing a rather small pool of bioactives that can be delivered transdermally and demonstrate therapeutic action [368,372]. To address these issues NEs can be employed providing the ability to solubilize and deliver highly lipophilic drugs and demonstrating easy penetration through the pores of the skin due to their small size thus reaching the systemic circulation [65,330,343,356,373]. Chemical penetration enhancers such as surfactants, solvents, and fatty acids can also enhance skin permeability by interacting with the lipids of the SC and modifying its microstructure [374,375] but they also increase the chance of skin irritation and toxicity [335,367]. However, the possibility of skin irritation can be reduced or completely dealt with in various ways such as the selection of an appropriate formulation. For example, systems that present pH values between 5-7 which are close to the pH of the skin surface, application of hydrogels, or systems providing controlled release have been reported to reduce the possibility of skin irritation caused either by the administered drug or the nanocarrier itself [376–379].

Table 1. Overall evaluation and comparison of the advantages and limitations of the three most commonly used delivery routes namely oral, intranasal, and transdermal.

Properties	Route of administration		
	Oral	Intranasal	Transdermal
Simple	√	√	√
Cost-effective	√	√	√
Patient compliance	√	√	√
Systemic delivery	√	√	√
Sustained delivery		√	√
Targeted delivery		√	√
Delivery of lipophilic drugs		√	√
Patient cooperation (Geriatric/pediatric/seizure patients)		√	√
Gastrointestinal problems		√	√
Circumvention of first-pass metabolism		√	√
Circumvention of enzymatic degradation			√
Administration of large doses	√		√
Easy removal in case of the appearance of side-effects			√
Possible topical irritation caused by long-term administration		√	
Direct CNS delivery		√	
Risk of overdosage	√		
Prolonged contact with the site of action			√

The aforementioned drawbacks that (trans)dermal delivery might present can be encountered by using suitable colloidal nanodispersions to act as carriers of the bioactive compounds of interest [380] leading to efficient delivery. More specifically, hybrid systems composed of a hydrogel or a cream in combination with liposomes or NEs like the NE-filled hydrogels that were developed in the present study have emerged as promising delivery vehicles for (trans)dermal application. Since these types of nanocarriers demonstrate the benefits of both systems, it is suggested that they could have great potential for (trans)dermal applications providing controlled delivery and enhanced bioavailability while decreasing the possibility of skin irritation [367].

All three routes of administration that have been mentioned previously, demonstrate both advantages and limitations. However, regarding the transdermal route, the benefits outweigh the disadvantages and since it also provides the possibility of topical as well as systemic administration, it has emerged as a promising delivery method for a variety of bioactive compounds including vitamins, analgesic compounds such as lidocaine and opioids or even hormones [381]. Hence, the transdermal route has been selected and investigated for the systemic delivery of CBD which was encapsulated in two different nanodispersions namely an O/W NE and the respective NE/HG to study their potential as delivery vehicles.

Chapter 2

Aim of the study

Chapter 2 – Aim of the study

In recent years there is an increasing interest towards natural compounds for use as therapeutic agents. This arises from the fact that they present multiple pharmacological actions and good safety profiles thus being ideal candidates for the treatment of various ailments. However, the administration of some natural substances is challenging due to their highly lipophilic nature which leads to low bioavailability and efficacy. Moreover, since they are considerably sensitive to processing, their incorporation in various formulations is difficult as they are easily degraded.

Therefore, the main objective of the present thesis consists of two parts with the first being the development and structural characterization of novel biocompatible nanodispersions for the encapsulation of natural bioactives and subsequently the *in vitro* and *ex vivo* biological assessment of the formulated systems. In particular, the main scope was the formulation of oil-in-water NE and NE-based hydrogels. These systems were utilized as carriers for the simultaneous encapsulation and delivery of various lipophilic compounds and a hydrophilic compound of pharmacological interest. An important part of the study was the elucidation of the structure of the developed NEs as well as evaluating the effect of their incorporation into chitosan hydrogels. Nonetheless, the *in vitro* and *ex vivo* evaluation of the formulated systems was also essential in order to determine their suitability for the transdermal delivery as carriers of the compounds of interest.

Chapter 3

Description of the experimental procedure

Chapter 3 – Description of the experimental procedure

3.1. *Formulation of nanocarriers as delivery systems of bioactive compounds and structural study*

The first goal of the present thesis was the development of novel nanocarriers. Thus, initially various combinations of oils and biocompatible, non-toxic surfactants were used in order to prepare stable O/W NEs. For that purpose, two formulation methods were implemented, a low energy and a high energy one. The most stable NEs were selected for further investigation and for the encapsulation of three lipophilic bioactive compounds namely curcumin, vitamin D, and cannabidiol. For the second part of this study, diverse biocompatible and biodegradable polymers and their combinations were used in different concentrations for the formulation of the hydrogels. In the most stable system, the hydrophilic C-PC-extract from *Spirulina maxima* was embedded. Finally, the selected NE was incorporated into the developed hydrogels resulting in the novel hybrid systems, the NE-based hydrogels or emulgels.

Subsequently, the aforementioned nanodispersions were structurally characterized applying a variety of advanced techniques. To determine the size and homogeneity of the NEs Dynamic Light Scattering (DLS) was employed immediately after their formulation and in various time points in order to study their stability over time. Furthermore, Electron Paramagnetic Resonance (EPR) spectroscopy was performed for the structural characterization of the surfactants' monolayer in both the NEs and the NE-based hydrogels in absence and in presence of the bioactive compounds using appropriate spin-probes. This technique was applied to acquire information concerning the localization of the encapsulated lipophilic substances and estimate the possible effects of the incorporation of the Esogels. Then, advanced microscopy techniques such as Confocal laser scanning microscopy (CLSM) and Cryo-electron microscopy (CryoEM) were employed to obtain a visualization of the developed NE and the hybrid system as well.

Finally, Small-angle X-ray scattering (SAXS) provided an indication concerning the size and shape of the developed systems and the possible structural changes of the NE upon its incorporation in the hydrogel.

3.2. Biological evaluation of the formulated systems

In order to determine the suitability of the developed systems as effective carriers for the bioactive compounds of interest, their biological assessment was essential. The main goal of this part of the study was to compare the NEs and the hybrid systems in terms of biocompatibility and permeability. Initially, the most promising NEs and the respective NE-based hydrogels were studied to evaluate their possible cytotoxicity in various human cell lines in the absence of the bioactive compounds. Namely human nasal epithelial cells (RPMI 2650) and normal human fibroblasts (WS1) were used to assess the potential use of the developed systems in intranasal and transdermal administration respectively. Subsequently, the effect of the loaded systems on cell viability was investigated *in vitro* by applying the tetrazolium-based colorimetric MMT assay to assess the inhibition of cell proliferation induced.

Moreover, in order to estimate the potential permeation and retention in the stratum corneum of cannabidiol, an appropriate model was used to simulate human skin. Specifically, an *ex vivo* permeation protocol was performed using modified Franz diffusion cells and porcine ear skin as the model membrane. The quantity of the cannabidiol released to the receptor chamber over time was determined by LC-MS/MS method and subsequently, appropriate calculations were performed to obtain the release model of cannabidiol. Finally, the quantity of cannabidiol retained in the stratum corneum and the hair follicles of the porcine skin was evaluated by the differential tape stripping method in addition to LC-MS/MS technique.

Chapter 4

Materials & Methods

Chapter 4 – Materials & Methods

4.1. Materials

Nanoemulsions

Organic extra virgin olive oil (EVOO) from the Amfissa Variety, Pelion, Magnesia, Greece, (acidity b 0.4%, oleocanthal 124 mg/kg, oleacein 72 mg/kg, total hydroxytyrosol derivatives 140 mg/kg, total phenols analyzed 315 mg/kg) was generously donated by "Myrolion" startup company. Isopropyl tetradecanoate (IPM), 98% was from Alpha Aesar, Germany. Cholecalciferol (Vitamin D3) ≥ 98% was supplied from Sigma-Aldrich, Germany and Curcumin was a product of Sigma–Aldrich Co; St. Louis, MO, USA. CBD (99 % of cannabidiol) from Cannabis sativa L. was a gift from Ekati Alchemy Labs S.L, Barcelona, Spain. C-Phycocyanin extract was achieved by the Group of Biomimetics & Nanobiotechnology at the Institute of Chemical Biology (National Hellenic Research Foundation) Soybean lecithin (L-alpha phosphatidylocholine), 90% was from Alpha Aesar, Germany. Polyethoxylene 20 (Tween 20) was purchased from Merck Schuchardt, Germany and Polyoxyethylenesorbitan monooleate (Tween 80), pure, was purchased from Fisher BioReagents, NH, USA. Quillaja saponin (Q-Naturale®200V) was a generous gift of Ingredion, Germany GmbH. Glycerol monolinoleate (Maisine® CC) HLB 1, Diethylene glycol monoethyl ether (Transcutol® HP) and Caprylocaproyl Polyoxyl-8 glycerides (Labrasol®) HLB 12, were kindly donated by Gattefossé, France. Calcium citrate tetrahydrate, 99% was from Aldrich. Spin-probe 5-Doxyl stearic acid ammonium salt, >99% purity, was from Avanti Polar Lipids, Alabama, USA. 5-, 12- and 16-Doxyl stearic acid as well as the lipophilic dye Nile red were purchased from Sigma-Aldrich Chemie GmbH Munich, Germany. 4-hydroxy-TEMPOL was purchased from Alpha Aesar, Germany. Ethanol absolute, analytical grade was from Fisher Scientific, Loughborough, UK. Deionized water was used and highly purified water was obtained from a Millipore Milli Q Plus device.

Hydrogels

Chitosan (200-600 mPa·s, 0.5% in 0.5% Acetic Acid at 20°C) was purchased from TCI, Belgium. Xanthan gum from Xanthomonas campestris and Hydroxypropyl methylcellulose (HPMC) were supplied from Sigma-Aldrich, Chemie Gmbh Munich, Germany. Acetic Acid glacial 100% was from Merck, Darmstadt, Germany.

Cell culture

Two different cell lines were used for the evaluation of the biological effect of the formulated systems. The human nasal cell line RPMI 2650 (CCL-30) was provided by Prof. Fabio

Sonvico (University of Parma, Parma, Italy). Cells between passages 16–30 were grown at 37 °C in complete DMEM culture media supplemented with 10% (v/v) FBS and 1% (v/v) non-essential amino acid solution. The second cell line used was human skin normal fibroblasts WS1 which was purchased from the American Type Culture Collection (ATCC, Manassas, VA, USA). The cell line was grown in EMEM (containing 2 mM L-glutamine, 1 mM sodium pyruvate, and 1500 mg/L sodium bicarbonate), supplemented with 10% FBS and 1% penicillin/streptomycin (Gibco-Life Technologies). Both cell lines were grown in 75 cm^2 culture flasks, maintained in a humidified atmosphere of 95% air and 5% CO2 and were subsequently spread in 96-well tissue culture plates at a density of 5×10^3 per well for RPMI 2650 (CCL-30) and 1.6×10^4 per well for WS1 cells. Dulbecco's Modified Eagle's Medium (DMEM), *Eagle's Minimum Essential Medium (EMEM),* fetal bovine serum (FBS), 100 U/mL penicillin and 100 mg/mL streptomycin, phosphate-buffered saline (PBS) and trypsin-EDTA were purchased from Gibco (Life Technologies, Grand Island, NY, USA). Thiazolyl blue tetrazolium bromide (MTT) and dimethyl sulfoxide (DMSO) were obtained from Sigma-Aldrich (Taufkichen, Germany).

Ex vivo study

For the evaluation of the release of the bioactive compounds with vertical Franz diffusion cells, a synthetic cellulose membrane with molecular weight cut-off 14,000 and average flat width 43mm (Sigma-Aldrich Co St. Louis, MO, USA) and porcine ears (kindly donated by a local provider in Serbia, as the *ex vivo* experiments were performed in the Faculty of Pharmacy, University of Belgrade, Belgrade, Serbia) were used.

4.2. Methods

In this chapter, the methods and protocols used in the thesis will be presented in detail. Firstly, the formulation methods of a) the oil-in-water NEs both in the absence and presence of the bioactive compounds, b) the hydrogels and, c) the emulsion-filled gels, will be described. Then, the techniques employed for the structural characterization and the biological evaluation of the developed systems will be presented.

4.2.1. Formulation of the nanocarriers

In the present study the main objective was the development of novel nanocarriers for the encapsulation of three lipophilic and a hydrophilic compound. To that end, a series of stable O/W NEs were formulated and characterized and then three different bioactive compounds (vitamin D, curcumin, CBD) were encapsulated in the most promising systems. In addition, chitosan-based hydrogels were also prepared into which either C-phycocyanin to result loaded hydrogels was added or O/W NEs were incorporated resulting in hybrid systems, the NE/HG. Following, the formulation of the systems in the absence and presence of the bioactive compounds will be described in more detail.

4.2.1.1. Oil-in-water nanoemulsions and encapsulation of the bioactive compounds

To obtain stable and non-toxic O/W NEs various combinations of biocompatible surfactants and oils were used and two emulsification methods were performed.

4.2.1.1.1. Nanoemulsions in the absence of bioactive compounds

HIGH ENERGY METHOD

In this approach, high pressure homogenization was selected which was described in more detail in Chapter 1.2. To implement this two-step emulsification method, initially the appropriate amounts of surfactants and oils were weighted to prepare the oil phase and then coarse emulsions were formulated by mixing the oil phase with the aqueous phase using mechanical agitation in ambient temperature. The production of the final O/W NEs (H1-H4) was obtain by passing the coarse emulsions through a Panda PLUS1000 (GEA, Niro Soavi) high-pressure homogenizer at maximum pressure 700 bar applying up to 12 recirculation passages. After the homogenization procedure the final NEs from the exit of the homogenizer were immediately cooled using an ice bath. The compositions of the different NEs that were formulated are presented below in Table 2.

LOW ENERGY METHOD

As the low energy method, the isothermal spontaneous emulsification method which was also presented previously in Chapter 1.2, was selected. For the development of the low energy O/W NEs (L1-L4), proper amounts of the surfactants and oils presented in Table 1 were weighted and mixed in mild conditions using a magnetic stirrer to prepare the oil phase. Following, to achieve the formulation of the NEs the oily phase was added into the aqueous phase dropwise under constant magnetic stirring at room temperature.

4.2.1.1.2. Encapsulation of the bioactive compounds

For the formulation of the loaded NEs first stock solutions of the lipophilic bioactive compounds in oils were prepared to be used as the oil phase of the O/W NEs. Vitamin D and curcumin were solubilized in IPM while CBD was dissolved in a 1:1 mixture of IPM and EVOO. Appropriate amounts of these solutions were used to obtain NEs with different concentrations of the bioactives. The oil stock solutions were then mixed with surfactants to form the respective oil phases for the development of the three different loaded NEs by the low energy emulsification method as described above. Specifically, two loaded NEs were formulated using the L1 composition encapsulating 1mg/mL of either vitamin D or curcumin, respectively. For the formulation of the CBD-loaded systems, the composition of L4 NE was selected and three different concentrations of CBD were encapsulated, namely 1mg/mL, 5mg/mL and, 10mg/mL to determine the most appropriate amount that would not affect the NEs' stability.

Table 2. Composition of the NEs formulated using high-pressure homogenization (H1-H6) and isothermal spontaneous emulsification (L1-L4) methods.

Ingredients (% w/w)	Systems							
	H1	**H2**	**H3**	**H4**	**L1**	**L2**	**L3**	**L4**
Water	92	92	91	90	92	93	91	91
Tween 80	2	4	2	2	2	2	2	2
Labrasol	2	-	2	2	2	2	2	2
Lecithin	-	0.4	-	-	-	-	-	-
Maisine	1	-	1	1	1	1	1	1
Trancutol	1	-	-	1	1	-	-	-
IPM	2	-	2	2	2	0.4	4	2
EVOO	-	3.6	2	2	-	1.6	-	2

4.2.1.2. Formulation of hydrogels

For the formulation of the hydrogels either two single biopolymers namely chitosan (CS) and, hydroxypropyl methyl cellulose (HPMC) or combinations of two different types of monomers were used, resulting in homo-polymeric or co-polymeric networks, respectively.

Various hydrogels were prepared using different amounts of acetic acid solution 1% (v/v) of pH 3 (A.A. 1%) or water (H_2O) as the dispersion media in order to achieve a system easy to handle and with the desired sensory properties (Table 3). For the development of the hydrogels the desired amounts of polymers were weighted in glass tubes and next the dispersion medium was added providing systems with different concentrations. This mixture was gently stirred with a spatula to avoid the formation of bubbles until the polymer was uniformly distributed.

Table 3. Compositions of formulated hydrogels that were tested for the incorporation of C-Phycocyanin and for the development of the emulsion-filled hydrogels.

	Polymer	Dispersion medium	Concentrations % w/v (Min/Max)
1	Chitosan	A.A. 1%	Min: 0.8% Max: 4%
2	HPMC	H_2O	Min: 4% Max: 20%
3	Chitosan + HPMC	A.A. 1%	Min: 0.9% Max: 6.7%

4.2.1.3. C-Phycocyanin extraction and formulation of loaded hydrogels

C-Phycocyanin (C-PC) was initially studied as a hydrophilic model compound for the formulation of C-PC loaded hydrogels. Two separate hydrogels comprised one of CS and the other of HPMC were selected for the incorporation of the C-PC extract and for further investigation. The C-PC extract that was used, was obtained by our lab implementing an extraction and purification protocol based on techniques widely used for this purpose [382–385]. Dried biomass of the cyanobacterium *Arthrospira platensis* was used and was attempted to obtain an extract with the highest possible c-phycocyanin content.

The procedure started with the weighing of an appropriate amount of arthrospira powder and the lysis of the cells overnight using phosphate buffer solutions and constant stirring. Following, the solution was centrifuged at 10000 g for 10 minutes at 4°C to remove the biomass and collect the supernatant. The supernatant was then saturated with ammonium sulfate (AS) [$(NH_4)_2SO_4$] to achieve protein precipitation. After centrifugation, the precipitate was collected and redissolved in phosphate buffer (pH 7) to perform dialysis. The C-PC content and relative purity of each fraction obtained by the described methodology was assessed by measuring absorbance at 280 and 620 nm. The entire process occurred in temperature of 4°C and in the dark to avoid C-PC degradation. Finally, the obtained C-PC extract was lyophilized providing a powder of bright blue color as illustrated in figure 24.

The lyophilized C-PC extract was then used for the formulation of the loaded hydrogels. Four different concentrations of C-PC extract (10-40 mg) were incorporated into the CS and HPMC hydrogels and the resulting systems were optically observed over time and studied in terms of different pH values and temperatures to determine the effect of these parameters on the bright blue color of C-PC.

Figure 24. Final, lyophilized product obtained by C-PC extraction and purification protocol.

4.2.1.4. Formulation of nanoemulsion-filled hydrogels

For the formulation of the emulsion-filled hydrogels, the aforementioned O/W NEs were prepared both in the absence and presence of the three lipophilic compounds under study. To obtain this composite system, chitosan was selected to formulate an emulsion-filled hydrogel of 1.25% w/v final concentration. In order to incorporate the NE into the hydrogel, an amount of the A.A. solution was replaced by the NE resulting in a dispersion medium consisting of A.A. solution and NE in a ratio 1:1.

4.2.2. Structural study

One of the main objectives of the present thesis was the development of suitable nanocarriers with the perspective of encapsulating and releasing effectively various lipophilic bioactive compounds. To this end a crucial aspect was the elucidation of the structure of the formulated NEs in the absence and presence of the bioactive substances in order to determine the effect of their encapsulation on the properties of the systems. It was also essential to investigate whether the incorporation of the NE into the hydrogel matrix affects its structure and interfacial properties.

Thus, in order to study the formulated systems in terms of size, homogeneity, shape, and interfacial properties, advanced analytical techniques were implemented. In particular, Dynamic Light Scattering (DLS), Electron Paramagnetic Resonance Spectroscopy (EPR), Confocal Microscopy (CLSM), Cryo-Electron Microscopy (Cryo-EM) and, Small-angle X-ray Scattering (SAXS) were applied. These methods provide useful information concerning the

structure of the systems and, the interfacial properties of the NEs indicating the suitability of the formulated nanocarriers to act as delivery vehicles.

4.2.2.1. Dynamic Light Scattering (DLS)

When developing a new nanocarrier for the delivery of bioactive compounds it is essential to elucidate the size and homogeneity of the system. It is well established that these features have a great impact on the formulation of an effective vehicle since they affect its stability over time as well as its efficacy, cellular uptake, bioavailability and clearance, possible toxicity and in general determine whether the formulated nanocarrier is suitable for a specific route of administration. In addition, the diameter and size distribution of the nanocarrier affects the processability, appearance and overall performance of the final product [32,386–390].

Thus, Dynamic Light Scattering (DLS) is a well-established technique for the investigation of the size and homogeneity of colloidal delivery systems such as NEs [391,392]. The principle of this technique lies on the fact that the particles in a suspension moving according to Brownian motion scatter an incident light beam in all directions with different intensities dependent on their size and shape [393]. The Brownian motion theory explains the perpetual movement of the particles in a dispersion which is caused by their random collision with the solvent molecules that surround them [393]. An important effect arising from that theory is that small particles move faster compared to larger ones leading to the Stokes-Einstein equation that expresses the particle size in relation to its velocity which is referred to as translational diffusion coefficient (D) [394,395]. Thus, the hydrodynamic radius (R) of the particles can be determined by the following Stokes-Einstein equation (1):

$$R = \frac{kT}{6\pi\eta D} \quad (1)$$

Where k is the Boltzmann constant ($1.38064852 \times 10^{-23}$ J/K), T is the temperature of the suspending medium in Kelvin degrees, η is its viscosity, and D the translational diffusion coefficient.

When a monochromatic laser collides with the particles of a dispersion, light is scattered spherically in all directions with an intensity proportional to the sixth power of their radii [396] as can be observed by the following equation (2):

$$I = I_0 \frac{16\pi^4}{\lambda^4} \frac{1+\cos^2\theta}{2s^2} \left(\frac{n^2-1}{n^2+2}\right)^2 r^6 \quad (2)$$

Since the diameter of the dispersed particles plays crucial role to the intensinty of the scattered light, two different theories have been expressed concerning the type of the scattering depending on the size of the particles. The observed scattering of particles with diameter smaller (<λ/10) than the incident light carries the same energy towards all directions and is angle-independent and is characterized as Rayleigh scattering [397]. On the other hand, when the radii of the dispersed particles exceed the aforementioned size threshold, anisotropic Mie scattering is detected according to which the scattered light is angle-dependent and scattered more intensely towards the direction of the incident light [398,399]. The two described scattering types and their differences are illustrated below in figure 25.

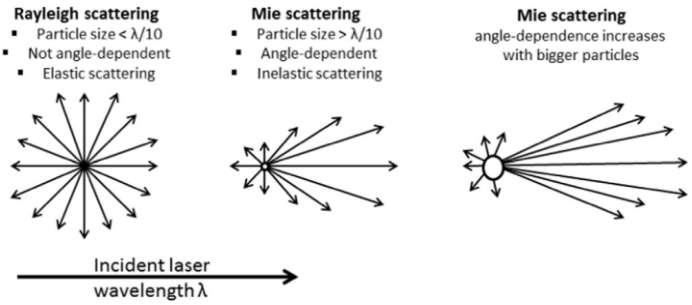

Figure 25. Schematic representation of the Rayleigh and Mie scattering types according to the dispersed particle radii.

Hence, DLS is actually based on the two assumptions that 1) the particles in the suspension follow the Brownian motion and 2) are spherical with small diameter and exploits these features of colloidal dispersions in order to determine the hydrodynamic radius (R) of the nanoparticles [400].

Another important feature of nanodispersions that can be investigated using DLS is the particle size distribution expressed by the polydispersity index (PdI) [401,402]. The values of this dimensionless index range from 0 to 1 demonstrating perfectly homogenous distribution of particle size or a highly polydisperse system with multiple particle size populations, respectively. Concerning the lipid-based nanocarriers, it is generally accepted that when the PdI value is 0.3 or below, the system under study is monodispersed with a homogenous population of oil nanodroplets [391,403–405]. Below, in figure 26 a typical intensity particle size distribution graph is illustrated.

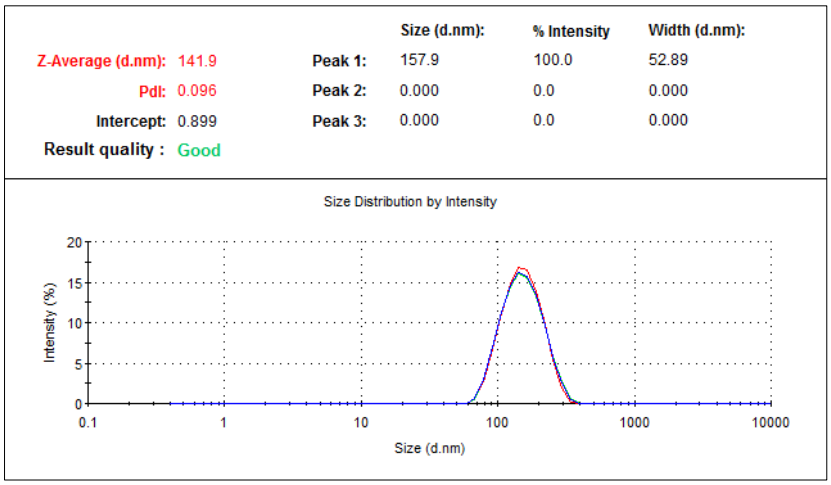

Figure 26. Picture from the experimental procedure demonstrating a typical intensity size distribution graph.

DLS is a fast, simple, reproducible method which is non-invasive and does not require complex sample preparation. Therefore, it is frequently used for the investigation of the size of nanodispersions and the particle distribution as a powerful analytical tool [391,394]. Furthermore, this technique is user-friendly since it is essentially automized and the available instruments are compact and affordable. A typical DLS instrumentation and its mode of operation are demonstrated in figure 27. An important feature of the more current instruments is the backscatter detection system at 173° which is also present in the Zetasizer Nano ZS (ZEN3600) from Malvern Instruments (UK) used for the measurements of the formulated NEs. The specific detector enables the investigation of highly concentrated systems reducing the phenomenon of multiple scattering by excluding excess scattered light. On the same time, it enhances the signal of smaller particles while avoiding the scattering contribution of large particles providing more reliable results [393,406].

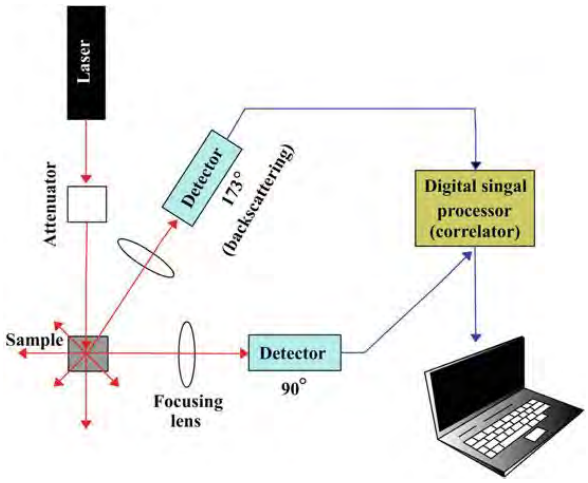

Figure 27. Schematic representation of Dynamic Light Scattering instrumentation.

In the present study, DLS was implemented for the investigation of the formulated NEs in terms of size and particle size distribution (PdI) both in the absence and in presence of the bioactive compounds. Measurements were carried out immediately after the preparation of the NEs and at various time points. To obtain more accurate results for each system three separate sample were taken and each of them was measured three times. Hence, the resulting PdI values and the hydrodynamic radius mentioned were the average of nine measurements. All samples were filtered prior to the measurements using 0.45 μm filters and the temperature during the experiment was stable at 25°C. The measurements were conducted at the scattering angle of 173° using a Zetasizer Nano ZS (ZEN3600) from Malvern Instruments (UK) equipped with a He-Ne laser (632.8 nm) using a noninvasive back scatter (NIBS) technology. For the process of the results the Malvern Zetasizer Nano software was employed which fits a spherical model of diffusing particles with low polydispersity and the mean diameter of the nanodroplets was calculated by the Stokes-Einstein law as mentioned before. Furthermore, the size and homogeneity of the formulated NEs was investigated over time in order to determine possible changes and the stability of the systems.

In spite the fact that DLS allows the detection of particle sizes even down to 1nm in diameter [407,408], it is unable to distinguish the aggregates from one single vehicle and does not provide information about the shape and morphology of the system [32]. Hence, it is necessary to implement additional structural techniques to obtain supplementary information in order to fully characterize the developed nanocarrier.

4.2.2.2. Electron Paramagnetic Resonance Spectroscopy (EPR)

Electron Paramagnetic Resonance is a spectroscopic technique based on the absorption of microwave radiation by paramagnetic centers with one or more unpaired electrons. Through this method it is possible to measure the energy of separation (splitting) of unpaired electrons, when exposed to a magnetic field. This technique is also referred to as Electron Spin Resonance (ESR) and is considered suitable for the study of structure and membrane dynamics of an interface. The implementation of EPR has been described for many applications provided that unpaired electrons exist including the study of free radical reactions [409,410], structural study of physicochemical systems [70,279,411] as well as biological systems [412,413].

As a principal, the spin of an electron is $m_s = \pm 1/2$ however, in the presence of magnetic field the electron could be oriented parallel or antiparallel to the magnetic field adopting the lower ($m_s = -1/2$) or higher ($m_s = +1/2$) energy state respectively. In EPR spectroscopy, when microwave energy is absorbed, a transition occurs between the two energy states which is described by the following equation (3):

$$\Delta E = h\nu = g\beta H_0 \quad (3)$$

where ΔE is the energy difference between the two states, h the Plank's constant, v refers to the radiation frequency of the microwaves, g is a dimensionless isotropic factor/coefficient, β is the Bohr constant, and finally H_0 represents the magnetic field intensity [414].

Specifically, in the field of NEs the investigation of the surfactants' monolayer properties is crucial hence, EPR spectroscopy using the spin-probing technique is a useful tool. This method is a valuable method since it is non-invasive and provides information concerning the localization of the bioactive molecules, the structure and dynamics of the surfactants' monolayer and also an indication of the ability of the nanocarrier under study to release the encapsulated compounds. EPR spectroscopy using the spin-probing technique plays an important role in the elucidation of the structure of surfactant interfaces near species with unpaired electrons, which are referred as spin-probes. Nitroxides are one of the most used categories of molecules as spin-probes since they possess the necessary unpaired electrons. In spite the fact that, they are free radicals they demonstrate exceptional stability due to the chemical protection provided by the methyl groups located near the nitroxide ring. In the present study, three amphiphilic fatty acid derivatives labelled at different positions of the aliphatic chain were used to probe membrane dynamics at different depths namely 5-, 12-

and 16- doxyl stearic acids (5-DSA, 12-DSA, 16-DSA) whose chemical structure is depicted in figure 28(a,b,c) below.

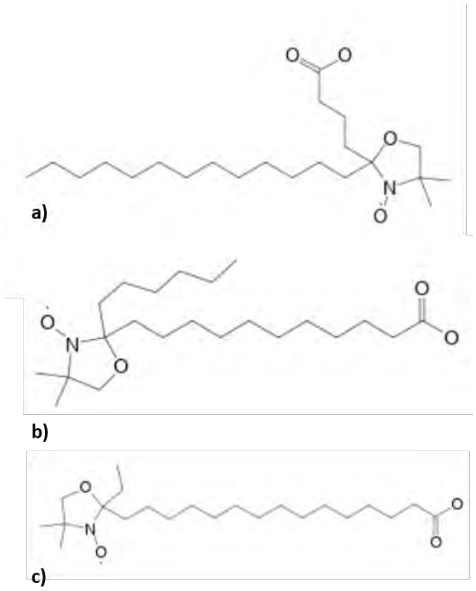

Figure 28. Molecular structures of the three nitroxides that were used as free radical in the present study namely, a) 5-DSA, b) 12-DSA and c) 16-DSA (source: https://spectrabase.com/).

These compounds have the ability to interact with the surfactant molecules creating the monolayer and provide spectra with three distinct peaks which give indirect information about the membrane dynamics closest to the surfactant tails (5-DSA) or the nanodroplets' oil core (16-DSA) depending on the position of the nitroxide ring. Since the obtained spectrum of each spin-probe is affected by its microenvironment, any change can by associated with structural changes of the NE for example absence or presence of an encapsulated bioactive compound. In figure 29, a characteristic EPR spectrum of 5-DSA is illustrated. From its analysis three values can be calculated. The correlation time τ_R (equation 4) which demonstrates the ability of the spin-probe to rotate, order parameter S (equation 5) which is indicative of the surfactants' monolayer rigidity and finally, the isotropic hyperfine coupling constant α_0 expressing the micro-polarity of the environment near the spin probe.

Specifically, parameter τ_R can be calculated by the following equation:

$$\tau_R = 6 \times 10^{-10}[(h_0/h_{+1})^{1/2} + (h_0/h_{-1})^{1/2} - 2]\Delta H_0 \quad (4)$$

where h_{+1}, h_o and h_{-1} represent the intensity of the three spectrums' peaks respectively and ΔH_0 refers to the width of the central line as illustrated in figure 29. This relationship can be

applied either for fast ($10^{-11} < \tau_R < 3\times10^{-9}$ s) or slow ($\tau_R > 3\times10^{-9}$ s) motion region however, for the first one is more accurate since they depict precisely the molecular motion of the spin probe [411].

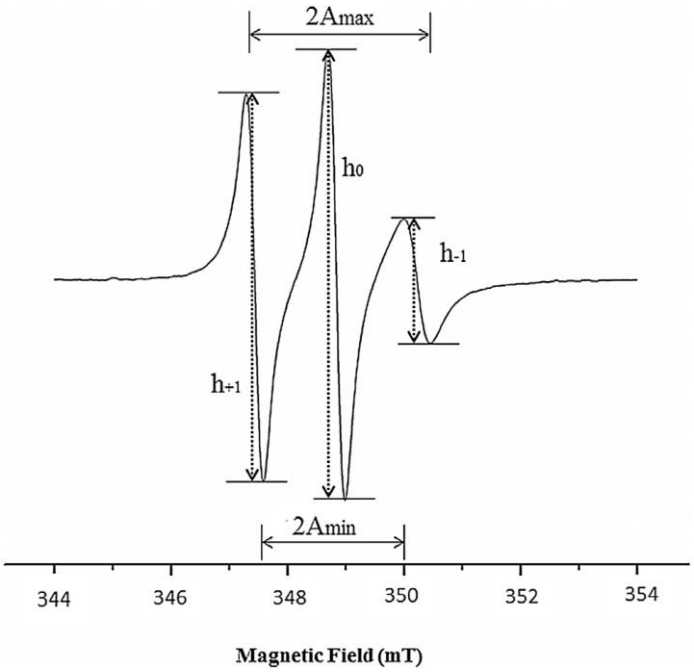

Figure 29. Illustration of a typical EPR spectrum of a nitroxide spin-probe with the three distinct peaks. Parameters A_{max} and A_{min} are also presented [415].

Order parameter S provides a measure of the spin probe's arrangement and can take values between 0 for the completely random state and 1 for the completely ordered state suggesting increase rigidity of the surfactants' monolayer. From the analysis of the obtained spectrum, using equation 5 order parameter can be calculated [411]:

$$S = (A_{||}-A\perp)/[A_{ZZ}-1/2(A_{XX}+A_{YY})](\alpha_o/\alpha'_o) \quad (5)$$

Where $A_{\|}$ refers to the half-distance of the outer EPR lines ($2A_{max}$) and $A_{\perp}$ represents the half-distance of the inner EPR lines and are the hyperfine splitting constants. Parameters A_{ZZ}= 33.6 G, A_{XX}= 6.3 G and A_{YY}= 5.8 G are the single crystal values. The ratio (α_o/α'_o) is the polarity correction where $\alpha_o = (A_{XX} + A_{YY} + A_{ZZ})/3$ and $\alpha'_o = (A_{\|} + 2A_{\perp})/3$ represents the isotropic hyperfine splitting constant for the spin probe in the membrane. The latter parameter (α'_o) depends on the polarity of the spin-probes' environment and is increasing when the nitroxide paramagnetic ring is located in a more polar environment [411].

To prepare the samples for the EPR measurements, initially stock solutions (2 mM) of each spin-probe (5-, 12-, 16-DSA) in ethanol were prepared. Following, appropriate amounts of the aforementioned stock solutions were inserted in eppendorf tubes. After ethanol evaporation, 1 mL of the NEs was added and let for 48 hours in order for the spin-probe to incorporate to the membrane of the surfactants. For the preparation of the respective hybrid systems the former NEs were incorporated into the chitosan hydrogels. Both the NEs and the hybrids had 0.02 mM final concentration of the spin-probes. EPR measurements were conducted at room temperature with an EMX EPR spectrometer (Bruker BioSpin GmbH, Germany) functioning at the X-Band (9.8 GHz). To obtain the EPR measurements both systems were inserted in a low dielectric constant quartz flat cell suitable for aqueous samples (Wilmad-LabGlass, Cortecnet Europe, France). The EPR settings were set up as follows: center field of 0.348 T, scan range 0.01 T, gain of 5.64×10^3, time constant of 5.12 ms, conversion time of 5 ms, modulation amplitude of 0.4 mT. The programs Bruker WinEPR acquisition and processing (Bruker BioSpin GmbH, Germany) were used to perform data collection and analysis respectively.

4.2.2.3. Confocal Fluorescence Microscopy (CFM)

The method of Confocal Fluorescence Microscopy is an analytical tool that can be used in diverse applications. It is most commonly used in the field of cell biology [416–418] however due to the advantages that this technique presents, efforts are being made to utilize it as well for the physicochemical characterization of pharmaceutical formulations such as microspheres, tablets, hydrophilic matrices and, colloidal nanodispersions [419]. Specifically, concerning the latter formulation, CFM has been employed for the investigation of structural changes or the detection of destabilization mechanisms [419].

In order to perform CFM an essential step is the labeling of the formulation under study using a suitable fluorophore. As fluorophores are characterized molecules which have the ability to absorb light energy with result the excitation of their orbital electrons to higher energy. Subsequently, when they return to their ground the absorbed energy is lost as emitted photons. Each of these molecules possess distinct spectral characteristics depending on their specific electronic configurations. Hence, a particular fluorophore is sensitive to a particular range of excitation wavelengths referred to as the excitation spectrum and in turn has the ability to emit fluorescence at longer wavelengths [419]. To obtain a CFM measurement an excitation laser beam targets the sample under study. A fluorescence light produced by the dye molecules is emitted directly back following the same optical path while passing through an aperture and then reaches the detector (photomultiplier). Due to the fact that the focal

point in the sample and the aperture are situated in conjugate planes the photomultiplier can detect only light derived from the focal plane since the light coming from other planes cannot pass through the aperture. Due to the described optical arrangement of the focal points this method is referred to as “confocal”. The sensitivity of this technique can be adjusted sinc416e by decreasing the size of the aperture, the stray or out-of-focus areas of the sample light that reaches the detector is minimized [416].

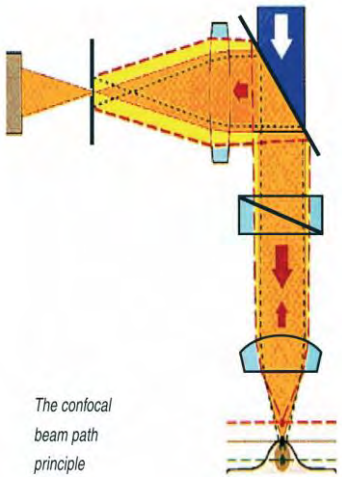

Figure 30. Schematic representation of the experimental set up of a laser fluorescence microscope and illustration of the confocal principle [416].

This method has attracted much attention recently for the morphological study of colloids since it presents sensitivity and selectivity due to the ability to label a specific phase of the dispersion using a particular fluorophore as a dye. Furthermore, it is considerably versatile and provides the possibility to image up to three separate fluorophores at once [419]. In addition, CFM is exceptionally valuable for the structural investigation of colloidal systems in their native state and in room temperature without the need to implement complicate conditions for sample preparation such as freezing or decreased pressure in contrast to other microscopic techniques like electron microscopy [420,421]. The implementation of CFM demonstrates favorable features compared to conventional microscopic techniques allowing improved visualization due to reduced blurring of the image, increased resolutions as well as enhanced signal-to-noise ratio [419].

In order to acquire visualization of the NEs’ oil phase and investigate whether its structure and size is affected by the incorporation into the hydrogel confocal fluorescence microscopy was performed. In spite the fact that this method is not extensively used for the imaging of nanodispersions without the simultaneous use of living cells, it was selected in the

present study as a preliminary imaging technique since it was simple and rapid. Firstly, the NEs and the respective hybrids in the absence of bioactive compound were prepared for visualization via the confocal microscope as follows. The lipophilic dye Nile red was used to stain the oil phase (1:1 mixture of IPM/EVOO) and then NEs and the corresponding NE-filled hydrogels were formulated as mentioned in previous paragraphs 4.2.1.1.1. and 4.2.1.2. respectively using the aforementioned oil phase. Subsequently, one drop of the stained samples was placed on a slide and covered with a cover slip cautiously in order to avoid the formation of air bubbles. All the samples were mounted on a confocal laser scanning microscope (Leica TCS SPE, Leica Microsystems, Heidelberg, Germany) and visualized with an excitation wavelength at 488 nm and emission wavelength at 500 nm. The LAS AF software (Leica Microsystems) was used for acquisition of the images.

4.2.2.4. Cryo-Electron Microscopy (Cryo-EM)

Cryo-Electron Microscopy (Cryo-EM) constitutes an invaluable tool for the investigation of the actual morphology of colloidal nanodispersions. It is widely used to study the structure of colloidal systems in terms of size and shape providing reliable data at the supramolecular level (1–2 nm resolution). This method is widely used especially for the elucidation of the structure of NEs in their native state since it has the ability to acquire detailed information about their internal structure as well as detect surfactant aggregates or other minor structural changes that would not be obvious with other methods [422,423].

A typical transmission electron microscope (TEM) could be described as an inverted light microscope with the difference that the sample is illuminated by an electron beam [424]. Specifically, the TEM operation is based on the illumination of a sample by an electron beam which is produced by an electron gun located at the top of the microscope column and focused on the sample by a system of electromagnetic lenses. The transmitted electrons are then projected onto a viewing screen or an image recording device providing the visualization of the sample. In this method, the contrast is achieved by the interaction of the electrons with the formulation under study. However, in order to obtain accurate imaging, the appropriate sample preparation is crucial. There are various ways to prepare a sample for visualization via TEM including negative staining, freeze-fracture and vitrification by plunge freezing and the appropriate method must be chosen conscientiously as different information can be obtained by each of them concerning the colloidal structures. In this study particularly, vitrification by plunge freezing was selected since it provides direct investigation of colloids in the vitrified, frozen-hydrated state which is very close to the native state of the NEs [425–427].

Furthermore, since electrons poorly penetrate matter, it is also essential to achieve a thin sample to obtain its morphological study.

The resolution can also be adjusted since it is correlated to the acceleration voltage of the electrons. Consequently, when the voltage is increased causes a decrease of the electrons' wavelength resulting in higher resolution and vice versa the contrast decreases when the acceleration voltage is increased since the scattering of the electrons is inversely related to their velocity. Hence, for the elucidation of the structure of colloidal nanodispersions the values of the applied voltage are usually between 80 and 200 kV.

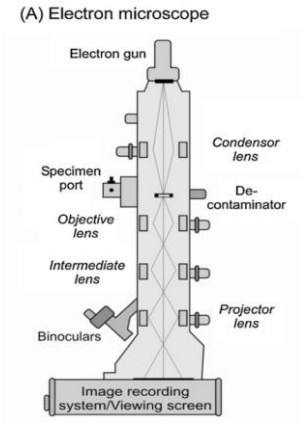

Figure 31. Illustration of an experimental set up of a transmission electron microscope [423].

In the present study cryogenic transmission electron microscopy method (Cryo-TEM) was implemented for the investigation of the CBD-loaded and empty NEs' morphology. For that purpose, quantifoil® R2/1 grids were used as a substrate. The grids were prepared using Vitrobot Mark IV System (Thermo Fisher Scientific) with 95% humidity, ashless filter paper (Standard Vitrobot Filter Paper, Ø55/20mm, Grade 595) and blotting time of 4 sec [428]. After their preparation they were then loaded in a ThermoFisher Scientific Vitrobot Mark IV grid plunger. The chamber of the grid plunger was adjusted at 4 °C and >95% relative humidity. A 3.5 μL aliquot from each sample was applied on the prepared grids and blotted using type 595 filter paper for 6 seconds. The blotted grids were plunged in liquified ethane were further assembled in autogrids and loaded inside the ThermoFisher Scientific Glacios 200 kV CryoEM under cryogenic conditions. The micrographs were acquired at the pixel size of 3.17 Å/pixel and 30 e/Å2 electron dose using ThermoFisher Scientific EPU V 2.11 software. The experiments were performed at the Martin Luther University Halle-Wittenberg in Halle (Saale), Germany.

4.2.2.5. Small-angle X-ray Scattering (SAXS)

SAXS is a well-established, rapid and non-destructive analytical method implemented for the structural investigation of nanostructures in liquids and solids. It has the ability to probe the colloidal length scales of 1–1000 nm and therefore is an appropriate method to determine the size and the structure of colloidal systems such as NE and NE/HG.

This method demonstrates significant versatility providing the ability to investigate the morphology of a wide range of formulations. Some of the most commonly studied systems using SAXS are colloids, polymers, minerals and metals as well as samples containing biological materials such as proteins, and peptides. Due to its widespread applicability SAXS has evolved to a powerful tool in the fields of pharmaceutical research, material science and biochemistry [429–432]. This technique is frequently used since it presents high sensitivity to particle size. More specifically, a radius increase by a factor of 10 could affect the signal intensity at zero angle by a factor of 10^6. In addition, the sample preparation is easy and straightforward in contrast to other structural methods that may require intricate procedures such as crystallization, vitrification or, fixation decreasing the risk of artefacts induced by preparation [429]. However, SAXS is more beneficial when acting as a complementary technique to confirm structural results already obtained by other techniques such as DLS and (cryo) electron microscopy (EM) [433] .

The principle of operation of a SAXS instrument is illustrated below in figure 32. Initially, an aligned monochromatic beam of X-rays encounters the sample. The elastic collision between the existing inhomogeneities in the nanometer range and the X-rays cause radiation scattering at low angles generally between 0.1-10° creating a scattering pattern which is picked up by a detector situated behind the sample. More specifically it is located perpendicular to the direction of the beam that hits the sample. The obtained scattering pattern provides information concerning the morphology, shape, and size of the system under study [431,434,435].

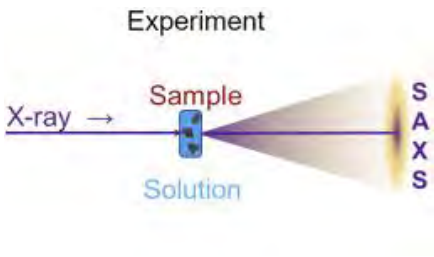

Figure 32. Schematic representation of the principle of method of a SAXS experiment [431].

From the obtained SAXS profile results the scattered radiation intensity I(q), which is measured as a function of the scattering vector q which is described by the following equation (6) [431,436]:

$$|\mathbf{q}| = \frac{4\pi}{\lambda}\sin\theta \quad (6)$$

With λ being the wavelength and θ the scattering angle.

A well-established method which is commonly used for the interpretation of SAXS data is the Indirect Fourier transformation [437]. However, it is applicable only for the study of dilute solutions where the particle interactions are neglectable resulting a direct relation between the particle and the achieved scattering data. Specifically, for the evaluation of SAXS data concerning monodisperse, homogeneous, globular particles the scattering intensity can be defined by the following equation (7):

$$I(q) = NS(q)P(q) \quad (7)$$

Where N is the number of particles, S(q) refers to the structure factor which corresponds to the interparticle scattering and P(q) is the form factor expressing the intraparticle scattering. However, for ideally diluted solutions, structure factor S(q) is a constant and equals one [438].

In the present study, Small Angle X-ray Scattering (SAXS) experiments were carried out on a XEUSS 2.0 device (XENOCS, Grenoble, France). Coupled to a FOX 3D single reflection optical mirror centered on the Cu Kα radiation (λ = 1.54 Å), the GeniX 3D source delivers an 8 keV beam which is collimated and defined by a set of 2 motorized scatterless slits. The samples were put in thin glass capillaries (optical path 2 mm) which were then airtight sealed. The data were collected by a two-dimensional PILATUS-300k detector (DECTRIS, Switzerland) placed at different distances from the sample, giving access to the angle range 0.056° – 2.26° (0.04 nm^{-1} – 1.6 nm^{-1}*).* A thermostatically controlled module makes it possible to carry out studies in T from -30 °C to 150 °C. The measurements were performed at room temperature. The experiments were conducted at the Centre de Recherche Paul Pascal (CRPP) at the University of Bordeaux in France.

4.2.3. Biological evaluation

A particularly important factor for the development of nanodispersions to be used as delivery vehicles for various bioactive compounds of pharmaceutical interest is the biocompatibility of the carrier itself. In addition, the ability of the nanocarrier to effectively release the bioactive compounds is of paramount importance particularly when the system is intended for topical or transdermal delivery. To that end, a biological evaluation was carried out *in vitro* and *ex vivo* in order to evaluate the suitability of the formulated nanocarriers as delivery systems for cannabidiol. The most stable NEs and NE-filled hydrogels demonstrating promising structural characteristics were investigated in terms of cell viability *in vitro* using two different cells lines as presented below. Subsequently, both the NEs and the respective NE/HGs with encapsulated cannabidiol were evaluated using an *ex vivo* permeation model and the differential tape stripping technique in order to estimate the amount of cannabidiol released from the carriers and retained by the skin. The combination of the methods that will be presented below provides a valuable indication about the suitability of the developed nanodispersions to act as effective delivery systems.

4.2.3.1. Cell culture

In order to conduct the cell viability assessment, initially, cell culture was prepared under the appropriate conditions and using the suitable culture media. Two different cell lines were used for the cytotoxicity evaluation of the developed nanodispersions. Specifically, human nasal cell line RPMI 2650 (CCL-30) between the passages 16-30 was provided by Prof. Fabio Sonvico (University of Parma, Parma, Italy) and WS1 human skin normal fibroblasts purchased from the American Type Culture Collection (ATCC, Manassas, VA, USA) and used for the cell culture between passages 2-5. The cell lines were grown in monolayer cultures using complete DMEM and EMEM media (containing 2 mM L-glutamine, 1 mM sodium pyruvate, and 1500 mg/L sodium bicarbonate) respectively. Both culture media were additionally supplemented with 10% (*v*/*v*) FBS and 1% (*v*/*v*) penicillin/streptomycin as an antibiotic mixture. Furthermore, 1% (v/v) non-essential amino acid solution was also added for the preparation of the DMEM culture medium. The cells were cultured in flasks filled with the appropriate amount of the respective media depending on the size of the culture surface and were incubated at humidified atmosphere at constant temperature conditions of 37^{o}C with 95% air and 5% CO_2 supply.

Subsequently, in order to detach the cells from the surface of the flask, trypsinization was performed. Initially, the culture medium was removed and the cells were rinsed twice with 1XPBS solution and then a solution of the enzyme trypsin was added to detach the

adherent cells from their growth surface. Since trypsin is a proteolytic enzyme, it has the ability to break down the proteins specifically at the carboxyl side of the amino acids' lysine or arginine. This leads to the dissociation of the adherent cells from the bottom of the flask. The exact time needed for the trypsinization depends on the cell type but it normally lasts no more than 5 minutes. When the cells are detached from the surface of the vessel, trypsin has to be deactivated thus culture medium is added which stops the action of trypsin due to the presence of serum. Then, the dispersed cells in the trypsin-culture medium solution are collected, centrifuged (1800 rpm, 5 minutes, 25^{o}C) and the supernatant is removed. Finally, the cell pellet is resuspended in medium and the number of cells is measured using a Neubauer counting chamber.

4.2.3.1. Cell viability assay (MTT assay)

A crucial factor during the development of novel nanocarriers is their biocompatibility both in the absence and presence of the encapsulated bioactive compound. Hence, in order to evaluate the potential toxicity of a system and determine the maximum concentration which is safe for administration, *in vitro* biological assays using different human or animal cell lines are applied [439]. Specifically, cytotoxicity assays are broadly utilized for the development of new formulations of pharmaceutical interest [440] in order to assess their toxicity.

Cytotoxicity assays are one of the fundamental tools for the identification of toxic compounds *in vitro* and they are frequently selected since they are rapid, cost-effective and do not involve hazardous reagents [439]. In principle, these methods are based on the detection of direct or indirect changes in certain biological functions of the cells such as number of live and dead cells, enzyme activity and cell proliferation and their correlation with the cytotoxic activity of the administered nanodispersion and/or bioactive compound [440]. These methods can be categorized depending on the measured feature in two categories. The first one includes the techniques measuring the total protein content such as Kenacid Blue test and sulforhodamine B staining while the second group contains the methods which are based on the evaluation of the redox activity of the cells like Alamar Blue assay and XTT and MTT tests [439].

In the present thesis MTT assay was implemented for the investigation of the potential cytotoxicity of the formulated nanodispersions both the NEs and the NE/HGs in the absence and presence of CBD. MTT test which was first reported in 1983, is a quantitative colorimetric assay that enables the assessment of toxicity of an administered system or compound via the indirect measurement of the number of living cells [441]. This technique is

frequently used for cytotoxicity evaluation since it is quick, enables the simultaneous testing of a large number of samples and presents high sensitivity [440]. In principle, this assay is based on the conversion of tetrazolium salt (MTT) into water-insoluble formazan crystals due to reduction of pyridine occurred by specific dehydrogenase enzymes of the living cells [442,443]. This process can be also detected visually since the initial yellow color of MTT is transformed into an intense violet-colored solution when formazan crystals are solubilized with the use of appropriate solvents like isopropanol or DMSO [439].

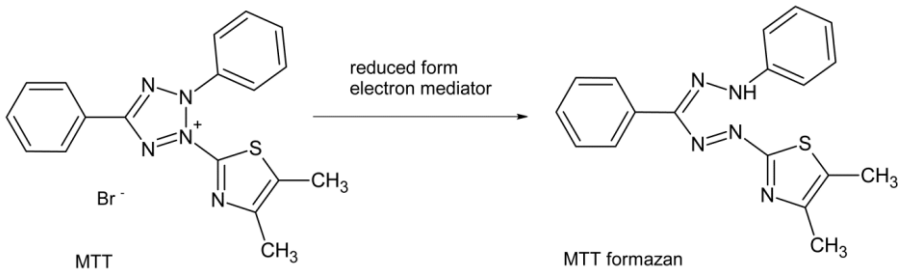

Figure 33. Reaction occurred when MTT is reduced to formazan crystals [444]

Since only cells that are metabolically active have the ability to carrie out the reduction of pyridine, MTT assay provides an indication of the surviving cell number after the administration of the system of interest [439,445] .

For the evaluation of the cytotoxic effects of the systems under study initially the appropriate number of the selected cells with 200 μl of the culture medium were placed in 96-well plates and left for 24 hours to adhere on the bottom of the wells. After that period of time, the culture medium was removed and properly diluted samples corresponding to increasing concentrations of the systems into the culture medium were prepared and administered in each column of the plate. The first one was renewed with plain culture medium and was used as the control., The plates were incubated for 72 hours at the end of which the inhibition of cell proliferation was evaluated after treatment by the MTT (3-(4,5-Dimethyl-2-thiazolyl)-2,5-diphenyl-2H-tetrazolium bromide) assay according to the manufacturer's standard protocol: Briefly, a stock solution was prepared by solubilisation of MTT in PBS and proper amount was added to each well. The plates were then incubated for 3 hours. The MTT solution was then discarded and the amount of the produced formazan crystals was quantified spectrophotometrically after their solubilization in a mixture of isopropanol/DMSO (1:1).

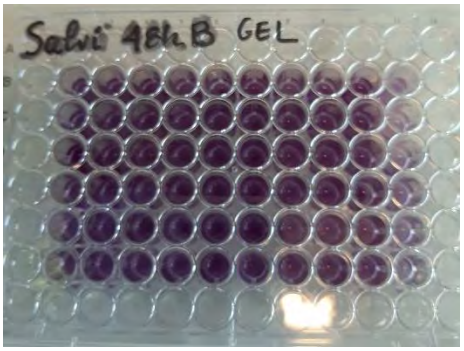

Figure 34. Picture of a 96-well plate during an MTT assay conducted for the present thesis. The more intense the purple color, the greater the percentage of cell viability.

Finally, the absorbance of the converted dye was measured at 570 nm and the cell viability was calculated by the following equation and was expressed as a percentage.

Cell viability (%) = (OD of treated cells)/ (OD of control) x 100

where, OD is the optical density.

Depending on the calculated absorption values, the toxicity of the administered system is estimated, the concentrations resulting in viability less than 80% are considered as toxic [439].

4.2.3.2. In vitro and ex vivo permeation studies

In the present study, the transdermal route was selected for the administration of cannabidiol. As mentioned before in Chapter 1.7, this delivery route offers many advantages since it is simple and non-invasive offering the patients the possibility of self-administration. A crucial parameter that needs to be evaluated during the development of formulations intended for transdermal delivery is the ability of the delivery system to release the encapsulated compound of interest. For that reason, the use of vertical Franz diffusion cells is widely employed providing an insight of the release model. A typical experimental setup as well as a more detailed illustration of a Franz cell are depicted in figure 35. As can be observed the cell consists of a donor compartment where the formulation under study is placed and a receptor compartment filled with a buffer solution suitable for the experiment. In the present study it was a mixture of PBS 1X solution and ethanol 96% V/V (1:1) which was preheated and kept under constant stirring at 500 rpm using a magnet. Between the donor and the receptor compartment was placed a synthetic cellulose membrane with molecular weight cut-off 14,000 and average flat width 43mm. The membrane was hydrated in the buffer solution for 24 h before the experiments were conducted. The cells used for the implementation of the permeation study using a synthetic membrane had an effective diffusion surface area of 0.785

cm^2 (1 cm diameter orifice) and were filled with 5 mL of the buffer solution. The cells were surrounded by water-jacket and connected to a thermostatically controlled water bath in order to maintain the temperature of the solution stable at 32 ± 0.5 °C. With this method the preliminary study was carry out in order to investigate the release profiles of VD and CU from the developed NEs and the respective NE/HGs.

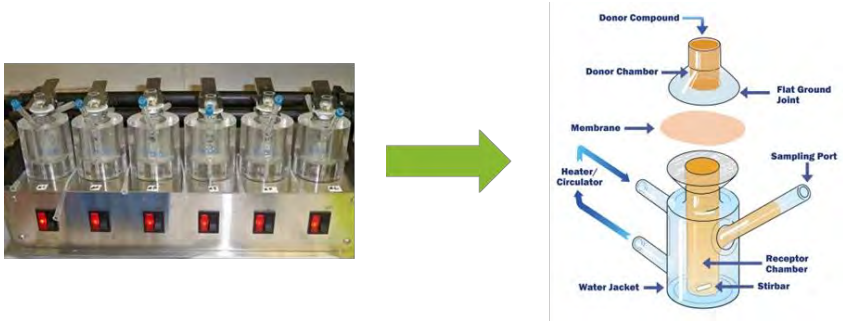

Figure 35. Vertical Franz diffusion cell experimental setup and schematic representation of a cell.

However, synthetic membranes usually are not able to provide results comparable to the respective in vivo studies since it is not possible to display the intricate interactions between the skin and the formulation under study [446].

For that reason, an in vitro permeation protocol was implemented in the present study using full-thickness porcine ear skin as the model membrane in order to properly evaluate the skin permeation of CBD from the NEs and the corresponding NE/HGs. The porcine ears were purchased from a regional slaughter house in Serbia and were processed appropriately in order for the SC to remain as intact as possible. Firstly, immediately after slaughter the porcine ears were washed with cold tap water, dried cautiously with soft tissue, wrapped with aluminum foil and then stored at –20 °C for preservation until use. For the implementation of the *in vitro* protocol, the porcine ears were defrosted at room temperature and then to achieve a sufficiently clear surface the hair were shortened carefully with electric trimmer without destroying hair follicles or damage the SC. Subsequently, as illustrated in figure 36, the full-thickness skin was detached from the cartilage using a scalpel and punched with a custom-made spherical cutter of a 25 mm diameter to obtain discs with the appropriate size in order to be used as membranes for the experiment. Furthermore, trans-epidermal water loss (TEWL) (Tewameter® TM 210; Courage+Khazaka, Köln, Germany) was measured in order to ensure the integrity of the skin barrier. The obtained full-thickness skin discs were placed on modified Franz diffusion cells with a surface of 2.01 cm^2 and a receptor chamber of 12 mL volume (Gauer Glas, Germany) and the water-bath temperature was set at a constant

of 32 °C in order to corespond with the mean temperature of the skin surface. The porcine full-thickness skin was placed between the donor and receptor compartments with the SC towards the first one and after 30 min of equilibration, the donor chambers were filled evenly with 0.5 mL of the systems (CBD-loaded NEs or NE/HGs). It should be noted that as can be observed below in figure 36, the donor compartments were covered with Parafilm® to avoid evaporation.

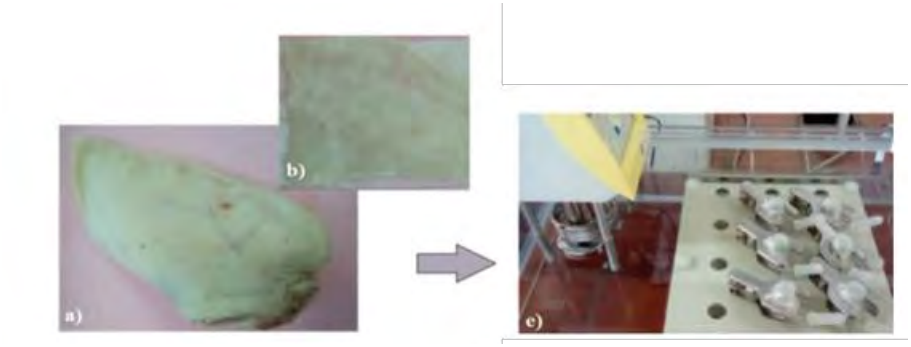

Figure 36. Steps followed for the implementation of ex vivo permeation study with porcine ear skin as the model membrane.

Every 2 hours samples of 500 μL volume were collected, for a total of 30 hours of experiment with the initial time point being the formulation application. Each time after sampling the receptor compartments were filled again with an equivalent volume of fresh pre-warmed medium. To quantify the amount of CBD in the receptor chamber through time a LC-MS/MS method described in the following (paragraph 4.2.3.5.) was used. From the obtained results were evaluated the release profiles from the two nanocarriers under study and were calculated the steady-state flux (J_{ss}), cumulative amount of CBD permeated through the skin at the end of the 30 h of the experiment (Q_{30h}), and permeability coefficient (K_p) [447]. The experiments were carried out at the Department of Pharmaceutical Technology and Cosmetology of the University of Belgrade in Serbia.

4.2.3.3. Tape stripping experiments

In order to evaluate the two systems under study in terms of CBD penetration through the SC the technique of tape stripping was implemented using porcine ear [448]. For the specific experiment was used a porcine ear preserved as described in the previous chapter (4.2.3.3.). The ear was initially thawed, the hair was removed with a trimmer, and then it was fixed on Styrofoam plates without separating the skin from the cartilage. For the determination of the appropriate time point to administer the formulation the TEWL was measured periodically using a Tewameter® TM 210 and when it reached a value of approximately 15 g.m-2.h-2 [449] the CBD-loaded systems were applied carefully on the

marked skin sites like shown in the picture of demonstrated below in figure 37. In order to obtain more accurate results five independent experiments were performed.

Figure 37. Picture of a differential tape stripping performed for the present thesis. The green circles mark the surfaces to which the CBD-loaded NE and the respective NE/HG have been administered.

Both the *in vitro* permeation study using Franz diffusion cells and the penetration experiment described in this paragraph can be performed either under finite or infinite dose regiment depending on the amount of the bioactive substance and in general the formulation that is applied on the skin [450]. Both these administration methods present different advantages and drawbacks and they have different applications in transdermal delivery studies. Specifically, as finite dosing is characterized the application of a small volume of formulation resembling the consumer exposure and provides evaluation of the bioactive concentration in different skin layers and its total amount present in the receptor compartment after 24 h. On the other hand, infinite dose regiment represents the application of an amount of formulation that exceeds the typical exposure conditions and provides information concerning steady-state flux, diffusion constant and permeability [450,451]. While the first application methodology resembles the consumer administration, it presents erratic bioactive concentration due to its evaporation or penetration/permeation through the skin. However, when the aim is the investigation of the fundamental permeation characteristics or the evaluation of the effects of penetration enhancers on transdermal absorption of the bioactive compound under study infinite dose regiment is commonly employed.

The present study was performed under infinite dose regimen, using the same dosing conditions as for *in vitro* skin permeation study (1 mL of each of the formulations were left on the skin for 2 h (effective diffusion area: 4.02 cm^2)) in order to preserve a constant rate of absorption of the CBD through the skin or as it is also referred to the steady-state flux and with this method it is generally accepted that there is no change in the bioactive concentration within the formulation during the experiment [452]. To determine the quantity of SC removed,

each adhesive tape was weighted precisely before starting the tape stripping. When the 2 h incubation time was over, the excess nanodispersions were carefully removed using dry cotton swabs and started the procedure of gradual removal of the SC, for which were used 30 adhesive D-squame® discs (CuDerm Corporation, USA). For this process the adhesive tapes were pressed onto the skin with a roller to avoid any wrinkling and following were removed with a fast motion. After that the weighing was repeated and, each tape was inserted into a centrifuge tube to extract the CBD. To obtain that, 4 ml of ethanol (70%, v/v) was added in each tube and followed sonication (Sonorex RK 120H, Bandelin, Berlin, Germany) for 15 min and the centrifugation at 4000 rpm for 5 min (Centrifuge MPW-56; MPW Med. Instruments, Warszawa, Poland). The final supernatant was accumulated and analysed for CBD content using LC-MS/MS method that will be presented below in paragraph 4.2.3.5. [448]. The experiments were performed at the Department of Pharmaceutical Technology and Cosmetology of the University of Belgrade in Serbia.

4.2.3.4. Liquid chromatography- mass spectrometry (LC MS/MS Method)

In order to detect and quantify the CBD contained in the samples obtained by the in vitro permeation study (paragraph 4.2.3.3.) and the tape stripping experiments (paragraph 4.2.3.4.) the high-pressure liquid chromatography method was implemented in combination with mass spectrometry also referred as LC-MS. In general, liquid chromatography (LC) being one of the most valuable tools of analytical chemistry is widely used since it provides the ability to separate, identify and quantify the substances of a complex sample dissolved in a liquid [453]. This method is widely used since it is adaptable, demonstrates high sensitivity and provides the ability to analyze non-volatile and thermosensitive species [454,455].

Specifically, High Performance Liquid Chromatography (HPLC) was implemented in the present study. In this method the sample is inserted into the instrument through an injection valve and eluted into the column by the mobile phase which is a solvent forced into the column by a high-pressure pump. The separation takes place in the mobile phase and the effluent of the column is guided to a detector generating a signal which in turn is gathered by a software, processed and finally converted into a chromatogram [454]. The use of high-performance liquid chromatography in combination with mass spectrometry (HPLC–MS) or in our case tandem mass spectrometry (HPLC–MS–MS) has proven to be the analytical method of choice for an abundance of assays implemented in various steps of drug discovery [456]. The main MS instrumentation is depicted below in figure 38 and includes firstly a sample insertion system and, an ion source into which the samples' components are transformed to positive or negative ions. These are then accelerated towards the third MS segment the mass

analyzer where the ions are separated based on their mass to electrical charge ratio which is represented by the relationship, m/z. The fourth part is the detector which receives the separated ions and transforms the ion current into electrical signals which are then processed through the final MS components the data system.

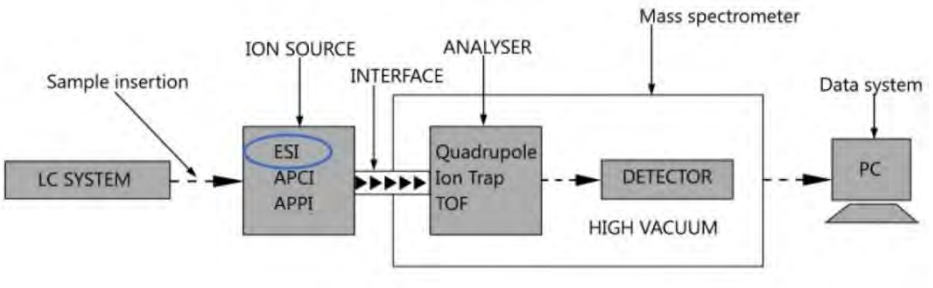

Figure 38. Schematic representation of the basic instrumentation of a typical LC-MS.

To determine the CBD in aliquots obtained by the *in vitro* penetration and permeation experiments an LC-MS/MS method was performed. A liquid chromatographic system Accela 1000 (Thermo Fisher Scientific, San Jose, California, USA) was used which consists of an auto sampler and quaternary pump. Chromatographic separation was obtained using Infinity Lab Poroshell 120 EC-C18 (100 mm x 4.6 mm, 2.7 µm; Agilent Technologies, USA) at 40 °C. To achieve isocratic elution at flow rate of 500 µL/min a mixture of acetonitrile and 0.1% formic acid (80:20, v/v) was used. The complete analysis time was 6 min. For the mass analysis was used a TSQ Quantum Access MAX triple quadripole spectrometer equipped with electrospray ionization source and worked with nitrogen as nebulizing gas. ESI source parameters were optimized by syringe infusion (20 µL/min) of CBD standard solution. For data acquisition selected reaction monitoring (SRM) positive scan mode was used. ESI source and mass spectrometry parameters were the following: spray voltage 3500 V; vaporizer temperature 400 °C; sheath gas pressure 50 units; ion sweep gas 0 units; auxiliary gas 45 units; ion transfer capillary temperature 250 °C; capillary offset 35 units; tube lens offset 50 units; skimmer offset 0 units; peak width relating to resolution 0.7 for Q1; scan with (m/z) 0.02; scan time 200 ms. Xcalibur software v. 2.1.0.1139 was used for data acquisition and processing (Thermo Fisher Scientific, San Jose, CA, USA). Mass spectrometry was employed in order to detect specific ions for analyte identification. MS full-scan mass spectra indicated that in ESI source [M+H]+ was the dominant ion for CBD (m/z 315.3). The setting of SRM transition channel for CBD monitoring was selected product ions at m/z 193.2 (collision energy was 19 V). The experiments were implemented at the Department of Pharmaceutical Technology and Cosmetology of the University of Belgrade in Serbia.

Chapter 5

Experimental results & Discussion

Chapter 5 –Experimental results & Discussion

5.1. Nanoemulsions as carriers of naturally derived lipophilic bioactive compounds

In the present thesis, the main goal was the formulation of stable nanocarriers, suitable for the encapsulation, protection, and release of diverse lipophilic bioactive compounds. The ultimate objective was the development of a nanodispersion with improved characteristics that could provide enhanced delivery of the bioactives under study. Specifically, as mentioned in previous chapters (Chapter 1.5. and 4.2.1.1.1.), three different molecules with the potential to act as therapeutic agents, namely vitamin D_3 (VD), curcumin (CU) and cannabidiol (CBD) (figure 39) were selected as model compounds in order to confirm the ability of the formulated nanodispersions to act as delivery vehicles.

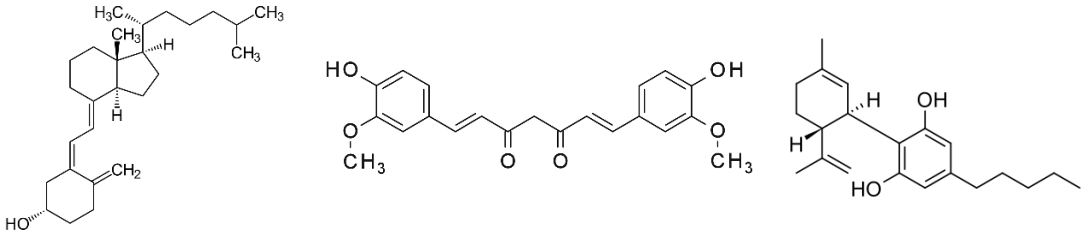

a) b) c)

Figure 39. Chemical structure of the encapsulated model lipophilic compounds a) vitamin D_3, b) curcumin and, c) cannabidiol.

Initially, O/W NEs were developed using non-toxic and biocompatible ingredients. As the oil phase were selected isopropyl myristate (IPM), extra virgin olive oil (EVOO), and a mixture of these two. At first, a concentration of 2 % w/w of oil phase was selected which was subsequently increased up to 4 % w/w to enable the encapsulation of a higher concentration of the bioactives. For the stabilization of the developed systems, a combination of hydrophilic and lipophilic surfactants including Tween 80 (T80), Labrasol (LS), and Maisine (MS) was used at a concentration of 5% w/w. In some cases, Transcutol at a concentration of 1 % w/w was also added as a co-surfactant and solubilizer to enhance the stability of the formulated NEs and the solubilization of the encapsulated compounds. The exact composition of the O/W NEs developed in the present thesis is mentioned in Table 2 (Chapter 4.2.1.1.1.). All the components of the systems were selected bearing in mind their potential health benefits (in the case of EVOO) or toxicity in order to develop biocompatible formulations. Particularly, T80 is a non-ionic surfactant commonly utilized for the development of stable and biocompatible O/W NEs [395,457,458]. Moreover, all the systems contained a 2:1 mixture of two other non-

ionic surfactants namely Labrasol (caprylocaproyl polyoxyl-8 glycerides) and Maisine (glyceryl monolinoleate). This combination was considered appropriate since caprylocaproyl polyoxyl-8 glycerides have been previously reported in the literature as suitable for the formulation of biocompatible O/W NEs [77,459] while glyceryl monolinoleate is a vegetable oil derivative.

It is well established in the literature that using a combination of surfactants leads to increased solubilization of the oil and aqueous phases resulting in the formulation of more stable systems [460,461]. Thus, a mixture of surfactants with different hydrophilic lipophilic balance (HLB) values presented below in table 4, were selected for the preparations of the O/W NEs developed in the present thesis.

Table 4. Surfactants and co-surfactants used for the formulation of the O/W NEs and their respective HLB values.

Surfactant	HLB value
Tween 80	15.0
Labrasol ALF	12.0
Maisine CC	1.0
Lecithin	4.0
Transcutol HP	4.2

When a mixture of surfactants is used for the preparation of a NE, the HLB value resulting from this combination depends on the percentage and the HLB value of each individual surfactant. More specifically, the following equation (9) is applied for the calculation of the HLB value of a mixture of two or more surfactants:

$$HLB_{desired} = (\%\ \text{surfactant A}) \times (\text{HLB surfactant A}) + (\%\ \text{surfactant B}) \times (\text{HLB surfactant B}) \quad (9)$$

Thus, in the present thesis, the HLB value of the surfactant mixture Tween 80/Labrasol/Maisine was calculated using the aforementioned equation and was determined equal to 11 which is a value capable of producing O/W NEs [462]. An attempt was made to use the hydrophilic T80 and the lipophilic lecithin as a mixture of surfactants for the preparation of stable biocompatible systems since the latter is widely used as a biocompatible and biodegradable emulsifier in various pharmaceutical, food and cosmetic products [70,77,463]. The resulting HLB of the Tween80/Lecithin mixture was also calculated as aforementioned and despite the fact that it was found equal to 14 which is a slightly higher value, it did not demonstrate increased stability.

5.2. *Nanoemulsions as carriers of naturally derived lipophilic bioactive compounds*

5.2.1. Stability study of O/W nanoemulsions by Dynamic Light Scattering (DLS)

Since NEs with different compositions were developed implementing either high- or low-emulsification methods the study of their stability was essential. Stability is a crucial factor for the use of a NE as a carrier for bioactive compounds. Thus, DLS was employed for the study of all the formulated systems in terms of size and homogeneity (PdI) which are indicative of their overall stability.

In total, eight O/W NEs were developed. Four NEs (H1, H2, H3, H4) were formulated using high-pressure homogenization as the high-energy method and the other four (L1, L2, L3, L4) were formulated through isothermal spontaneous emulsification which was the low-energy method. All the developed NEs, were measured with DLS immediately after their preparation and at different time intervals in order to determine their initial size and homogeneity as well as their changes over time. In table 5 below are presented the days of storage stability for each NE as well as the hydrodynamic diameter and PdI of the formulated NEs in the absence of bioactive compounds on the first day of their formulation compared to the last day they appeared stable. All the formulated systems demonstrated PdI < 0.250 indicating satisfactory homogeneity. Regarding the droplet size and the stability of the developed NEs there are indications that they are strongly affected by the formulation method as well as the presence of the co-solvent transcutol and the type of the selected oil phase.

More specifically, concerning the low-energy NEs (L1-L4) it was observed that L1 that contains 2% IPM in combination with the co-solvent transcutol demonstrates lower PdI values and adequate stability remaining optically clear for 60 days. On the other hand, when transcutol was omitted and simultaneously a part of the oil phase is replaced with EVOO like in the case of L2, higher values of both PdI and droplet size occur and as demonstrated in figure 40 a sharp increase is observed in both the PdI and the droplet size leading to rapid destabilization after 22 days. However, since there are indications in the literature suggesting that transcutol may present toxicity [464–466], efforts have been focused on achieving the preparation of stable systems without this ingredient. In addition, the use of higher concentrations of the oil phase was investigated in order to obtain the solubilization of a higher amount of bioactive substances. Hence, NEs L3 and L4 were stabilized with 5% w/w of

the same mixture of surfactants but different oil phases. More specifically, the L3 contained 4% w/w IPM while the L4 contained 4% w/w of a 1:1 IPM and EVOO mixture. The presence of EVOO in NE L4 leads to higher PdI value and increased droplet size (0.237 ± 0.009 and 204.0 ± 5.1 nm) as compared to NE L3 (0.155 ± 0.004 and 0.155 ± 0.004 nm), however L4 remained stable for an additional 10 days.

Table 5. Days of stability, PdI, and size of all the developed NEs.

Systems	Days of stability	PdI (Day 0)	PdI (final day)	Size (nm) (Day 0)	Size (nm) (final day)
H1	30	0.088 ± 0.013	0.079 ± 0.009	142. 9 ± 4.6	318.6 ± 2.5
H2	50	0.225 ± 0.007	0.226 ± 0.002	220.5 ± 4.8	240.2 ± 1.9
H3	50	0.201 ± 0.003	0.199 ± 0.008	241.6 ± 1.4	231.3 ± 1.4
H4	60	0.212 ± 0.014	0.090 ± 0.032	139.1 ± 7.6	260.9 ± 4.4
L1	60	0.092 ± 0.003	0.080 ± 0.010	78.6 ± 0.2	292.7 ± 0.6
L2	22	0.122 ± 0.007	0.235 ± 0.012	41.8 ± 0.3	570.7 ± 23.2
L3	80	0.155 ± 0.004	0.086 ± 0.007	62.1 ± 0.9	154.9 ± 0.5
L4	90	0.237 ± 0.009	0.170 ± 0.022	204.0 ± 5.1	382.6 ± 11.3

On the other hand, when NEs formulated using the high-energy technique (H1- H4) were tested, much larger oil droplets were observed in comparison to the respective systems prepared with the low-energy method. More specifically, when NEs were prepared with the same composition as L1 ones but implementing the high-energy technique (H1) a low polydispersity (<0.1) was indeed achieved however the resulting hydrodynamic diameter was 142.9 ± 4.6 nm which was significantly higher compared to the diameter of L1 (78.6 ± 0.2) and remained stable for half the time. As aforementioned, the NE L3 that was developed by omitting transcutol and containing a higher amount of oil phase which also included EVOO, presented Increased stability by 1 month. hence the respective NE H3 was prepared by HPH. Even though the two systems (L4 and H3) contain the same components, the high-energy one exhibited lower polydispersity values (0.201 ± 0.003) compared with the low-energy system (0.237 ± 0.009), it presented larger nanodroplets and remained stable for fewer days. The comparison of the above low- and high-energy NEs provides a strong indication that the formulation method affects the physicochemical characteristics of the developed systems. In addition, by the formulation of NE H4 was observed that the addition of transcutol provided a decreased nanodroplet size, but did not contribute significantly to the improvement of the homogeneity or stability of the system. Thus, in an attempt to develop a NE comprised basically of ingredients of natural origin such as EVOO and the natural emulsifier lecithin in combination with Tween 80 system H2 was prepared. Although it exhibited satisfactory

polydispersity (0.225 ± 0.007) and hydrodynamic diameter (220.5 ± 4.8 nm) the fact that energy input was inevitable for its formulation and remained stable for fewer days were decisive factors for which the system L4 was eventually selected for further investigation.

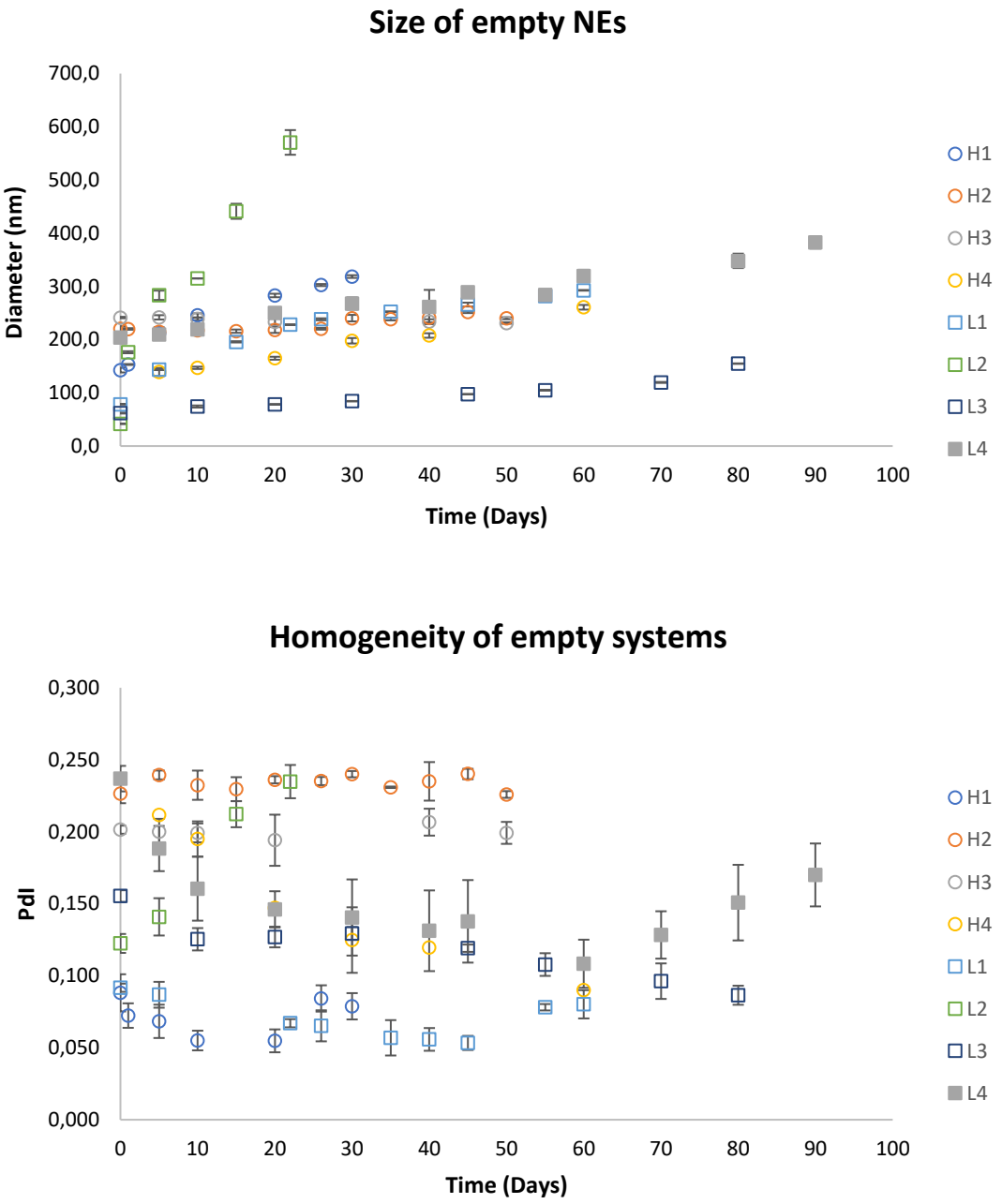

Figure 40. DLS study of O/W NEs: a) Droplet size and b) polydispersity index (PdI) as a function of time.

5.2.2. Stability study of loaded O/W nanoemulsions by Dynamic Light Scattering (DLS)

In order to determine the suitability of the formulated NEs to act as carriers of lipophilic bioactives two model compounds of pharmacological interest were encapsulated to conduct the preliminary study. Namely vitamin D3 and curcumin were encapsulated into the oil cores of low-energy O/W NE L1 as described previously in Methods (Chapter 4.2.1.1.1.) both at a concentration of 1 mg/g. The effect of their presence on polydispersity, droplet size, and stability was examined using DLS. As described in previous chapters of the introduction, these parameters are crucial since they affect various properties of the nanocarriers. Their overall efficacy to act as delivery vehicles via different administration routes, their uptake and permeation through the epithelia and their absorption profile are directly dependent on the droplet size and homogeneity of the formulated nanodispersion. Hence, their investigation is of great importance for the potential application of the developed NEs as potent nanocarriers.

DLS measurements indicated that the addition of both bioactives in the dispersed oil phase causes changes in the polydispersity as well as the size of the NE as can be observed in figure 41. Particularly, VD3-loaded NEs demonstrated a small increase in the size of the oil droplets from 78.6 ± 0.2 nm to 83.6 ± 0.3 nm (figure 42) and also a slight increase of PdI from 0.092 ± 0.003 to 0.102 ± 0.005. This behavior is commonly observed when VD3 is encapsulated in O/W NEs regardless of the mixture of the selected surfactants or the concentration used and the droplet size increases in a concentration-dependent manner [70,77]. This could be an indication that VD3 interacts with the surfactants' monolayer affecting the interfacial tension as well as the overall stability of the system.

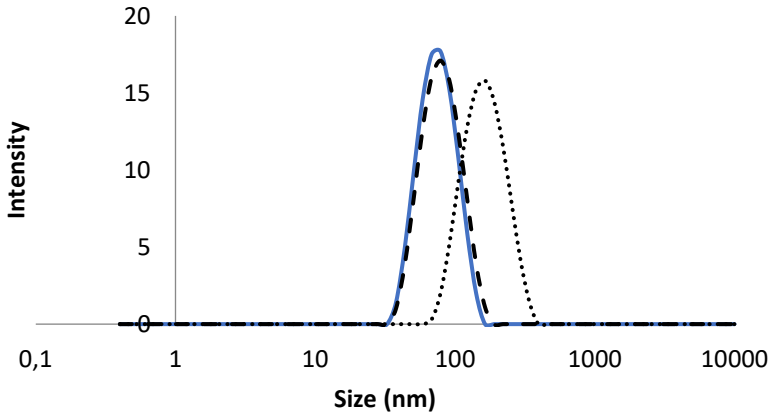

Figure 41. Droplet size distribution of both the empty and loaded L1 NEs measured by DLS. Encapsulation of vitamin D3 and curcumin in low-energy O/W NE based on water, IPM, Tween 80, Labrasol, Maisine, and Transcutol (L1). (–): empty, (- - -): loaded with vitamin D3, (…): loaded with curcumin.

Regarding the CU-loaded NE L1, DLS measurements also exhibited an increase of droplet size from 78.6 ± 0.2 nm to 165.6 ± 1.0 nm, however, PdI decreased from 0.092 ± 0.003 to 0.072 ± 0.008 (figure 41). This behavior has been previously mentioned in the literature concerning the formulation of low-energy CU-loaded NEs and a concentration-dependent increase in the droplet size has been observed [231,467]. Specifically, the study performed by Sharma et al., suggested the interfacial location of CU which could be related to the observed increase in the droplet size.

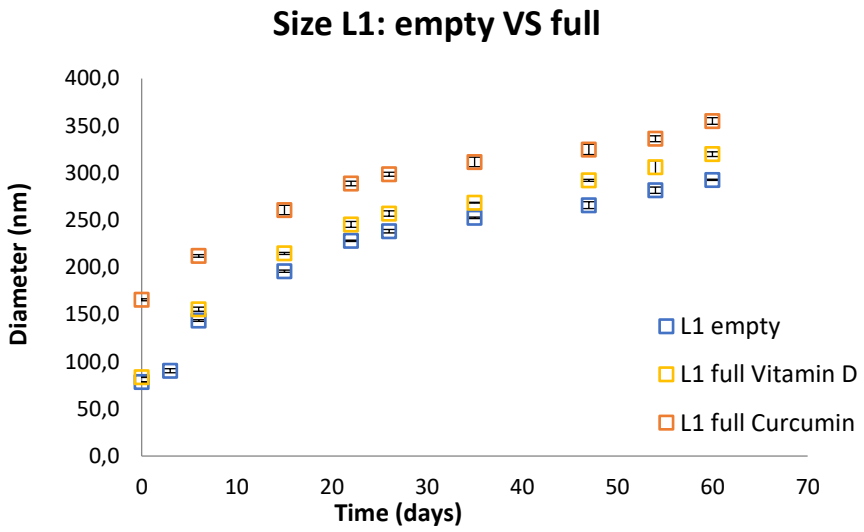

Figure 42. DLS study of the differences in droplet size of the low-energy O/W NE L1 in the absence of bioactive compounds and the vitamin D-loaded and curcumin-loaded NEs.

In addition, the examination of droplet size over time using DLS provided an indication of the storage stability of VD3 and CU-loaded NEs at 25 °C (figure 42). Although the diameter of the oil droplets of both the VD3-loaded and CU-loaded NEs was gradually increased with time up to 320 nm and 355 nm respectively, both NEs remained physically stable for 60 days.

Subsequently, CBD was encapsulated in a low-energy NE. However, in order to avoid the possibility of toxicity due to transcutol [464–466] and because an increased amount of oil was required for the solubilization of higher concentrations of the bioactive, system L4 was eventually selected for the encapsulation of CBD which was the main lipophilic bioactive compound under study. Initially, CBD was added into the oil phase at four different concentrations resulting in NEs containing 1 mg/g, 3 mg/g, 5 mg/g, and, 10 mg/g of the bioactive compound. The investigation of the appropriate CBD concentration that would be

encapsulated into the developed systems was crucial in order to determine its effect on the droplet size and stability of the NEs. In fact, as can be observed in figure 43 below, immediately after formulation, all four loaded NEs presented smaller nanodroplets compared to the empty system suggesting possible interaction of CBD and the monolayer of surfactants. In addition, the dispersion index PdI which reflects the distribution of particle size, was below 0.3 indicating uniform dispersions. The PdI and hydrodynamic radius values obtained by DLS were investigated to study the NEs in terms of stability over time. It was observed that NE with 3 mg/g of the bioactive compound demonstrated a sharp increase in the droplet size leading to destabilization after 75 days. Furthermore, it exhibited the highest PdI (0,295 ± 0,040) and size (201,3 ± 12,2 nm) of the rest of the systems. Regarding NE L4 prepared in the presence of 1 mg/g CBD, oil droplets of 126.5±3.1 nm diameter and 0.18±0.01 PdI were formulated demonstrating the lowest values amongst the loaded systems. Nevertheless, it was discarded since it would be difficult to detect and assess the effect of CBD in such a small concentration. Between the remaining three CBD-loaded NEs with the different CBD concentrations (3mg/g, 5 mg/g, 10 mg/g), the one containing 5 mg/g of CBD demonstrated the lowest PdI (0,240 ± 0,010) similar to the value of the empty NE (0,237 ± 0,009). In spite of the fact that the NEs containing 5 mg/g CBD and those with 10 mg/g CBD did not exhibit any significant difference in the homogeneity presenting PdI 0,240 ± 0,010 and 0,258 ± 0,029 respectively, the first one demonstrated smaller droplet size (102,4 ± 2,9 nm) compared to the other (170,3 ± 6,6 nm) and even in comparison to the empty one (204,0 ± 5,1 nm). Thus, NE L4 containing 5 mg/g CBD was selected for further investigation. In all four cases mean oil droplet diameter was increased over time as presented in figure 43 while the PdI initially decreased and then remained practically unchanged and lower than 0.2.

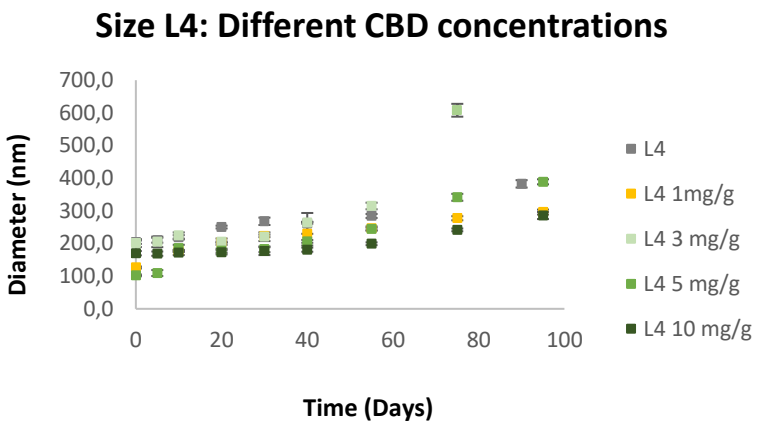

Figure 43. DLS study of the alterations in droplet size of the low-energy O/W NE L4 in the absence of CBD and the loaded NEs with three different CBD concentrations namely 3 mg/mL, 5 mg/mL, and 10 mg/mL.

These findings suggest that the presence of CBD in the oil nanodroplets of the NEs influences certain physicochemical characteristics. This behaviour could be attributed to the structure of the particular bioactive compound. The molecule of CBD possesses a lipophilic tail making it soluble to oil however, the two carbon rings present in the compound and specifically the 1,3-Dihydroxybenzene decrease slightly the overall lipophilicity of CBD. Thus, CBD could interact with the surfactant monolayer causing the observed changes in the nanodroplet sizes and enhancing the stability of the NEs. In addition, the encapsulation of CBD and its interaction with the surfactant monolayer and the oil core could induce structural alterations at the oil–water interface possibly associated to an increase of the interfacial tension.

This behaviour has been observed previously in literature with studies mentioning alterations in droplet size when a bioactive compound is encapsulated in O/W NEs. These changes have been reported upon encapsulation of vitamin D, curcumin and, lycopene among others, and seem to depend on the structure and concentration of the bioactive and its interaction with the surfactant monolayer. More specifically, in another study performed by our group, an increase of the nanodroplet size was also observed when VD or CU were encapsulated in EVOO-based O/W NEs indicating that the loading of bioactives affects the system [71]. In addition, a previous publication concerning the encapsulation of VD in NEs with different oils used as the oil phase demonstrated a concentration dependent increase in droplet size that could be attributed to the vitamin's interaction with the surfactants layer influencing the interfacial tension as well as the overall emulsion stabilization [70]. A concentration depended increase of the droplet size was also detected by Nikolić et al., when CU was encapsulated in low-energy NEs stabilized by polysorbate 80 and soybean lecithin droplet size growth with increase in the concentration of curcumin was also observed. The microstructural investigation that was carried out demonstrated the interfacial location of the active compound explaining the observed changes in the droplet size upon CU encapsulation [468]. In a different study performed by the same group, low-energy NEs were developed as carriers of CU for dermal administration. The empty and drug-loaded NEs were compared regarding their physicochemical properties indicating that the presence of CU in the formulation caused a significant particle size increment [467].

On the other hand, in a study investigating the effect of the encapsulation of different lycopene concentrations in protein-stabilized NEs it was demonstrated that the particle size of the prepared system did not change linearly as the bioactives concentration increased [469]. Three different oils were used as the oil phase, namely sesame oil, linseed oil and walnut

oil to examine the effect of lycopene encapsulation however this behavior was observed regardless the type of oil phase. These results could be associated with the limited solubility of lycopene in oil and are more in accordance with the behavior that the systems of the present thesis demonstrated since as aforementioned, it was observed that the changes of the nanodroplet size were not proportional to the concentration of the encapsulated molecule.

5.3. Hydrogels for the incorporation of C-Phycocyanin extract and stability study

As mentioned in the beginning of this chapter, the focus of the present thesis was the development of nanocarriers with considerable stability in order to encapsulate diverse lipophilic compounds. More specifically, the overall purpose of the developed nanodispersions was their use for the effective delivery of the bioactive molecules of interest through alternative routes of administration including intranasal and/or transdermal. However, NEs are not considered appropriate for these administration routes since due to their liquid nature it is impossible to remain in contact with the target site long enough for the bioactive to be released and delivered. Hence, a strategy followed in the recent years, is the combination of NEs with hydrogel matrices creating a novel hybrid system with physicochemical properties such as increased viscosity which is essential for both intranasal and transdermal delivery [470].

The hydrogel matrix selected for the incorporation of the formulated NEs is of paramount importance. It is crucial that it does not affect the structural characteristics of the embedded NE in order to obtain the desired release of the encapsulated bioactive [277,280,471,472]. Thus, it was essential to prepare a hydrogel network possessing the appropriate features in order to incorporate effectively the developed NEs for the formulation of the hybrid systems. It was crucial to prepare a hydrogel that would act as a suitable matrix maintaining its rheology and presenting stability over time before and after the NE incorporation in order to protect it effectively. Various hydrogels were formulated as described in methods (chapter 4.2.1.2.) using two different polymers namely chitosan (CS) and hydroxypropyl methyl cellulose (HPMC) as well as their combination. Initially, hydrogels were prepared with diverse concentrations of the polymers in the appropriate dispersion media in order to determine the ideal consistency. As can be observed below in figure 44 the viscosity decreased with increasing amount of the dispersion medium, providing hydrogels demonstrating water-like consistency at low polymer concentrations.

Figure 44. Image from the experimental procedure illustrating the difference in viscosity depending on the polymer concentration in the dispersion medium.

Hydrogels prepared using CS, HPMC, and their combination in various concentrations presented in table 3 (Chapter 4.2.1.2.) were optically observed at room temperature for three months to detect changes in their viscosity, color, or possible spoilage. Hydrogels prepared using HPMC and water as the dispersion medium as well as those comprised of both polymers in acetic acid solution 1% v/v appeared less viscous over time. This observation could suggest that the network slowly lost its cohesion losing its capacity to retain water. In addition, after three weeks spoilage was observed at the top layers of those systems due to the growth of microorganisms (mold). On the other hand, CS hydrogels remained stable for a period of three months and did not demonstrate any changes during optical observation. This behavior could be observed probably due to the use of acetic acid as the dispersion medium which simultaneously acts as a preservative [473,474]. In addition, it is well-estblished that CS possess antimicrobial properties which could also prevent the appearance of spoilage due to mold or microorganisms [475,476]. Hence, a CS hydrogel at a concentration of 1. solution 1% v/v was selected for the incorporation of C-PC extract as well as for the development of the hybrid systems since it was easy to prepare, remained stable for three months and it was convenient to spread without leaking.

Subsequently, C-PC extract was incorporated to examine the ability of the formulated CS HG to provide a protective matrix. Initially, the incorporation of different concentrations of C-PC extract was examined. As illustrated below in figure 45, various amounts of the extract

were added into the CS HG in order to determine the maximum concentration that could be incorporated. The lyophilized extract powder was added in the HG at concentrations up to 40 mg/g without optically observing any obvious sedimentation or any other change in the color of the extract or the structure of the matrix. Solely the color of the dispersion was affected (figure 45) becoming more intense with increasing extract concentration. All the systems showed stability over time and retained the bright blue color of the C-PC extract for three months without needing any additional protection against light degradation.

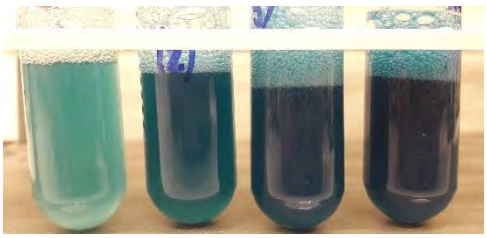

Figure 45. Different concentrations of C-PC extract 10 mg/g, 20 mg/g, 30 mg/g, and 40 mg/g starting from the left.

Following, the effect of temperature on the structure of chitosan hydrogels and HPMC hydrogels was investigated. Moreover, fructose was added to these systems to examine its efficacy as a preservative in order to maintain the bright blue color of C-PC extract which disappears after heating up to 45 ^{o}C due to C-PC degradation [477–479]. Thus, the aforementioned hydrogels were prepared both in the absence and presence of 1 % w/w fructose and 10 mg/g of C-PC extract and were incubated in two different thermal conditions namely 50 ^{o}C and 80 ^{o}C for 30 mins at each temperature. During the first heating, the hydrogels managed to function as a protective carrier resulting in the preservation of the color of the C-PC extract regardless of whether they contained fructose or not. In addition, all the systems under study did not demonstrate any significant alterations in terms of structure upon optical observation. However, as can be observed below in figure 46 after 30 mins of incubation at 80 ^{o}C the color was reduced significantly in all four systems. Moreover, the HPMC hydrogel foamed intensely and did not return to its original state even after cooling to room temperature. This result indicates that HPMC hydrogel most likely collapses during heating in contrast to the chitosan one which remained stable. Hence, based on the aforementioned investigation, chitosan hydrogel of concentration 1.25% w/v was selected as most appropriate for the incorporation of the NE.

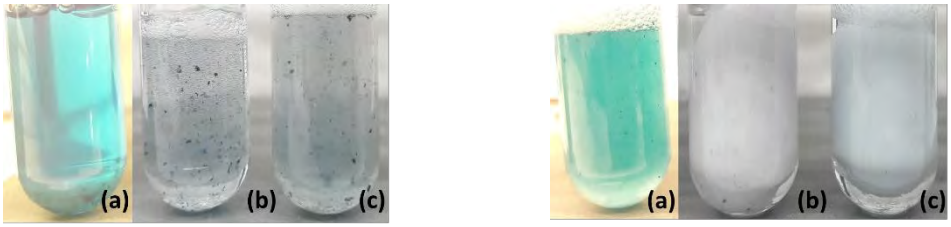

Figure 46. Pictures of hydrogels containing C-PC-extract. On the left: Chitosan hydrogel with C-PC-extract (a) before heating (b) after 30 min incubation in 80 °C without fructose (c) after 30 min incubation in 80 °C with fructose. On the right: HPMC hydrogel with C-PC-extract (a) before heating (b) after 30 min incubation in 80 °C without fructose (c) after 30 min incubation in 80 °C with fructose.

5.4. Nanoemulsion-filled hydrogels structural study

As mentioned previously, a fundamental objective of the present thesis was the development of a novel nanodispersion providing increased efficiency for the delivery of lipophilic compounds. Hence, based on the aforementioned studies which highlighted i) the stability of the developed O/W NEs and their suitability as carriers for lipophilic compounds and ii) the ability of chitosan hydrogels to act as carriers, a NE/HG also referred to as emulgel was formulated as described in chapter 4.2.1.4.

Nowadays, it is established that the structure of the developed nanocarriers is of paramount importance affecting various physicochemical properties as well as the release of the encapsulated bioactive molecules [480–483]. Thus, an essential part of this study was the structural characterization of the developed NEs and NE/HGs which is presented in the following chapters. By implementing diverse techniques, the localization of the encapsulated molecules was determined. It was also investigated whether the NEs structure is affected after its incorporation into the hydrogel. This study was of paramount importance in order to establish whether the NEs structure is preserved maintaining its ability to act as a carrier, resulting in the formulation of a carrier-in-carrier type system.

5.4.1. Electron Paramagnetic Resonance Spectroscopy (EPR)

In order to achieve information regarding the dynamics of the surfactant monolayer as well as the location of the encapsulated molecules in the carriers, EPR spin probing technique was applied. This method was implemented on the developed O/W NEs and the respective NE/HGs in the absence and presence of the bioactives using three different amphiphilic spin probes namely 5-, 12-, and 16-DSA as mentioned previously in chapter 4.2.1.6.

These spin-labelled fatty acids are located at the oil/water interface and have the ability to interact with the surfactant molecules due to their amphiphilic nature thus providing useful information regarding their mobility and the rigidity of the environment [484]. EPR spectra obtained by nitroxide spin probes like the ones used in the present thesis, present three peaks due to the hyperfine interaction between the spin of the nitrogen nucleus (I=1) and that of the unpaired electron (S=1/2). Below, in figure 47 the characteristic three-peak EPR spectrum of doxyl derivatives (5-DSA) when they are free in a solution, is presented. As can be observed, when the spin-probe is located in disordered fluid phases such as non-viscous solvents it moves freely and fast leading to isotropic hyperfine coupling represented by three symmetric narrow peaks [485].

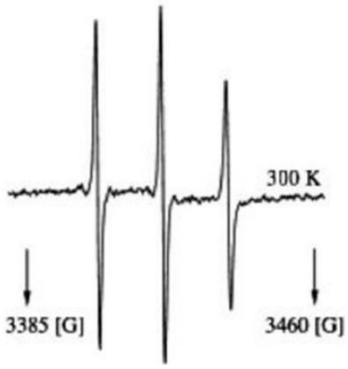

Figure 47. Typical EPR spectrum of the spin probe 5-DSA in solution [486].

On the other hand, in phases that demonstrate higher order such as the surfactant monolayer of NEs, the movement of the spin probe is hindered resulting in anisotropic hyperfine interaction, represented by asymmetric EPR peaks. Generally, EPR spectra of unequal heights and widths suggest that the spin probe demonstrates a restrictive motion in the environment where it is located [70,485,487]. This behavior can be observed in figures 48 and 49 illustrating the 5-DSA spectra of spin-probe interacting with the surfactant monolayer of the developed O/W NEs and the respective hybrid systems. These figures demonstrate the spectra obtained both in the absence and presence of the bioactives under study. In al cases, the three characteristic peaks of the nitroxide group are distinct and they appear to have unequal heights and widths suggesting restricted mobility of the spin probe in the surfactant layer.

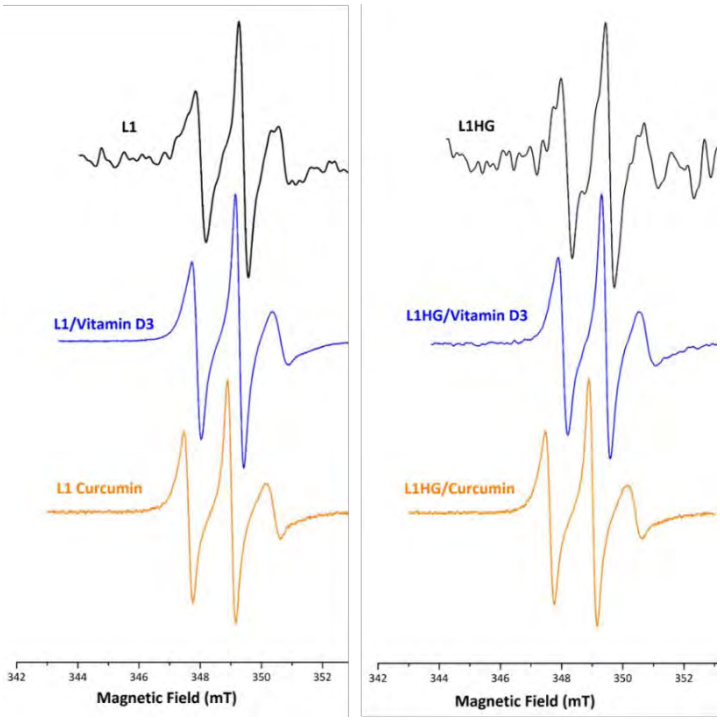

Figure 48. EPR spectra of 5-DSA in O/W NE based on water, IPM, Tween 80, Labrasol, Maisine, and Transcutol (L1) (left) and the respective hybrid systems (right). In black are represented the empty systems, in blue those with encapsulated vitamin D3, and in orange those with encapsulated curcumin.

Through the analysis of the obtained EPR spectra, mobility, order, and polarity across the surfactant monolayer off the formulated systems, were acquired. The calculation of these parameters is feasible since the spectroscopic behavior and thus the resulting spectra of the spin probes are highly susceptible on the environment surrounding them [488]. Therefore, changes in the structure of a nanodispersion that can occur after the encapsulation of a bioactive substance or its incorporation in a different environment (like a hydrogel matrix), can be detected by the changes in the resulting spectrum. The values of rotational correlation time, τ_R, order parameter, S, and isotropic hyperfine coupling constant, αN, were calculated from the experimental EPR spectra using equations (4) and (5) respectively (4.2.1.6.) providing a quantitative expression of the mobility of the probe and the rigidity of the interface [484]. The results of the EPR study for the empty L1 NE and the respective NE/HG as well as the VD and CU containing systems and for the NE L4 and the hybrid system in the absence and presence of CBD are presented in Table 6 and Table 7, respectively. The observed differences in these values are indicative of changes in different parts of the nanodroplets since the paramagnetic moiety of the spin probes is localized in different depths of the surfactant monolayer. More specifically, 5-DSA is oriented closer to the polar head groups of the surfactant monolayer as opposed to 16-DSA which is penetrated deeper closer to the oil core.

In other words, 5-DSA perceives variations closer to the aqueous phase whereas 16-DSA recognizes changes in the oil phase that penetrates the lipophilic surfactant chains [489].

Hence, the observed increase of the τ_R and S values of 5-DSA in comparison to the corresponding ones of 16-DSA suggests that the first one is located in a region where the surfactants are organized more tightly in contrast to the more flexible environment near the oil phase where 16-DSA is located. Furthermore, in order to examine the polarity profile across the surfactant monolayer the hyperfine coupling constants (α_N) of both spin-probes were also calculated from the resulting EPR spectra since this parameter is directly related to the distance between the peaks. Comparing the obtained values for 5- and 16-DSA, it can be observed that the latter presents higher hyperfine coupling constants in all systems (Table 6). This could be a verification regarding the location of 16-DSA near the oil phase since in all cases the values of α_N are comparable to these of pure solvent which in this case was IPM [411].

More specifically, regarding the spin probe 5-DSA, encapsulation of VD in the O/W NEs resulted in increased τ_R values from 2.73 ns to 3.62 ns with a simultaneous decrease of order parameters from 0.16 to 0.11. As observed previously by DLS measurements, droplet size increases upon VD addition which in turn causes a decrease in the curvature of the surfactants layer. When this occurs the hydrocarbon chains of the surfactants become tighter packed, thus hindering the motion of the amphiphilic spin probes. Hence, these results are in accordance with the ones obtained by DLS indicating that VD interacts with the surfactant monolayer of the O/W NEs increasing its rigidity. Similar behavior has been observed during the encapsulation of VD in edible O/W NEs developed for various food applications [70,77]. On the other hand, when 16-DSA was incorporated into the systems the obtained values of τ_R and S were not affected by the presence of VD which could be related to the negligible interaction of the encapsulated compound with the spin probe at the deeper depth of the monolayer near the oil core where is located.

In the case of CU encapsulation, both spin probes demonstrated a decrease in the values τ_R as compared to the empty systems as can be observed in Table 6. This suggests that CU influences the movement of the spin probes regardless of the depth they are located in the membrane. Since CU molecules are symmetric possessing two aromatic ring systems and a bent conformation, it is most likely that they create free space among tightly packed surfactant molecules, due to their chemical structure. Hence, CU encapsulation enables both 5-DSA and 16-DSA to rotate more freely resulting in the observed τ_R decrease [490]. However,

this phenomenon is more distinct for the spin probe 5-DSA of which the N–O· moiety is localized closer to the surfactants' polar head groups. According to the obtained results of the present study, CU seems to be closer to the polar region of the surfactant monolayer. In the case that CU did not interact with the surfactant molecules and was located closer to the oil core, more pronounced changes in 16-DSA dynamics would be detected. Regarding the values of order parameter S, the decrease from 0.16 to 0.11 is observed regarding 5-DSA and is probably due to the increase of droplet size upon CU encapsulation and the resulting decrease in the curvature of the surfactant's monolayer as aforementioned. These findings are in agreement with studies carried out previously investigating the structure of low energy O/W NEs where it was also observed the interfacial location of CU [468].

Regarding local polarity α_N, it was not affected significantly either by the encapsulation of VD or CU. This is an indication that the nitroxide group of both spin probes employed in this study remains in their initial location and is not displaced in an environment with different polarity when the bioactives are encapsulated in the nanodroplets.

Table 6.Calculated values of rotational correlation time (τ_R), order parameter (S), and isotropic hyperfine coupling constant (α_N) from the EPR spectra of 5-DSA and 16-DSA obtained in empty and loaded NEs (L1, L1/VD3, L1/CU) and the respective NE/HGs (L1HG, L1HG/VD3, L1HG/CU).

System	5-DSA			16-DSA		
	τ_R (ns)	S	α_N (x10^{-4} T)	τ_R (ns)	S	α_N (x10^{-4} T)
L1	2.73	0.16	13.8	0.36	0.02	14.8
L1/Vitamin D3	3.62	0.11	13.8	0.35	0.04	14.7
L1/Curcumin	2.14	0.11	14.0	0.33	0.04	14.8
L1HG	2.73	0.17	13.6	0.37	0.04	14.6
L1HG/VD3	3.61	0.13	13.8	0.35	0.04	14.7
L1HG/Curcumin	2.23	0.11	14.0	0.36	0.04	14.7

Interestingly, the values τ_R, S, and α_N obtained by the respective NE/HGs were affected in a similar way as in NEs indicating maintaining a consistent behavior even after their incorporation into the hydrogel matrix. This finding suggests that the chitosan hydrogel used as a carrier to achieve the thickening of the formulated NEs at a concentration of 1.25% w/v does not affect the rigidity or the polarity of the surfactants' monolayer. In other words, the

hydrogel matrix has the ability to act as a carrier without the chitosan absorbing onto the droplet interface or interacting with the non-ionic surfactants as it has been mentioned for other gelling agents such as small molecules or triblock copolymers [491].

Subsequently, the corresponding investigation was carried out for the NE L4 and the respective hybrid system in the absence and presence of CBD using 5-DSA ammonium salt and 12-DSA as the spin probes. In contrast to the L1 NE, L4 was formulated without the use of the co-solvent transcutol and twice as much oil was used as the oil phase containing also EVOO in combination with IPM in 1:1 ratio.

The obtained EPR experimental spectra of 5-DSA ammonium salt in empty and CBD-loaded O/W NEs and the respective NE/HGs are illustrated below in figure 49. The characteristic three-line EPR spectra of doxyl derivatives, when located in membranes, are also observed in this case. The peaks show unequal heights and widths in all cases, similar to the ones achieved from the two aforementioned systems.

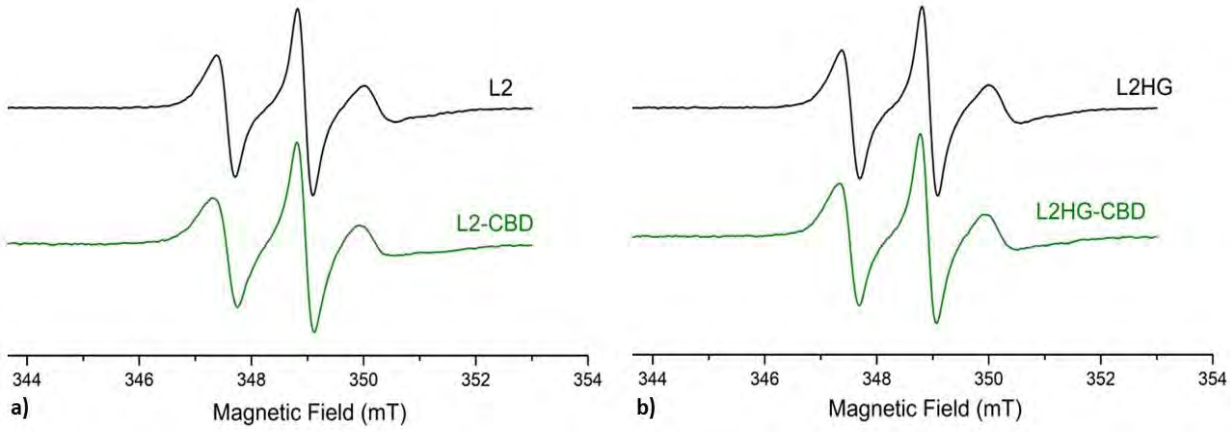

Figure 49. EPR spectra of 5-DSA ammonium salt in O/W NE based on water, IPM, EVOO, Labrasol, and Maisine (a) empty (L4) and CBD-loaded (L4-CBD) O/W NEs and (b) empty (L4HG) and CBD-loaded (L4HG-CBD) hybrids.

The three parameters τ_R, S, and α_N calculated from the above EPR spectra in the absence and presence of CBD are presented in Table 7. More specifically, the values τ_R and S obtained in the case of 5-DSA demonstrate an increase upon CBD encapsulation in the oil core of the O/W NEs. Particularly, as indicated in Table 7 τ_R was increased from 2.5 ± 0.1 ns to 3.2 ± 0.1 ns providing an indication of a more hindered motion of the spin probe located close to the surfactants' polar head groups. In addition, the values of parameter S also demonstrated an increase from 0.13 ± 0.01 to 0.19 ± 0.01 suggesting a higher rigidity in the same area. These alterations imply that CBD penetrates between the surfactant molecules and interacts with

them rendering the surfactants' monolayer more viscous and less flexible. On the other hand, the values of the isotropic hyperfine splitting, α_N, did not exhibit any significant changes regardless of the presence of CBD. Similar behavior was detected when 12-DSA was used for the implementation of the study. However, the corresponding values of parameters τ_R and S were lower in comparison to those of 5-DSA which could be attributed to the different locations of 12-DSA in the membrane. Concerning the isotropic hyperfine splitting, α_N, 12-DSA displayed higher values than 5-DSA both in the presence and absence of CBD suggesting differences in the micro polarity at the diverse depths of the surfactants' monolayer where the two spin probes are located. These results are in accordance with previous studies regarding the encapsulation of lipophilic compounds such as Vitamin D3 or curcumin in O/W NEs based on various oils [22,70,77].

Table 7. Calculated values of rotational correlation time (τ_R), order parameter (S), and isotropic hyperfine coupling constant (α_N) from the EPR spectra of 5-DSA and 12-DSA obtained by empty and loaded NEs (L4, L4-CBD) and NE/HGs (L4HG, L4HG-CBD).

System	5-DSA			12-DSA		
	τ_R (ns)	S	α_N (x10^{-4} T)	τ_R (ns)	S	α_N (x10^{-4} T)
L4 Empty	2.47 ± 0.06	0.13 ± 0.01	13.8 ± 0.03	1.42 ± 0.03	0.08 ± 0.01	14.4 ± 0.03
L4HG Empty	2.45 ± 0.17	0.15 ± 0.02	13.5 ± 0.11	1.47 ± 0.06	0.09 ± 0.01	14.4 ± 0.11
L4 Full	3.24 ± 0.10	0.19 ± 0.01	13.5 ± 0.04	2.33 ± 0.07	0.14 ± 0.01	14.0 ± 0.08
L4HG Full	2.68 ± 0.08	0.15 ± 0.02	13.6 ± 0.12	1.55 ± 0.02	0.09 ± 0.01	14.3 ± 0.07

Then, hybrid systems prepared based on the aforementioned L4 O/W NE were investigated using 5-DSA ammonium salt and 12-DSA as spin probes. Regarding the NE/HG in the absence of CBD, membrane dynamics as expressed by τ_R, S, and α_N parameters were similar to the corresponding NE (Table 7). These results indicate that the use of a chitosan matrix at a concentration of 1.25 % w/v for the increase of the NEs' viscosity does not affect the local viscosity, order, and polarity. On the other hand, the CBD-loaded NE/HG was less affected by the encapsulation of the lipophilic compound in comparison to the corresponding NE. More specifically, the CBD-loaded NE/HGs demonstrated only a slight increase in the rotational correlation time (τ_R) while order parameter (S) and local polarity remained similar to values achieved by the empty hybrid systems. These findings suggest that the NE when incorporated

into the hydrogel obtains a less rigid surfactant monolayer and hence the hybrid system could probably be a more effective carrier for the transdermal delivery of CBD.

To summarize the obtained τ_R and S values of all the spin probes demonstrated that the surfactant monolayer is affected by the encapsulation of all three lipophilic compounds regardless of their structure. However, the increase or decrease of the monolayers' rigidity appears to be dependent on the localization of the encapsulated bioactive molecule. Nevertheless, the results obtained by the present EPR study indicate that the NEs' interface is not affected by the incorporation into the hydrogel matrix. This finding suggests that NE retains its characteristics, properties, and functionality as a carrier, and hence its combination with the hydrogel could provide a promising delivery system possessing novel rheological characteristics suitable for use in transdermal delivery.

5.4.2. Confocal Fluorescence Microscopy (CFM)

In spite of the fact that the aforementioned technique provided useful information on whether the NEs surfactant monolayer is affected by its incorporation into the hydrogel, an actual visualization of the nanodroplets was essential. Thus, confocal fluorescence microscopy (CFM) was implemented in order to achieve an initial depiction of the NEs structure and the possible changes in the size and shape of the formulated nanodroplets after incorporation in the chitosan hydrogels.

Typically, CFM is utilized in combination with cells in order to distinguish the live from the dead ones, to examine the integrity of their membrane after the administration with diverse systems [492,493] or to investigate the intracellular release of a lipophilic bioactive compound under study [494]. Furthermore, this method has been commonly utilized for the monitoring of morphological changes of delivery systems when subjected to simulated digestion through *in vitro* models [495–497]. However, quite recently this technique has been applied for the microstructural characterization of O/W NEs by staining the oil phase with various lipophilic stains. In the current thesis the lipophilic dye Nile red was used to stain the oil phase of the developed NEs in order to obtain a visualization of the oil nanodroplets in their native state. As demonstrated below in figure 50, this method achieved a direct depiction of the nanodroplets providing an instantaneous and straightforward comparison of the NEs structure before and after its incorporation into the chitosan hydrogel. The obtained images suggested that the oil droplets of the O/W NEs had a spherical shape and a diameter of approximately 120 nm (figure 50) which is in accordance with the results achieved by DLS. Furthermore, confocal micrographs acquired for the respective NE/HGs did not demonstrate

any significant changes in the shape or size of the incorporated NEs (figure 50). Hence, in both the NE and the NE/HG systems, a uniform dispersion of the oil nanodroplets was observed and no obvious aggregation or other changes were detected. This finding indicates that NE did not collapse after its incorporation in the hydrogel and maintained its structure intact. As a result, CBD remaining in the NEs oil core can be dispersed throughout the hydrogel network. Since CBD is a lipophilic compound its dispersion in hydrophilic carriers as hydrogels would not be possible without the NEs. Hence, hybrid systems emerge as ideal candidates for the encapsulation and delivery of lipophilic compounds in cases where increased viscosity is required for effective administration.

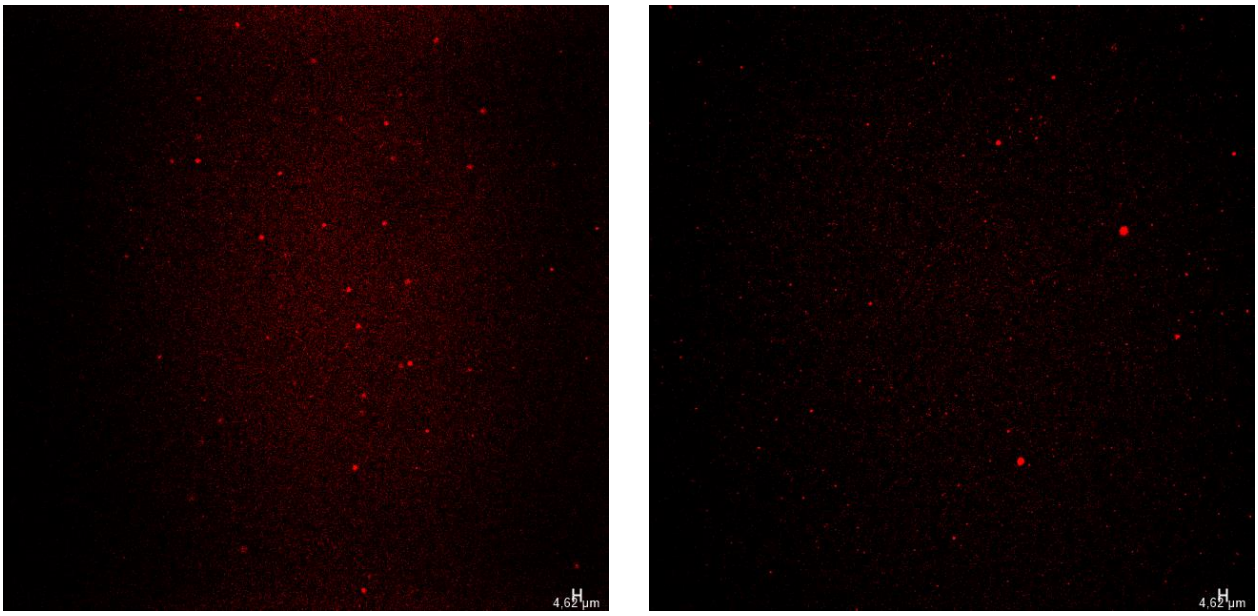

Figure 50. Images obtained by confocal fluorescence microscopy illustrating the Nile red-stained oil mixture of the formulated NEs (left) and the respective NE/HGs (right) (X 40 magnification).

There are recent studies also utilizing CFM for the visualization of the microstructure of diverse systems. Nonetheless, similarly to the present thesis, this technique is regularly utilized as a supplementary tool in combination with DLS or Cryo-TEM methods in order to provide a complete image of the nanodispersion under study. The use of different dyes including fluorescein [498]**,** cumarin [499] or nile red [493,500,501] has been mentioned for the staining of the oil phases of the systems under study with the latter being the most commonly used. To date, this technique has been implemented in NEs to gain information on their microstructure and detect any possible alterations upon different environmental conditions such pH, temperature and salt concentrations [501], to evaluate the preparation method and determine the ideal process [498] or simply as an additional tool for the depiction

of a NEs' oil phase [493,499,500]. Corresponding to the findings of the group Li et al. [501], that did not observe any significant changes in the NE microstructure in different pH, the NEs developed in this thesis also maintained their structure intact after their embodiment in the HG. This result suggests the suitability of the CS HS as a matrix for the development of a novel system with the appropriate physicochemical properties.

5.4.3. Cryo-Electron Microscopy (Cryo-TEM)

As an alternative technique to achieve direct observation of the structure of NEs and the respective CBD-loaded formulations, cryogenic electron microscopy (cryo-EM) was employed. This method is frequently used as an additional tool to DLS to confirm the assumption that the developed nanodispersions possess indeed a spherical structure [502]. Furthermore, due to the high-resolution images, the identification of any co-existent structure or aggregate that may remain undetected through DLS [422] is enabled To implement this method all specimens were vitrified by plunge-freezing as described in a previous chapter (Chapter 4.2.1.8.) to avoid the formation of ice crystals that perturbs their structure. The use of cryogenic techniques for sample preparation has been proven an invaluable tool since they provide the possibility to examine the nanodispersions under study in their native state. Thus, a more representative visualization is obtained providing high accuracy information [422]. The vitrification conditions selected in the present thesis were proved to be indeed applicable for all the samples and cryo-EM data were achieved for NE L4 in the absence and presence of CBD. Hence, direct investigation of both unloaded and CBD-loaded formulations as depicted below in figure 51 was achieved, establishing that cryo-EM analysis could be a valuable tool for the visualization of NEs.

The images acquired demonstrate that the formulated nanodroplets possess a highly spherical structure as can be observed in figure 51 below. Such spherical shapes have been also observed in O/W microemulsions intended as carriers for an analog compound of Vemurafenib [503]. However, in that case the nanodispersions morphology was investigated in the absence of the bioactive compound. In the present thesis, the NEs' structure was examined both in the absence and in presence of CBD in order to investigate the effect of the bioactive compound on the structure of the nanocarrier. The obtained micrographs illustrate the existence of spherical structures that demonstrate slight variations in their size ranging from ~ 80 to 130 nm and ~75 to 134 nm for the NEs in the absence and presence of CBD, respectively. This kind of variation in the nanodroplet size is often observed in corresponding NEs since Cryo-TEM provides high-precision imaging [422,504,505]. Particularly, a considerably high variation in the size of the observed nanodroplets was mentioned in a

previous study performed by Brenelli et al. regarding the formulation of an O/W NE using an emulsifier derived from natural source where nanodroplets of diameter from ~50 to ~500 nm were detected [505]. The dark dots detected in figures 51A and C, correspond to the oil phase dispersed in the aqueous one (grey areas) with the average size of the empty and loaded NEs being 113 nm and 124 nm, respectively. Therefore, can be concluded that cryo-EM and DLS data are in agreement with the first one confirming the DLS findings. The cryo-EM technique was also implemented for the characterization of NEs with considerably larger diameters (figure 51B) that could be suitable carriers for the delivery of more complex molecules in terms of size. It is also observed the localization of the empty O/W NEs in thick vitreous ice regions, consistently forming spherical signatures (figure 51A). It can be observed that the O/W NE under study had preferential distribution in thicker vitreous ice similar to polymersomes previously illustrated with cryo-EM [506–508]. This behavior has also been detected in more viscous NEs that are adsorbed strongly onto the carbon coated grid making difficult their removal by filter paper and it could be demonstrated due to the presence of EVOO in the oil phase which increases the overall viscosity of the NEs under study [422].

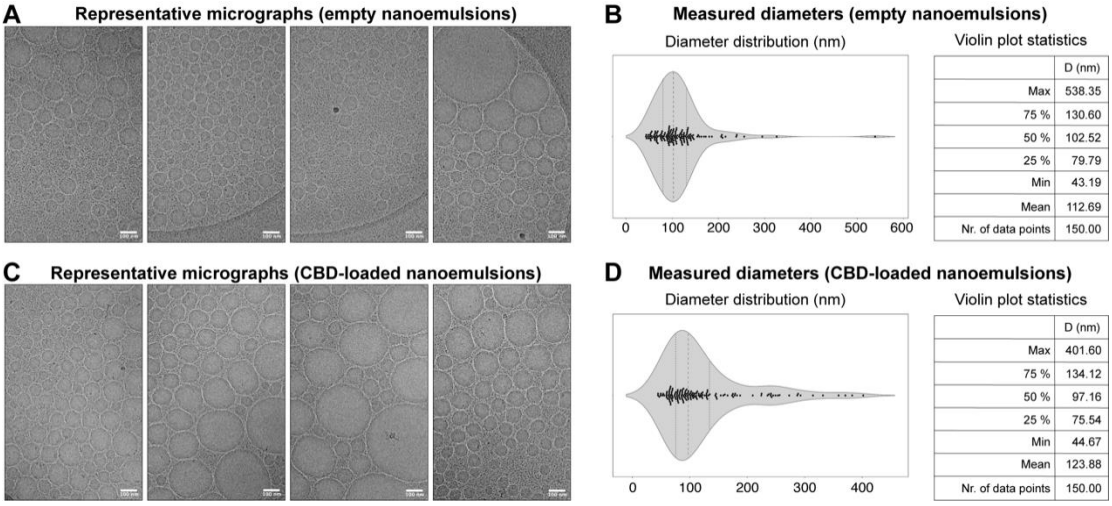

Figure 51. Cryo-EM study of L4 NEs. (A) Representative micrographs of empty NEs illustrate their distribution, which is regulated by ice thickness (the thicker the ice, the highest the odds to identify the particles). Background black dots identified in the micrographs represent possible surfactants. (B) Violin plot demonstrating the measurements of diameters for 150 single-particle NEs including the underlying statistics in the accompanying table. The dots in the violin plots represent each single data point. (C) Same as (A), but for CBD-loaded NEs. (D) is the same as (C), but for CBD-loaded NEs.

Regarding the morphology of the formulated NEs, both the empty as well as the CBD-loaded ones, demonstrated comparable structural properties (figure 51C). Statistical analysis

of their nanodroplet diameters did not exhibit any significant change in their observed shapes (figure 51D). This finding suggests that the encapsulation of CBD does not affect substantially the systems' structural rigidity and ultrastructure, indicating minimal perturbations upon drug encapsulation. This result is in good agreement with the micrographs obtained previously by two other groups that prepared carriers for the encapsulation of quercetin [509,510]. In the first case TEM was implemented to visualize the quercetin-loaded O/W NEs. Those NEs contained 37.5 % w/w of a 1:1 mixture of Labrasol and Tween 80 which was much higher than the 4% w/w used for the formulation of the NEs of the present investigation. However, the quercetin-loaded NEs prepared by the group of Pangeni et al. also demonstrated spherical nanodroplets with a uniform distribution [509]. In another similar study performed by Dario et al., nanodroplets of spherical structure with a relative fluctuation in their size were also illustrated when O/W NEs containing quercetin concentration respective to the CBD encapsulated in the nanocarriers of the present thesis were subjected to Cryo-TEM [510]. These findings indicate that the NEs proposed in the present study could be suitable for the encapsulation of a lipophilic compound of pharmacological interest, like CBD.

5.4.4. Small-angle X-ray scattering (SAXS)

SAXS is an analytical and non-destructive method to investigate nanostructures in liquids and solids. This method is able to probe the colloidal length scales of 10–1000 Å and therefore is an appropriate technique to determine the size and the structure of colloidal systems such as microemulsions, NEs, and hydrogels [511]. However, reaching the upper limit requires specific equipment and favourable systems. In the present study this method was implemented in order to investigate possible changes in the NEs' structure a) upon encapsulation of different CBD concentrations and b) after the incorporation of NEs into the hydrogel matrix.

Below, the obtained intensity profiles of the systems under study in the absence and presence of various CBD concentrations in the so-called Porod representation, are depicted. Due to the relatively large characteristic sizes, the scattering intensity I is dominated by the asymptotic power-law decay $1/q^4$ in the investigated range of the scattering wave vector q which is also referred to as Porod's law. The Porod representation ($I \cdot q^4$ vs. q), amplifies deviations from Porod's law, unravelling the structure [511,512]. In the specific technique, a practical limitation arises due to the low contrast of organic matter in relation to water and the consequent low signal-to-noise ratio. Nevertheless, some robust structural information still emerges from the data processing, at least in a semi-quantitative sense. However, there is still some unavoidable background superimposed to the scattering data in spite of the fact

that the whole radiation pathway (including the sample chamber) is entirely in vacuum, and the use of a pixel detector (PILATUS-300 k). Since background would be challenging to be measured directly, it has been estimated using the standard approach described below. Firstly, it has been accepted that the background level was q-independent in the investigated range of scattering wave vector. More specifically, the background level B has been determined by fitting the function A +Bq^4 to the data A +Bq^4 to the data q^4· R (R is the raw scattering data) in the so-called asymptotic range of wave vector values. From the data depicted in the Porod representation, the asymptotic regime typically starts above q≈0.02 Å−1. Below the results are illustrated as I · q^4 vs q (figure. 52) where a red line was used as a model fit that was obtained and drawn from a model by exploiting the usual form factor of a sphere. The spectra illustrated in figure 52 provide an indication of the NEs' structure. The two peaks located at 3.54/R and 3.51/R resulting from the empty NEs and the NE/HGs respectively provide an indication regarding the mean diameter and dispersity parameter of the NE before and after its incorporation into the hydrogel. More specifically, for the empty NEs was suggested an assembly of non-interacting, identical spheres with a mean diameter of approximately 118 nm and dispersity parameter of 0.28. In the case of NE/HGs, a decreased mean diameter of 90 nm was observed while the same dispersity parameter (0.28) was estimated.

Following, the effect of the encapsulation of two different CBD concentrations, namely 1 mg/g and 5 mg/g, was investigated and the loaded systems were compared with the respective NEs in absence of the bioactive of interest. The (truncated) «peak» detected at around 0.0045 A-1 for the CBD-free system was moved to a slightly larger value, ca. 0.005 A-1 with CBD concentration. This alteration could be associated with the decrease of the NEs' droplet size when CBD is encapsulated in the system. However, no significant changes in size are detected between the two loaded NEs indicating that the encapsulation of different CBD concentrations does not influence the developed system in terms of size. However, as could be observed from the SAXS curves (figure 52a) the diameter of the oil nanodroplets calculated by fitting SAXS data appeared always smaller compared to the values obtained by DLS. This difference was expected since DLS does not measure just the nanodroplets' size but also the hydration layer that moves with the nanodroplets [513].

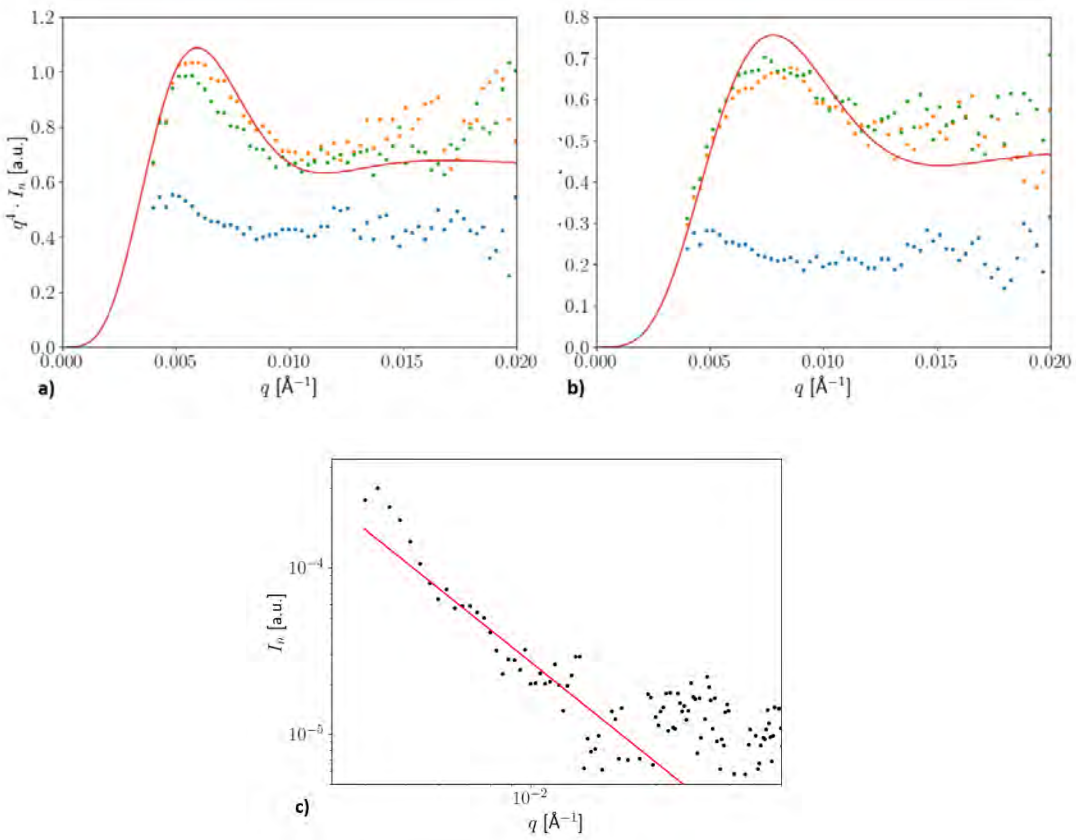

Figure 52. a) Data of SAXS in the Porod representation for empty and loaded NEs. Empty NEs (blue ●) and loaded systems with 1 mg/g CBD (orange ●) and 5 mg/g CBD (green ●), the red line is a model fit. b) Empty NE/HGs (blue ●) and loaded systems with 0.5 mg/g CBD (orange ●) and 2.5 mg/g CBD (green ●), the red line is a model fit. c) Chitosan hydrogel (black ●), the red line is a model fit.

In addition, the structure of the chitosan hydrogel was examined. As can be observed from the spectrum depicted in figure 52c it could be described as two-dimensional (thin, with large lateral dimensions) objects like platelets. No better fit could be obtained since the data achieved by the chitosan hydrogel was rather noisy. Nevertheless, for the drawing of the model fit line (figure 52c), a scaling exponent equal to 2 which is in accordance with what is expected for membranes, was selected.

Finally, the NEs' size after their incorporation into the hydrogels was investigated to determine possible changes. For this purpose, the hybrid systems were formulated by incorporating NEs both in the absence and in presence of CBD in the chitosan hydrogel. In figure 52b the hybrid systems in the absence and presence of CBD, are illustrated. More particularly, two different CBD concentrations were investigated namely, 0.5 mg/g and 2.5 mg/g. These systems as the aforementioned ones were also evaluated in terms of size and structure. The spectrum depicted in figure 52b illustrates that the size and the spherical structure of the Nes were not influenced by their incorporation in the HGs, with the system in

the absence of CBD exhibiting again a larger characteristic size in comparison to both CBD-loaded systems.

To summarize, the findings acquired by the SAXS complement those obtained by EPR and confocal microscopy indicating that indeed the NEs' incorporation in the chitosan-based hydrogel could provide protection to them without affecting significantly their structural properties.

5.5. *Biological evaluation of oil-in-water nanoemulsions & nanoemulsion-filled hydrogels*

An essential objective of the present thesis was the development of nanocarriers that could be used as delivery vehicles for various lipophilic bioactives through alternative routes of administration. Thus, the biological evaluation of the developed systems in terms of toxicity as well as the assessment of their ability to act as suitable carriers to deliver the bioactives through the skin were of paramount importance.

Since the developed nanodispersions were intended either for intranasal or transdermal administration, it was deemed necessary to investigate their effect in two different cell lines to determine whether they demonstrate any cytotoxicity. Hence, two cell lines were selected for the evaluation of toxicity, namely human nasal epithelial cells (RPMI 2650) and normal human fibroblasts (WS1). Initially, NEs L3 and L4 were selected for investigation. This was due to the fact that they were easy to prepare and did not contain the co-surfactant Transcutol which is known to present toxicity. Subsequently, the most promising NE in terms of toxicity as well as the corresponding hybrid system were further evaluated in terms of transdermal delivery using synthetic membranes as well as porcine ears which served as a model of the human skin.

The results obtained from the biological evaluation of the developed NEs and the respective NE/HGs are reported below.

5.5.1. Cell viability assay

To investigate the effect of NEs L3 and L4 (compositions presented in Table 8) on cell viability *in vitro*, the colorimetric MTT assay was performed. As aforementioned in a previous chapter (4.2.3.2. Cell viability assay (MTT assay)), during the particular tetrazolium-based assay the viable cells are evaluated by measuring the reduction of tetrazolium salt by intracellular dehydrogenases occurring in their mitochondria [444]. Since the evaluation of

the nanodispersion itself is of paramount importance in order to determine its suitability as a carrier, the study was initially performed using NEs in the absence of any bioactive compound. Thus, to carry out this assay, human nasal epithelial cells (RPMI 2650) were treated with unloaded NEs L3 and L4, at a concentration range of 0.05 to 2.5 mg/mL in the cell culture medium.

Table 8. Composition of the NEs L3 and L4 that were selected for biological evaluation.

NEs	Ingredients (% w/w)					
	Water	T80	Labrasol	Maisine	IPM	EVOO
L3	91	2	2	1	4	-
L4	91	2	2	1	2	2

As can be observed in figure 53 below, both NEs did not exhibit any cytotoxic effect up to the concentration threshold of 0.5 mg/mL in the cell culture medium. It should be mentioned that this is a rather high concentration compared to previous studies conducted using NEs with similar composition. Particularly, in a study performed by Espinoza et al. O/W NEs were prepared based on a mixture of the surfactants Labrasol/Tween 80/Transcutol P and Capryol 90 as the oil phase in order to be used for nose-to-brain delivery of Donepezil [514]. The drug-loaded NEs demonstrated cell viability greater than 80% when administered in the cell culture at concentrations ranging from 3.125 to 25 μg/mL.

Nevertheless, further increase of the NEs' concentration led to an increase of the cytotoxic effect, a result that could be associated with the increased concentration of the systems' components in the culture medium. More specifically, it is well established that surfactants, including Tween 80, are capable to disrupt the cell membrane of epithelial cells. As has been previously reported, Tween 80 in particular, significantly decreases the viability of RPMI 2650 cells in a dose-dependent way [21,515]. On the other hand, the EVOO-containing NE L4 did not exhibit the same behavior as the L3 especially at higher concentrations. More specifically, NE L4 did not demonstrate any cytotoxicity up to the concentration threshold of 0.75mg/mL of the culture medium in comparison to the 0.5mg/mL observed regarding L3 NE which did not contain EVOO. In addition, in higher concentrations (1.75mg/mL and 2.5mg/mL) while both L3 and L4 NEs displayed cytotoxicity, nevertheless L4 still presented higher cell viability. These findings could be attributed to the health benefits of EVOO which are well-established and mentioned in the literature in abundance. To the best of our knowledge there are no available studies performed investigating the effect of EVOO specifically on the nasal cell line used in the present thesis. However, throughout the years

several studies have been performed suggesting the antioxidant, anti-inflammatory and antimicrobial properties of EVOO [81,83,84,102,105]. Particularly, in a recent review are highlighted the effects of EVOO on the proper cell function which are mainly attributed especially to the phenolic fracture it contains. In this review is mentioned that the polyphenols contained in EVOO are involved in the modulation of a variety of cellular pathways maintaining the genomic stability of the cells and protecting their nuclear and mitochondrial DNA against damage induced by oxidative stress [516]. Therefore, there are compelling indications based on the literature that the improved cell viability upon L4 administration could be attributed to the presence of EVOO. Since NE L4 demonstrated reduced cytotoxic effect in cell line RPMI 2650 even at higher concentrations, it was selected for further investigation.

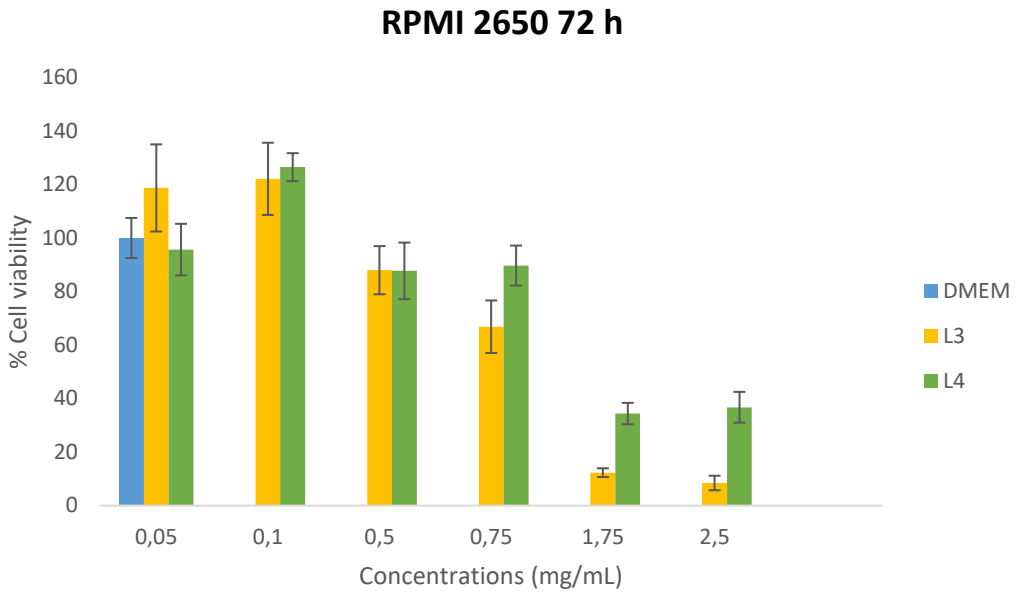

Figure 53. Cell viability results in nasal epithelial cell line (RPMI 2650) after 72 h of treatment with L3 and L4 NEs using the MTT cell proliferation assay. Each column represents the mean of six replicates ± SD.

The nanodispersions proposed in the present thesis were formulated to provide the possibility of delivery with alternative routes of administration. Thus, L4 NE which demonstrated a more favorable cytotoxic profile in the nasal epithelial cells, and the respective NE/HG both in the absence and presence of CBD were evaluated for potential toxicity in normal human fibroblasts (WS1). This study was carried out in order to investigate whether these systems could be suitable for topical use and possibly for wound healing due to the potentially proliferative properties of EVOO. Accordingly, NE L4 and the corresponding

NE/HG were administered to WS1 cells in the absence and presence of CBD at a concentration range of 0.5 to 1.5 mg/mL and the biocompatibility of these two colloidal delivery systems was compared. As can be observed in figure 54 presented below, neither the NEs nor the NE/HGs exhibited any cytotoxic impact up to the concentration threshold of 1.5 mg/mL in the cell culture medium. The high biocompatibility of the nanodispersions under study is possibly attributed to the fairly low concentration of surfactants (5 % w/w) as well as the presence of EVOO. In fact, the specific investigation suggests that the treatment of the WS1 cells with the empty systems could induce a dose-dependent cell proliferation.

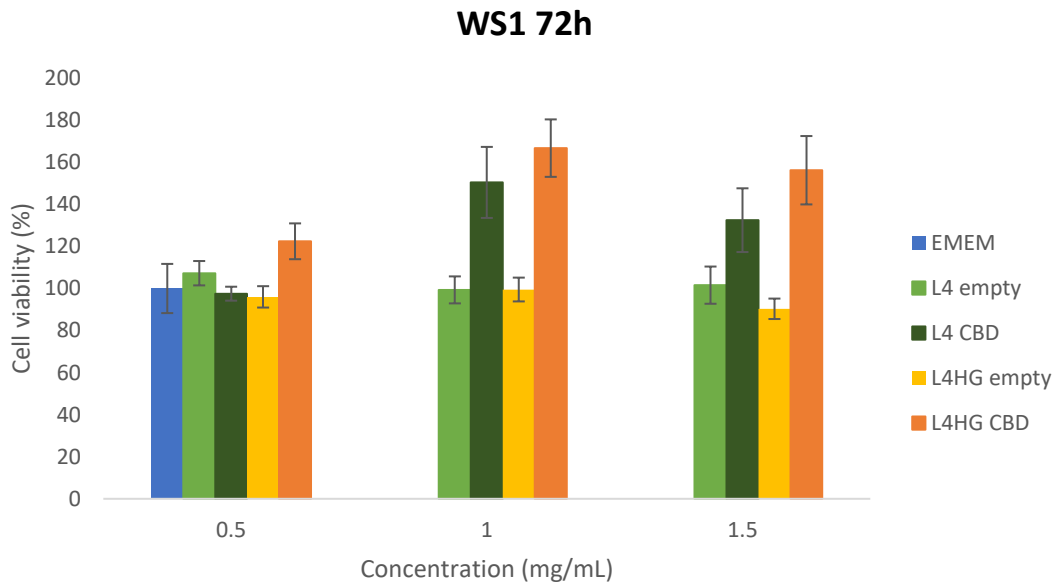

Figure 54. Cell viability testing results in human fibroblasts cell line (WS1) after 72 h of treatment with L4 NE and the respective L4/HG NE/HG in the absence and presence of CBD using the MTT cell proliferation assay. Each column represents the mean of five replicates ± SD.

This finding could be attributed possibly to the EVOO-containing oil phase [84,517] as well as the presnce of chitosan in the hybrid systems. More specifically, in a previous study conducted by Howling et al. [518] a strong stimulation of fibroblast proliferation was demonstrated when highly deacetylated chitosan, like the one used in the present thesis was adminstered to the cells. Despite the fact that the chitosans' exact mechanism of action has not been elucidated yet, there are indications that it has the ability to bind to serum factors, such as growth factors inducing cell proliferation [519]. In addition, at higher concentrations, the CBD-loaded systems demonstrated an increased cell viability suggesting that the particular bioactive molecule could also stimulate the proliferation of fibroblasts. Since as until recently, the most common delivery route for CBD was the oral administration, there is no comparable literature

investigating the effect of CBD on normal human fibroblasts. Nevertheless, there studies performed using murine models indicating the engagement of the endocannabinoid system with the wound healing response in fibroblast cells via the upregulation of epidermal growth factors [520]. Another study recently performed by Nigro et al. investigated the effect of the cell viability of fibroblasts after their treatment with NE/HG formulated for the topical delivery of coenzyme Q10 (coQ10) [521]. It is worth mentioning that the colloidal systems developed in the present theseis were administered at noticeably increased concentrations in comparison to the aforementioned study without demonstrating the corresponding cytotoxic effect.

In conclusion, the results described above regarding the cell viability assessment *in vitro* using two different cell lines indicate that both delivery systems under study display considerably high biocompatibility. Furthermore, the effect of these colloidal systems on the WS1 cell line provides an indication that they could stimulate skin fibroblast proliferation making them ideal candidates for topical applications where wound healing is required. Hence, this study suggests that both the NEs and the corresponding NE/HGs could be suitable candidates for the delivery of various lipophilic bioactive compounds through diverse administration routes including intranasal and (trans)dermal administration for a number of applications.

5.5.2. *In vitro* release Study

A crucial parameter indicating the suitability of nanocarriers to act as potent delivery systems is their ability to effectively release the encapsulated compound. Thus, a preliminary study was conducted using vertical glass Franz diffusion cells and a synthetic cellulose membrane in order to investigate *in vitro* the release of encapsulated VD and CU from NE L4 and the respective NE/HG.

In order to perform this study, 1 mL of each loaded nanocarrier was placed in the donor compartment of each cell. The *in vitro* release profiles of VD and CU both from the NEs and the NE/HGs were examined for 26 and 28 h, respectively, in 1:1 PBS buffer/ethanol solution. Samples were collected from the receiver compartment at different time intervals and the corresponding amount was replaced with fresh buffer. The permeated amounts of each bioactive molecule were calculated by a Cary UV-VIS spectrophotometer at the wavelength of peak absorption. For this calculation standard curves were prepared for both VD and CU using appropriate amounts to prepare standard solutions of known concentrations which were then measured at the appropriate wavelengths, namely 259 nm and 213 nm. The

equations obtained by plotting the standard curves of VD (y = 0.037x, R^2 = 0.993) and CU (y = 0.158x, R^2 = 0.999) were used to determine the concentration of the bioactive substance released over time from the nanodispersions. The membrane permeation profiles of the bioactives VD and CU from the colloidal systems under study are depicted in the diagrams below in figure 55, illustrating the cumulative amount of compound permeated in the receiver compartment as a function of time. The concentration of both VD and CU in the receptor compartment increased over time regardless of the investigated system. However, the two bioactives demonstrated distinctive release profiles and different cumulative amounts were detected in the receiver medium.

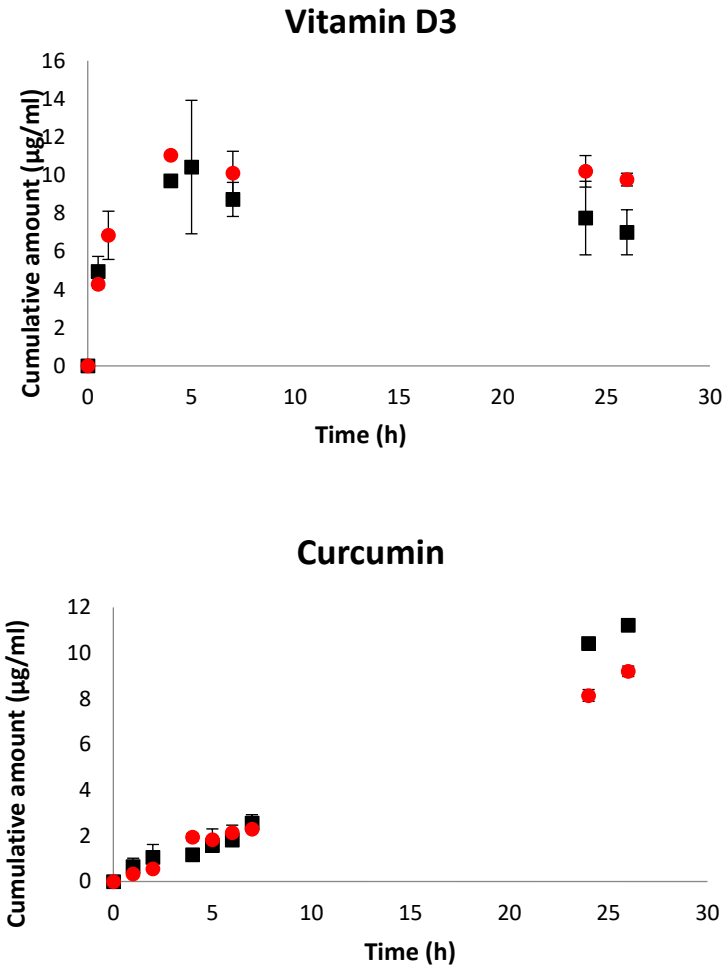

Figure 55. In vitro release of encapsulated (a) vitamin D_3 and (b) curcumin from (■) NE L4 and (●) the respective NE/HG at 32 ± 0.5 °C. The results are presented as average ± S.D.

Regarding VD, the amount released during the 26 h that the study was conducted, was up to 12% and 33% from the NE and the NE/HG, respectively. According to the release

rate obtained by the slope achieved from the plot of the cumulative amount as a function of time the release occurred in two stages. As illustrated in figure 55, an initial stage of burst release was observed during the first 5 h and following the release rate was significantly decreased during the second stage. Since VD is typically intended for oral administration, its release is most commonly investigated using *in vitro* gastrointestinal models [522,523] and therefore, to the best of our knowledge there are no similar investigations discussed in the literature. However, this release model of two stages has been previously mentioned by Marcos Bruschi [524], suggesting that the burst release observed at the first stage of the present study indicates the ability of the proposed nanodispersions to initially deliver the necessary therapeutic dose of VD rapidly. Following, due to the decrease of the release rate the developed nanodispersions could provide a steady rate of the concentration of the bioactive agent in the blood or the preferred site of action as long as possible, resulting in a sustained release rate and duration [524].

In the case of CU, after 28 h at the end of the study, 8% and 13% of the bioactive was released from the NE and the NE/HG, respectively. The release from both colloidal nanodispersions followed the zero-order kinetic described with a linear relationship of the cumulative amount of the released drug as a function of time. It is worth noting that both the NE and the NE/HG released the encapsulated CU with the same release kinetic indicating that the NE maintained its structure and properties after its incorporation into the hydrogel matrix. On the other hand, in a study performed by Rachmawati et. al [525], comparing the *in vitro* release of a NE and the corresponding nanoemulgel it was observed that the two developed systems followed a different release kinetic. More specifically, similarly to the NEs developed in the present thesis, zero-order kinetic was observed during the release of CU from the NE of this group. However, the release kinetic of CU changed to a Higuchi release profile when the NE was incorporated to a Viscolam AT 100P hydrogel matrix. The research group suggested that a burst release of the CU is obtained due to the hydrophilic nature of the polymer comprising the gel matrix. The high hydrophilicity of the gel resulted in the formation of loose channels within the network leading to burst release [525]. These findings indicate that the hydrogel matrix selected for the incorporation of the loaded NE could affect its structure and therefore alter the release profile of the encapsulated substance of interest. These results suggest that the CS HG proposed for the incorporation of the developed NE is an appropriate matrix that could provide protection against burst release while maintaining the NEs' properties.

As can be observed from the plots illustrated in figure 55, the release rate of both lipophilic molecules from the NEs was comparable to the corresponding ones from the NE/HGs at 32 ± 0.5 °C indicating that the release rate of the bioactives is not affected by the structure of the developed nanocarriers. However, VD and CU are released following a different kinetic model and at different release rates with VD being released to a greater extent. This difference between the released amounts of the two bioactive substances could be attributed to their contrasting solubilities in ethanol which are 30mg/mL for VD versus 1mg/mL for CU. In addition, the diverse release rates are in accordance with the literature suggesting that release rate constants are depended on the composition of the nanocarrier as well as the structure of the incorporated bioactive compound [526]. However, in the present study the composition of the nanocarrier does not seem to have a decisive effect on the release of the encapsulated compounds probably because the NE maintains its structure after the incorporation into the CS HG.

5.5.3. *Ex vivo* permeation study

As mentioned above, investigation of the release of an encapsulated substance with pharmacological interest from a carrier is crucial. It provides a significant indication regarding the bioavailability of the compound under study and the suitability of the nanocarrier as a delivery vehicle. In the present study, both NEs and the corresponding NE/HGs were examined as delivery vehicles of CBD and compared in terms of release of the encapsulated molecule. The structural difference of these two systems could be expected to affect their ability to release and deliver the encapsulated bioactive compound into/through the skin [23]. Therefore, various characteristics were evaluated including the release profile and rate and the cumulative amount of the released bioactive in order to determine the suitability of the developed nanodispersions as delivery vehicles for (trans)dermal administration.

In spite the fact that synthetic membranes are very popular for the implementation of *in vitro* release studies due to the ease of application, more than often they demonstrate important shortcomings. Foremost, the major challenges are the inability to correlate the results obtained from the synthetic membrane with the *in vivo* performance and the difficulty to detect possible differences in release due to different structure of the vehicle encapsulating the bioactive [527]. For that reason, in the present thesis the *in vitro* permeation protocol described in Chapter 4.2.3.3. was implemented following the preliminary study that was performed using cellulose membranes. In order to perform this study, modified Franz diffusion cells were used and full-thickness porcine ear skin was selected as the model membrane. Throughout the years, the similarity of the porcine ear skin to its human

counterpart has been established via various studies including biophysical characterization [528]. More specifically, porcine ear and human skin are strikingly comparable in terms of structure, thickness, collagen, sweat glands and hair follicle content. In addition, they demonstrate similar biophysical properties and the lipids of which they are composed display corresponding behaviors resulting to equivalent penetration for topically administered compounds [529–533]. Hence, the suitability of porcine ear skin to simulate *in vivo* results in human skin has been established and is frequently utilized as model membrane for diverse studies including transdermal delivery as well as wound healing, dermal toxicology and radiation effects [530].

Thus, an *ex vivo* permeation study using full-thickness porcine ear skin as a membrane was performed in order detect potential differences regarding the rate and extent of CBD delivery through the skin from the investigated samples. The study was conducted under infinite dose regimen. Although the amount of formulation which is used in these experiments is significantly higher than the actual amount applied by patients, infinite dose experiments allow determining the maximum flux of the CBD from a formulation and therefore enable to parametrically compare investigated formulations.

The cumulative permeation profiles of CBD and the corresponding *ex vivo* permeation parameters are presented in figure 56 and table 9, respectively. Interestingly, no CBD has permeated through the porcine skin at the beginning of the test. More specifically, as can be observed below in figure 56, CBD was initially detected in the receiving cells 24 and 22 h after administration of NEs and NE/HGs, respectively. Before these time intervals, CBD concentration was below the LC/MS-MS quantification limit. At later sampling time intervals, NE/HG displayed higher CBD release in comparison to NEs.

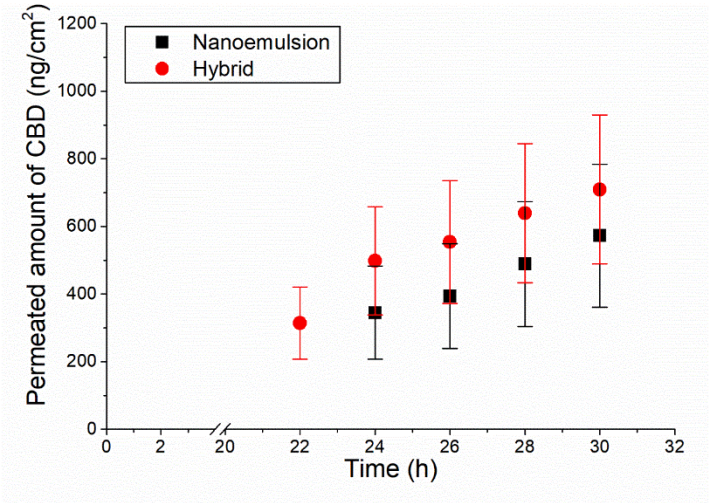

Figure 56. Permeation profiles of CBD determined across the full-thickness pig ear skin (mean ± SD, n=6) reflecting the influence of differences in nanocarrier type on the ex vivo skin absorption of CBD. (=8)

As demonstrated in Table 9, NE/HGs exhibited higher permeation rate and permeation coefficient which suggest enhanced transdermal absorption. Furthermore, by the end of the 30-h incubation time, the cumulative amount of CBD that was detected in the acceptor compartment of the cells where NE/HG were administered was also higher in comparison to the NE ones.

Table 9. Ex vivo skin penetration data for the different investigated colloidal systems after 30 h of application (mean ± SD, n=6). (=4)

	steady-state flux ($\mu g/cm^2h^{-1}$)	Q_{30h} Cumulative amount of CBD permeated through the skin (μg/cm)	Permeation coefficient (ng/cm^2h)
NEs	403.37 ± 130.09	572.56 ± 211.11	80.67 ± 211.11
NE/HGs	475.68 ± 162.57	709.22 ± 220.62	95.14 32.51

These findings could be attributed to the presence of CS in the NE/HGs which functions as a penetration enhancer. This phenomenon occurs due to the ability of CS to interact with the SC in diverse ways including the modification of its protein structure and to act as a moisturizing agent increasing the SCs' water content [534,535]. It is well-established that the percutaneous absorption of any bioactive compound is significantly affected by variations in skin hydration since it influences the structure of the SC [536]. Skin occlusion even for a short period of time, can lead to increased SC hydration, while extended skin hydration (>8h) causes a swelling of corneocytes, creating inter-corneocyte ruptures, and causes microstructural changes in lipid self-assembly. Hence, the percutaneous absorption of the bioactives of interest is influenced by the swelling of the corneocytes and possibly by the modification of the intercellular lipid phase structure and organization [537–541]. Therefore, the penetration of the administered compounds is enhanced with increasing duration of occlusion. This behavior could also be related to the increased viscosity of the NE/HG which leaves a thicker and more occlusive residue on the skin leading to enhanced skin permeation due to an increase in hydration [542]. In addition, the presence of EVOO in the oil phase of the systems could also enhance the percutaneous absorption of CBD. This could be related to the ability of fatty acids such as oleic acid, which is in abundance in EVOO, to function as penetration or permeation enhancers boosting the CBD permeation through the skin [543].

Therefore, the obtained results indicate that the NE/HG itself contributed to the improved penetration of CBD. Nevertheless, it is important to emphasize that the observed permeation parameters of the two nanodispersions under study did not present significant

difference, probably due to high variability of the achieved results. The high variation is frequently reported in the literature and is highly expected since porcine ear skin that was used is a biological membrane with diverse properties related to different characteristics of the animals including age, sex, breeding and diet conditions.

5.5.4. Tape stripping experiments

The results obtained by the aforementioned *in vitro* permeation study suggest that the physicochemical characteristics of the vehicles used for the encapsulation of CBD can induce a reversible disruption of the skin layers. Furthermore, during the 30-h *in vitro* skin permeation studies it was observed that the used nanodispersions were able to promote higher degree of skin hydration and probably induce changes of the porcine ear skin reducing its barrier function. Thus, preliminary differential tape stripping experiments were performed on porcine ear skin in order to investigate the quantity of CBD that penetrated through the superficial skin layers after a shorter exposure time.

As opposed to the *in vitro* permeation study mentioned above where the skin was excised from the porcine ears, during the present investigation the skin remained intact on the cartilage. However, the same infinite dose setting was administered. The samples were collected 2 h after the administration of the two colloidal systems and LC-MS/MS was used for the quantification of the CBD amount. In addition, it is important to mention that a preliminary study was initially carried out in order to determine the number of tapes required for the complete removal of the CBD localized in the SC. The obtained results revealed that after the removal of 30 tapes there was still CBD detected in the SC indicating a rapid penetration of the compound in the SC. During the experiments it was decided to discard the first two tapes removed since a very high amount of CBD was detected in these samples. This phenomenon was notably observed in the skin surface where the NE/HGs were administered, which could be related to the bioadhesive properties of chitosan [544]. The detection of higher amounts of bioactives in the first tapes has been mentioned previously by other research groups and was attributed to the adhesive properties of the nanodispersions applied on the skin surface, resulting in the creation of a dense film on the skin following the water evaporation [545,546].

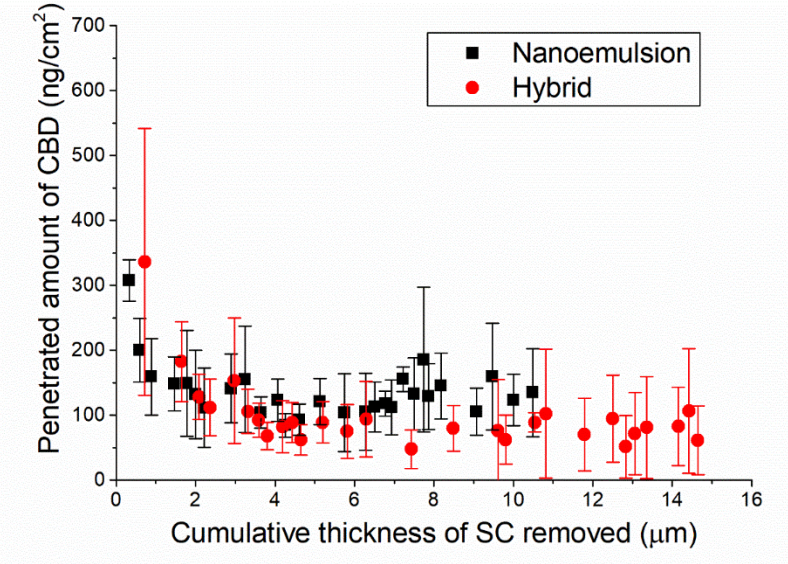

Figure 57. Diagram representing the stratum corneum concentration of CBD in relation to the cumulative thickness of stratum corneum removed profiles following a 2h application of tested samples (mean ± SE, n=4). (=9)

In the present study the total quantity of CBD recovered in the SC where NE was applied was slightly increased (3853.20 ± 543.06 ng/cm2) in comparison to the NE/HG (2745.41 ± 1022.44 ng/cm^2). Nevertheless, no statistically significant difference was observed, despite the fact that the two formulations under study demonstrated differences in viscosity. However, an obvious difference was observed between NEs and NE/HGs regarding the penetration depth of CBD as illustrated in figure 57. More specifically, significantly increased amount of SC was removed with 28 tapes after the administration of the NE/HG (14.644 ± 8.338 μm) in comparison to the NE (10.493 ± 3.958 μm). This finding indicates that the cohesion of the corneocytes was probably decreased after application of the hybrid system due to the presence of CS interacting with the SC as suggested in the previous chapter (5.5.3). Additionally, comparing this finding with *in vitro* permeation results, it appears that skin occlusion potentiated the observed effect, leading to improved CBD delivery during the prolonged test duration.

The obtained results are in agreement with various studies conducted by other research groups in the past. Particularly, there is a previous study investigating the effect of viscosity of various formulations on drug penetration through porcine ear skin. The group of Binder et al. examined formulations of different viscosities in comparison to a liquid system. Their findings indicate that the penetration of the drug was independent of this parameter. However, it was observed that the penetration depth of the drug was greatly affected by the concentration of the gelling agent used in the evaluated formulations. In addition,

corresponding to the results presented in the current study, significantly lower quantity of the administered drug was recovered from the SC in the surface where the liquid control was applied. This was attributed to the higher viscosity of the hydrogel formulations, adhering more effectively on the skin surface thus leaving an increased residue on the skin even after thorough removal of the excess formulation [547]. Furthermore, another research group established that increased viscosity and skin penetration of a bioactive present a positive correlation probably due to improved and prolonged contact with the skin [548].

These findings suggest a rapid and increased permeation through the SC indicating that the proposed nanodispersions are promising candidates for the transdermal delivery of CBD. However, the hybrid system in particular due to its characteristics and the presence of CS demonstrated enhanced properties as a delivery vehicle for percutaneous delivery.

Chapter 6

Conclusions

Chapter 6 – Conclusions

In the present thesis, the main objective was the development of biocompatible nanocarriers in order to be used as delivery vehicles for various lipophilic compounds. Ultimately, the formulated nanodispersions were proposed for the delivery of bioactives of pharmacological interest through alternative routes of administration including intranasal and transdermal.

Initially, biocompatible oil-in-water NEs were developed using non-toxic, GRAS oils, surfactants and co-surfactants. Particularly, isopropyl myristate, extra virgin olive oil and their combination were used as the oil phase. Stable systems were obtained by implementing both high- and low-energy emulsification methods and using various combinations of the selected components. The nanodroplet size and the homogeneity of the developed systems were evaluated using DLS in order to determine the most promising systems in terms of stability. Two low-energy NEs monodispersed and stable for three months containing IPM and a combination of IPM and EVOO as the oil phase were selected for the encapsulation of the bioactives and the development of the hybrid systems. In addition, these NEs were prepared in the absence of co-solvent or any permeation enhancers that could cause toxicity. Thus, the three lipophilic bioactives of interest namely, VD, CU and, CBD were successfully encapsulated in the developed NEs. All three compounds induced slight changes to the NEs in terms of nanodroplet size and homogeneity, however, they still remained stable for three months indicating that the developed NEs are suitable carriers.

Moreover, hydrogels were formulated using various polymers and their combinations. In order to determine the most suitable hydrogel matrix, C-PC extract was incorporated in them. After optical observation and carrying out studies in different temperature conditions and pH, a chitosan hydrogel of concentration 1.25% w/v was finally selected for the development of the hybrid systems. This HG demonstrated the most satisfactory properties and no changes were optically observed for at least three months. Therefore, it was considered as the most suitable matrix for the incorporation of the NEs in order to obtain the desired “carrier in carrier” colloidal formulations.

Both NEs and NE/HGs were structurally characterized by performing EPR, SAXS, confocal microscopy and cryo-EM. Regarding the hybrid systems, the investigation of the NEs’ structure after its incorporation into the HG was of special interest in order to elucidate possible structural changes. Particularly, EPR spin probing indicated that the rigidity of the

surfactant monolayer was affected differently depending on the bioactive compound encapsulated in the system. However, all NE/HGs under study demonstrated less viscous interfacial films in comparison to the corresponding NEs providing the indication that they could release the encapsulated compounds more efficiently. The spherical structure of the NEs that remained unaffected upon incorporation into the HG matrix was confirmed by a combination of methods acting in a complementary manner. Initially, confocal micrographs demonstrated the presence of spherical oil droplets of comparable sizes in both formulations. In addition, SAXS results also suggested that the spherical structure as well as the size of the NEs were not affected by their embodiment in the HG, indicating that they maintained their properties as colloidal systems. Furthermore, SAXS exhibited that the encapsulation of different CBD concentrations had no significant effect on the NEs' structure and the size of the nanodroplets both before and after its incorporation into the hydrogel. Finally, NEs in the absence and presence of CBD were characterized via cryo-EM which also demonstrated the presence of spherical structures and confirmed the droplet diameters that were obtained by DLS.

Subsequently, the developed nanocarriers were examined using *in vitro* and *ex vivo* assays in order to evaluate their suitability as delivery vehicles. First of all, a cell viability assessment was of paramount importance in order to establish that the carriers themselves in the absence of bioactive compounds do not demonstrate any cytotoxic effect. Hence, the two most promising NEs were administered to human nasal epithelial cells (RPMI 2650) in various concentrations. The system containing EVOO in the oil phase exhibited increased cell viability even when administered in particularly high concentrations in the cell culture medium. Therefore, it was selected for the encapsulation of CBD and for the formulation of the hybrid systems. Subsequently, NEs in the absence and presence of CBD as well as the corresponding NE/HGs were administered to human normal fibroblasts (WS1). Cell viability assessment indicated that both colloidal delivery systems present increased biocompatibility even at very high concentrations. Secondly, a preliminary *in vitro* permeation study using synthetic cellulose membranes was carried out to investigate the ability of the nanodispersions to release the bioactives. It was demonstrated that the release kinetics was independent of the nanocarrier, however, it was related to the structure of the encapsulated compound and its interaction with the surfactant monolayer. Both VD and CU were effectively released, however, increased amounts were released from the NE/HG. This finding was confirmed through an *in vitro* permeation study in which porcine's ear skin was used as the model membrane. This study was performed in order to evaluate the suitability of NEs and

NE/HGs as vehicles for the transdermal delivery of CBD. Improved penetration of CBD was observed for both NEs and NE/ HGs which was related to the presence of surfactants at the interface, inducing structural changes and solubilizing the lipids and proteins of the SC. Moreover, tape stripping experiments demonstrated enhanced penetration of CBD with administration of the NE/HG system that could be attributed to the presence of chitosan further affecting the structure of the SC.

Overall, the present thesis indicates that the proposed colloidal delivery systems, can be ideal candidates for the efficient transdermal delivery of bioactive compounds of highly lipophilic nature. The increased cell viability and the enhanced penetration properties are essential characteristics of a nanodispersion to be used for the administration of substances of pharmacological interest. Finally, the comparison between NEs and NE/HGs demonstrated that the hybrid systems exhibit improved penetration through SC making them more appropriate for transdermal administration versus the corresponding NEs. In the future, the ability of the developed nanocarriers to simultaneously encapsulate lipophilic and hydrophilic bioactive compounds in order to achieve synergistic action and improved biological effects remains to be investigated. Nevertheless, the foremost benefit of the proposed systems is that they could provide simple and non-invasive alternative routes of delivery which are of paramount importance for people who are not able to take medication orally or they want to avoid painful ways of delivery such as injection.

Supplementary Data

Supplementary data

The results that were presented above in the chapters 5.5.3. *Ex vivo* permeation study and 5.5.4. Tape stripping experiments were obtained using the following raw data. These data were obtained using the technique of Liquid chromatography- mass spectrometry (LC MS/MS) in combination with a standard curve that was prepared using known CBD concentrations.

Standard curve

Table 10. Illustration of the peaks obtained by performing liquid chromatography-mass spectrometry in CBD samples with known concentrations.

Concentration (ng/mL)	Peak 1	Peak 2	Average
5	36259	29178	32718,5
10	68375	48042	58208,5
20	111812	93986	102899
50	222641	211023	216832
100	395630	385322	390476
200	667234	660329	663781,5
500	1421767	1413245	1417506

Using the results illustrated in the table, the following standard curve was obtained which was then used for the processing of the raw data.

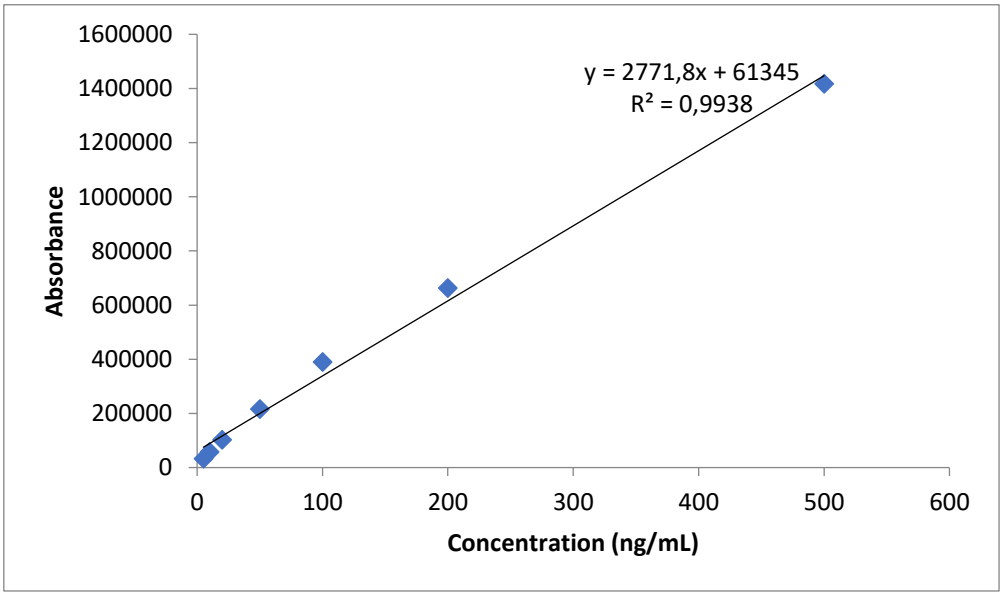

Figure 58. Standard curve diagram that was prepared using solutions with known concentrations of CBD.

***Ex vivo* permeation study**

In order to obtain as accurate results as possible, NEs and NE/HGs were each applied in six Franz diffusion cells. The obtained raw data representing the CBD concentrations that were detected over time in each cell are presented in the table below.

Table 11. Raw date obtained during the ex vivo permeation study using the LC MS/MS method.

Time (h)	Sample	Abs	C (ng/mL)
2	NE 1	0	< LOQ
	NE 2	0	< LOQ
	NE 3	343	< LOQ
	NE 4	2510	< LOQ
	NE 5	299	< LOQ
	NE 6	4619	< LOQ
	NE/HG 7	0	< LOQ
	NE/HG 8	108	< LOQ
	NE/HG 9	120	< LOQ
	NE/HG 10	1988	< LOQ
	NE/HG 11	214	< LOQ
	NE/HG 12	326	< LOQ

Time (h)	Abs	C (ng/mL)
4	142	< LOQ
	549	< LOQ
	274	< LOQ
	2332	< LOQ
	1703	< LOQ
	5483	< LOQ
	302	< LOQ
	884	< LOQ
	3267	< LOQ
	2330	< LOQ
	194	< LOQ
	719	< LOQ

Time (h)	Abs	C (ng/mL)
6	680	< LOQ
	2673	< LOQ
	381	< LOQ
	2847	< LOQ
	7465	1,12
	4820	< LOQ
	2347	< LOQ
	3343	< LOQ
	10417	4,78
	1726	< LOQ
	1173	< LOQ
	2369	< LOQ

Time (h)	Sample	Abs	C (ng/mL)
8	NE 1	1845	< LOQ
	NE 2	5876	< LOQ
	NE 3	633	< LOQ
	NE 4	3067	< LOQ
	NE 5	13215	8,26
	NE 6	5685	< LOQ

Time (h)	Abs	C (ng/mL)
22	361	< LOQ
	836	< LOQ
	89	< LOQ
	218	< LOQ
	2230	< LOQ
	1298	< LOQ

Time (h)	Abs	C (ng/mL)
24	39351	40,74
	125806	148,17
	21868	19,01
	34687	34,94
	164089	195,74
	43374	45,74

	NE/HG 7	6938	0,46
	NE/HG 8	7681	1,38
	NE/HG 9	21830	18,97
	NE/HG 10	2425	< LOQ
	NE/HG 11	3147	< LOQ
	NE/HG 12	5456	< LOQ

	89943	103,60
	71615	80,83
	195918	235,29
	10308	4,65
	42772	44,99
	29799	28,87

	137355	162,52
	87715	100,84
	210262	253,12
	12185	6,98
	46069	49,09
	76403	86,78

Time (h)	Sample	Abs	C (ng/mL)
26	NE 1	42466	44,61
	NE 2	136686	161,69
	NE 3	24390	22,15
	NE 4	36424	37,10
	NE 5	187423	224,74
	NE 6	48580	52,21
	NE/HG 7	153714	182,85
	NE/HG 8	95129	110,05
	NE/HG 9	229717	277,29
	NE/HG 10	13324	8,40
	NE/HG 11	47416	50,76
	NE/HG 12	82961	94,93

Time (h)	Abs	C (ng/mL)
28	46198	49,25
	160006	190,67
	30478	29,71
	47684	51,09
	212680	256,12
	57550	63,35
	175957	210,49
	106035	123,60
	260384	315,40
	16337	12,14
	55188	60,42
	95252	110,20

Time (h)	Abs	C (ng/mL)
30	55202	60,43
	178964	214,22
	35524	35,98
	52025	56,49
	227338	274,33
	63809	71,13
	192260	230,75
	110964	129,73
	285903	347,11
	19533	16,11
	64608	72,12
	106142	123,73

Tape stripping experiments

Since porcine ears demonstrate significant variation in their structure, it was deemed necessary to conduct five independent experiments in order to achieve results as accurate as possible. The raw data obtained using the LC MS/MS method and the aforementioned standard curve are presented in the tables below.

Table 12. Raw data obtained during tape stripping experiments using the LC MS/MS method (experiments 1-3).

Sample	Absorbance	Concentration (ng/mL)	Absorbance	Concentration (ng/mL)	Absorbance	Concentration (ng/mL)
G1	551660	677,34	236017	285,12	504074	618,21
G2	324373	394,91	152400	181,21	273672	331,91
G3	106624	124,33	126604	149,16	380710	464,92
G4	117148	137,41	75507	85,67	113079	132,35
G5	84376	96,69	60989	67,63	81780	93,46
G6	52870	57,54	51627	55,99	104222	121,35
G7	51482	55,81	183183	219,47	64910	72,50
G8	42866	45,11	69422	78,10	90467	104,26
G9	49317	53,12	48762	52,43	77764	88,47
G10	43481	45,87	35570	36,04	47628	51,02
G11	28111	26,77	51320	55,61	86613	99,47
G12	64895	72,48	34113	34,23	77998	88,76
G13	31749	31,29	32205	31,86	56944	62,60
G14	74132	83,96	32048	31,66	66746	74,78
G15	28788	27,61	47696	51,11	88511	101,83
G16	91879	106,01	17494	13,58	92118	106,31
G17	28614	27,40	16383	12,20	59641	65,95
G18	407504	498,21	51151	55,40	86416	99,22
G19	224047	270,25	24883	22,76	125065	147,25
G20	39850	41,36	26880	25,24	78331	89,18
G21	47853	51,30	62215	69,15	68693	77,20
G22	32598	32,35	47719	51,14	159538	190,08
G23	12397	7,24	29133	28,04	83228	95,26
G24	20636	17,48	118977	139,68	66999	75,09
G25	11781	6,48	7291	0,90	79762	90,95
G26	19533	16,11	26785	25,12	106934	124,72
G27	43098	45,39	17130	13,13	126118	148,56
G28	23941	21,59	42729	44,94	109946	128,46
G29	155831	185,48	23124	20,57	66056	73,92
G30	27507	26,02	28258	26,95	92681	107,01
N1	273257	331,39	439006	537,36	348366	424,73
N2	97637	113,17	328531	400,08	333028	405,67
N3	75517	85,68	211043	254,09	200528	241,02
N4	68042	76,39	119432	140,25	127795	150,64
N5	47235	50,53	88574	101,90	94637	109,44

N6	101182	117,57	96120	111,28	114470	134,08
N7	86324	99,11	108036	126,09	57762	63,62
N8	37515	38,46	93110	107,54	48356	51,93
N9	32746	32,53	70269	79,16	46265	49,33
N10	33728	33,75	135188	159,83	86059	98,78
N11	70817	79,84	80538	91,92	1534711	1898,90
N12	69628	78,36	52975	57,67	88502	101,81
N13	41166	42,99	110051	128,59	65403	73,11
N14	32429	32,14	72102	81,43	48064	51,56
N15	44267	46,85	65735	73,52	43101	45,40
N16	42993	45,26	96831	112,16	77771	88,48
N17	33769	33,80	47677	51,08	42431	44,57
N18	36454	37,14	42533	44,69	37088	37,93
N19	30158	29,31	43603	46,02	81157	92,69
N20	44113	46,66	76874	87,36	68315	76,73
N21	48204	51,74	60912	67,53	47628	51,02
N22	44962	47,71	98256	113,93	87281	100,30
N23	40424	42,07	47402	50,74	123630	145,46
N24	46079	49,10	58992	65,14	213213	256,78
N25	44846	47,57	43118	45,42	85733	98,37
N26	35498	35,95	90126	103,83	57599	63,41
N27	27366	25,84	73746	83,48	43189	45,51
N28	33016	32,87	60150	66,58	172194	205,81
N29	43422	45,80	46993	50,23	93344	107,83
N30	37076	37,91	48674	52,32	143487	170,14

Table 13. . Raw data obtained during tape stripping experiments using the LC MS/MS method (experiments 4,5).

Sample	Absorbance	Concentration (ng/mL)	Absorbance	Concentration (ng/mL)
G1	803934	990,83	429743	525,85
G2	345298	420,91	313385	381,26
G3	258673	313,27	235179	284,08
G4	133832	158,14	167238	199,65
G5	106841	124,60	112951	132,19
G6	105458	122,88	91265	105,25
G7	112476	131,60	100901	117,22
G8	113799	133,25	83089	95,09
G9	69452	78,14	76277	86,62
G10	118199	138,72	65869	73,69
G11	108456	126,61	61818	68,66
G12	90261	104,00	65823	73,63
G13	64541	72,04	56697	62,29
G14	141679	167,89	71139	80,24
G15	491291	602,33	45078	47,85
G16	557923	685,13	54589	59,67

G17	156105	185,82	38264	39,39
G18	173876	207,90	36867	37,65
G19	98233	113,91	33605	33,60
G20	125	< LOQ	33864	33,92
G21	131050	154,68	65198	72,86
G22	125305	147,55	36156	36,77
G23	146240	173,56	73476	83,14
G24	91555	105,61	51641	56,01
G25	72471	81,89	33491	33,46
G26	62407	69,39	37485	38,42
G27	373360	455,78	38261	39,38
G28	5797156	7195,51	52295	56,82
G29	653703	804,15	41554	43,48
G30	122108	143,57	27315	25,78
N1	493260	604,78	721278	888,12
N2	350193	427,00	337340	411,03
N3	166253	198,43	200686	241,22
N4	98793	114,60	170226	203,37
N5	75768	85,99	156640	186,48
N6	61573	68,35	1105643	1365,74
N7	227844	274,96	164055	195,70
N8	582020	715,07	143112	169,67
N9	54019	58,96	128635	151,68
N10	57223	62,95	93462	107,98
N11	43808	46,28	122162	143,64
N12	67696	75,96	71877	81,16
N13	71557	80,76	80350	91,68
N14	50821	54,99	61573	68,35
N15	66683	74,70	78541	89,44
N16	50695	54,83	96788	112,11
N17	68179	76,56	122583	144,16
N18	100479	116,70	104329	121,48
N19	100123	116,25	77580	88,24
N20	95504	110,51	74112	83,93
N21	105473	122,90	86815	99,72
N22	113620	133,03	107329	125,21
N23	106782	124,53	74079	83,89
N24	81096	92,61	127261	149,98
N25	95869	110,97	116456	136,55
N26	133273	157,45	100099	116,22
N27	69829	78,61	97693	113,23
N28	110457	129,10	73521	83,20
N29	101106	117,48	86944	99,88
N30	97646	113,18	66019	73,88

References

[1] O.C. Farokhzad, R. Langer, Impact of nanotechnology on drug delivery, ACS Nano. 3 (2009) 16–20. https://doi.org/10.1021/NN900002M/ASSET/IMAGES/LARGE/NN-2009-00002M_0001.JPEG.

[2] S. Bayda, M. Adeel, T. Tuccinardi, M. Cordani, F. Rizzolio, The History of Nanoscience and Nanotechnology: From Chemical–Physical Applications to Nanomedicine, Molecules 2020, Vol. 25, Page 112. 25 (2019) 112. https://doi.org/10.3390/MOLECULES25010112.

[3] Home | National Nanotechnology Initiative, (n.d.). https://www.nano.gov/ (accessed October 10, 2022).

[4] D.J. McClements, Nanoemulsions versus microemulsions: terminology, differences, and similarities, Soft Matter. 8 (2012) 1719–1729. https://doi.org/10.1039/C2SM06903B.

[5] M.C. García Vior, E. Monteagudo, L.E. Dicelio, J. Awruch, A comparative study of a novel lipophilic phthalocyanine incorporated into nanoemulsion formulations: Photophysics, size, solubility and thermodynamic stability, Dyes and Pigments. 91 (2011) 208–214. https://doi.org/10.1016/J.DYEPIG.2011.03.011.

[6] J. Rao, D.J. McClements, Lemon oil solubilization in mixed surfactant solutions: Rationalizing microemulsion & nanoemulsion formation, Food Hydrocoll. 26 (2012) 268–276. https://doi.org/10.1016/J.FOODHYD.2011.06.002.

[7] N. Anton, J.P. Benoit, P. Saulnier, Design and production of nanoparticles formulated from nano-emulsion templates—A review, Journal of Controlled Release. 128 (2008) 185–199. https://doi.org/10.1016/J.JCONREL.2008.02.007.

[8] N. Sadurní, C. Solans, N. Azemar, M.J. García-Celma, Studies on the formation of O/W nano-emulsions, by low-energy emulsification methods, suitable for pharmaceutical applications, European Journal of Pharmaceutical Sciences. 26 (2005) 438–445. https://doi.org/10.1016/J.EJPS.2005.08.001.

[9] Q. Huang, H. Yu, Q. Ru, Bioavailability and Delivery of Nutraceuticals Using Nanotechnology, J Food Sci. 75 (2010) R50–R57. https://doi.org/10.1111/J.1750-3841.2009.01457.X.

[10] M. Kong, X.G. Chen, D.K. Kweon, H.J. Park, Investigations on skin permeation of hyaluronic acid based nanoemulsion as transdermal carrier, Carbohydr Polym. 86 (2011) 837–843. https://doi.org/10.1016/J.CARBPOL.2011.05.027.

[11] J. Patra, G. Das, L. Fraceto, E. Campos, M. Rodriguez-Torres, L. Acosta-Torres, L. Diaz-Torres, R. Grillo, M. Swamy, S. Sharma, S. Habtemariam, H. Shin, Nano based drug delivery systems: recent developments and future prospects, J Nanobiotechnology. 16 (2018) 1–33. https://doi.org/https://doi.org/10.1186/s12951-018-0392-8.

[12] J.E. Hulla, S.C. Sahu, A.W. Hayes, Nanotechnology: History and future, Hum Exp Toxicol. 34 (2015) 1318–1321. https://doi.org/10.1177/0960327115603588.

[13] J.A. Beutler, Natural Products as a Foundation for Drug Discovery, Curr Protoc Pharmacol. 46 (2009) 9.11.1-9.11.21. https://doi.org/10.1002/0471141755.PH0911S46.

[14] A.G. Atanasov, B. Waltenberger, E.M. Pferschy-Wenzig, T. Linder, C. Wawrosch, P. Uhrin, V. Temml, L. Wang, S. Schwaiger, E.H. Heiss, J.M. Rollinger, D. Schuster, J.M. Breuss, V. Bochkov, M.D. Mihovilovic, B. Kopp, R. Bauer, V.M. Dirsch, H. Stuppner, Discovery and resupply of pharmacologically active plant-derived natural products: A review, Biotechnol Adv. 33 (2015) 1582–1614. https://doi.org/10.1016/J.BIOTECHADV.2015.08.001.

[15] P. Vega-Vásquez, N.S. Mosier, J. Irudayaraj, Nanoscale Drug Delivery Systems: From Medicine to Agriculture, Front Bioeng Biotechnol. 8 (2020). https://doi.org/10.3389/FBIOE.2020.00079/FULL.

[16] M. Namdari, A. Eatemadi, M. Soleimaninejad, A.T. Hammed, A brief review on the application of nanoparticle enclosed herbal medicine for the treatment of infective endocarditis, Biomedicine & Pharmacotherapy. 87 (2017) 321–331. https://doi.org/10.1016/J.BIOPHA.2016.12.099.

[17] T. Safra, F. Muggia, S. Jeffers, D.D. Tsao-Wei, S. Groshen, O. Lyass, R. Henderson, G. Berry, A. Gabizon, Pegylated liposomal doxorubicin (doxil): Reduced clinical cardiotoxicity in patients reaching or exceeding cumulative doses of 500 mg/m2, Annals of Oncology. 11 (2000) 1029–1034. https://doi.org/10.1023/A:1008365716693.

[18] M.M.A. Abdel-Mottaleb, D. Neumann, A. Lamprecht, Lipid nanocapsules for dermal application: A comparative study of lipid-based versus polymer-based nanocarriers, European Journal of Pharmaceutics and Biopharmaceutics. 79 (2011) 36–42. https://doi.org/10.1016/J.EJPB.2011.04.009.

[19] I. Theochari, E. Mitsou, I. Nikolic, T. Ilic, V. Dobricic, V. Pletsa, V. Papadimitriou, Colloidal nanodispersions for the topical delivery of Ibuprofen: Structure, dynamics and bioperformances, J Mol Liq. 334 (2021). https://doi.org/https://doi.org/10.1016/j.molliq.2021.116021.

[20] M. Chaari, I. Theochari, V. Papadimitriou, A. Xenakis, E. Ammar, Encapsulation of carotenoids extracted from halophilic Archaea in oil-in-water (O/W) micro- and nano-emulsions, Colloids Surf B Biointerfaces. 161 (2018) 219–227. https://doi.org/10.1016/J.COLSURFB.2017.10.042.

[21] E. Mitsou, V. Pletsa, G. Sotiroudis, P. Panine, M. Zoumpanioti, A. Xenakis, Development of a microemulsion for encapsulation and delivery of gallic acid. The role of chitosan, Colloids Surf B Biointerfaces. 190 (2020). https://doi.org/https://doi.org/10.1016/j.colsurfb.2020.110974.

[22] I. Nikolic, E. Mitsou, I. Pantelic, D. Randjelovic, B. Markovic, V. Papadimitriou, S. Savic, Microstructure and biopharmaceutical performances of curcumin-loaded low-energy nanoemulsions containing eucalyptol and pinene: Terpenes' role, European Journal of Pharmaceutical Sciences. 142 (2020). https://doi.org/https://doi.org/10.1016/j.ejps.2019.105135.

[23] V. Savić, M. Todosijević, T. Ilić, M. Lukić, E. Mitsou, V. Papadimitriou, S. Savić, Tacrolimus loaded biocompatible lecithin-based microemulsions with improved skin penetration: Structure characterization and in vitro/in vivo performances, Int J Pharm. 529 (2017) 491–505. https://doi.org/https://doi.org/10.1016/j.ijpharm.2017.07.036.

[24] M. Ferrari, Cancer nanotechnology: opportunities and challenges, Nature Reviews Cancer 2005 5:3. 5 (2005) 161–171. https://doi.org/10.1038/nrc1566.

[25] K. Thanki, R.P. Gangwal, A.T. Sangamwar, S. Jain, Oral delivery of anticancer drugs: Challenges and opportunities, Journal of Controlled Release. 170 (2013) 15–40. https://doi.org/10.1016/J.JCONREL.2013.04.020.

[26] I. Theochari, A. Xenakis, V. Papadimitriou, Nanocarriers for effective drug delivery, Smart Nanocontainers: Micro and Nano Technologies. (2020) 315–341. https://doi.org/10.1016/B978-0-12-816770-0.00019-8.

[27] B. Mishra, B.B. Patel, S. Tiwari, Colloidal nanocarriers: a review on formulation technology, types and applications toward targeted drug delivery, Nanomedicine. 6 (2010) 9–24. https://doi.org/10.1016/J.NANO.2009.04.008.

[28] S. Gupta, S.P. Moulik, Biocompatible Microemulsions and Their Prospective Uses in Drug Delivery, J Pharm Sci. 97 (2008) 22–45. https://doi.org/10.1002/JPS.21177.

[29] A. Zeeshan, M.• Farhan, A. Siddiqui, Nanomedicine and drug delivery: a mini review, International Nano Letters 2014 4:1. 4 (2014) 1–7. https://doi.org/10.1007/S40089-014-0094-7.

[30] A.Z. Wilczewska, K. Niemirowicz, K.H. Markiewicz, H. Car, Nanoparticles as drug delivery systems, Pharmacological Reports. 64 (2012) 1020–1037. https://doi.org/10.1016/S1734-1140(12)70901-5.

[31] Z. Zhu, Y. Li, X. Yang, W. Pan, H. Pan, The reversion of anti-cancer drug antagonism of tamoxifen and docetaxel by the hyaluronic acid-decorated polymeric nanoparticles, Pharmacol Res. 126 (2017) 84–96. https://doi.org/10.1016/J.PHRS.2017.07.011.

[32] M. Danaei, M. Dehghankhold, S. Ataei, F. Hasanzadeh Davarani, R. Javanmard, A. Dokhani, S. Khorasani, M.R. Mozafari, Impact of Particle Size and Polydispersity Index on the Clinical Applications of Lipidic Nanocarrier Systems, Pharmaceutics 2018, Vol. 10, Page 57. 10 (2018) 57. https://doi.org/10.3390/PHARMACEUTICS10020057.

[33] H.R. Dhanasekaran, C.P. Sharma, P. Haridoss, Drug delivery nanosystems—An introduction, Drug Delivery Nanosystems for Biomedical Applications. (2018) 1–12. https://doi.org/10.1016/B978-0-323-50922-0.00001-8.

[34] A. Sangtani, O.K. Nag, L.D. Field, J.C. Breger, J.B. Delehanty, Multifunctional nanoparticle composites: progress in the use of soft and hard nanoparticles for drug delivery and imaging, Wiley Interdiscip Rev Nanomed Nanobiotechnol. 9 (2017) e1466. https://doi.org/10.1002/WNAN.1466.

[35] X. Chen, Y. Tang, B. Cai, H. Fan, 'One-pot' synthesis of multifunctional GSH–CdTe quantum dots for targeted drug delivery, Nanotechnology. 25 (2014) 235101. https://doi.org/10.1088/0957-4484/25/23/235101.

[36] F. Gu, L. Zhang, B.A. Teply, N. Mann, A. Wang, A.F. Radovic-Moreno, R. Langer, O.C. Farokhzad, Precise engineering of targeted nanoparticles by using self-assembled biointegrated block copolymers, Proceedings of the National Academy of Sciences. 105 (2008) 2586–2591. https://doi.org/10.1073/PNAS.0711714105.

[37] E. Roger, F. Lagarce, E. Garcion, J.P. Benoit, Biopharmaceutical parameters to consider in order to alter the fate of nanocarriers after oral delivery, Future Medicine. 5 (2010) 287–306. https://doi.org/10.2217/NNM.09.110.

[38] H.H. Tayeb, F. Sainsbury, Nanoemulsions in drug delivery: formulation to medical application, Future Medicine. 13 (2018) 2507–2525. https://doi.org/10.2217/NNM-2018-0088.

[39] S. Ganta, M. Talekar, A. Singh, T. Coleman, M.A.-A. Pharmscitech, undefined 2014, Nanoemulsions in translational research—opportunities and challenges in targeted cancer therapy, AAPS PharmSciTech . 15 (2014) 694–708.

[40] D.J. McClements, Food Emulsions : Principles, Practices, and Techniques, Second Edition, (2004). https://doi.org/10.1201/9781420039436.

[41] Y. Singh, J.G. Meher, K. Raval, F.A. Khan, M. Chaurasia, N.K. Jain, M.K. Chourasia, Nanoemulsion: Concepts, development and applications in drug delivery, Journal of Controlled Release. 252 (2017) 28–49. https://doi.org/10.1016/J.JCONREL.2017.03.008.

[42] N. Haziqah Che Marzuki, R. Abdul Wahab, M. Abdul Hamid, An overview of nanoemulsion: concepts of development and cosmeceutical applications, Biotechnology & Biotechnological Equipment. 33 (2019) 779–797. https://doi.org/10.1080/13102818.2019.1620124.

[43] J.S. Komaiko, D.J. Mcclements, Formation of Food-Grade Nanoemulsions Using Low-Energy Preparation Methods: A Review of Available Methods, Compr Rev Food Sci Food Saf. 15 (2016) 331–352. https://doi.org/10.1111/1541-4337.12189.

[44] Z. Zhang, D.M.- Nanoemulsions, undefined 2018, Overview of nanoemulsion properties: stability, rheology, and appearance, Elsevier. (n.d.). https://www.sciencedirect.com/science/article/pii/B9780128118382000023 (accessed February 12, 2023).

[45] A. Gupta, B.H. Eral, A.T. Hatton, P.S. Doyle, Nanoemulsions: formation, properties and applications, Soft Matter. 12 (2016) 2826–2841. https://doi.org/10.1039/C5SM02958A.

[46] D.J. McClements, Nanoemulsion-based oral delivery systems for lipophilic bioactive components: nutraceuticals and pharmaceuticals, Future Science. 4 (2013) 841–857. https://doi.org/10.4155/TDE.13.46.

[47] E Acosta, Bioavailability of nanoparticles in nutrient and nutraceutical delivery, Curr Opin Colloid Interface Sci. 14 (2009) 3–15.

[48] M.- Kohn, J.B. Đokovi´cđokovi´c, S. Demisli, S.M. Savi´csavi´c, B.D. Markovi´c, N.D. Ceki´cceki´c, D. v Randjelovic, J.R. Mitrovi´cmitrovi´c, D.J. Lunter, V. Papadimitriou, A. Xenakis, S.D. Savi´csavi´c, The Impact of the Oil Phase Selection on Physicochemical

Properties, Long-Term Stability, In Vitro Performance and Injectability of Curcumin-Loaded PEGylated, Pharmaceutics. 14 (2022). https://doi.org/10.3390/pharmaceutics14081666.

[49] Y. Zhang, Z. Shang, C. Gao, M. Du, S. Xu, H. Song, T. Liu, Nanoemulsion for solubilization, stabilization, and in vitro release of pterostilbene for oral delivery, AAPS PharmSciTech. 15 (2014) 1000–1008. https://doi.org/10.1208/S12249-014-0129-4/METRICS.

[50] N. Garti, M. Frenkel, R. Shwartz, MULTIPLE EMULSIONS. PART II: PROPOSED TECHNIQUE TO OVERCOME UNPLEASANT TASTE OF DRUGS, J Dispers Sci Technol. 4 (2007) 237–252. https://doi.org/10.1080/01932698308943369.

[51] M.M. Fryd, T.G. Mason, Advanced Nanoemulsions, Annu Rev Phys Chem. 63 (2012) 493–518. https://doi.org/10.1146/ANNUREV-PHYSCHEM-032210-103436.

[52] S. Abrol, A. Trehan, O.P. Katare, Comparative Study of Different Silymarin Formulations: Formulation, Characterisation and In Vitro / In Vivo Evaluation, Curr Drug Deliv. 2 (2005) 45–51. https://doi.org/10.2174/1567201052772870.

[53] S.P. Jiang, S.N. He, Y.L. Li, D.L. Feng, X.Y. Lu, Y.Z. Du, H.Y. Yu, F.Q. Hu, H. Yuan, Preparation and characteristics of lipid nanoemulsion formulations loaded with doxorubicin, Int J Nanomedicine. 8 (2013) 3141–3150. https://doi.org/10.2147/IJN.S47708.

[54] S. Banasaz, K. Morozova, G. Ferrentino, M. Scampicchio, Encapsulation of Lipid-Soluble Bioactives by Nanoemulsions, Molecules 2020, Vol. 25, Page 3966. 25 (2020) 3966. https://doi.org/10.3390/MOLECULES25173966.

[55] D.J. McClements, J. Rao, Food-Grade Nanoemulsions: Formulation, Fabrication, Properties, Performance, Biological Fate, and Potential Toxicity, Critical Reviews in Food Science and Nutrition . 51 (2011) 285–330. https://doi.org/10.1080/10408398.2011.559558.

[56] M.X. Quintanilla-Carvajal, B.H. Camacho-Díaz, L.S. Meraz-Torres, J.J. Chanona-Pérez, L. Alamilla-Beltrán, A. Jimenéz-Aparicio, G.F. Gutiérrez-López, Nanoencapsulation: A new trend in food engineering processing, Food Engineering Reviews. 2 (2010) 39–50. https://doi.org/10.1007/S12393-009-9012-6/METRICS.

[57] P. Sanguansri, M.A. Augustin, Nanoscale materials development – a food industry perspective, Trends Food Sci Technol. 17 (2006) 547–556. https://doi.org/10.1016/J.TIFS.2006.04.010.

[58] N. Anton, T.F. Vandamme, The universality of low-energy nano-emulsification, Int J Pharm. 377 (2009) 142–147. https://doi.org/10.1016/J.IJPHARM.2009.05.014.

[59] I. Solè, A. Maestro, C. González, C. Solans, J.M. Gutiérrez, Optimization of nano-emulsion preparation by low-energy methods in an ionic surfactant system, Langmuir. 22 (2006) 8326–8332. https://doi.org/10.1021/LA0613676/ASSET/IMAGES/MEDIUM/LA0613676N00001.GIF.

[60] J. Mewis, N.J. Wagner, Colloidal Suspension Rheology, 2012.

[61] K. Rahn-Chique, A.M. Puertas, M.S. Romero-Cano, C. Rojas, G. Urbina-Villalba, Nanoemulsion stability: Experimental evaluation of the flocculation rate from turbidity measurements, Adv Colloid Interface Sci. 178 (2012) 1–20. https://doi.org/10.1016/J.CIS.2012.05.001.

[62] M. Jaiswal, R. Dudhe, P.K. Sharma, Nanoemulsion: an advanced mode of drug delivery system, 3 Biotech. 5 (2015) 123–127. https://doi.org/10.1007/S13205-014-0214-0/METRICS.

[63] A. Kabalnov, Ostwald Ripening and Related Phenomena, J Dispers Sci Technol. 22 (2007) 1–12. https://doi.org/10.1081/DIS-100102675.

[64] T. Delmas, H. Piraux, A.C. Couffin, I. Texier, F. Vinet, P. Poulin, M.E. Cates, J. Bibette, How to prepare and stabilize very small nanoemulsions, Langmuir. 27 (2011) 1683–1692. https://doi.org/10.1021/LA104221Q/SUPPL_FILE/LA104221Q_SI_001.PDF.

[65] H. Choudhury, B. Gorain, B. Chatterjee, U. K. Mandal, P. Sengupta, R. K. Tekade, Pharmacokinetic and Pharmacodynamic Features of Nanoemulsion Following Oral, Intravenous, Topical and Nasal Route, Curr Pharm Des. 23 (2017). https://doi.org/10.2174/1381612822666161201143600.

[66] Y. Kawabata, K. Wada, M. Nakatani, S. Yamada, S. Onoue, Formulation design for poorly water-soluble drugs based on biopharmaceutics classification system: Basic approaches and practical applications, Int J Pharm. 420 (2011) 1–10. https://doi.org/10.1016/J.IJPHARM.2011.08.032.

[67] M. Pandey, H. Choudhury, O.C. Yeun, H.M. Yin, T.W. Lynn, C.L.Y. Tine, N.S. Wi, K.C.C. Yen, C.S. Phing, P. Kesharwani, S.K. Bhattamisra, B. Gorain, Perspectives of Nanoemulsion Strategies in The Improvement of Oral, Parenteral and Transdermal Chemotherapy, Curr Pharm Biotechnol. 19 (2018) 276–292. https://doi.org/10.2174/1389201019666180605125234.

[68] Z. Xia, Y. Han, H. Du, D.J. McClements, Z. Tang, H. Xiao, Exploring the effects of carrier oil type on in vitro bioavailability of β-carotene: A cell culture study of carotenoid-enriched nanoemulsions, LWT. 134 (2020) 110224. https://doi.org/10.1016/J.LWT.2020.110224.

[69] L. Yang, J. Gu, T. Luan, X. Qiao, Y. Cao, C. Xue, J. Xu, Influence of oil matrixes on stability, antioxidant activity, bioaccessibility and bioavailability of astaxanthin ester, J Sci Food Agric. 101 (2021) 1609–1617. https://doi.org/10.1002/JSFA.10780.

[70] I. Golfomitsou, E. Mitsou, A. Xenakis, V. Papadimitriou, Development of food grade O/W nanoemulsions as carriers of vitamin D for the fortification of emulsion based food matrices: A structural and activity study, J Mol Liq. 268 (2018) 734–742. https://doi.org/10.1016/J.MOLLIQ.2018.07.109.

[71] S. Demisli, E. Mitsou, V. Pletsa, A. Xenakis, V. Papadimitriou, Development and study of nanoemulsions and nanoemulsion-based hydrogels for the encapsulation of lipophilic compounds, Nanomaterials. 10 (2020). https://doi.org/10.3390/nano10122464.

[72] H. Choudhury, B. Gorain, S. Karmakar, E. Biswas, G. Dey, R. Barik, M. Mandal, T.K. Pal, Improvement of cellular uptake, in vitro antitumor activity and sustained release

profile with increased bioavailability from a nanoemulsion platform, Int J Pharm. 460 (2014) 131–143. https://doi.org/10.1016/J.IJPHARM.2013.10.055.

[73] C. Fernandes, U. Soni, V. Patravale, Nano-interventions for neurodegenerative disorders, Pharmacol Res. 62 (2010) 166–178. https://doi.org/10.1016/J.PHRS.2010.02.004.

[74] J. Edmond, Essential polyunsaturated fatty acids and the barrier to the brain: The components of a model for transport, Journal of Molecular Neuroscience. 16 (2001) 181–193. https://doi.org/10.1385/JMN:16:2-3:181/METRICS.

[75] B. Sapra, P. Thatai, S. Bhandari, J. Sood, M. Jindal, A. Tiwary, A critical appraisal of microemulsions for drug delivery: part I, 4 (2013) 1547–1564. https://doi.org/10.4155/TDE.13.116.

[76] R. Richa, A. Roy Choudhury, Exploration of polysaccharide based nanoemulsions for stabilization and entrapment of curcumin, Int J Biol Macromol. 156 (2020) 1287–1296. https://doi.org/10.1016/J.IJBIOMAC.2019.11.167.

[77] S. Demisli, I. Theochari, P. Christodoulou, M. Zervou, A. Xenakis, V. Papadimitriou, Structure, activity and dynamics of extra virgin olive oil-in-water nanoemulsions loaded with vitamin D3 and calcium citrate, J Mol Liq. 306 (2020). https://doi.org/https://doi.org/10.1016/j.molliq.2020.112908.

[78] V. Solfrizzi, F. Panza, V. Frisardi, D. Seripa, G. Logroscino, B.P. Imbimbo, A. Pilotto, Diet and Alzheimer's disease risk factors or prevention: the current evidence, Expert Rev Neurother. 11 (2014) 677–708. https://doi.org/10.1586/ERN.11.56.

[79] J. López-Miranda, F. Pérez-Jiménez, E. Ros, R. de Caterina, L. Badimón, M.I. Covas, E. Escrich, J.M. Ordovás, F. Soriguer, R. Abiá, C. Alarcón de la Lastra, M. Battino, D. Corella, J. Chamorro-Quirós, J. Delgado-Lista, D. Giugliano, K. Esposito, R. Estruch, J.M. Fernandez-Real, J.J. Gaforio, C. la Vecchia, D. Lairon, F. López-Segura, P. Mata, J.A. Menéndez, F.J. Muriana, J. Osada, D.B. Panagiotakos, J.A. Paniagua, P. Pérez-Martinez, J. Perona, M.A. Peinado, M. Pineda-Priego, H.E. Poulsen, J.L. Quiles, M.C. Ramírez-Tortosa, J. Ruano, L. Serra-Majem, R. Solá, M. Solanas, V. Solfrizzi, R. de la Torre-Fornell, A. Trichopoulou, M. Uceda, J.M. Villalba-Montoro, J.R. Villar-Ortiz, F. Visioli, N. Yiannakouris, Olive oil and health: Summary of the II international conference on olive oil and health consensus report, Jaén and Córdoba (Spain) 2008, Nutrition, Metabolism and Cardiovascular Diseases. 20 (2010) 284–294. https://doi.org/10.1016/J.NUMECD.2009.12.007.

[80] A. D'Alessandro, G. de Pergola, Mediterranean Diet and Cardiovascular Disease: A Critical Evaluation of A Priori Dietary Indexes, Nutrients. 7 (2015) 7863–7888. https://doi.org/10.3390/NU7095367.

[81] L. Lucas, A. Russell, R. Keast, Molecular Mechanisms of Inflammation. Anti-Inflammatory Benefits of Virgin Olive Oil and the Phenolic Compound Oleocanthal, Curr Pharm Des. 17 (2011) 754–768. https://doi.org/10.2174/138161211795428911.

[82] A. Camargo, J. Ruano, J.M. Fernandez, L.D. Parnell, A. Jimenez, M. Santos-Gonzalez, C. Marin, P. Perez-Martinez, M. Uceda, J. Lopez-Miranda, F. Perez-Jimenez, Gene expression changes in mononuclear cells in patients with metabolic syndrome after

acute intake of phenol-rich virgin olive oil, BMC Genomics. 11 (2010) 1–11. https://doi.org/10.1186/1471-2164-11-253/FIGURES/3.

[83] J. Salas-Salvadó, A. Garcia-Arellano, R. Estruch, F. Marquez-Sandoval, D. Corella, M. Fiol, E. Gómez-Gracia, E. Viñoles, F. Arós, C. Herrera, C. Lahoz, J. Lapetra, J.S. Perona, D. Muñoz-Aguado, M.A. Martínez-González, E. Ros, Components of the mediterranean-type food pattern and serum inflammatory markers among patients at high risk for cardiovascular disease, European Journal of Clinical Nutrition 2008 62:5. 62 (2007) 651–659. https://doi.org/10.1038/sj.ejcn.1602762.

[84] L. Melguizo-Rodríguez, R. Illescas-Montes, V. Costela-Ruiz, J. Ramos-Torrecillas, E. de Luna-Bertos, O. García-Martínez, C. Ruiz, Antimicrobial properties of olive oil phenolic compounds and their regenerative capacity towards fibroblast cells, J Tissue Viability. 30 (2021) 372–378. https://doi.org/https://doi.org/10.1016/j.jtv.2021.03.003.

[85] F. Pérez-Jiménez, J. Ruano, P. Perez-Martinez, F. Lopez-Segura, J. Lopez-Miranda, The influence of olive oil on human health: not a question of fat alone, Mol Nutr Food Res. 51 (2007) 1199–1208. https://doi.org/10.1002/MNFR.200600273.

[86] M.I. Covas, K. Nyyssönen, H.E. Poulsen, J. Kaikkonen, H.J.F. Zunft, H. Kiesewetter, A. Gaddi, R. de La Torre, J. Mursu, H. Bäumler, S. Nascetti, J.T. Salonen, M. Fitó, J. Virtanen, J. Marrugat, The effect of polyphenols in olive oil on heart disease risk factors: A randomized trial, Ann Intern Med. 145 (2006) 333–341. https://doi.org/10.7326/0003-4819-145-5-200609050-00006.

[87] A. Romani, F. Ieri, S. Urciuoli, A. Noce, G. Marrone, C. Nediani, R. Bernini, Health Effects of Phenolic Compounds Found in Extra-Virgin Olive Oil, By-Products, and Leaf of Olea europaea L., Nutrients 2019, Vol. 11, Page 1776. 11 (2019) 1776. https://doi.org/10.3390/NU11081776.

[88] M. Gorzynik-Debicka, P. Przychodzen, F. Cappello, A. Kuban-Jankowska, A.M. Gammazza, N. Knap, M. Wozniak, M. Gorska-Ponikowska, Potential Health Benefits of Olive Oil and Plant Polyphenols, International Journal of Molecular Sciences 2018, Vol. 19, Page 686. 19 (2018) 686. https://doi.org/10.3390/IJMS19030686.

[89] D. del Rio, A. Rodriguez-Mateos, J.P.E. Spencer, M. Tognolini, G. Borges, A. Crozier, Dietary (poly)phenolics in human health: Structures, bioavailability, and evidence of protective effects against chronic diseases, Antioxid Redox Signal. 18 (2013) 1818–1892.
https://doi.org/10.1089/ARS.2012.4581/ASSET/IMAGES/LARGE/FIGURE41.JPEG.

[90] R. Aparicio, J. Harwood, Handbook of olive oil: Analysis and properties, Handbook of Olive Oil: Analysis and Properties. (2013) 1–772. https://doi.org/10.1007/978-1-4614-7777-8/COVER.

[91] R.J. Widmer, A.J. Flammer, L.O. Lerman, A. Lerman, The Mediterranean Diet, its Components, and Cardiovascular Disease, Am J Med. 128 (2015) 229–238. https://doi.org/10.1016/J.AMJMED.2014.10.014.

[92] I. Castro-Quezada, B. Román-Viñas, L. Serra-Majem, The Mediterranean Diet and Nutritional Adequacy: A Review, Nutrients 2014, Vol. 6, Pages 231-248. 6 (2014) 231–248. https://doi.org/10.3390/NU6010231.

[93] A. Bach-Faig, E.M. Berry, D. Lairon, J. Reguant, A. Trichopoulou, S. Dernini, F.X. Medina, M. Battino, R. Belahsen, G. Miranda, L. Serra-Majem, J. Aranceta, T. Atinmo, J.M. Barros, S. Benjelloun, I. Bertomeu-Galindo, B. Burlingame, M. Caballero-Bartolí, C. Clapés-Badrinas, S. Couto, I. Elmadfa, R. Estruch, A. Faig, F. Fidanza, S. Franceschi, J. Hautvast, E. Helsing, D. Julià-Llobet, C. la Vecchia, A. Lemtouni, A. Mariné, M.A. Martínez-González, R. Mokni, F. Mombiela, I. Noain, B. Obrador, G. Pekcan, S. Piscopo, B. Raidó-Quintana, E. Ros, S. Sáez-Almendros, J. Salas-Salvadó, F. Sensat, D. Trichopoulos, J.A. Tur, M.D. Vaz Da Almeida, W.C. Willett, M.J. Amiot-Carlin, A. Bellio, C. Cannella, R. Capone, D. Cassi, L.M. Donini, C. Lacirignola, G. Maiani, M. Mancini, N. Merendino, M. Padilla, S. Padulosi, Mediterranean diet pyramid today. Science and cultural updates, Public Health Nutr. 14 (2011) 2274–2284. https://doi.org/10.1017/S1368980011002515.

[94] R. Estruch, E. Ros, J. Salas-Salvadó, M.-I. Covas, D. Corella, F. Arós, E. Gómez-Gracia, V. Ruiz-Gutiérrez, M. Fiol, J. Lapetra, R.M. Lamuela-Raventos, L. Serra-Majem, X. Pintó, J. Basora, M.A. Muñoz, J. v. Sorlí, J.A. Martínez, M.A. Martínez-González, Primary prevention of cardiovascular disease with a mediterranean diet, Zeitschrift Fur Gefassmedizin. 10 (2013) 28. https://doi.org/10.1056/NEJMOA1200303/SUPPL_FILE/NEJMOA1200303_DISCLOSURES.PDF.

[95] R. García-Villalba, A. Carrasco-Pancorbo, C. Oliveras-Ferraros, A. Vázquez-Martín, J.A. Menéndez, A. Segura-Carretero, A. Fernández-Gutiérrez, Characterization and quantification of phenolic compounds of extra-virgin olive oils with anticancer properties by a rapid and resolutive LC-ESI-TOF MS method, J Pharm Biomed Anal. 51 (2010) 416–429. https://doi.org/10.1016/J.JPBA.2009.06.021.

[96] M. el Riachy, F. Priego-Capote, L. León, L. Rallo, M.D. Luque de Castro, Hydrophilic antioxidants of virgin olive oil. Part 1: Hydrophilic phenols: A key factor for virgin olive oil quality, European Journal of Lipid Science and Technology. 113 (2011) 678–691. https://doi.org/10.1002/EJLT.201000400.

[97] M. Stefani, S. Rigacci, Beneficial properties of natural phenols: Highlight on protection against pathological conditions associated with amyloid aggregation, BioFactors. 40 (2014) 482–493. https://doi.org/10.1002/BIOF.1171.

[98] N.S.A. Malik, J.M. Bradford, Changes in oleuropein levels during differentiation and development of floral buds in 'Arbequina' olives, Sci Hortic. 110 (2006) 274–278. https://doi.org/10.1016/J.SCIENTA.2006.07.016.

[99] S.D.' Angelo, P. Galletti, C. Manna, S. D'angelo, V. Migliardi, E. Loffredi, O. Mazzoni, P. Morrica, V. Zappia, Protective effect of the phenolic fraction from virgin olive oils against oxidative stress in human cells, J Agric Food Chem. 50 (2002) 6521–6526. https://doi.org/10.1021/jf020565.

[100] R.W. Owen, A. Giacosa, W.E. Hull, R. Haubner, B. Spiegelhalder, H. Bartsch, The antioxidant/anticancer potential of phenolic compounds isolated from olive oil, Eur J Cancer. 36 (2000) 1235–1247. https://doi.org/10.1016/S0959-8049(00)00103-9.

[101] E. Tripoli, M. Giammanco, G. Tabacchi, D. di Majo, S. Giammanco, M. la Guardia, The phenolic compounds of olive oil: structure, biological activity and beneficial effects on human health, Nutr Res Rev. 18 (2005) 98–112. https://doi.org/10.1079/NRR200495.

[102] G.O. Bisi Gnan, A.T. Omain O, R. LO Cascio, G. Useppe Crisafi, N. Uccella, A.N. Antonella Sa Ija, A. Saija, On the In-vitro Antimicrobial Activity of Oleuropein and Hydroxytyrosol, Journal of Pharmacy and Pharmacology. 51 (2010) 971–974. https://doi.org/10.1211/0022357991773258.

[103] H.P. Fleming, Jr. W. M. Walter, J.L. Etchells, Antimicrobial Properties of Oleuropein and Products of Its Hydrolysis from Green Olives, Appl Environ Microbiol. 26 (1973) 777–782. https://doi.org/10.1128/AM.26.5.777-782.1973.

[104] F. Federici, G. Bongi, Improved Method for Isolation of Bacterial Inhibitors from Oleuropein Hydrolysis, Appl Environ Microbiol. 46 (1983) 509–510. https://doi.org/10.1128/AEM.46.2.509-510.1983.

[105] M.A. Carluccio, L. Siculella, M.A. Ancora, M. Massaro, E. Scoditti, C. Storelli, F. Visioli, A. Distante, R. De Caterina, Olive oil and red wine antioxidant polyphenols inhibit endothelial activation: Antiatherogenic properties of Mediterranean diet phytochemicals, Arterioscler Thromb Vasc Biol. 23 (2003) 622–629. https://doi.org/10.1161/01.ATV.0000062884.69432.A0.

[106] P. Rodríguez-López, J. Lozano-Sanchez, I. Borrás-Linares, T. Emanuelli, J.A. Menéndez, A. Segura-Carretero, Structure–Biological Activity Relationships of Extra-Virgin Olive Oil Phenolic Compounds: Health Properties and Bioavailability, Antioxidants 2020, Vol. 9, Page 685. 9 (2020) 685. https://doi.org/10.3390/ANTIOX9080685.

[107] W.F. Bergfeld, F.A.C.P.; Donald, V. Belsito, R.A. Hill, C.D. Klaassen, D.C. Liebler, J.G. Marks, R.C. Shank, T.J.; Slaga, P.W. Snyder, Amended Safety Assessment of Alkyl Esters as Used in Cosmetics Panel Meeting Date The 2013 Cosmetic Ingredient Review Expert Panel members are: Chairman, (2013).

[108] R.L. Campbell, R.D. Bruce, Comparative dermatotoxicology: I. Direct comparison of rabbit and human primary skin irritation responses to isopropylmyristate, Toxicol Appl Pharmacol. 59 (1981) 555–563. https://doi.org/10.1016/0041-008X(81)90310-0.

[109] M.E. Lane, Skin penetration enhancers, Int J Pharm. 447 (2013) 12–21. https://doi.org/10.1016/J.IJPHARM.2013.02.040.

[110] M. v. Michalun, J.C. DiNardo, Skin Care and Cosmetic Ingredients Dictionary, 2014. https://books.google.gr/books?hl=el&lr=&id=AePNAgAAQBAJ&oi=fnd&pg=PR3&dq=International+Cosmetic+Ingredient+Dictionary+and+Handbook&ots=RUDcg76L0W&sig=9sEavTT6sGlPbDqTJdLYy3e00QM&redir_esc=y#v=snippet&q=isopropyl%20myristate&f=false (accessed February 19, 2023).

[111] M. Hori, S. Satoh, H.I. Maibach, Classification of percutaneous penetration enhancers: A conceptional diagram, Journal of Pharmacy and Pharmacology. 42 (2011) 71–72. https://doi.org/10.1111/J.2042-7158.1990.TB05356.X.

[112] P. Liu, M. Cettina, J. Wong, Effects of Isopropanol–Isopropyl Myristate Binary Enhancers on In Vitro Transport of Estradiol in Human Epidermis: A Mechanistic Evaluation, J Pharm Sci. 98 (2009) 565–572. https://doi.org/10.1002/JPS.21459.

[113] T.N. Engelbrecht, B. Demé, B. Dobner, R.H.H. Neubert, Study of the Influence of the Penetration Enhancer Isopropyl Myristate on the Nanostructure of Stratum Corneum Lipid Model Membranes Using Neutron Diffraction and Deuterium Labelling, Skin Pharmacol Physiol. 25 (2012) 200–207. https://doi.org/10.1159/000338538.

[114] K. Sato, K. Sugibayashi, Y. Morimoto, Effect and mode of action of aliphatic esters on the in vitro skin permeation of nicorandil, Int J Pharm. 43 (1988) 31–40. https://doi.org/10.1016/0378-5173(88)90055-5.

[115] A. Eichner, S. Stahlberg, S. Sonnenberger, S. Lange, B. Dobner, A. Ostermann, T.E. Schrader, T. Hauß, A. Schroeter, D. Huster, R.H.H. Neubert, Influence of the penetration enhancer isopropyl myristate on stratum corneum lipid model membranes revealed by neutron diffraction and 2H NMR experiments, Biochimica et Biophysica Acta (BBA) - Biomembranes. 1859 (2017) 745–755. https://doi.org/10.1016/J.BBAMEM.2017.01.029.

[116] Milton J. Rosen, Joy T. Kunjappu, Surfactants and Interfacial Phenomena, 2012. https://books.google.gr/books?hl=el&lr=&id=pdTsgREZp5QC&oi=fnd&pg=PR15&dq=Rosen+MJ,+Kunjappu+JT.+Surfactants+and+interfacial+phenomena,+4th+ed.,+New+Jersey:+John+Wiley+%26+Sons,+Inc.%3B+2012&ots=-88E2otSqM&sig=mMVbbX_6oGXJEr8ZJrfu6Tb-HRA&redir_esc=y#v=onepage&q&f=false (accessed February 19, 2023).

[117] Tadros Tharwat F., Applied Surfactants: Principles and Applications, 2006. https://books.google.gr/books?hl=el&lr=&id=KimqCBg0s8QC&oi=fnd&pg=PR7&dq=Tadros+TF.+Applied+surfactants+principles+and+applications,+1st+ed.,+Germany:+WILEY-VCH+Verlag+GmbH+%26+Co.%3B+2005.&ots=ahzGgKirQ4&sig=oCQUf2jh568TdZY681VMVQEszBc&redir_esc=y#v=onepage&q&f=false (accessed February 19, 2023).

[118] I. Kralova, J. Sjöblom, Surfactants Used in Food Industry: A Review, J Dispers Sci Technol. 30 (2009) 1363–1383. https://doi.org/10.1080/01932690902735561.

[119] D.J. McClements, Food Emulsions : Principles, Practices, and Techniques, Second Edition, (2004). https://doi.org/10.1201/9781420039436.

[120] I. Solè, A. Maestro, C.M. Pey, C. González, C. Solans, J.M. Gutiérrez, Nano-emulsions preparation by low energy methods in an ionic surfactant system, Colloids Surf A Physicochem Eng Asp. 288 (2006) 138–143. https://doi.org/10.1016/J.COLSURFA.2006.02.013.

[121] A. Majeed, R. Bashir, S. Farooq, M. Maqbool, Preparation, Characterization and Applications of Nanoemulsions: An Insight, Journal of Drug Delivery and Therapeutics. 9 (2019) 520–527. https://doi.org/10.22270/JDDT.V9I2.2410.

[122] R. Bnyan, I. Khan, T. Ehtezazi, I. Saleem, S. Gordon, F. O'Neill, M. Roberts, Surfactant Effects on Lipid-Based Vesicles Properties, J Pharm Sci. 107 (2018) 1237–1246. https://doi.org/10.1016/J.XPHS.2018.01.005.

[123] M. Nejadmansouri, S.M.H. Hosseini, M. Niakosari, G.H. Yousefi, M.T. Golmakani, Physicochemical properties and oxidative stability of fish oil nanoemulsions as affected by hydrophilic lipophilic balance, surfactant to oil ratio and storage temperature,

Colloids Surf A Physicochem Eng Asp. 506 (2016) 821–832. https://doi.org/10.1016/J.COLSURFA.2016.07.075.

[124] K. Katsuta, K. Tsutsui, E. Maruyama, M. Miura, Classification of surface-active agents by "HLB," J. Soc. Cosmet. Chem. 1 (1949) 311–325. https://doi.org/10.5458/JAG.49.145.

[125] Eric. Dickinson, D.Julian. McClements, Advances in food colloids, Blackie Academic & Professional, 1996. https://link.springer.com/book/9780751402032 (accessed February 19, 2023).

[126] S. Bahadur, D.M. Pardhi, J. Rautio, J.M. Rosenholm, K. Pathak, Intranasal Nanoemulsions for Direct Nose-to-Brain Delivery of Actives for CNS Disorders, Pharmaceutics 2020, Vol. 12, Page 1230. 12 (2020) 1230. https://doi.org/10.3390/PHARMACEUTICS12121230.

[127] K. Bouchemal, S. Briançon, E. Perrier, H. Fessi, Nano-emulsion formulation using spontaneous emulsification: solvent, oil and surfactant optimisation, Int J Pharm. 280 (2004) 241–251. https://doi.org/10.1016/J.IJPHARM.2004.05.016.

[128] K.M. Hosny, Z.M. Banjar, The formulation of a nasal nanoemulsion zaleplon in situ gel for the treatment of insomnia, 10 (2013) 1033–1041. https://doi.org/10.1517/17425247.2013.812069.

[129] R.N. Gursoy, S. Benita, Self-emulsifying drug delivery systems (SEDDS) for improved oral delivery of lipophilic drugs, Biomedicine & Pharmacotherapy. 58 (2004) 173–182. https://doi.org/10.1016/J.BIOPHA.2004.02.001.

[130] C.M. Pey, A. Maestro, I. Solé, C. González, C. Solans, J.M. Gutiérrez, Optimization of nano-emulsions prepared by low-energy emulsification methods at constant temperature using a factorial design study, Colloids Surf A Physicochem Eng Asp. 288 (2006) 144–150. https://doi.org/10.1016/J.COLSURFA.2006.02.026.

[131] V. Uskoković, M. Drofenik, SYNTHESIS OF MATERIALS WITHIN REVERSE MICELLES, Surface Review and Letters. 12 (2012) 239–277. https://doi.org/10.1142/S0218625X05007001.

[132] G.D. Rees, R. Evans-Gowing, S.J. Hammond, B.H. Robinson, Formation and Morphology of Calcium Sulfate Nanoparticles and Nanowires in Water-in-Oil Microemulsions, Langmuir. 15 (1999) 1993–2002. https://doi.org/10.1021/LA981026V.

[133] I. Som, K. Bhatia, M. Yasir, Status of surfactants as penetration enhancers in transdermal drug delivery, J Pharm Bioallied Sci. 4 (2012) 2. https://doi.org/10.4103/0975-7406.92724.

[134] C.J.H. Porter, C.W. Pouton, J.F. Cuine, W.N. Charman, Enhancing intestinal drug solubilisation using lipid-based delivery systems, Adv Drug Deliv Rev. 60 (2008) 673–691. https://doi.org/10.1016/J.ADDR.2007.10.014.

[135] S. Chakraborty, D. Shukla, B. Mishra, S. Singh, Lipid – An emerging platform for oral delivery of drugs with poor bioavailability, European Journal of Pharmaceutics and Biopharmaceutics. 73 (2009) 1–15. https://doi.org/10.1016/J.EJPB.2009.06.001.

[136] S. Sood, K. Jain, K. Gowthamarajan, Optimization of curcumin nanoemulsion for intranasal delivery using design of experiment and its toxicity assessment, Colloids Surf B Biointerfaces. 113 (2014) 330–337. https://doi.org/10.1016/J.COLSURFB.2013.09.030.

[137] A. Azeem, M. Rizwan, F.J. Ahmad, Z. Iqbal, R.K. Khar, M. Aqil, S. Talegaonkar, Nanoemulsion Components Screening and Selection: a Technical Note, AAPS PharmSciTech 2009 10:1. 10 (2009) 69–76. https://doi.org/10.1208/S12249-008-9178-X.

[138] N. Garti, A. Yaghmur, M.E. Leser, V. Clement, H.J. Watzke, Improved Oil Solubilization in Oil/Water Food Grade Microemulsions in the Presence of Polyols and Ethanol, J Agric Food Chem. 49 (2001) 2552–2562. https://doi.org/10.1021/JF001390B.

[139] S. Shafiq-un-Nabi, F. Shakeel, S. Talegaonkar, J. Ali, S. Baboota, A. Ahuja, R.K. Khar, M. Ali, Formulation development and optimization using nanoemulsion technique: A technical mote, AAPS PharmSciTech. 8 (2007) E12–E17. https://doi.org/10.1208/PT0802028/METRICS.

[140] J. Shokri, A. Nokhodchi, A. Dashbolaghi, D. Hassan-Zadeh, T. Ghafourian, M. Barzegar Jalali, The effect of surfactants on the skin penetration of diazepam, Int J Pharm. 228 (2001) 99–107. https://doi.org/10.1016/S0378-5173(01)00805-5.

[141] E.A. Thackaberry, S. Kopytek, P. Sherratt, K. Trouba, B. McIntyre, Comprehensive Investigation of Hydroxypropyl Methylcellulose, Propylene Glycol, Polysorbate 80, and Hydroxypropyl-Beta-Cyclodextrin for use in General Toxicology Studies, Toxicological Sciences. 117 (2010) 485–492. https://doi.org/10.1093/TOXSCI/KFQ207.

[142] M.J. Cappel, J. Kreuter, Effect of nonionic surfactants on transdermal drug delivery: I. Polysorbates, Int J Pharm. 69 (1991) 143–153. https://doi.org/10.1016/0378-5173(91)90219-E.

[143] E. Limpongsa, K. Umprayn, Preparation and evaluation of diltiazem hydrochloride diffusion-controlled transdermal delivery system, AAPS PharmSciTech. 9 (2008) 464–470. https://doi.org/10.1208/S12249-008-9062-8/METRICS.

[144] D. Kumar, M. Aqil, M. Rizwan, Y. Sultana, M. Ali, Investigation of a nanoemulsion as vehicle for transdermal delivery of amlodipine, Pharmazie. 64 (2009) 80–85. https://doi.org/10.1691/PH.2009.8200.

[145] A. Arellano, S. Santoyo, C. Martn, P. Ygartua, Surfactant effects on the in vitro percutaneous absorption of diclofenac sodium, (n.d.).

[146] M. Kreilgaard, E.J. Pedersen, J.W. Jaroszewski, NMR characterisation and transdermal drug delivery potential of microemulsion systems, Journal of Controlled Release. 69 (2000) 421–433. https://doi.org/10.1016/S0168-3659(00)00325-4.

[147] Labrasol®, (n.d.). https://www.gattefosse.com/pharmaceuticals-products/labrasol (accessed February 19, 2023).

[148] I. Nardin, S. Köllner, Successful development of oral SEDDS: screening of excipients from the industrial point of view, Adv Drug Deliv Rev. 142 (2019) 128–140. https://doi.org/10.1016/J.ADDR.2018.10.014.

[149] Z. Hu, R. Tawa, T. Konishi, N. Shibata, K. Takada, A novel emulsifier, Labrasol, enhances gastrointestinal absorption of gentamicin, Life Sci. 69 (2001) 2899–2910. https://doi.org/10.1016/S0024-3205(01)01375-3.

[150] Y.V.R. Prasad, T. Minamimoto, Y. Yoshikawa, N. Shibata, S. Mori, A. Matsuura, K. Takada, In situ intestinal absorption studies on low molecular weight heparin in rats using Labrasol as absorption enhancer, Int J Pharm. 271 (2004) 225–232. https://doi.org/10.1016/J.IJPHARM.2003.11.013.

[151] F. McCartney, V. Jannin, S. Chevrier, H. Boulghobra, D.R. Hristov, N. Ritter, C. Miolane, Y. Chavant, F. Demarne, D.J. Brayden, Labrasol® is an efficacious intestinal permeation enhancer across rat intestine: Ex vivo and in vivo rat studies, Journal of Controlled Release. 310 (2019) 115–126. https://doi.org/10.1016/J.JCONREL.2019.08.008.

[152] P. Guo, N. Li, L. Fan, J. Lu, B. Liu, B. Zhang, Y. Wu, Z. Liu, J. Li, J. Pi, D. Qi, Study of penetration mechanism of labrasol on rabbit cornea by Ussing chamber, RT-PCR assay, Western blot and immunohistochemistry, Asian J Pharm Sci. 14 (2019) 329–339. https://doi.org/10.1016/J.AJPS.2018.05.005.

[153] S. Eaimtrakarn, Y. v. Rama Prasad, T. Ohno, T. Konishi, Y. Yoshikawa, N. Shibata, K. Takada, Absorption Enhancing Effect of Labrasol on the Intestinal Absorption of Insulin in Rats, Journal of Drug Targeting . 10 (2008) 255–260. https://doi.org/10.1080/10611860290022688.

[154] K. Koga, Y. Kusawake, Y. Ito, N. Sugioka, N. Shibata, K. Takada, Enhancing mechanism of Labrasol on intestinal membrane permeability of the hydrophilic drug gentamicin sulfate, European Journal of Pharmaceutics and Biopharmaceutics. 64 (2006) 82–91. https://doi.org/10.1016/J.EJPB.2006.03.011.

[155] K.A. Hamid, H. Katsumi, T. Sakane, A. Yamamoto, The effects of common solubilizing agents on the intestinal membrane barrier functions and membrane toxicity in rats, Int J Pharm. 379 (2009) 100–108. https://doi.org/10.1016/J.IJPHARM.2009.06.018.

[156] S. Maher, J. Heade, F. McCartney, S. Waters, S.B. Bleiel, D.J. Brayden, Effects of surfactant-based permeation enhancers on mannitol permeability, histology, and electrogenic ion transport responses in excised rat colonic mucosae, Int J Pharm. 539 (2018) 11–22. https://doi.org/10.1016/J.IJPHARM.2018.01.008.

[157] J. Heade, S. Maher, S.B. Bleiel, D.J. Brayden, Labrasol® and Salts of Medium-Chain Fatty Acids Can Be Combined in Low Concentrations to Increase the Permeability of a Macromolecule Marker Across Isolated Rat Intestinal Mucosae, J Pharm Sci. 107 (2018) 1648–1655. https://doi.org/10.1016/J.XPHS.2018.02.012.

[158] Z. Liu, X. Zhang, J. Li, R. Liu, L. Shu, J. Jin, Effects of Labrasol on the corneal drug delivery of baicalin, Drug Deliv. 16 (2009) 399–404. https://doi.org/10.1080/10717540903126165.

[159] D.Z. Liu, E.L. Lecluyse, D.R. Thakker, Dodecylphosphocholine-mediated enhancement of paracellular permeability and cytotoxicity in Caco-2 cell monolayers, J Pharm Sci. 88 (1999) 1161–1168. https://doi.org/10.1021/JS990094E.

[160] M.A. Kassem, M.H. Aboul-Einien, M.M. el Taweel, Dry Gel Containing Optimized Felodipine-Loaded Transferosomes: a Promising Transdermal Delivery System to

Enhance Drug Bioavailability, AAPS PharmSciTech. 19 (2018) 2155–2173. https://doi.org/10.1208/S12249-018-1020-5/METRICS.

[161] D. Izgelov, E. Shmoeli, A.J. Domb, A. Hoffman, The effect of medium chain and long chain triglycerides incorporated in self-nano emulsifying drug delivery systems on oral absorption of cannabinoids in rats, Int J Pharm. 580 (2020) 119201. https://doi.org/10.1016/J.IJPHARM.2020.119201.

[162] C.J.H. Porter, N.L. Trevaskis, W.N. Charman, Lipids and lipid-based formulations: optimizing the oral delivery of lipophilic drugs, Nature Reviews Drug Discovery 2007 6:3. 6 (2007) 231–248. https://doi.org/10.1038/nrd2197.

[163] Z. Niu, I. Conejos-Sánchez, B.T. Griffin, C.M. O'Driscoll, M.J. Alonso, Lipid-based nanocarriers for oral peptide delivery, Adv Drug Deliv Rev. 106 (2016) 337–354. https://doi.org/10.1016/J.ADDR.2016.04.001.

[164] C.J.H. Porter, A.M. Kaukonen, B.J. Boyd, G.A. Edwards, W.N. Charman, Susceptibility to lipase-mediated digestion reduces the oral bioavailability of danazol after administration as a medium-chain lipid-based microemulsion formulation, Pharm Res. 21 (2004) 1405–1412. https://doi.org/10.1023/B:PHAM.0000036914.22132.CC/METRICS.

[165] S.M. Khoo, D.M. Shackleford, C.J.H. Porter, G.A. Edwards, W.N. Charman, Intestinal lymphatic transport of halofantrine occurs after oral administration of a unit-dose lipid-based formulation to fasted dogs, Pharm Res. 20 (2003) 1460–1465. https://doi.org/10.1023/A:1025718513246/METRICS.

[166] R.G. Strickley, Solubilizing Excipients in Oral and Injectable Formulations, Pharm Res. 21 (2004) 201–230. https://doi.org/10.1023/B:PHAM.0000016235.32639.23/METRICS.

[167] N.L. Trevaskis, D.M. Shackleford, W.N. Charman, G.A. Edwards, A. Gardin, S. Appel-Dingemanse, O. Kretz, B. Galli, C.J.H. Porter, Intestinal lymphatic transport enhances the post-prandial oral bioavailability of a novel cannabinoid receptor agonist via avoidance of first-pass metabolism, Pharm Res. 26 (2009) 1486–1495. https://doi.org/10.1007/S11095-009-9860-Z/METRICS.

[168] N.L. Trevaskis, C.L. McEvoy, M.P. Mcintosh, G.A. Edwards, R.M. Shanker, W.N. Charman, C.J.H. Porter, The role of the intestinal lymphatics in the absorption of two highly lipophilic cholesterol ester transfer protein inhibitors (CP524,515 and CP532,623), Pharm Res. 27 (2010) 878–893. https://doi.org/10.1007/S11095-010-0083-0/METRICS.

[169] N.L. Trevaskis, L.M. Kaminskas, C.J.H. Porter, From sewer to saviour — targeting the lymphatic system to promote drug exposure and activity, Nature Reviews Drug Discovery 2015 14:11. 14 (2015) 781–803. https://doi.org/10.1038/nrd4608.

[170] Maisine® CC, (n.d.). https://www.gattefosse.com/pharmaceuticals-products/maisine-cc (accessed February 19, 2023).

[171] K. Bunchongprasert, J. Chen, J. Shao, Effect of double bond in unsaturated long-chain monoglyceride in self-emulsified nanoemulsion on tight junction opening, J Drug Deliv Sci Technol. 60 (2020) 101972. https://doi.org/10.1016/J.JDDST.2020.101972.

[172] A. Zgair, J.B. Lee, J.C.M. Wong, D.A. Taha, J. Aram, D. di Virgilio, J.W. Mcarthur, Y.-K. Cheng, I.M. Hennig, D.A. Barrett, P.M. Fischer, C.S. Constantinescu, P. Gershkovich, Oral administration of cannabis with lipids leads to high levels of cannabinoids in the intestinal lymphatic system and prominent immunomodulation OPEN, Sci Rep. 7 (2017) 1–12. https://doi.org/10.1038/s41598-017-15026-z.

[173] A. Zgair, J.C.M. Wong, J.B. Lee, J. Mistry, O. Sivak, K.M. Wasan, I.M. Hennig, D.A. Barrett, C.S. Constantinescu, P.M. Fischer, P. Gershkovich, Dietary fats and pharmaceutical lipid excipients increase systemic exposure to orally administered cannabis and cannabis-based medicines, Am J Transl Res. 8 (2016) 3448. /pmc/articles/PMC5009397/ (accessed February 19, 2023).

[174] P. Verma, A. Ram, A.K. Jha, A. Mishra, A. Thakur, PHOSPHATIDYLCHOLINE: A REVOLUTION IN DRUG DELIVERY TECHNOLOGY, Int J Pharm Sci Res. 1 (2010) 1–12. www.ijpsr.com (accessed February 19, 2023).

[175] A. Spernath, A. Aserin, A.C. Sintov, N. Garti, Phosphatidylcholine embedded micellar systems: Enhanced permeability through rat skin, J Colloid Interface Sci. 318 (2008) 421–429. https://doi.org/10.1016/J.JCIS.2007.10.036.

[176] M. Kirjavainen, A. Urtti, J. Mönkkönen, J. Hirvonen, Influence of lipids on the mannitol flux during transdermal iontophoresis in vitro, European Journal of Pharmaceutical Sciences. 10 (2000) 97–102. https://doi.org/10.1016/S0928-0987(99)00080-9.

[177] D.Z. Liu, S.L. Morris-Natschke, L.S. Kucera, K.S. Ishaq, D.R. Thakker, Structure—activity relationships for enhancement of paracellular permeability by 2-alkoxy-3-alkylamidopropylphosphocholines across Caco-2 cell monolayers, J Pharm Sci. 88 (1999) 1169–1174. https://doi.org/10.1021/JS9900957.

[178] A. Spernath, A. Aserin, L. Ziserman, D. Danino, N. Garti, Phosphatidylcholine embedded microemulsions: Physical properties and improved Caco-2 cell permeability, Journal of Controlled Release. 119 (2007) 279–290. https://doi.org/10.1016/J.JCONREL.2007.02.014.

[179] L.M. Lichtenberger, Z.M. Wang, J.J. Romero, C. Ulloa, J.C. Perez, M.N. Giraud, J.C. Barreto, Non-steroidal anti-inflammatory drugs (NSAIDs) associate with zwitterionic phospholipids: Insight into the mechanism and reversal of NSAID-induced gastrointestinal injury, Nature Medicine 1995 1:2. 1 (1995) 154–158. https://doi.org/10.1038/nm0295-154.

[180] B.S. Anand, J.J. Jim, S.K. Sanduja, L.M. Lichtenberger, Phospholipid association reduces the gastric mucosal toxicity of aspirin in human subjects., Am J Gastroenterol. 94 (1999) 1818–1822. https://doi.org/10.1111/j.1572-0241.1999.01211.x.

[181] T. Garg, A. K. Goyal, Liposomes: Targeted and Controlled Delivery System, Drug Deliv Lett. 4 (2014) 62–71.

[182] D.W. Osborne, J. Musakhanian, Skin Penetration and Permeation Properties of Transcutol®—Neat or Diluted Mixtures, AAPS PharmSciTech. 19 (2018) 3512–3533. https://doi.org/10.1208/S12249-018-1196-8/FIGURES/23.

[183] D.W. Osborne, Diethylene glycol monoethyl ether: an emerging solvent in topical dermatology products, J Cosmet Dermatol. 10 (2011) 324–329. https://doi.org/10.1111/J.1473-2165.2011.00590.X.

[184] D.W. Sullivan, S.C. Gad, M. Julien, A review of the nonclinical safety of Transcutol®, a highly purified form of diethylene glycol monoethyl ether (DEGEE) used as a pharmaceutical excipient, Food and Chemical Toxicology. 72 (2014) 40–50. https://doi.org/10.1016/J.FCT.2014.06.028.

[185] Transcutol® HP, (n.d.). https://www.gattefosse.com/pharmaceuticals-products/transcutol-hp (accessed February 19, 2023).

[186] W.A. RITSCHEL, A.S. HUSSAIN, Influence of selected solvents on penetration of griseofulvin in rat skin, in vitro, Pharmazeutische Industrie. 50 (1988) 483–486.

[187] A. Ganem-Quintanar, C. Lafforgue, F. Falson-Rieg, P. Buri, Evaluation of the transepidermal permeation of diethylene glycol monoethyl ether and skin water loss, Int J Pharm. 147 (1997) 165–171. https://doi.org/10.1016/S0378-5173(96)04809-0.

[188] Gattefossé | Personal care ingredients & pharmaceutical excipients, (n.d.). https://www.gattefosse.com/ (accessed February 19, 2023).

[189] P.H. Dugard, M. Walker, S.J. Mawdsley, R.C. Scott, Absorption of some glycol ethers through human skin in vitro, Environ Health Perspect. VOL. 57 (1984) 193–197. https://doi.org/10.1289/EHP.8457193.

[190] E. Papakostantinou, K. Xenos, S.L. Markantonis, S. Druska, A. Stratigos, A. Katsambas, Efficacy of 2 weeks' application of theophylline ointment in psoriasis vulgaris, Journal of Dermatological Treatment. 16 (2009) 169–170. https://doi.org/10.1080/09546630510043202.

[191] G. Chadha, S. Sathigari, D.L. Parsons, R.J. Babu, In vitro percutaneous absorption of genistein from topical gels through human skin, Drug Dev Ind Pharm. 37 (2011) 498–505. https://doi.org/10.3109/03639045.2010.525238.

[192] F. Shakeel, S. Baboota, A. Ahuja, J. Ali, M. Aqil, S. Shafiq, Nanoemulsions as vehicles for transdermal delivery of aceclofenac, AAPS PharmSciTech. 8 (2007) 1–9. https://doi.org/10.1208/PT0804104/METRICS.

[193] G.C. Ceschel, V. Bergamante, P. Maffei, S.L. Borgia, V. Calabrese, S. Biserni, C. Ronchi, Solubility and Transdermal Permeation Properties of a Dehydroepiandrosterone Cyclodextrin Complex from Hydrophilic and Lipophilic Vehicles, Drug Deliv. 12 (2008) 275–280. https://doi.org/10.1080/10717540500176563.

[194] A.G. Sandig, A.C.C. Campmany, F.F. Campos, M.J.M. Villena, B.C. Naveros, Transdermal delivery of imipramine and doxepin from newly oil-in-water nanoemulsions for an analgesic and anti-allodynic activity: Development, characterization and in vivo evaluation, Colloids Surf B Biointerfaces. 103 (2013) 558–565. https://doi.org/10.1016/J.COLSURFB.2012.10.061.

[195] D.K. Parikh, T.K. Ghosh, Feasibility of transdermal delivery of fluoxetine, AAPS PharmSciTech. 6 (2005) E144–E149. https://doi.org/10.1208/PT060222/METRICS.

[196] A. Fini, V. Bergamante, G.C. Ceschel, C. Ronchi, C.A.F. Moraes, Control of transdermal permeation of hydrocortisone acetate from hydrophilic and lipophilic formulations, AAPS PharmSciTech. 9 (2008) 762–768. https://doi.org/10.1208/S12249-008-9107-Z/FIGURES/4.

[197] S. Wang, P. Chen, L. Zhang, C. Yang, G. Zhai, Formulation and evaluation of microemulsion-based in situ ion-sensitive gelling systems for intranasal administration of curcumin, J Drug Target. 20 (2012) 831–840. https://doi.org/10.3109/1061186X.2012.719230.

[198] J. Yao, L. Hou, J.P. Zhou, Z.Q. Zhang, L. Sun, Preparation of lorazepam-loaded microemulsions for intranasal delivery and its pharmacokinetics, Pharmazie. 64 (2009) 642–647. https://doi.org/10.1691/PH.2009.9082.

[199] S.C. Gad, C.D. Cassidy, N. Aubert, B. Spainhour, H. Robbe, Nonclinical Vehicle Use in Studies by Multiple Routes in Multiple Species, Int J Toxicol. 25 (2006) 499–521. https://doi.org/10.1080/10915810600961531.

[200] A. Piotrowska, J. Wierzbicka, M.A. Zmijewski, Vitamin D in the skin physiology and pathology., Acta Biochim Pol. 63 (2016) 17–29. https://doi.org/10.18388/ABP.2015_1104.

[201] M. Wacker, M.F. Holick, Sunlight and Vitamin D, Dermatoendocrinol. 5 (2013) 51–108. https://doi.org/10.4161/DERM.24494.

[202] J. Jakobsen, E.A. Wreford Andersen, T. Christensen, R. Andersen, S. Bügel, Vitamin D Vitamers Affect Vitamin D Status Differently in Young Healthy Males, Nutrients 2018, Vol. 10, Page 12. 10 (2017) 12. https://doi.org/10.3390/NU10010012.

[203] P. Lips, Vitamin D physiology, Prog Biophys Mol Biol. 92 (2006) 4–8. https://doi.org/10.1016/J.PBIOMOLBIO.2006.02.016.

[204] F.J. Navarro-Triviño, S. Arias-Santiago, Y. Gilaberte-Calzada, Vitamin D and the Skin: A Review for Dermatologists, Actas Dermo-Sifiliográficas (English Edition). 110 (2019) 262–272. https://doi.org/10.1016/J.ADENGL.2019.04.001.

[205] K.Y.Z. Forrest, W.L. Stuhldreher, Prevalence and correlates of vitamin D deficiency in US adults, Nutrition Research. 31 (2011) 48–54. https://doi.org/10.1016/J.NUTRES.2010.12.001.

[206] R. Moretti, M.E. Morelli, P. Caruso, Vitamin D in Neurological Diseases: A Rationale for a Pathogenic Impact, International Journal of Molecular Sciences 2018, Vol. 19, Page 2245. 19 (2018) 2245. https://doi.org/10.3390/IJMS19082245.

[207] M.A. Zmijewski, Vitamin D and Human Health, International Journal of Molecular Sciences 2019, Vol. 20, Page 145. 20 (2019) 145. https://doi.org/10.3390/IJMS20010145.

[208] D. Meena, Vitamin D and skin diseases: A review, Asian Journal of Multidimensional Research. 10 (2021) 451–458. https://doi.org/10.5958/2278-4853.2021.01028.4.

[209] A. Saggini, Immunomodulatory effects of vitamin D on skin inflammation, Article in Journal of Biological Regulators and Homeostatic Agents. (2015). https://www.researchgate.net/publication/282277031 (accessed February 20, 2023).

[210] E. Alia, P.E. Kerr, Vitamin D: Skin, sunshine, and beyond, Clin Dermatol. 39 (2021) 840–846. https://doi.org/10.1016/J.CLINDERMATOL.2021.05.025.

[211] M. Pereira, A. Dantas Damascena, L.M. Galvão Azevedo, T. de Almeida Oliveira, J. da Mota Santana, Vitamin D deficiency aggravates COVID-19: systematic review and meta-analysis, Crit Rev Food Sci Nutr. 62 (2020) 1308–1316. https://doi.org/10.1080/10408398.2020.1841090.

[212] V. Kalia, G.P. Studzinski, S. Sarkar, Role of vitamin D in regulating COVID-19 severity—An immunological perspective, J Leukoc Biol. 110 (2021) 809–819. https://doi.org/10.1002/JLB.4COVR1020-698R.

[213] J.K. Stroehlein, J. Wallqvist, C. Iannizzi, A. Mikolajewska, M.I. Metzendorf, C. Benstoem, P. Meybohm, M. Becker, N. Skoetz, M. Stegemann, V. Piechotta, Vitamin D supplementation for the treatment of COVID-19: a living systematic review, Cochrane Database of Systematic Reviews. 2021 (2021). https://doi.org/10.1002/14651858.CD015043.

[214] K.S. Vimaleswaran, N.G. Forouhi, K. Khunti, Vitamin D and covid-19, BMJ. 372 (2021). https://doi.org/10.1136/BMJ.N544.

[215] G.C. Deluca, S.M. Kimball, J. Kolasinski, S. v. Ramagopalan, G.C. Ebers, Review: The role of vitamin D in nervous system health and disease, Neuropathol Appl Neurobiol. 39 (2013) 458–484. https://doi.org/10.1111/NAN.12020.

[216] L., S.Y., M.J.E., P.S., M.W., M.K., . . . & S.H.D. Wang, Circulating 25-hydroxy-vitamin D and risk of cardiovascular disease: a meta-analysis of prospective studies., Circ Cardiovasc Qual Outcomes. 5 (2012) 819–829.

[217] M. Gonnet, L. Lethuaut, F. Boury, New trends in encapsulation of liposoluble vitamins, Journal of Controlled Release. 146 (2010) 276–290. https://doi.org/10.1016/J.JCONREL.2010.01.037.

[218] M.F. Holick, T.C. Chen, Vitamin D deficiency: a worldwide problem with health consequences, Am J Clin Nutr. 87 (2008) 1080S-1086S. https://doi.org/10.1093/AJCN/87.4.1080S.

[219] M. F. Holick, Vitamin D: Evolutionary, Physiological and Health Perspectives, (n.d.).

[220] S.J. Park, C. v. Garcia, G.H. Shin, J.T. Kim, Development of nanostructured lipid carriers for the encapsulation and controlled release of vitamin D3, Food Chem. 225 (2017) 213–219. https://doi.org/10.1016/J.FOODCHEM.2017.01.015.

[221] M. Shah, W. Murad, S. Mubin, O. Ullah, N.U. Rehman, M.H. Rahman, Multiple health benefits of curcumin and its therapeutic potential, Environmental Science and Pollution Research. 29 (2022) 43732–43744. https://doi.org/10.1007/S11356-022-20137-W/METRICS.

[222] R.K. Maheshwari, A.K. Singh, J. Gaddipati, R.C. Srimal, Multiple biological activities of curcumin: A short review, Life Sci. 78 (2006) 2081–2087. https://doi.org/10.1016/J.LFS.2005.12.007.

[223] S.C. Gupta, S. Patchva, B.B. Aggarwal, Therapeutic roles of curcumin: Lessons learned from clinical trials, AAPS Journal. 15 (2013) 195–218. https://doi.org/10.1208/S12248-012-9432-8/METRICS.

[224] S. Roy, J.W. Rhim, Antioxidant and antimicrobial poly(vinyl alcohol)-based films incorporated with grapefruit seed extract and curcumin, J Environ Chem Eng. 9 (2021) 104694. https://doi.org/10.1016/J.JECE.2020.104694.

[225] M.S. Algahtani, M.Z. Ahmad, I.H. Nourein, J. Ahmad, Co-Delivery of Imiquimod and Curcumin by Nanoemugel for Improved Topical Delivery and Reduced Psoriasis-Like Skin Lesions, Biomolecules 2020, Vol. 10, Page 968. 10 (2020) 968. https://doi.org/10.3390/BIOM10070968.

[226] A. Jain, S. Doppalapudi, A.J. Domb, W. Khan, Tacrolimus and curcumin co-loaded liposphere gel: Synergistic combination towards management of psoriasis, Journal of Controlled Release. 243 (2016) 132–145. https://doi.org/10.1016/J.JCONREL.2016.10.004.

[227] X.Y. Xu, X. Meng, S. Li, R.Y. Gan, Y. Li, H. bin Li, Bioactivity, Health Benefits, and Related Molecular Mechanisms of Curcumin: Current Progress, Challenges, and Perspectives, Nutrients 2018, Vol. 10, Page 1553. 10 (2018) 1553. https://doi.org/10.3390/NU10101553.

[228] A. El-Sayed, L. Aleya, M. Kamel, Microbiota's role in health and diseases, Environmental Science and Pollution Research 2021 28:28. 28 (2021) 36967–36983. https://doi.org/10.1007/S11356-021-14593-Z.

[229] A. Sharma, H. Khan, T.G. Singh, A.K. Grewal, A. Najda, M. Kawecka-Radomska, M. Kamel, A.E. Altyar, M.M. Abdel-Daim, Pharmacological Modulation of Ubiquitin-Proteasome Pathways in Oncogenic Signaling, International Journal of Molecular Sciences 2021, Vol. 22, Page 11971. 22 (2021) 11971. https://doi.org/10.3390/IJMS222111971.

[230] K.M. Nelson, J.L. Dahlin, J. Bisson, J. Graham, G.F. Pauli, M.A. Walters, The Essential Medicinal Chemistry of Curcumin, J Med Chem. 60 (2017) 1620–1637. https://doi.org/10.1021/ACS.JMEDCHEM.6B00975/ASSET/IMAGES/LARGE/JM-2016-009757_0003.JPEG.

[231] R.A. Sharma, A.J. Gescher, W.P. Steward, Curcumin: The story so far, Eur J Cancer. 41 (2005) 1955–1968. https://doi.org/10.1016/J.EJCA.2005.05.009.

[232] S.A. Bonini, M. Premoli, S. Tambaro, A. Kumar, G. Maccarinelli, M. Memo, A. Mastinu, Cannabis sativa: A comprehensive ethnopharmacological review of a medicinal plant with a long history, J Ethnopharmacol. 227 (2018) 300–315. https://doi.org/10.1016/J.JEP.2018.09.004.

[233] C.M. Andre, J.F. Hausman, G. Guerriero, Cannabis sativa: The plant of the thousand and one molecules, Front Plant Sci. 7 (2016) 19. https://doi.org/10.3389/FPLS.2016.00019/BIBTEX.

[234] L.O. Hanuš, S.M. Meyer, E. Muñoz, O. Taglialatela-Scafati, G. Appendino, Phytocannabinoids: a unified critical inventory, Nat Prod Rep. 33 (2016) 1357–1392. https://doi.org/10.1039/C6NP00074F.

[235] P.F. Whiting, R.F. Wolff, S. Deshpande, M. di Nisio, S. Duffy, A. v. Hernandez, J.C. Keurentjes, S. Lang, K. Misso, S. Ryder, S. Schmidlkofer, M. Westwood, J. Kleijnen, Cannabinoids for Medical Use: A Systematic Review and Meta-analysis, JAMA. 313 (2015) 2456–2473. https://doi.org/10.1001/JAMA.2015.6358.

[236] C. Ibeas Bih, T. Chen, A.V.W. Nunn, M. Bazelot, M. Dallas, B.J. Whalley, Molecular Targets of Cannabidiol in Neurological Disorders, Neurotherapeutics 2015 12:4. 12 (2015) 699–730. https://doi.org/10.1007/S13311-015-0377-3.

[237] G.A. Cabral, T.J. Rogers, A.H. Lichtman, Turning Over a New Leaf: Cannabinoid and Endocannabinoid Modulation of Immune Function, Journal of Neuroimmune Pharmacology. 10 (2015) 193–203. https://doi.org/10.1007/S11481-015-9615-Z/METRICS.

[238] A. Mastinu, M. Premoli, G. Ferrari-Toninelli, S. Tambaro, G. Maccarinelli, M. Memo, S.A. Bonini, Cannabinoids in health and disease: Pharmacological potential in metabolic syndrome and neuroinflammation, Horm Mol Biol Clin Investig. 36 (2018). https://doi.org/10.1515/HMBCI-2018-0013/ASSET/GRAPHIC/J_HMBCI-2018-0013_FIG_004.JPG.

[239] C. Rong, Y. Lee, N.E. Carmona, D.S. Cha, R.M. Ragguett, J.D. Rosenblat, R.B. Mansur, R.C. Ho, R.S. McIntyre, Cannabidiol in medical marijuana: Research vistas and potential opportunities, Pharmacol Res. 121 (2017) 213–218. https://doi.org/10.1016/J.PHRS.2017.05.005.

[240] R.G. Pertwee, The diverse CB1 and CB2 receptor pharmacology of three plant cannabinoids: Δ9-tetrahydrocannabinol, cannabidiol and Δ9-tetrahydrocannabivarin, Br J Pharmacol. 153 (2008) 199–215. https://doi.org/10.1038/SJ.BJP.0707442.

[241] P. Fusar-Poli, J. Crippa, S. Bhattacharyya, S.J. Borgwardt, P. Allen, R. Martin-Santos, M. Seal, S.A. Surguladze, C. O'Carrol, Z. Atakan, A.W. Zuardi, P.K. McGuire, Distinct Effects of Δ9-Tetrahydrocannabinol and Cannabidiol on Neural Activation During Emotional Processing, Arch Gen Psychiatry. 66 (2009) 95–105. https://doi.org/10.1001/ARCHGENPSYCHIATRY.2008.519.

[242] A.S. Laun, S.H. Shrader, K.J. Brown, Z.H. Song, GPR3, GPR6, and GPR12 as novel molecular targets: their biological functions and interaction with cannabidiol, Acta Pharmacologica Sinica 2018 40:3. 40 (2018) 300–308. https://doi.org/10.1038/s41401-018-0031-9.

[243] O. Devinsky, J.H. Cross, L. Laux, E. Marsh, I. Miller, R. Nabbout, I.E. Scheffer, E.A. Thiele, S. Wright, Trial of Cannabidiol for Drug-Resistant Seizures in the Dravet Syndrome, New England Journal of Medicine. 376 (2017) 2011–2020. https://doi.org/10.1056/NEJMOA1611618/SUPPL_FILE/NEJMOA1611618_DISCLOSURES.PDF.

[244] M.H.N. Chagas, A.W. Zuardi, V. Tumas, M.A. Pena-Pereira, E.T. Sobreira, M.M. Bergamaschi, A.C. dos Santos, A.L. Teixeira, J.E.C. Hallak, J.A.S. Crippa, Effects of cannabidiol in the treatment of patients with Parkinson's disease: An exploratory double-blind trial, Journal of Psychopharmacology. 28 (2014) 1088–1092. https://doi.org/10.1177/0269881114550355.

[245] P. McGuire, P. Robson, W.J. Cubala, D. Vasile, P.D. Morrison, R. Barron, A. Taylor, S. Wright, Cannabidiol (CBD) as an adjunctive therapy in schizophrenia: A multicenter randomized controlled trial, American Journal of Psychiatry. 175 (2018) 225–231. https://doi.org/10.1176/APPI.AJP.2017.17030325/ASSET/IMAGES/LARGE/APPI.AJP.2017.17030325F2.JPEG.

[246] A. Hazekamp, The Trouble with CBD Oil, Med Cannabis Cannabinoids. 1 (2018) 65–72. https://doi.org/10.1159/000489287.

[247] L.L. Romano, A. Hazekamp, Cannabis Oil: chemical evaluation of an upcoming cannabis-based medicine, Cannabinoids. 1 (2013) 1–11. www.cannabis-med.org (accessed February 21, 2023).

[248] W.S. Park, H.J. Kim, M. Li, D.H. Lim, J. Kim, S.S. Kwak, C.M. Kang, M.G. Ferruzzi, M.J. Ahn, Two Classes of Pigments, Carotenoids and C-Phycocyanin, in Spirulina Powder and Their Antioxidant Activities, Molecules 2018, Vol. 23, Page 2065. 23 (2018) 2065. https://doi.org/10.3390/MOLECULES23082065.

[249] M. Safaei, H. Maleki, H. Soleimanpour, A. Norouzy, H.S. Zahiri, H. Vali, K.A. Noghabi, Development of a novel method for the purification of C-phycocyanin pigment from a local cyanobacterial strain Limnothrix sp. NS01 and evaluation of its anticancer properties, Scientific Reports 2019 9:1. 9 (2019) 1–16. https://doi.org/10.1038/s41598-019-45905-6.

[250] S. Chethana, C.A. Nayak, M.C. Madhusudhan, K.S.M.S. Raghavarao, Single step aqueous two-phase extraction for downstream processing of C-phycocyanin from Spirulina platensis, J Food Sci Technol. 52 (2015) 2415–2421. https://doi.org/10.1007/S13197-014-1287-9/METRICS.

[251] T. Kato, Blue pigment from Spirulina, New Food Industry. 29 (1994) 17–21. https://scholar.google.gr/scholar?hl=el&as_sdt=0%2C5&q=T.+Kato%2C+%E2%80%9CBlue+pigment+from+Spirulina%2C%E2%80%9D+New+Food+Industry%2C+vol.+29%2C+pp.+17%E2%80%9321%2C+1994.%2C+&btnG= (accessed February 21, 2023).

[252] T. Hirata, M. Tanaka, M. Ooike, T. Tsunomura, M. Sakaguchi, Antioxidant activities of phycocyanobilin prepared from Spirulina platensis, J Appl Phycol. 12 (2000) 435–439. https://doi.org/10.1023/A:1008175217194/METRICS.

[253] D. Dranseikienė, G. Balčiūnaitė-Murzienė, J. Karosienė, D. Morudov, N. Juodžiukynienė, N. Hudz, R.J. Gerbutavičienė, N. Savickienė, Cyano-Phycocyanin: Mechanisms of Action on Human Skin and Future Perspectives in Medicine, Plants 2022, Vol. 11, Page 1249. 11 (2022) 1249. https://doi.org/10.3390/PLANTS11091249.

[254] Ch. Romay, R. Gonzalez, N. Ledon, D. Remirez, V. Rimbau, C-Phycocyanin: A Biliprotein with Antioxidant, Anti-Inflammatory and Neuroprotective Effects, Curr Protein Pept Sci. 4 (2005) 207–216. https://doi.org/10.2174/1389203033487216.

[255] P. Spolaore, C. Joannis-Cassan, E. Duran, A. Isambert, Blue-green algae as an immuno-enhancer and biomodulator, J. Am. Nutraceutical Assoc. 3 (2001) 24–30. https://doi.org/10.1263/JBB.101.87.

[256] D.W. Grainger, Connecting drug delivery reality to smart materials design, Int J Pharm. 454 (2013) 521–524. https://doi.org/10.1016/J.IJPHARM.2013.04.061.

[257] P. Kakkar, B. Madhan, Fabrication of keratin-silica hydrogel for biomedical applications, Materials Science and Engineering: C. 66 (2016) 178–184. https://doi.org/10.1016/J.MSEC.2016.04.067.

[258] P.A.G. Soares, A.I. Bourbon, A.A. Vicente, C.A.S. Andrade, W. Barros, M.T.S. Correia, A. Pessoa, M.G. Carneiro-Da-Cunha, Development and characterization of hydrogels based on natural polysaccharides: Policaju and chitosan, Materials Science and Engineering: C. 42 (2014) 219–226. https://doi.org/10.1016/J.MSEC.2014.05.009.

[259] F. Ullah, M.B.H. Othman, F. Javed, Z. Ahmad, H.M. Akil, Classification, processing and application of hydrogels: A review, Materials Science and Engineering: C. 57 (2015) 414–433. https://doi.org/10.1016/J.MSEC.2015.07.053.

[260] E.M. Ahmed, Hydrogel: Preparation, characterization, and applications: A review, J Adv Res. 6 (2015) 105–121. https://doi.org/10.1016/J.JARE.2013.07.006.

[261] N. Bhattarai, J. Gunn, M. Zhang, Chitosan-based hydrogels for controlled, localized drug delivery, Adv Drug Deliv Rev. 62 (2010) 83–99. https://doi.org/10.1016/J.ADDR.2009.07.019.

[262] R. Batista, C. Otoni, P. Espitia, Fundamentals of chitosan-based hydrogels: elaboration and characterization techniques, Materials for Biomedical Engineering. (2019) 61–81. https://doi.org/https://doi.org/10.1016/B978-0-12-816901-8.00003-1.

[263] M.K. Lima-Tenório, E.T. Tenório-Neto, M.R. Guilherme, F.P. Garcia, C. v. Nakamura, E.A.G. Pineda, A.F. Rubira, Water transport properties through starch-based hydrogel nanocomposites responding to both pH and a remote magnetic field, Chemical Engineering Journal. 259 (2015) 620–629. https://doi.org/10.1016/J.CEJ.2014.08.045.

[264] M.C.G. Pellá, M.K. Lima-Tenório, E.T. Tenório-Neto, M.R. Guilherme, E.C. Muniz, A.F. Rubira, Chitosan-based hydrogels: From preparation to biomedical applications, Carbohydr Polym. 196 (2018) 233–245. https://doi.org/10.1016/J.CARBPOL.2018.05.033.

[265] R.A.A. Muzzarelli, C. Muzzarelli, Chitin and chitosan hydrogels, Handbook of Hydrocolloids: Second Edition. (2009) 849–888. https://doi.org/10.1533/9781845695873.849.

[266] N.M. Alves, J.F. Mano, Chitosan derivatives obtained by chemical modifications for biomedical and environmental applications, Int J Biol Macromol. 43 (2008) 401–414. https://doi.org/10.1016/J.IJBIOMAC.2008.09.007.

[267] N. Sereni, A. Enache, G. Sudre, A. Montembault, C. Rochas, P. Durand, M.H. Perrard, G. Bozga, J.P. Puaux, T. Delair, L. David, Dynamic Structuration of Physical Chitosan Hydrogels, Langmuir. 33 (2017) 12697–12707. https://doi.org/10.1021/ACS.LANGMUIR.7B02997/SUPPL_FILE/LA7B02997_SI_001.PDF.

[268] S. Baghaie, M.T. Khorasani, A. Zarrabi, J. Moshtaghian, Wound healing properties of PVA/starch/chitosan hydrogel membranes with nano Zinc oxide as antibacterial wound dressing material, Journal of Biomaterials Science, Polymer Edition . 28 (2017) 2220–2241. https://doi.org/10.1080/09205063.2017.1390383.

[269] G.R. Mahdavinia, M. Soleymani, H. Etemadi, M. Sabzi, Z. Atlasi, Model protein BSA adsorption onto novel magnetic chitosan/PVA/laponite RD hydrogel nanocomposite beads, Int J Biol Macromol. 107 (2018) 719–729. https://doi.org/10.1016/J.IJBIOMAC.2017.09.042.

[270] E. Caló, V. v. Khutoryanskiy, Biomedical applications of hydrogels: A review of patents and commercial products, Eur Polym J. 65 (2015) 252–267. https://doi.org/10.1016/J.EURPOLYMJ.2014.11.024.

[271] M. Dash, F. Chiellini, R.M. Ottenbrite, E. Chiellini, Chitosan—A versatile semi-synthetic polymer in biomedical applications, Prog Polym Sci. 36 (2011) 981–1014. https://doi.org/10.1016/J.PROGPOLYMSCI.2011.02.001.

[272] V.R. Sinha, A.K. Singla, S. Wadhawan, R. Kaushik, R. Kumria, K. Bansal, S. Dhawan, Chitosan microspheres as a potential carrier for drugs, Int J Pharm. 274 (2004) 1–33. https://doi.org/10.1016/J.IJPHARM.2003.12.026.

[273] Vipin Bansal, Pramod Kumar Sharma, Nitin Sharma, Om Prakash, Rishabha Malviya, Applications of Chitosan and Chitosan Derivatives in Drug Delivery, Adv Biol Res (Rennes). 5 (2011) 28–37.

[274] N.A. Peppas, K.M. Wood, J.O. Blanchette, Hydrogels for oral delivery of therapeutic proteins, Expert Opin Biol Ther. 4 (2005) 881–887. https://doi.org/10.1517/14712598.4.6.881.

[275] A. Nayak, O. Olatunji, D.B. Das, G. Vladisavljević, Pharmaceutical applications of natural polymers, Natural Polymers: Industry Techniques and Applications. (2015) 263–313. https://doi.org/10.1007/978-3-319-26414-1_9/COVER.

[276] O. Olatunji, Natural polymers: Industry techniques and applications, Natural Polymers: Industry Techniques and Applications. (2015) 1–370. https://doi.org/10.1007/978-3-319-26414-1/COVER.

[277] B.C. Ciobanu, A.N. Cadinoiu, M. Popa, J. Desbrières, C.A. Peptu, Modulated release from liposomes entrapped in chitosan/gelatin hydrogels, Materials Science and Engineering: C. 43 (2014) 383–391. https://doi.org/10.1016/J.MSEC.2014.07.036.

[278] S. Demisli, M. Chatzidaki, A. Xenakis, V. Papadimitriou, Recent progress on nano-carriers fabrication for food applications with special reference to olive oil-based systems, Current Opinion in Food. 43 (2022) 146–154. https://doi.org/https://doi.org/10.1016/j.cofs.2021.11.012.

[279] E. Vassiliadi, E. Mitsou, S. Avramiotis, C.L. Chochos, F. Pirolt, M. Medebach, O. Glatter, A. Xenakis, M. Zoumpanioti, Structural Study of (Hydroxypropyl)Methyl Cellulose Microemulsion-Based Gels Used for Biocompatible Encapsulations, Nanomaterials 2020, Vol. 10, Page 2204. 10 (2020) 2204. https://doi.org/10.3390/NANO10112204.

[280] M.W. Jøraholmen, P. Basnet, M.J. Tostrup, S. Moueffaq, N. Škalko-Basnet, Localized Therapy of Vaginal Infections and Inflammation: Liposomes-In-Hydrogel Delivery System for Polyphenols, Pharmaceutics 2019, Vol. 11, Page 53. 11 (2019) 53. https://doi.org/10.3390/PHARMACEUTICS11020053.

[281] O. Torres, N. Tena, B. Murray, A. Sarkar, Novel starch based emulsion gels and emulsion microgel particles: Design, structure and rheology, Carbohydr Polym. 178 (2017) 86–94. https://doi.org/https://doi.org/10.1016/j.carbpol.2017.09.027.

[282] I.M. Geremias-Andrade, N.P.B.G. Souki, I.C.F. Moraes, S.C. Pinho, Rheology of Emulsion-Filled Gels Applied to the Development of Food Materials, Gels 2016, Vol. 2, Page 22. 2 (2016) 22. https://doi.org/10.3390/GELS2030022.

[283] E. Dickinson, Understanding Food Structures: The Colloid Science Approach, Food Structures, Digestion and Health. (2014) 3–49. https://doi.org/10.1016/B978-0-12-404610-8.00001-3.

[284] M., Boland, M., Golding, H. Singh, eds., Food Structures, Digestion and Health, Academic Press, n.d.

[285] E. Dickinson, Emulsion gels: The structuring of soft solids with protein-stabilized oil droplets, Food Hydrocoll. 28 (2012) 224–241. https://doi.org/10.1016/J.FOODHYD.2011.12.017.

[286] T. Farjami, A. Madadlou, An overview on preparation of emulsion-filled gels and emulsion particulate gels, Trends Food Sci Technol. 86 (2019) 85–94. https://doi.org/10.1016/J.TIFS.2019.02.043.

[287] J. Chen, E. Dickinson, Effect of surface character of filler particles on rheology of heat-set whey protein emulsion gels, Colloids Surf B Biointerfaces. 12 (1999) 373–381. https://doi.org/10.1016/S0927-7765(98)00091-5.

[288] E. Dickinson, Emulsion gels: The structuring of soft solids with protein-stabilized oil droplets, Food Hydrocoll. 28 (2012) 224–241. https://doi.org/10.1016/J.FOODHYD.2011.12.017.

[289] L. Oliver, L. Berndsen, G.A. van Aken, E. Scholten, Influence of droplet clustering on the rheological properties of emulsion-filled gels, Food Hydrocoll. 50 (2015) 74–83. https://doi.org/10.1016/J.FOODHYD.2015.04.001.

[290] T. van Vliet, Rheological properties of filled gels. Influence of filler matrix interaction, Colloid Polym Sci. 266 (1988) 518–524. https://doi.org/10.1007/BF01420762/METRICS.

[291] G. Sala, F. van de Velde, M.A. Cohen Stuart, G.A. van Aken, Oil droplet release from emulsion-filled gels in relation to sensory perception, Food Hydrocoll. 21 (2007) 977–985. https://doi.org/10.1016/J.FOODHYD.2006.08.009.

[292] J. Kokini, G. van Aken, Discussion session on food emulsions and foams, Food Hydrocoll. 20 (2006) 438–445. https://doi.org/10.1016/J.FOODHYD.2005.10.003.

[293] E.A. Foegeding, E.L. Bowland, C.C. Hardin, Factors that determine the fracture properties and microstructure of globular protein gels, Food Hydrocoll. 9 (1995) 237–249. https://doi.org/10.1016/S0268-005X(09)80254-3.

[294] Q. Guo, A. Ye, M. Lad, D. Dalgleish, H. Singh, The breakdown properties of heat-set whey protein emulsion gels in the human mouth, Food Hydrocoll. 33 (2013) 215–224. https://doi.org/10.1016/J.FOODHYD.2013.03.008.

[295] L. Mao, Y.H. Roos, S. Miao, Study on the rheological properties and volatile release of cold-set emulsion-filled protein gels, J Agric Food Chem. 62 (2014) 11420–11428. https://doi.org/10.1021/JF503931Y/ASSET/IMAGES/MEDIUM/JF-2014-03931Y_0009.GIF.

[296] D.B. Genovese, Shear rheology of hard-sphere, dispersed, and aggregated suspensions, and filler-matrix composites, Adv Colloid Interface Sci. 171–172 (2012) 1–16. https://doi.org/10.1016/J.CIS.2011.12.005.

[297] E. Dickinson, Y. Yamamoto, Viscoelastic Properties of Heat-Set Whey Protein-Stabilized Emulsion Gels with Added Lecithin, J Food Sci. 61 (1996) 811–816. https://doi.org/10.1111/J.1365-2621.1996.TB12208.X.

[298] D.J. McCLEMENTS, F.J. MONAHAN, J.E. KINSELLA, EFFECT OF EMULSION DROPLETS ON THE RHEOLOGY OF WHEY PROTEIN ISOLATE GELS, J Texture Stud. 24 (1993) 411–422. https://doi.org/10.1111/J.1745-4603.1993.TB00051.X.

[299] O. Torres, N.M. Tena, B. Murray, A. Sarkar, Novel starch based emulsion gels and emulsion microgel particles: Design, structure and rheology, Carbohydr Polym. 178 (2017) 86–94. https://doi.org/10.1016/J.CARBPOL.2017.09.027.

[300] E. Dickinson, J. Chen, Heat-set whey protein emulsion gels: Role of active and inactive filler particles, J Dispers Sci Technol. 20 (2007) 197–213. https://doi.org/10.1080/01932699908943787.

[301] D.J. McClements, E.A. Decker, J. Weiss, Emulsion-Based Delivery Systems for Lipophilic Bioactive Components, J Food Sci. 72 (2007) R109–R124. https://doi.org/10.1111/J.1750-3841.2007.00507.X.

[302] X.L., Zhang, R., Zhao, W. Qian, Preparation of an emulgel for treatment of aphthous ulcer on the basis of carbomers, Chin Pharm J. 30 (1995) 417–418.

[303] E. Rahmani-Neishaboor, R. Jallili, R. Hartwell, V. Leung, N. Carr, A. Ghahary, Topical application of a film-forming emulgel dressing that controls the release of stratifin and acetylsalicylic acid and improves/prevents hypertrophic scarring, Wound Repair and Regeneration. 21 (2013) 55–65. https://doi.org/10.1111/J.1524-475X.2012.00857.X.

[304] P., Devada, A., Jain, N., Vyas, S. Jain, Development of antifungal emulsion based gel for topical fungal infection, Int J Pharm Res Dev. 3 (2011) 18–25.

[305] G.M. Eccleston, Emulsions and creams., Aulton's Pharmaceutics, The Design and Manufacture of Medicines, 2003. https://books.google.co.uk/books?hl=el&lr=&id=rrtGKQxcoWIC&oi=fnd&pg=PA435&dq=Emulsions+and+creams.&ots=-tCbzaLJKp&sig=oIAfhGB1IoM4HkFXjBvr3KuzZVM&redir_esc=y#v=onepage&q=Emulsions%20and%20creams.&f=false (accessed February 28, 2023).

[306] Z. Zhang, E.A. Decker, D.J. McClements, Encapsulation, protection, and release of polyunsaturated lipids using biopolymer-based hydrogel particles, Food Research International. 64 (2014) 520–526. https://doi.org/10.1016/J.FOODRES.2014.07.020.

[307] Ajazuddin, A. Alexander, A. Khichariya, S. Gupta, R.J. Patel, T.K. Giri, D.K. Tripathi, Recent expansions in an emergent novel drug delivery technology: Emulgel, Journal of

Controlled Release. 171 (2013) 122–132. https://doi.org/10.1016/J.JCONREL.2013.06.030.

[308] G. di Colo, A. Baggiani, Y. Zambito, G. Mollica, M. Geppi, M.F. Serafini, A new hydrogel for the extended and complete prednisolone release in the GI tract, Int J Pharm. 310 (2006) 154–161. https://doi.org/10.1016/J.IJPHARM.2005.12.002.

[309] Z. Zhang, R. Zhang, L. Chen, Q. Tong, D.J. McClements, Designing hydrogel particles for controlled or targeted release of lipophilic bioactive agents in the gastrointestinal tract, Eur Polym J. 72 (2015) 698–716. https://doi.org/10.1016/J.EURPOLYMJ.2015.01.013.

[310] H.M. Shewan, J.R. Stokes, Review of techniques to manufacture micro-hydrogel particles for the food industry and their applications, J Food Eng. 119 (2013) 781–792. https://doi.org/10.1016/J.JFOODENG.2013.06.046.

[311] M.J. Kutyła, M.W. Boehm, J.R. Stokes, P.N. Shaw, N.M. Davies, R.P. McGeary, J. Tuke, B.P. Ross, Cyclodextrin-crosslinked poly(acrylic acid): Adhesion and controlled release of diflunisal and fluconazole from solid dosage forms, AAPS PharmSciTech. 14 (2013) 301–311. https://doi.org/10.1208/S12249-012-9903-3/METRICS.

[312] J. Jung, R.D. Arnold, L. Wicker, Pectin and charge modified pectin hydrogel beads as a colon-targeted drug delivery carrier, Colloids Surf B Biointerfaces. 104 (2013) 116–121. https://doi.org/10.1016/J.COLSURFB.2012.11.042.

[313] Z. Zhang, R. Zhang, E.A. Decker, D.J. McClements, Development of food-grade filled hydrogels for oral delivery of lipophilic active ingredients: pH-triggered release, Food Hydrocoll. 44 (2015) 345–352. https://doi.org/10.1016/J.FOODHYD.2014.10.002.

[314] S. Ray, S. Banerjee, S. Maiti, B. Laha, S. Barik, B. Sa, U.K. Bhattacharyya, Novel interpenetrating network microspheres of xanthan gum–poly(vinyl alcohol) for the delivery of diclofenac sodium to the intestine—in vitro and in vivo evaluation, Drug Deliv. 17 (2010) 508–519. https://doi.org/10.3109/10717544.2010.483256.

[315] L. Chen, G.E. Remondetto, M. Subirade, Food protein-based materials as nutraceutical delivery systems, Trends Food Sci Technol. 17 (2006) 272–283. https://doi.org/10.1016/J.TIFS.2005.12.011.

[316] R. Dubey, Microencapsulation technology and applications., Def Sci J. 59 (2009) 82. https://citeseerx.ist.psu.edu/document?repid=rep1&type=pdf&doi=e205cf57fda2024156582660d59d6614cc936055 (accessed February 28, 2023).

[317] Y. Li, J. Kim, Y. Park, D.J. McClements, Modulation of lipid digestibility using structured emulsion-based delivery systems: Comparison of in vivo and in vitro measurements, Food Funct. 3 (2012) 528–536. https://doi.org/10.1039/C2FO10273K.

[318] M.I. Mohamed, Optimization of chlorphenesin emulgel formulation, AAPS Journal. 6 (2004) 1–7. https://doi.org/10.1208/AAPSJ060326/METRICS.

[319] R. Khullar, D. Kumar, N. Seth, S. Saini, Formulation and evaluation of mefenamic acid emulgel for topical delivery, Saudi Pharmaceutical Journal. 20 (2012) 63–67. https://doi.org/10.1016/J.JSPS.2011.08.001.

[320] S.P. Stanos, Topical Agents for the Management of Musculoskeletal Pain, J Pain Symptom Manage. 33 (2007) 342–355. https://doi.org/10.1016/J.JPAINSYMMAN.2006.11.005.

[321] F. Vanpariya, M. Shiroya, M. Malaviya, Emulgel: A Review, Article in International Journal of Science and Research. (2021). https://doi.org/10.21275/SR21311095015.

[322] C. Sarisozen, I. Vural, T. Levchenko, A.A. Hincal, V.P. Torchilin, PEG-PE-based micelles co-loaded with paclitaxel and cyclosporine A or loaded with paclitaxel and targeted by anticancer antibody overcome drug resistance in cancer cells, Drug Deliv. 19 (2012) 169–176. https://doi.org/10.3109/10717544.2012.674163.

[323] L. Perioli, C. Pagano, S. Mazzitelli, C. Rossi, C. Nastruzzi, Rheological and functional characterization of new antiinflammatory delivery systems designed for buccal administration, Int J Pharm. 356 (2008) 19–28. https://doi.org/10.1016/J.IJPHARM.2007.12.027.

[324] D.A. El-Setouhy, S.M. Ahmed El-Ashmony, Ketorolac trometamol topical formulations: release behaviour, physical characterization, skin permeation, efficacy and gastric safety, Journal of Pharmacy and Pharmacology. 62 (2010) 25–34. https://doi.org/10.1211/JPP.62.01.0002.

[325] A. Kaur, S.S. Katiyar, V. Kushwah, S. Jain, Nanoemulsion loaded gel for topical co-delivery of clobitasol propionate and calcipotriol in psoriasis, Nanomedicine. 13 (2017) 1473–1482. https://doi.org/10.1016/J.NANO.2017.02.009.

[326] L. Perioli, V. Ambrogi, L. Venezia, S. Giovagnoli, C. Pagano, C. Rossi, Formulation studies of benzydamine mucoadhesive formulations for vaginal administration, Drug Dev Ind Pharm. 35 (2009) 769–779. https://doi.org/10.1080/03639040802592435.

[327] M. López-Cervantes, J.J. Escobar-Chvez, N. Casas-Alancaster, D. Quintanar-Guerrero, A. Ganem-Quintanar, Development and characterization of a transdermal patch and an emulgel containing kanamycin intended to be used in the treatment of mycetoma caused by Actinomadura madurae, Drug Dev Ind Pharm. 35 (2009) 1511–1521. https://doi.org/10.3109/03639040903037215.

[328] R. Kaur, M. Ajitha, Formulation of transdermal nanoemulsion gel drug delivery system of lovastatin and its in vivo characterization in glucocorticoid induced osteoporosis rat model, J Drug Deliv Sci Technol. 52 (2019) 968–978. https://doi.org/10.1016/J.JDDST.2019.06.008.

[329] I.B. Pathan, R. Juvrag, S. Shelke, W. Ambekar, Terbinafine Hydrochloride Nanoemulsion Gel for Transdermal Delivery in Fungal Infection: Ex-vivo and In-vivo Evaluation, Current Nanomedicine. 8 (2018) 251–263. https://doi.org/10.2174/2211352516666180425153510.

[330] Prakash U. R.T., P., Thiagarajan, Nanoemulsions for drug delivery through different routes, Research in Biotechnology. 2 (2011). https://agris.fao.org/agris-search/search.do?recordID=AE2019100853.

[331] B. Homayun, X. Lin, H.J. Choi, Challenges and Recent Progress in Oral Drug Delivery Systems for Biopharmaceuticals, Pharmaceutics 2019, Vol. 11, Page 129. 11 (2019) 129. https://doi.org/10.3390/PHARMACEUTICS11030129.

[332] K. Thanki, R.P. Gangwal, A.T. Sangamwar, S. Jain, Oral delivery of anticancer drugs: Challenges and opportunities, Journal of Controlled Release. 170 (2013) 15–40. https://doi.org/10.1016/J.JCONREL.2013.04.020.

[333] J., Posner, J.P., Griffin, G.R. Barker, eds., The Textbook of Pharmaceutical Medicine, John Wiley & Sons, 2013. https://books.google.co.uk/books?hl=el&lr=&id=PpfT6bSF4kcC&oi=fnd&pg=PT13&dq=The+Textbook+of+Pharmaceutical+Medicine+&ots=HeX8-4OnHG&sig=oX0p7kWVJfwwKVLwkSuwury478U&redir_esc=y#v=onepage&q=The%20Textbook%20of%20Pharmaceutical%20Medicine&f=false (accessed February 28, 2023).

[334] E. Flynn, Pharmacokinetic Parameters, XPharm: The Comprehensive Pharmacology Reference. (2007) 1–3. https://doi.org/10.1016/B978-008055232-3.60034-0.

[335] B. Homayun, X. Lin, H.J. Choi, Challenges and Recent Progress in Oral Drug Delivery Systems for Biopharmaceuticals, Pharmaceutics 2019, Vol. 11, Page 129. 11 (2019) 129. https://doi.org/10.3390/PHARMACEUTICS11030129.

[336] S.V. Sastry, J.R. Nyshadham, J.A. Fix, Recent technological advances in oral drug delivery – a review, Pharm Sci Technol Today. 3 (2000) 138–145. https://doi.org/10.1016/S1461-5347(00)00247-9.

[337] F. Kong, R.P. Singh, Disintegration of Solid Foods in Human Stomach, J Food Sci. 73 (2008) R67–R80. https://doi.org/10.1111/J.1750-3841.2008.00766.X.

[338] A. Rubinstein, Y. v. Pathak, J. Kleinstern, A. Reches, S. Benita, In Vitro Release and Intestinal Absorption of Physostigmine Salicylate from Submicron Emulsions, J Pharm Sci. 80 (1991) 643–647. https://doi.org/10.1002/JPS.2600800706.

[339] E. Roger, F. Lagarce, E. Garcion, J.P. Benoit, Biopharmaceutical parameters to consider in order to alter the fate of nanocarriers after oral delivery, Nanomedicine. 5 (2010) 287–306. https://doi.org/10.2217/NNM.09.110.

[340] P. Arora, S. Sharma, S. Garg, Permeability issues in nasal drug delivery, Drug Discov Today. 7 (2002) 967–975. https://doi.org/10.1016/S1359-6446(02)02452-2.

[341] A. Rapoport, P. Winner, Nasal Delivery of Antimigraine Drugs: Clinical Rationale and Evidence Base, Headache: The Journal of Head and Face Pain. 46 (2006) S192–S201. https://doi.org/10.1111/J.1526-4610.2006.00603.X.

[342] A. Pires, A. Fortuna, G. Alves, A. Falcão, Intranasal Drug Delivery: How, Why and What for?, Journal of Pharmacy & Pharmaceutical Sciences. 12 (2009) 288–311. https://doi.org/10.18433/J3NC79.

[343] S.A., K.F.C., A.A.A. Chime, Nanoemulsions—advances in formulation, characterization and applications in drug delivery., Application of Nanotechnology in Drug Delivery. 3 (2014) 77–126.

[344] A.K. Leonard, A.P. Sileno, G.C. Brandt, C.A. Foerder, S.C. Quay, H.R. Costantino, In vitro formulation optimization of intranasal galantamine leading to enhanced bioavailability and reduced emetic response in vivo, Int J Pharm. 335 (2007) 138–146. https://doi.org/10.1016/J.IJPHARM.2006.11.013.

[345] R.J. Salib, P.H. Howarth, Safety and Tolerability Profiles of Intranasal Antihistamines and Intranasal Corticosteroids in the Treatment of Allergic Rhinitis, Drug Safety 2003 26:12. 26 (2012) 863–893. https://doi.org/10.2165/00002018-200326120-00003.

[346] T. Furubayashi, A. Kamaguchi, K. Kawaharada, Y. Masaoka, M. Kataoka, S. Yamashita, Y. Higashi, T. Sakane, Evaluation of the Contribution of the Nasal Cavity and Gastrointestinal Tract to Drug Absorption Following Nasal Application to Rats, Biol Pharm Bull. 30 (2007) 608–611. https://doi.org/10.1248/BPB.30.608.

[347] M.I. Ugwoke, R.U. Agu, N. Verbeke, R. Kinget, Nasal mucoadhesive drug delivery: Background, applications, trends and future perspectives, Adv Drug Deliv Rev. 57 (2005) 1640–1665. https://doi.org/10.1016/J.ADDR.2005.07.009.

[348] H.R. Costantino, L. Illum, G. Brandt, P.H. Johnson, S.C. Quay, Intranasal delivery: Physicochemical and therapeutic aspects, Int J Pharm. 337 (2007) 1–24. https://doi.org/10.1016/J.IJPHARM.2007.03.025.

[349] L. Illum, Nasal drug delivery: new developments and strategies, Drug Discov Today. 7 (2002) 1184–1189. https://doi.org/10.1016/S1359-6446(02)02529-1.

[350] S.B. Bhise, A.V. Yadav, A.M. Avachat, R. Malayandi, Bioavailability of intranasal drug delivery system, Asian Journal of Pharmaceutics (AJP). 2 (2008). https://doi.org/10.22377/AJP.V2I4.203.

[351] S. Grassin-Delyle, A. Buenestado, E. Naline, C. Faisy, S. Blouquit-Laye, L.J. Couderc, M. le Guen, M. Fischler, P. Devillier, Intranasal drug delivery: An efficient and non-invasive route for systemic administration: Focus on opioids, Pharmacol Ther. 134 (2012) 366–379. https://doi.org/10.1016/J.PHARMTHERA.2012.03.003.

[352] M.I. Ugwoke, N. Verbeke, R. Kinget, The biopharmaceutical aspects of nasal mucoadhesive drug delivery, Journal of Pharmacy and Pharmacology. 53 (2001) 3–22. https://doi.org/10.1211/0022357011775145.

[353] T. Matsuyama, T. Morita, Y. Horikiri, H. Yamahara, H. Yoshino, Enhancement of nasal absorption of large molecular weight compounds by combination of mucolytic agent and nonionic surfactant, Journal of Controlled Release. 110 (2006) 347–352. https://doi.org/10.1016/J.JCONREL.2005.09.047.

[354] D.S. Quintana, A.J. Guastella, L.T. Westlye, O.A. Andreassen, The promise and pitfalls of intranasally administering psychopharmacological agents for the treatment of psychiatric disorders, Molecular Psychiatry 2016 21:1. 21 (2015) 29–38. https://doi.org/10.1038/mp.2015.166.

[355] S. Mujica Ascencio, C.S. Choe, M.C. Meinke, R.H. Müller, G. v. Maksimov, W. Wigger-Alberti, J. Lademann, M.E. Darvin, Confocal Raman microscopy and multivariate statistical analysis for determination of different penetration abilities of caffeine and propylene glycol applied simultaneously in a mixture on porcine skin ex vivo, European Journal of Pharmaceutics and Biopharmaceutics. 104 (2016) 51–58. https://doi.org/10.1016/J.EJPB.2016.04.018.

[356] A.D. Metcalfe, M.W.J. Ferguson, Tissue engineering of replacement skin: the crossroads of biomaterials, wound healing, embryonic development, stem cells and

regeneration, J R Soc Interface. 4 (2006) 413–437. https://doi.org/10.1098/RSIF.2006.0179.

[357] D. Cosco, C. Celia, F. Cilurzo, E. Trapasso, D. Paolino, Colloidal carriers for the enhanced delivery through the skin, Expert Opin Drug Deliv. 5 (2008) 737–755. https://doi.org/10.1517/17425247.5.7.737.

[358] D.I.J. Morrow, P.A. McCarron, A.D. Woolfson, R.F. Donnelly, Innovative Strategies for Enhancing Topical and Transdermal Drug Delivery, The Open Drug Delivery Journal. 1 (2007) 36–59. https://doi.org/10.2174/1874126600701010036.

[359] J. Mueller, J.S.L. Oliveira, R. Barker, M. Trapp, A. Schroeter, G. Brezesinski, R.H.H. Neubert, The effect of urea and taurine as hydrophilic penetration enhancers on stratum corneum lipid models, Biochimica et Biophysica Acta (BBA) - Biomembranes. 1858 (2016) 2006–2018. https://doi.org/10.1016/J.BBAMEM.2016.05.010.

[360] I.A. Chacko, V.M. Ghate, L. Dsouza, S.A. Lewis, Lipid vesicles: A versatile drug delivery platform for dermal and transdermal applications, Colloids Surf B Biointerfaces. 195 (2020) 111262. https://doi.org/10.1016/J.COLSURFB.2020.111262.

[361] M.B. Brown, G.P. Martin, S.A. Jones, F.K. Akomeah, Dermal and Transdermal Drug Delivery Systems: Current and Future Prospects, Drug Deliv. 13 (2008) 175–187. https://doi.org/10.1080/10717540500455975.

[362] C.C. Müller-Goymann, Physicochemical characterization of colloidal drug delivery systems such as reverse micelles, vesicles, liquid crystals and nanoparticles for topical administration, European Journal of Pharmaceutics and Biopharmaceutics. 58 (2004) 343–356. https://doi.org/10.1016/J.EJPB.2004.03.028.

[363] B.W. Barry, Breaching the skin's barrier to drugs, Nat Biotechnol. 22 (2004) 165–167.

[364] A.A. Moshfeghi, G.A. Peyman, Micro- and nanoparticulates, Adv Drug Deliv Rev. 57 (2005) 2047–2052. https://doi.org/10.1016/J.ADDR.2005.09.006.

[365] H. Rosen, T. Abribat, The rise and rise of drug delivery, Nature Reviews Drug Discovery 2005 4:5. 4 (2005) 381–385. https://doi.org/10.1038/nrd1721.

[366] L. Kikwai, R.J. Babu, R. Prado, A. Kolot, C.A. Armstrong, J.C. Ansel, M. Singh, In vitro and in vivo evaluation of topical formulations of Spantide II, AAPS PharmSciTech. 6 (2005) E565–E572. https://doi.org/10.1208/PT060471/METRICS.

[367] K.S. Paudel, M. Milewski, C.L. Swadley, N.K. Brogden, P. Ghosh, A.L. Stinchcomb, Challenges and opportunities in dermal/transdermal delivery, Ther Deliv. 1 (2010) 109–131. https://doi.org/10.4155/TDE.10.16.

[368] S. Lee, D.J. McAuliffe, T.J. Flotte, N. Kollias, A.G. Doukas, Photomechanical Transcutaneous Delivery of Macromolecules, Journal of Investigative Dermatology. 111 (1998) 925–929. https://doi.org/10.1046/J.1523-1747.1998.00415.X.

[369] Y.S. Rhee, J.G. Choi, E.S. Park, S.C. Chi, Transdermal delivery of ketoprofen using microemulsions, Int J Pharm. 228 (2001) 161–170. https://doi.org/10.1016/S0378-5173(01)00827-4.

[370] M.H.F. Sakeena, M.F. Yam, S.M. Elrashid, A.S. Munavvar, M.N. Azmin, Anti-inflammatory and Analgesic Effects of Ketoprofen in Palm Oil Esters Nanoemulsion, J Oleo Sci. 59 (2010) 667–671. https://doi.org/10.5650/JOS.59.667.

[371] W. Leppert, M. Malec-Milewska, R. Zajaczkowska, J. Wordliczek, Transdermal and Topical Drug Administration in the Treatment of Pain, Molecules 2018, Vol. 23, Page 681. 23 (2018) 681. https://doi.org/10.3390/MOLECULES23030681.

[372] J.D. Bos, M.M.H.M. Meinardi, The 500 Dalton rule for the skin penetration of chemical compounds and drugs, Exp Dermatol. 9 (2000) 165–169. https://doi.org/10.1034/J.1600-0625.2000.009003165.X.

[373] K. Rehman, M.H. Zulfakar, Recent advances in gel technologies for topical and transdermal drug delivery, Drug Dev Ind Pharm. 40 (2014) 433–440. https://doi.org/10.3109/03639045.2013.828219.

[374] M.R. Prausnitz, R. Langer, Transdermal drug delivery, Nature Biotechnology 2008 26:11. 26 (2008) 1261–1268. https://doi.org/10.1038/nbt.1504.

[375] Y. Chen, P. Quan, X. Liu, M. Wang, L. Fang, Novel chemical permeation enhancers for transdermal drug delivery, Asian J Pharm Sci. 9 (2014) 51–64. https://doi.org/10.1016/J.AJPS.2014.01.001.

[376] M.H. Schmid-Wendtner, H.C. Korting, The pH of the Skin Surface and Its Impact on the Barrier Function, Skin Pharmacol Physiol. 19 (2006) 296–302. https://doi.org/10.1159/000094670.

[377] J.L. Antoine, J.L. Contreras, D.J. van Neste, pH influence of surfactant-induced skin irritation. A non-invasive, multiparametric study with sodium laurylsulfate., Derm Beruf Umwelt. 37 (1989) 96–100. https://europepmc.org/article/med/2743874 (accessed March 1, 2023).

[378] J.F.G.M. HURKMANS, H.E. BODDÉ, L.M.J. van DRIEL, H. van DOORNE, H.E. JUNGINGER, Skin irritation caused by transdermal drug delivery systems during long-term (5 days) application, British Journal of Dermatology. 112 (1985) 461–467. https://doi.org/10.1111/J.1365-2133.1985.TB02321.X.

[379] R.C. Wester, R. Patel, S. Nacht, J. Leyden, J. Melendres, H. Maibach, Controlled release of benzoyl peroxide from a porous microsphere polymeric system can reduce topical irritancy, J Am Acad Dermatol. 24 (1991) 720–726. https://doi.org/10.1016/0190-9622(91)70109-F.

[380] S. Münch, J. Wohlrab, R.H.H. Neubert, Dermal and transdermal delivery of pharmaceutically relevant macromolecules, European Journal of Pharmaceutics and Biopharmaceutics. 119 (2017) 235–242. https://doi.org/10.1016/J.EJPB.2017.06.019.

[381] Scheindlin, Stanley, Transdermal Drug Delivery: PAST, PRESENT, FUTURE, Mol Interv. 4 (2004) 308. https://doi.org/10.1124/MI.4.6.1.

[382] G. Patil, S. Chethana, A.S. Sridevi, K.S.M.S. Raghavarao, Method to obtain C-phycocyanin of high purity, J Chromatogr A. 1127 (2006) 76–81. https://doi.org/10.1016/J.CHROMA.2006.05.073.

[383] C.C. Moraes, S.J. Kalil, Strategy for a protein purification design using C-phycocyanin extract, Bioresour Technol. 100 (2009) 5312–5317. https://doi.org/10.1016/J.BIORTECH.2009.05.026.

[384] X. Liao, B. Zhang, X. Wang, H. Yan, X. Zhang, Purification of C-phycocyanin from spirulina platensis by single-step ion-exchange chromatography, Chromatographia. 73 (2011) 291–296. https://doi.org/10.1007/S10337-010-1874-5/METRICS.

[385] Y. Li, Z. Zhang, M. Paciulli, A. Abbaspourrad, Extraction of phycocyanin—A natural blue colorant from dried spirulina biomass: Influence of processing parameters and extraction techniques, J Food Sci. 85 (2020) 727–735. https://doi.org/10.1111/1750-3841.14842.

[386] E. Fröhlich, The role of surface charge in cellular uptake and cytotoxicity of medical nanoparticles, Int J Nanomedicine. 7 (2012) 5577–5591. https://doi.org/10.2147/IJN.S36111.

[387] S. Bhattacharjee, D. Ershov, K. Fytianos, J. van der Gucht, G.M. Alink, I.M.C.M. Rietjens, A.T.M. Marcelis, H. Zuilhof, Cytotoxicity and cellular uptake of tri-block copolymer nanoparticles with different size and surface characteristics, Part Fibre Toxicol. 9 (2012) 1–19. https://doi.org/10.1186/1743-8977-9-11/FIGURES/12.

[388] P.M. Favi, M. Gao, L. Johana Sepúlveda Arango, S.P. Ospina, M. Morales, J.J. Pavon, T.J. Webster, Shape and surface effects on the cytotoxicity of nanoparticles: Gold nanospheres versus gold nanostars, J Biomed Mater Res A. 103 (2015) 3449–3462. https://doi.org/10.1002/JBM.A.35491.

[389] S. Bhattacharjee, I.M.C.M. Rietjens, M.P. Singh, T.M. Atkins, T.K. Purkait, Z. Xu, S. Regli, A. Shukaliak, R.J. Clark, B.S. Mitchell, G.M. Alink, A.T.M. Marcelis, M.J. Fink, J.G.C. Veinot, S.M. Kauzlarich, H. Zuilhof, Cytotoxicity of surface-functionalized silicon and germanium nanoparticles: the dominant role of surface charges, Nanoscale. 5 (2013) 4870–4883. https://doi.org/10.1039/C3NR34266B.

[390] L.A.S. Bahari, H. Hamishehkar, The Impact of Variables on Particle Size of Solid Lipid Nanoparticles and Nanostructured Lipid Carriers; A Comparative Literature Review, Adv Pharm Bull. 6 (2016) 143. https://doi.org/10.15171/APB.2016.021.

[391] S. Bhattacharjee, DLS and zeta potential – What they are and what they are not?, Journal of Controlled Release. 235 (2016) 337–351. https://doi.org/10.1016/J.JCONREL.2016.06.017.

[392] W.I. Goldburg, Dynamic light scattering, Am J Phys. 67 (1999) 1152. https://doi.org/10.1119/1.19101.

[393] J. Stetefeld, S.A. McKenna, T.R. Patel, Dynamic light scattering: a practical guide and applications in biomedical sciences, Biophys Rev. 8 (2016) 409–427. https://doi.org/10.1007/S12551-016-0218-6/METRICS.

[394] P.A. Hassan, S. Rana, G. Verma, Making sense of Brownian motion: Colloid characterization by dynamic light scattering, Langmuir. 31 (2015) 3–12. https://doi.org/10.1021/LA501789Z/ASSET/IMAGES/MEDIUM/LA-2014-01789Z_0013.GIF.

[395] A. Kalaitzaki, N.E. Papanikolaou, F. Karamaouna, V. Dourtoglou, A. Xenakis, V. Papadimitriou, Biocompatible colloidal dispersions as potential formulations of natural pyrethrins: A structural and efficacy study, Langmuir. 31 (2015) 5722–5730. https://doi.org/10.1021/ACS.LANGMUIR.5B00246/SUPPL_FILE/LA5B00246_SI_001.PDF.

[396] P. Rademeyer, D. Carugo, J.Y. Lee, E. Stride, Microfluidic system for high throughput characterisation of echogenic particles, Lab Chip. 15 (2014) 417–428. https://doi.org/10.1039/C4LC01206B.

[397] X. Fan, W. Zheng, D.J. Singh, Light scattering and surface plasmons on small spherical particles, Light: Science & Applications 2014 3:6. 3 (2014) e179–e179. https://doi.org/10.1038/lsa.2014.60.

[398] S.H. Hong, J. Winter, Size dependence of optical properties and internal structure of plasma grown carbonaceous nanoparticles studied by in situ Rayleigh-Mie scattering ellipsometry, J Appl Phys. 100 (2006) 064303. https://doi.org/10.1063/1.2338132.

[399] D.J. Ross, R. Sigel, Mie scattering by soft core-shell particles and its applications to ellipsometric light scattering, Phys Rev E Stat Nonlin Soft Matter Phys. 85 (2012) 056710. https://doi.org/10.1103/PHYSREVE.85.056710/FIGURES/15/MEDIUM.

[400] J. Lim, S.P. Yeap, H.X. Che, S.C. Low, Characterization of magnetic nanoparticle by dynamic light scattering, Nanoscale Res Lett. 8 (2013) 1–14. https://doi.org/10.1186/1556-276X-8-381/FIGURES/10.

[401] U.L.F. Nobbmann, Polydispersity–what does it mean for DLS and chromatography., Material-Talks. Com. (2014).

[402] B. Bera, Nanoporous Silicon Prepared by Vapour Phase Strain Etch and Sacrificial Technique, Int J Comput Appl. (n.d.) 975–8887.

[403] M. Badran, FORMULATION AND IN VITRO EVALUATION OF FLUFENAMIC ACID LOADED DEFORMABLE LIPOSOMES FOR IMPROVED SKIN DELIVERY, Dig J Nanomater Biostruct. 9 (n.d.) 83–91.

[404] M. Chen, X. Liu, A. Fahr, Skin penetration and deposition of carboxyfluorescein and temoporfin from different lipid vesicular systems: In vitro study with finite and infinite dosage application, Int J Pharm. 408 (2011) 223–234. https://doi.org/10.1016/J.IJPHARM.2011.02.006.

[405] D. Christin Ayuning Putri, R. Dwiastuti, A. Kharis Nugroho, OPTIMIZATION OF MIXING TEMPERATURE AND SONICATION DURATION IN LIPOSOME PREPARATION, 14 (2017) 2527–7146. https://doi.org/10.24071/jpsc.142728.

[406] S. Amin, G. v. Barnett, J.A. Pathak, C.J. Roberts, P.S. Sarangapani, Protein aggregation, particle formation, characterization & rheology, Curr Opin Colloid Interface Sci. 19 (2014) 438–449. https://doi.org/10.1016/J.COCIS.2014.10.002.

[407] B. Maherani, O. Wattraint, Liposomal structure: A comparative study on light scattering and chromatography techniques, J Dispers Sci Technol. 38 (2017) 1633–1639. https://doi.org/10.1080/01932691.2016.1269651.

[408] M.R. Mozafari, C.J. Reed, C. Rostron, Prospects of anionic nanolipoplexes in nanotherapy: Transmission electron microscopy and light scattering studies, Micron. 38 (2007) 787–795. https://doi.org/10.1016/J.MICRON.2007.06.007.

[409] D. Skoutas, D. Haralabopoulos, S. Avramiotis, T.G. Sotiroudis, A. Xenakis, Virgin olive oil: Free radical production studied with spin-trapping electron paramagnetic resonance spectroscopy, J Am Oil Chem Soc. 78 (2001) 1121–1125. https://doi.org/10.1007/S11746-001-0399-4.

[410] V. Papadimitriou, T.G. Sotiroudis, A. Xenakis, N. Sofikiti, V. Stavyiannoudaki, N.A. Chaniotakis, Oxidative stability and radical scavenging activity of extra virgin olive oils: An electron paramagnetic resonance spectroscopy study, Anal Chim Acta. 573–574 (2006) 453–458. https://doi.org/10.1016/J.ACA.2006.02.007.

[411] S. Avramiotis, V. Papadimitriou, E. Hatzara, V. Bekiari, P. Lianos, A. Xenakis, Lecithin organogels used as bioactive compounds carriers. A microdomain properties investigation, Langmuir. 23 (2007) 4438–4447. https://doi.org/10.1021/LA0634995/ASSET/IMAGES/MEDIUM/LA0634995N00001.GIF.

[412] C.J. Pickard, F. Mauri, First-Principles Theory of the EPR g Tensor in Solids: Defects in Quartz, Phys Rev Lett. 88 (2002) 086403. https://doi.org/10.1103/PhysRevLett.88.086403.

[413] M. Panneerselvam, S.S. Ali, J.C. Finley, S.E. Kellerhals, M.Y. Migita, B.P. Head, P.M. Patel, D.M. Roth, H.H. Patel, Epicatechin regulation of mitochondrial structure and function is opioid receptor dependent, Mol Nutr Food Res. 57 (2013) 1007–1014. https://doi.org/10.1002/MNFR.201300026.

[414] S. Kempe, H. Metz, K. Mäder, Application of Electron Paramagnetic Resonance (EPR) spectroscopy and imaging in drug delivery research – Chances and challenges, European Journal of Pharmaceutics and Biopharmaceutics. 74 (2010) 55–66. https://doi.org/10.1016/J.EJPB.2009.08.007.

[415] V. Savić, M. Todosijević, T. Ilić, M. Lukić, E. Mitsou, V. Papadimitriou, S. Avramiotis, B. Marković, N. Cekić, S. Savić, Tacrolimus loaded biocompatible lecithin-based microemulsions with improved skin penetration: Structure characterization and in vitro/in vivo performances, Int J Pharm. 529 (2017) 491–505. https://doi.org/10.1016/J.IJPHARM.2017.07.036.

[416] Z. Földes-Papp, U. Demel, G.P. Tilz, Laser scanning confocal fluorescence microscopy: an overview, Int Immunopharmacol. 3 (2003) 1715–1729. https://doi.org/10.1016/S1567-5769(03)00140-1.

[417] H.M. Wong, J.J. Wang, C.H. Wang, In Vitro Sustained Release of Human Immunoglobulin G from Biodegradable Microspheres, Ind Eng Chem Res. 40 (2001) 933–948. https://doi.org/10.1021/IE0006256.

[418] K., S.S.P. Jichao, Determination of Diffusion Coefficient of a Small Hydrophobic Probe in Poly(lactide-co-glycolide) Microparticles by Laser Scanning Confocal Microscopy, Macromolecules. 36 (2003) 1324–1330.

[419] S.R. Pygall, J. Whetstone, P. Timmins, C.D. Melia, Pharmaceutical applications of confocal laser scanning microscopy: The physical characterisation of pharmaceutical systems, Adv Drug Deliv Rev. 59 (2007) 1434–1452. https://doi.org/10.1016/J.ADDR.2007.06.018.

[420] M.H. Chestnut, Confocal microscopy of colloids, Curr Opin Colloid Interface Sci. 2 (1997) 158–161. https://doi.org/10.1016/S1359-0294(97)80020-9.

[421] V. Prasad, … D.S.-J. of P., undefined 2007, Confocal microscopy of colloids, Iopscience.Iop.Org. 19 (2007) 25. https://doi.org/10.1088/0953-8984/19/11/113102.

[422] V. Klang, N. Matsko, C. Valenta, F.H.- Micron, undefined 2012, Electron microscopy of nanoemulsions: an essential tool for characterisation and stability assessment, Elsevier. (n.d.). https://www.sciencedirect.com/science/article/pii/S0968432811001235?casa_token=8Pl_VZRf3SQAAAAA:qwgTb4TRM2WpAGWWaxuakJ45IDK38wYzVArr3m763W08yIwTIFdB82V3IVMvoe64ew4zdna-ww (accessed September 24, 2022).

[423] J. Kuntsche, J. Horst, h Bunjes, Cryogenic transmission electron microscopy (cryo-TEM) for studying the morphology of colloidal drug delivery systems, Int J Pharm. 417 (2011) 120–137. https://doi.org/https://doi.org/10.1016/j.ijpharm.2011.02.001.

[424] D.B. Williams, C.B. Carter, The Transmission Electron Microscope, Transmission Electron Microscopy. (1996) 3–17. https://doi.org/10.1007/978-1-4757-2519-3_1.

[425] H. Friedrich, P.M. Frederik, G. de With, N.A.J.M. Sommerdijk, Imaging of Self-Assembled Structures: Interpretation of TEM and Cryo-TEM Images, Angewandte Chemie International Edition. 49 (2010) 7850–7858. https://doi.org/10.1002/ANIE.201001493.

[426] S.U. Egelhaaf, P. Schurtenberger, M. Müller, New controlled environment vitrification system for cryo-transmission electron microscopy: design and application to surfactant solutions, J Microsc. 200 (2000) 128–139. https://doi.org/10.1046/J.1365-2818.2000.00747.X.

[427] R.A. Grassucci, D.J. Taylor, J. Frank, Preparation of macromolecular complexes for cryo-electron microscopy, Nature Protocols 2007 2:12. 2 (2007) 3239–3246. https://doi.org/10.1038/nprot.2007.452.

[428] F. Hamdi, C. Tüting, D.A. Semchonok, K.M. Visscher, F.L. Kyrilis, A. Meister, I. Skalidis, L. Schmidt, C. Parthier, M.T. Stubbs, P.L. Kastritis, 2.7 Å cryo-EM structure of vitrified M. Musculus H-chain apoferritin from a compact 200 keV cryo-microscope, PLoS One. 15 (2020). https://doi.org/10.1371/JOURNAL.PONE.0232540.

[429] T.W. Gräwert, D.I. Svergun, Structural Modeling Using Solution Small-Angle X-ray Scattering (SAXS), J Mol Biol. 432 (2020) 3078–3092. https://doi.org/10.1016/J.JMB.2020.01.030.

[430] C.E. Blanchet, D.I. Svergun, Small-Angle X-Ray Scattering on Biological Macromolecules and Nanocomposites in Solution, Annu Rev Phys Chem. 64 (2013) 37–54. https://doi.org/10.1146/ANNUREV-PHYSCHEM-040412-110132.

[431] S. da Vela, D.I. Svergun, Methods, development and applications of small-angle X-ray scattering to characterize biological macromolecules in solution, Curr Res Struct Biol. 2 (2020) 164–170. https://doi.org/10.1016/J.CRSTBI.2020.08.004.

[432] A.F. Craievich, Synchrotron SAXS Studies of Nanostructured Materials and Colloidal Solutions: A Review, Materials Research. 5 (2002) 1–11. https://doi.org/10.1590/S1516-14392002000100002.

[433] W.C. Thomas, F.P. Brooks, A.A. Burnim, J.P. Bacik, J.A. Stubbe, J.T. Kaelber, J.Z. Chen, N. Ando, Convergent allostery in ribonucleotide reductase, Nature Communications 2019 10:1. 10 (2019) 1–13. https://doi.org/10.1038/s41467-019-10568-4.

[434] D.M.A.M. Luykx, R.J.B. Peters, S.M. van Ruth, H. Bouwmeester, A Review of Analytical Methods for the Identification and Characterization of Nano Delivery Systems in Food, J Agric Food Chem. 56 (2008) 8231–8247. https://doi.org/10.1021/JF8013926.

[435] P. Borthakur, P.K. Boruah, B. Sharma, M.R. Das, Nanoemulsion: preparation and its application in food industry, Emulsions. (2016) 153–191. https://doi.org/10.1016/B978-0-12-804306-6.00005-2.

[436] G. Fritz, A. Bergmann, O. Glatter, Evaluation of small-angle scattering data of charged particles using the generalized indirect Fourier transformation technique, J Chem Phys. 113 (2000) 9733. https://doi.org/10.1063/1.1321770.

[437] J. Brunner-Popela, O. Glatter, Small-Angle Scattering of Interacting Particles. I. Basic Principles of a Global Evaluation Technique, J Appl Crystallogr. 30 (1997) 431–442. https://doi.org/10.1107/S0021889896015749.

[438] A. Yaghmur, L. de Campo, A. Aserin, N. Garti, O. Glatter, Structural characterization of five-component food grade oil-in-water nonionic microemulsions, Physical Chemistry Chemical Physics. 6 (2004) 1524–1533. https://doi.org/10.1039/B314625C.

[439] M. Twarużek, E. Zastempowska, E. Soszczyńska, I. Ałtyn, The use of in vitro assays for the assessment of cytotoxicity on the example of MTT test, Acta Universitatis Lodziensis. Folia Biologica et Oecologica. 14 (2019) 23–32. https://doi.org/10.1515/FOBIO-2017-0006.

[440] J. van Meerloo, G.J.L. Kaspers, J. Cloos, Cell Sensitivity Assays: The MTT Assay, (2011) 237–245. https://doi.org/10.1007/978-1-61779-080-5_20.

[441] T. Mosmann, Rapid colorimetric assay for cellular growth and survival: Application to proliferation and cytotoxicity assays, J Immunol Methods. 65 (1983) 55–63. https://doi.org/10.1016/0022-1759(83)90303-4.

[442] T.F. Slater, B. Sawyer, U. Sträuli, Studies on succinate-tetrazolium reductase systems: III. Points of coupling of four different tetrazolium salts III. Points of coupling of four different tetrazolium salts, Biochim Biophys Acta. 77 (1963) 383–393. https://doi.org/10.1016/0006-3002(63)90513-4.

[443] Y. Liu, D.A. Peterson, H. Kimura, D. Schubert, Mechanism of Cellular 3-(4,5-Dimethylthiazol-2-yl)-2,5-Diphenyltetrazolium Bromide (MTT) Reduction, J Neurochem. 69 (1997) 581–593. https://doi.org/10.1046/J.1471-4159.1997.69020581.X.

[444] V. Kuete, O. Karaosmanoğlu, H. Sivas, Anticancer Activities of African Medicinal Spices and Vegetables, Medicinal Spices and Vegetables from Africa: Therapeutic Potential Against Metabolic, Inflammatory, Infectious and Systemic Diseases. (2017) 271–297. https://doi.org/10.1016/B978-0-12-809286-6.00010-8.

[445] M. Hanelt, M. Gareis, B. Kollarczik, Cytotoxicity of mycotoxins evaluated by the MTT-cell culture assay, Mycopathologia. 128 (1994) 167–174. https://doi.org/10.1007/BF01138479/METRICS.

[446] T. Ilić, I. Pantelić, D. Lunter, S. Đorđević, B. Marković, D. Ranković, R. Daniels, S. Savić, Critical quality attributes, in vitro release and correlated in vitro skin permeation—in vivo tape stripping collective data for demonstrating therapeutic (non)equivalence of topical semisolids: A case study of "ready-to-use" vehicles, Int J Pharm. 528 (2017) 253–267. https://doi.org/10.1016/J.IJPHARM.2017.06.018.

[447] I. Pantelić, T. Ilić, B. Marković, S. Savić, M. Lukić, S. Savić, A stepwise protocol for drug permeation assessment that combines heat-separated porcine ear epidermis and vertical diffusion cells, Doiserbia.Nb.Rs. 72 (2018) 47–53. https://doi.org/10.2298/HEMIND170726019P.

[448] T. Ilić, S. Savić, B. Batinić, B. Marković, M. Schmidberger, D. Lunter, S. Savić, Combined use of biocompatible nanoemulsions and solid microneedles to improve transport of a model NSAID across the skin: In vitro and in vivo studies, European Journal of Pharmaceutical Sciences. 125 (2018) 110–119. https://doi.org/https://doi.org/10.1016/j.ejps.2018.09.023.

[449] V. Klang, J. Schwarz, B. Lenobel, M. Nadj, J. Auböck, M. Wolzt, C. Valenta, In vitro vs. in vivo tape stripping: Validation of the porcine ear model and penetration assessment of novel sucrose stearate emulsions, Uropean Journal of Pharmaceutics and Biopharmaceutics. 80 (2012) 604–614. https://doi.org/https://doi.org/10.1016/j.ejpb.2011.11.009.

[450] L. Coderch, I. Collini, V. Carrer, C. Barba, C. Alonso, Assessment of Finite and Infinite Dose In Vitro Experiments in Transdermal Drug Delivery, Pharmaceutics 2021, Vol. 13, Page 364. 13 (2021) 364. https://doi.org/10.3390/PHARMACEUTICS13030364.

[451] T. Franz, P. Lehman, S. Franz, H. North-Root, J. Demetrulias, C. Kelling, S. Moloney, Gettings. SD, Percutaneous penetration of N-nitrosodiethanolamine through human skin (in vitro): comparison of finite and infinite dose applications from cosmetic vehicles, Fundamental and Applied Toxicology. 21 (1993) 213–221. https://doi.org/https://doi.org/10.1006/faat.1993.1091.

[452] W.M. Lau, K.W. Ng, Finite and infinite dosing, in: N., I. Dragicevic, H. Maibach (Eds.), Percutaneous Penetration Enhancers Drug Penetration Into/Through the Skin: Methodology and General Considerations, Springer Berlin Heidelberg, 2017: pp. 35–44. https://doi.org/10.1007/978-3-662-53270-6_3/FIGURES/4.

[453] M. Milhome, R. Castro, R. Silva, A. Nobre, R. do Nascimento, Advances in Liquid Chromatography Coupled to Mass Spectrometry for Determination of Pesticide Residues in Food, in: R. do Nascimento (Ed.), 1st ed., Avid Science, 2017. www.avidscience.com (accessed September 26, 2022).

[454] S. Kumar Bhardwaj, A Review: HPLC Method Development and Validation, (2015). http://www.urpjournals.com (accessed March 1, 2023).

[455] M. Thammana, Review on High Performance Liquid Chromatography (HPLC)., Res Rev J Pharm Anal RRJPA 5.2. 5 (2016) 22–28.

[456] W. Korfmacher, Foundation review: Principles and applications of LC-MS in new drug discovery, Drug Discov Today. 10 (2005) 1357–1367. https://doi.org/https://doi.org/10.1016/S1359-6446(05)03620-2.

[457] T. Mehmood, A. Ahmed, Tween 80 and Soya-Lecithin-Based Food-Grade Nanoemulsions for the Effective Delivery of Vitamin D, Langmuir. 36 (2020) 2886–2892. https://doi.org/10.1021/ACS.LANGMUIR.9B03944/ASSET/IMAGES/MEDIUM/LA9B03944_0005.GIF.

[458] A.S. Doost, C. v. Stevens, M. Claeys, P. van der Meeren, Fundamental Study on the Salt Tolerance of Oregano Essential Oil-in-Water Nanoemulsions Containing Tween 80, Langmuir. 35 (2019) 10572–10581. https://doi.org/10.1021/ACS.LANGMUIR.9B01620/ASSET/IMAGES/MEDIUM/LA-2019-01620D_0011.GIF.

[459] Z., Ding, Y., Jiang, X. Liu, Nanoemulsions-Based Drug Delivery for Brain Tumors, Nanotechnology-Based Targeted Drug Delivery Systems for Brain Tumors. (2018) 327–358. https://doi.org/10.1016/B978-0-12-812218-1.00012-9.

[460] M. Fanun, Microemulsions with mixed Nonionic surfactants, Microemulsion Properties and Applications. (2009) 87–134.

[461] L.C. Peng, C.H. Liu, C.C. Kwan, K.F. Huang, Optimization of water-in-oil nanoemulsions by mixed surfactants, Colloids Surf A Physicochem Eng Asp. 370 (2010) 136–142. https://doi.org/10.1016/J.COLSURFA.2010.08.060.

[462] Z.A. Sadeq, Review on Nanoemulsion: Preparation and Evaluation, International Journal of Drug Delivery Technology. 10 (2020) 187–189. https://doi.org/10.25258/ijddt.10.1.33.

[463] V. Klang, C. Valenta, Lecithin-based nanoemulsions, J Drug Deliv Sci Technol. 21 (2011) 55–76. https://doi.org/10.1016/S1773-2247(11)50006-1.

[464] D.W., Sullivan, S.C., Gad, M. Julien, A review of the nonclinical safety of Transcutol®, a highly purified form of diethylene glycol monoethyl ether (DEGEE) used as a pharmaceutical excipient, Food and Chemical Toxicology. 72 (2014) 40–50. https://doi.org/10.1016/J.FCT.2014.06.028.

[465] O.G. Strusovskaya, S. V. Poroiskii, A.G. Strusovskaya, Chemical Enhancers or Transcutaneous Conductors: Transcutol, Pharm Chem J. 52 (2019) 879–884. https://doi.org/10.1007/S11094-019-01920-5/METRICS.

[466] N. Panchal, M. Kaur, A. Tharmatt, S. Thakur, S.K. Jain, Development, Characterization and Evaluation of Parenteral Formulation of Diclofenac Sodium, AAPS PharmSciTech. 21 (2020) 1–13. https://doi.org/10.1208/S12249-020-01729-6/METRICS.

[467] I. Nikolic, D. Jasmin Lunter, D. Randjelovic, A. Zugic, V. Tadic, B. Markovic, N. Cekic, L. Zivkovic, D. Topalovic, B. Spremo-Potparevic, R. Daniels, S. Savic, Curcumin-loaded low-energy nanoemulsions as a prototype of multifunctional vehicles for different administration routes: Physicochemical and in vitro peculiarities important for dermal application, Int J Pharm. 550 (2018) 333–346. https://doi.org/10.1016/J.IJPHARM.2018.08.060.

[468] I. Nikolic, E. Mitsou, A. Damjanovic, V. Papadimitriou, J. Antic-Stankovic, B. Stanojevic, A. Xenakis, S. Savic, Curcumin-loaded low-energy nanoemulsions: Linking EPR spectroscopy-analysed microstructure and antioxidant potential with in vitro evaluated biological activity, J Mol Liq. 301 (2020). https://doi.org/10.1016/J.MOLLIQ.2020.112479.

[469] C. Zhao, L. Wei, B. Yin, F. Liu, J. Li, X. Liu, J. Wang, Encapsulation of lycopene within oil-in-water nanoemulsions using lactoferrin: Impact of carrier oils on physicochemical stability and bioaccessibility, Int J Biol Macromol. 153 (2020) 912–920. https://doi.org/https://doi.org/10.1016/j.ijbiomac.2020.03.063.

[470] B. Choudhary, S.R. Paul, S.K. Nayak, D. Qureshi, K. Pal, Synthesis and biomedical applications of filled hydrogels, Polymeric Gels. (2018) 283–302. https://doi.org/10.1016/B978-0-08-102179-8.00011-9.

[471] I. Muñoz-González, C. Ruiz-Capillas, M. Salvador, A.M. Herrero, Emulsion gels as delivery systems for phenolic compounds: Nutritional, technological and structural properties, Food Chem. 339 (2021) 128049. https://doi.org/10.1016/J.FOODCHEM.2020.128049.

[472] A. Billard, L. Pourchet, S. Malaise, P. Alcouffe, A. Montembault, C. Ladavière, Liposome-loaded chitosan physical hydrogel: Toward a promising delayed-release biosystem, Carbohydr Polym. 115 (2015) 651–657. https://doi.org/10.1016/J.CARBPOL.2014.08.120.

[473] M. Stratford, A. Plumridge, G. Nebe-von-Caron, D.B. Archer, Inhibition of spoilage mould conidia by acetic acid and sorbic acid involves different modes of action, requiring modification of the classical weak-acid theory, Int J Food Microbiol. 136 (2009) 37–43. https://doi.org/10.1016/J.IJFOODMICRO.2009.09.025.

[474] N. V. Narendranath, K.C. Thomas, W.M. Ingledew, Effects of acetic acid and lactic acid on the growth of Saccharomyces cerevisiae in a minimal medium, J Ind Microbiol Biotechnol. 26 (2001) 171–177. https://doi.org/10.1038/SJ.JIM.7000090/METRICS.

[475] I.J. Winayu, N. Ekantari, I.D. Puspita, Ustadi, W. Budhijanto, P.S. Nugraheni, The effect of reduced acetic acid concentration on nano-chitosan formulation as fish preservative, IOP Conf Ser Mater Sci Eng. 633 (2019) 012040. https://doi.org/10.1088/1757-899X/633/1/012040.

[476] C. Duan, X. Meng, J. Meng, M.I.H. Khan, L. Dai, A. Khan, X. An, J. Zhang, T. Huq, Y. Ni, Chitosan as A Preservative for Fruits and Vegetables: A Review on Chemistry and Antimicrobial Properties, Journal of Bioresources and Bioproducts. 4 (2019) 11–21. https://doi.org/10.21967/JBB.V4I1.189.

[477] M. Faieta, C. Toong, M.G. Corradini, R.D. Ludescher, P. Pittia, Degradation kinetics of C-Phycocyanin under isothermal and dynamic thermal treatments, Food Chem. 382 (2022) 132266. https://doi.org/10.1016/J.FOODCHEM.2022.132266.

[478] A. Adjali, I. Clarot, Z. Chen, E. Marchioni, A. Boudier, Physicochemical degradation of phycocyanin and means to improve its stability: A short review, J Pharm Anal. 12 (2022) 406–414. https://doi.org/10.1016/J.JPHA.2021.12.005.

[479] G. Martelli, C. Folli, L. Visai, M. Daglia, D. Ferrari, Thermal stability improvement of blue colorant C-Phycocyanin from Spirulina platensis for food industry applications, Process Biochemistry. 49 (2014) 154–159. https://doi.org/10.1016/J.PROCBIO.2013.10.008.

[480] T. Comunian, A. Babazadeh, A. Rehman, R. Shaddel, S. Akbari-Alavijeh, S. Boostani, S.M. Jafari, Protection and controlled release of vitamin C by different micro/nanocarriers, Crit Rev Food Sci Nutr. 62 (2020) 3301–3322. https://doi.org/10.1080/10408398.2020.1865258.

[481] N. Malekjani, S.M. Jafari, Modeling the release of food bioactive ingredients from carriers/nanocarriers by the empirical, semiempirical, and mechanistic models, Compr Rev Food Sci Food Saf. 20 (2021) 3–47. https://doi.org/10.1111/1541-4337.12660.

[482] A. Bahrami, R. Delshadi, S.M. Jafari, L. Williams, Nanoencapsulated nisin: An engineered natural antimicrobial system for the food industry, Trends Food Sci Technol. 94 (2019) 20–31. https://doi.org/10.1016/J.TIFS.2019.10.002.

[483] M. Gupta, U. Agrawal, S.P. Vyas, Nanocarrier-based topical drug delivery for the treatment of skin diseases, Expert Opin Drug Deliv. 9 (2012) 783–804. https://doi.org/10.1517/17425247.2012.686490.

[484] V. Papadimitriou, T.G. Sotiroudis, A. Xenakis, Olive oil microemulsions: Enzymatic activities and structural characteristics, Langmuir. 23 (2007) 2071–2077. https://doi.org/10.1021/LA062608C/ASSET/IMAGES/MEDIUM/LA062608CN00001.GIF.

[485] E. A. Abdel-Rahman, A.M. Mahmoud, A.M. Khalifa, S.S. Ali, Physiological and pathophysiological reactive oxygen species as probed by EPR spectroscopy: the underutilized research window on muscle ageing, J Physiol. 594 (2016) 4591–4613. https://doi.org/10.1113/JP271471.

[486] G. Martini, L. Ciani, Electron spin resonance spectroscopy in drug delivery, Physical Chemistry Chemical Physics. 11 (2009) 211–254. https://doi.org/10.1039/B808263D.

[487] O.H. Griffith, P.C. Jost, Spin Labeling: Theory and Applications, in: Lipid Spin Labels in Biological Membranes., 1st ed., 1976: pp. 453–523.

[488] A. Kogan, S. Rozner, S. Mehta, P. Somasundaran, A. Aserin, N. Garti, M.F. Ottaviani, Characterization of the Nonionic Microemulsions by EPR. I. Effect of Solubilized Drug on Nanostructure, Journal of Physical Chemistry B. 113 (2008) 691–699. https://doi.org/10.1021/JP807161G.

[489] E. Hatzara, E. Karatza, S. Avramiotis, A. Xenakis, Spectroscopic mobility probing studies of lecithin organogels, Trends in Colloid and Interface Science XVI. (2004) 94–97. https://doi.org/10.1007/978-3-540-36462-7_22.

[490] J. Ilnytskyi, T. Patsahan, O. Pizio, On the properties of the curcumin molecule in water. Exploration of the OPLS - United atom model by molecular dynamics computer simulation, J Mol Liq. 223 (2016) 707–715. https://doi.org/10.1016/J.MOLLIQ.2016.08.098.

[491] S.M. Hashemnejad, A.Z.M. Badruddoza, B. Zarket, C. Ricardo Castaneda, P.S. Doyle, Thermoresponsive nanoemulsion-based gel synthesized through a low-energy process, Nature Communications 2019 10:1. 10 (2019) 1–10. https://doi.org/10.1038/s41467-019-10749-1.

[492] C. Ji, A. Khademhosseini, F. Dehghani, Enhancing cell penetration and proliferation in chitosan hydrogels for tissue engineering applications, Biomaterials. 32 (2011) 9719–9729. https://doi.org/10.1016/J.BIOMATERIALS.2011.09.003.

[493] M. Liu, Y. Pan, M. Feng, W. Guo, X. Fan, L. Feng, J. Huang, Y. Cao, Garlic essential oil in water nanoemulsion prepared by high-power ultrasound: Properties, stability and its antibacterial mechanism against MRSA isolated from pork, Ultrason Sonochem. 90 (2022) 106201. https://doi.org/10.1016/J.ULTSONCH.2022.106201.

[494] I. Theochari, V. Papadimitriou, D. Papahatjis, N. Assimomytis, E. Pappou, H. Pratsinis, A. Xenakis, V. Pletsa, Oil-In-Water Microemulsions as Hosts for Benzothiophene-Based Cytotoxic Compounds: An Effective Combination, Biomimetics 2018, Vol. 3, Page 13. 3 (2018) 13. https://doi.org/10.3390/BIOMIMETICS3020013.

[495] B. Ozturk, S. Argin, M. Ozilgen, D. McClements, Nanoemulsion delivery systems for oil-soluble vitamins: Influence of carrier oil type on lipid digestion and vitamin D3 bioaccessibility, Food Chem. 187 (2015) 499–506. https://doi.org/https://doi.org/10.1016/j.foodchem.2015.04.065.

[496] S.J. Hur, E.A. Decker, D.J. McClements, Influence of initial emulsifier type on microstructural changes occurring in emulsified lipids during in vitro digestion, Food Chem. 114 (2009) 253–262. https://doi.org/10.1016/J.FOODCHEM.2008.09.069.

[497] X. Wang, A. Ye, A. Dave, H. Singh, In vitro digestion of soymilk using a human gastric simulator: Impact of structural changes on kinetics of release of proteins and lipids, Food Hydrocoll. 111 (2021) 106235. https://doi.org/10.1016/J.FOODHYD.2020.106235.

[498] X. Fu, Y. Gao, W. Yan, Z. Zhang, S. Sarker, Y. Yin, Q. Liu, J. Feng, J. Chen, Preparation of eugenol nanoemulsions for antibacterial activities, RSC Adv. 12 (2022) 3180–3190. https://doi.org/10.1039/D1RA08184E.

[499] A. Lewińska, M. Domżał-Kędzia, E. Maciejczyk, M. Łukaszewicz, U. Bazylińska, Design and engineering of “green” nanoemulsions for enhanced topical delivery of bakuchiol achieved in a sustainable manner: A novel eco-friendly approach to bioretinol, Int J Mol Sci. 22 (2021) 10091. https://doi.org/10.3390/IJMS221810091/S1.

[500] H.J. Joung, M.J. Choi, J.T. Kim, S.H. Park, H.J. Park, G.H. Shin, Development of Food-Grade Curcumin Nanoemulsion and its Potential Application to Food Beverage System: Antioxidant Property and In Vitro Digestion, J Food Sci. 81 (2016) N745–N753. https://doi.org/10.1111/1750-3841.13224.

[501] Q. Li, J. Shi, X. Du, D.J. McClements, X. Chen, M. Duan, L. Liu, J. Li, Y. Shao, Y. Cheng, Polysaccharide conjugates from Chin brick tea (Camellia sinensis) improve the physicochemical stability and bioaccessibility of β-carotene in oil-in-water nanoemulsions, Food Chem. 357 (2021) 129714. https://doi.org/10.1016/J.FOODCHEM.2021.129714.

[502] J. Pencer, F.R. Hallett, Effects of Vesicle Size and Shape on Static and Dynamic Light Scattering Measurements, Langmuir. 19 (2003) 7488–7497. https://doi.org/10.1021/LA0345439.

[503] I. Theochari, M. Goulielmaki, D. Danino, V. Papadimitriou, A. Pintzas, A. Xenakis, Drug nanocarriers for cancer chemotherapy based on microemulsions: The case of Vemurafenib analog PLX4720, Colloids Surf B Biointerfaces. 154 (2017) 350–356. https://doi.org/10.1016/J.COLSURFB.2017.03.032.

[504] T.P. Nordén, B. Siekmann, S. Lundquist, M. Malmsten, Physicochemical characterisation of a drug-containing phospholipid-stabilised o/w emulsion for intravenous administration, European Journal of Pharmaceutical Sciences. 13 (2001) 393–401. https://doi.org/10.1016/S0928-0987(01)00138-5.

[505] L.B. Brenelli, L.R.B. Mariutti, R. Villares Portugal, M.A. de Farias, N. Bragagnolo, A.Z. Mercadante, T.T. Franco, S.C. Rabelo, F.M. Squina, Modified lignin from sugarcane bagasse as an emulsifier in oil-in-water nanoemulsions, Ind Crops Prod. 167 (2021) 113532. https://doi.org/10.1016/J.INDCROP.2021.113532.

[506] L. Otrin, A. Witkowska, N. Marušič, Z. Zhao, R. Lira, F. Kyrilis, T. Vidaković-Koch, En route to dynamic life processes by SNARE-mediated fusion of polymer and hybrid membranes, Nat Commun. 12 (2021) 1–12. https://doi.org/https://doi.org/10.1038/s41467-021-25294-z.

[507] N. Marušič, L. Otrin, Z. Zhao, R.B. Lira, F.L. Kyrilis, F. Hamdi, P.L. Kastritis, T. Vidakovic-Koch, I. Ivanov, K. Sundmacher, R. Dimova, Constructing artificial respiratory chain in polymer compartments: Insights into the interplay between bo3 oxidase and the membrane, Proc Natl Acad Sci U S A. 117 (2020) 15006–15017. https://doi.org/10.1073/PNAS.1919306117.

[508] N. Marusic, L. Otrin, J. Rauchhaus, Z. Zhao, F.L. Kyrilis, F. Hamdi, P.L. Kastritis, R. Dimova, I. Ivanov, K. Sundmacher, Increased efficiency of charge-mediated fusion in polymer/lipid hybrid membranes, Proc Natl Acad Sci U S A. 119 (2022). https://doi.org/10.1073/PNAS.2122468119.

[509] R. Pangeni, S.W. Kang, M. Oak, E.Y. Park, J.W. Park, Oral delivery of quercetin in oil-in-water nanoemulsion: In vitro characterization and in vivo anti-obesity efficacy in mice, J Funct Foods. 38 (2017) 571–581. https://doi.org/10.1016/J.JFF.2017.09.059.

[510] M.F. Dario, M.S.C.S. Santos, A.S. Viana, E.P.G. Arêas, N.A. Bou-Chacra, M.C. Oliveira, M.E.M. da Piedade, A.R. Baby, M.V.R. Velasco, A high loaded cationic nanoemulsion for quercetin delivery obtained by sub-PIT method, Colloids Surf A Physicochem Eng Asp. 489 (2016) 256–264. https://doi.org/10.1016/J.COLSURFA.2015.10.031.

[511] M. Tomšič, M. Bešter-Rogač, A. Jamnik, W. Kunz, D. Touraud, A. Bergmann, O. Glatter, Nonionic surfactant Brij 35 in water and in various simple alcohols: structural

investigations by small-angle X-ray scattering and dynamic light scattering, ACS Publications. 108 (2004) 7021–7032. https://doi.org/10.1021/jp049941e.

[512] O. Glatter, O. Kratky, H. Kratky, Small angle x-ray scattering, Academic Press. (1982).

[513] J. de Oca-Avalos, C. Huck-Iriart, V. Borroni, K. Martínez, R. Candal, M. Herrera, Structural characterization of nanoemulsions stabilized with sodium caseinate and of the hydrogels prepared from them by acid-induced gelation, Curr Res Food Sci. 3 (2020) 113–121. https://doi.org/https://doi.org/10.1016/j.crfs.2020.03.010.

[514] L.C. Espinoza, M. Silva-Abreu, B. Clares, M. José Rodríguez-Lagunas, L. Halbaut, M.-A. Cañas, A.C. Calpena, Formulation strategies to improve nose-to-brain delivery of donepezil, Mdpi.Com. (2019). https://doi.org/10.3390/pharmaceutics11020064.

[515] L. Kürti, S. Veszelka, A. Bocsik, N.T.K. Dung, B. Ózsvári, L.G. Puskás, Á. Kittel, P. Szabó-Révész, M.A. Deli, The effect of sucrose esters on a culture model of the nasal barrier, Toxicology in Vitro. 26 (2012) 445–454. https://doi.org/10.1016/J.TIV.2012.01.015.

[516] G. Serreli, M. Deiana, Extra Virgin Olive Oil Polyphenols: Modulation of Cellular Pathways Related to Oxidant Species and Inflammation in Aging, Cells 2020, Vol. 9, Page 478. 9 (2020) 478. https://doi.org/10.3390/CELLS9020478.

[517] S. Martín-Peláez, M.I. Covas, M. Fitó, A. Kušar, I. Pravst, Health effects of olive oil polyphenols: Recent advances and possibilities for the use of health claims, Mol Nutr Food Res. 57 (2013) 760–771. https://doi.org/10.1002/MNFR.201200421.

[518] G. Howling, P. Dettmar, P. Goddard, F. Hampson, M. Dornish, E. Wood, The effect of chitin and chitosan on the proliferation of human skin fibroblasts and keratinocytes in vitro, Biomaterials. 22 (2001) 2959–2966. https://doi.org/https://doi.org/10.1016/S0142-9612(01)00042-4.

[519] A. Naseema, P. Padayatti, C. Paulose, Mechanism of wound healing induced by chitosan in streptozotocin diabetic rats, Curr Sci. 69 (1995) 461–464. https://doi.org/https://www.jstor.org/stable/24097159.

[520] Baswan Sudhir M, Klosner Allison E, Glynn Kelly, Rajgopal Arun, Malik Kausar, Yim Sunghan, Stern Nathan, Therapeutic potential of cannabidiol (CBD) for skin health and disorders, Clin Cosmet Investig Dermatol. 13 (2020). https://doi.org/10.2147/CCID.S286411.

[521] F. Nigro, C. Cerqueira, A. Rossi, V. Cardoso, A. Vermelho, E. Ricci-Júnior, C. Mansur, Development, characterization and in vitro toxicity evaluation of nanoemulsion-loaded hydrogel based on copaiba oil and coenzyme Q10, Colloids Surf A Physicochem Eng Asp. 586 (2020). https://doi.org/https://doi.org/10.1016/j.colsurfa.2019.124132.

[522] X. Zhang, R. Song, X. Liu, Y. Xu, R. Wei, Fabrication of vitamin D3 nanoemulsions stabilized by Tween 80 and Span 80 as a composite surface-active surfactant: Characterization and stability, Colloids Surf A Physicochem Eng Asp. 645 (2022) 128873. https://doi.org/10.1016/J.COLSURFA.2022.128873.

[523] Y. Jan, L.A. Al-Keridis, M. Malik, A. Haq, S. Ahmad, J. Kaur, M. Adnan, N. Alshammari, S.A. Ashraf, B.P. Panda, Preparation, modelling, characterization and release profile of

vitamin D3 nanoemulsion, LWT. 169 (2022) 113980. https://doi.org/10.1016/J.LWT.2022.113980.

[524] Marcos Luciano Bruschi, Mathematical models of drug release, in: Strategies to Modify the Drug Release from Pharmaceutical Systems, Woodhead Publishing, Cambridge, UK, 2015: pp. 63–86.

[525] H. Rachmawati, D.K. Budiputra, R. Mauludin, Curcumin nanoemulsion for transdermal application: formulation and evaluation, Drug Dev Ind Pharm. 41 (2015) 560–566. https://doi.org/10.3109/03639045.2014.884127.

[526] L. Montenegro, C. Carbone, G. Condorelli, R. Drago, G. Puglisi, Effect of Oil Phase Lipophilicity on In Vitro Drug Release from O/W Microemulsions with Low Surfactant Content, Drug Dev Ind Pharm. 32 (2008) 539–548. https://doi.org/10.1080/03639040600599806.

[527] V. Shah, A. Yacobi, F. Rădulescu, D. Miron, M. Lane, A science based approach to topical drug classification system (TCS), Int J Pharm. 491 (2015) 21–25. https://doi.org/https://doi.org/10.1016/j.ijpharm.2015.06.011.

[528] N. Sekkat, Y.N. Kalia, R.H. Guy, Biophysical Study of Porcine Ear Skin In Vitro and Its Comparison to Human Skin In Vivo, J Pharm Sci. 91 (2002) 2376–2381. https://doi.org/10.1002/JPS.10220.

[529] U. Jacobi, M. Kaiser, R. Toll, S. Mangelsdorf, H. Audring, N. Otberg, W. Sterry, J. Lademann, Porcine ear skin: an in vitro model for human skin, Skin Research and Technology. 13 (2007) 19–24. https://doi.org/10.1111/J.1600-0846.2006.00179.X.

[530] A. Summerfield, F. Meurens, M.E. Ricklin, The immunology of the porcine skin and its value as a model for human skin, Mol Immunol. 66 (2015) 14–21. https://doi.org/10.1016/J.MOLIMM.2014.10.023.

[531] F. Benech-Kieffer, P. Wegrich, R. Schwarzenbach, G. Klecak, T. Weber, J. Leclaire, H. Schaefer, Percutaneous Absorption of Sunscreens in vitro: Interspecies Comparison, Skin Models and Reproducibility Aspects, Skin Pharmacol Appl Skin Physiol. 13 (2000) 324–335. https://doi.org/10.1159/000029940.

[532] G.A. Simon, H.I. Maibach, The Pig as an Experimental Animal Model of Percutaneous Permeation in Man: Qualitative and Quantitative Observations – An Overview, Skin Pharmacol Appl Skin Physiol. 13 (2000) 229–234. https://doi.org/10.1159/000029928.

[533] R. NEUBERT, W. WOHLRAB, In vitro methods for the biopharmaceutical evaluation of topical formulations, Acta Pharmaceutica Technologica. 36 (1990) 197–206.

[534] J. Ma, Y. Wang, R. Lu, Mechanism and Application of Chitosan and Its Derivatives in Promoting Permeation in Transdermal Drug Delivery Systems: A Review, Pharmaceuticals. 15 (2022). https://doi.org/https://doi.org/10.3390/ph15040459.

[535] J. Berger, M. Reist, J. Mayer, O. Felt, N. Peppas, R. Gurny, Structure and interactions in covalently and ionically crosslinked chitosan hydrogels for biomedical applications, European Journal of Pharmaceutics and Biopharmaceutics. 57 (2004) 19–34. https://doi.org/https://doi.org/10.1016/S0939-6411(03)00161-9.

[536] T. Higuchi, Physical chemical analysis of percutaneous absorption process from creams and ointments, J Soc Cosmet Chem. 11 (1960) 85–97. https://doi.org/10.2745/DDS.18.459.

[537] G.L., Flynn, R.L., Bronaugh, H.I. Maibach, Percutaneous absorption, in: Effects of Occlusion, CRC Press, 1991: pp. 85–114. https://scholar.google.gr/scholar?hl=el&as_sdt=0%2C5&q=Bucks+D%2C+Guy+R%2C+Maibach+HI%3A+Effects+of+occlusion%3B+in+Bronaugh+RL%2C+Maibach+HI+%28eds%29%3A+In+vitro+Percutaneous+Absorption%3A+Principles%2C+Fundamentals%2C+and+Applications.+Boca+Raton%2C+CRC+Press%2C+1991%2C+pp+85%E2%80%93114.&btnG= (accessed May 9, 2023).

[538] Bucks D, Guy R, Maibach HI, In vitro Percutaneous Absorption: Principles, Fundamentals, and Applications, in: Marcel Dekker Inc. (Ed.), In Vitro Percutaneous Absorption: Principles, Fundamentals, and Applications, New York, 1991: pp. 85–114.

[539] M., Haftek, M.H., Teillon, D. Schmitt, Stratum corneum, corneodesmosomes and ex vivo percutaneous penetration, Microsc Res Tech. 43 (1998) 242–249.

[540] M.S. ROBERTS, M. WALKER, Water. The most natural penetration enhancer, Drugs and the Pharmaceutical Sciences. 59 (1993) 1–30.

[541] M.S., Roberts, J., Bouwstra, F., Pirot, F. Falson, Skin hydration-a key determinant in topical absorption, 1st ed., CRC Press, 2008. https://doi.org/10.3109/9780849375903-10/PART-II-SPECIFIC-FACTORS-AFFECTING-TARGETING-EFFICACY.

[542] S.E. Cross, R. Jiang, H.A.E. Benson, M.S. Roberts, Can Increasing the Viscosity of Formulations be used to Reduce the Human Skin Penetration of the Sunscreen Oxybenzone?, Journal of Investigative Dermatology. 117 (2001) 147–150. https://doi.org/10.1046/J.1523-1747.2001.01398.X.

[543] M.S. Roberts, H.S. Cheruvu, S.E. Mangion, A. Alinaghi, H.A.E. Benson, Y. Mohammed, A. Holmes, J. van der Hoek, M. Pastore, J.E. Grice, Topical drug delivery: History, percutaneous absorption, and product development, Adv Drug Deliv Rev. 177 (2021) 113929. https://doi.org/10.1016/J.ADDR.2021.113929.

[544] J. Hurler, N. Škalko-Basnet, Potentials of chitosan-based delivery systems in wound therapy: Bioadhesion study, J Funct Biomater. 3 (2012) 37–48. https://doi.org/10.3390/jfb3010037.

[545] H., Zhou, Y., Yue, G., Liu, Y., Li, J., Zhang, Q., Gong, M. Duan, Preparation and characterization of a lecithin nanoemulsion as a topical delivery system., Nanoscale Res Lett. 5 (2010) 224–230.

[546] V. Savić, T. Ilić, I. Nikolić, B. Marković, B. Čalija, N. Cekić, S. Savić, Tacrolimus-loaded lecithin-based nanostructured lipid carrier and nanoemulsion with propylene glycol monocaprylate as a liquid lipid: Formulation characterization and assessment of dermal delivery compared to referent ointment, Int J Pharm. 569 (2019) 118624. https://doi.org/10.1016/J.IJPHARM.2019.118624.

[547] L. Binder, J. Mazál, R. Petz, V. Klang, C. Valenta, The role of viscosity on skin penetration from cellulose ether-based hydrogels, Skin Research and Technology. 25 (2019) 725–734. https://doi.org/10.1111/SRT.12709.

[548] P. Batheja, L. Sheihet, J. Kohn, A.J. Singer, B. Michniak-Kohn, Topical drug delivery by a polymeric nanosphere gel: Formulation optimization and in vitro and in vivo skin distribution studies, Journal of Controlled Release. 149 (2011) 159–167. https://doi.org/10.1016/J.JCONREL.2010.10.005.